Mapping desertification:

Towards an approach for mapping regional land degradation in drylands.

Wesley Bell
BLLWES002

07 February 2020

THESIS SUBMITTED TO THE UNIVERSITY OF CAPE TOWN
In fulfilment of the requirements for the degree
Doctor of Philosophy (PhD)

Plant Conservation Unit
Department of Biological Sciences
UNIVERSITY OF CAPE TOWN

Supervisors:
Professor M Timm Hoffman, Plant Conservation Unit (UCT)
Dr. Vernon Visser, Centre for Statistics in Ecology, Environment and Conservation (UCT)

Declaration

By submitting this thesis electronically, I declare that the entirety of the work contained therein is my own original work, that I am the authorship owner thereof (unless to the extent explicitly otherwise stated) and that I have not previously in its entirety or in part submitted it for obtaining any qualification.

Signed by candidate

Date: 07 February 2020

Abstract

Land degradation in drylands (desertification) is an issue that potentially impacts nearly half of the world's human population living on over a third of the Earth's land surface. Despite global concern of the impact of desertification on people and the environment, there is no universal method to assess and map desertification. Methods to assess desertification at the local to regional scale that can fit into a broader global desertification narrative are more appropriate. The overall objective of this thesis is to assess regional desertification using field and Earth observation data for the Namaqualand Hardeveld bioregion of South Africa.

Field data on the condition of the land from 277 plots was analysed using Latent Class Analysis (LCA) and found to cluster into three separate states. The first state (S1) was comprised primarily of degraded plots. The third state (S3), on the other hand, was comprised primarily of non-degraded plots, while the plots in state two (S2) generally fell between those which were assigned to S1 and S3. Through the LCA, each plot was assigned a probability of belonging to each state, and the most important variables in distinguishing the three states (perennial plant cover and bare ground cover) were identified.

A total of 16 remote sensing variables were determined for the project area. Five vegetation indices (NDVI, EVI, SAVI, OSAVI, MSAVI), as well as spectral mixture analysis (SMA) cover estimates for perennial vegetation, bare ground and bare rock were calculated using both Landsat 8 and Sentinel-2A data. These variables were used in a series of Partial Least Squares regression (PLSr) models to predict either the probability of a plot belonging to one of the three latent states, or the field estimated perennial plant and bare ground cover. The best performing PLSr model had ten remote sensing variables predicting the field estimates of cover (R^2Ycum = 0.592; Q^2cum = 0.554). Both Sentinel-2A and Landsat 8 SMA cover estimates were better at predicting field cover than any of the vegetation indices. Estimates of bare ground and perennial plant cover were projected over the project area using the PLSr model and ground truthed using data from 61 independent field test plots. There was a significant correlation between the PLSr estimates and the field estimates for both perennial plant cover and bare ground cover for the test plots with the best correlation found to be

between the PLSr estimate of bare ground and field estimated bare ground cover ($r = 0.827$, $p < 0.001$, CI [0.727, 0.893]).

The trendline slope and percentile range of a time series of the Landsat SMA bare ground estimate were used to create raster images. These images, along with images for the PLSr bare ground and perennial plant cover estimates, were converted into images representing membership values between zero and one for the habitat condition archetype. These three images were then combined to produce one raster representing the overall membership of the project area to the habitat condition archetype. The importance of five potential drivers of land degradation (elevation, slope aspect, slope steepness, rainfall trend, and land tenure) in predicting PLSr-estimated perennial plant and bare ground cover were evaluated using a random forest model. All drivers were found to be important predictors of cover and were included in the construction of the final, multi-band archetype image.

If habitat condition classes are designated according to the mean archetype membership value ± one / two standard deviations, then 17% of the project area could be considered moderately degraded, with just over 3% severely degraded. This novel method of assessing and mapping desertification leads to improved accuracy in predicting habitat condition in the context of potential drivers of change. The utility of SMA over traditional vegetation indices is supported for this particular environment. This methodology can be improved with better endmember designation as well as improved spatial data on the potential drivers of change in drylands. The archetype approach ensures less subjectivity in map production, and the retention of pertinent information in map products. The approach developed in this thesis will allow for more accurate desertification reporting for UNCCD member states and will ultimately improve efforts to combat desertification globally.

Acknowledgements

I would firstly like to thank my supervisor, Prof. Timm Hoffman for his crucial contributions and guidance throughout, and for the confidence that he has shown in me from the start. Thank you for the positivity and encouragement, factors that became all the more important the closer the submission date loomed.

I would also like to thank my co-supervisor, Dr. Vernon Visser, whose help and insights with the statistical analyses in particular were invaluable. Thanks also to the various members of the PCU, past and present, who helped in any way throughout the three years. Particular thanks to Zander Venter for GEE scripts and advice, and to Saúl Manzano, for bringing a fantastic new energy to the office.

Thank you to my whole family for the support and encouragement, and Zola for taking my mind off thesis thoughts during our morning walks. The biggest thanks of all is reserved for my wife Courtnee, who saw everything, experienced it all with me and was my constant pillar throughout. It has been one heck of a chapter and I'm so happy and grateful to be starting a new one together. With you, everything is possible.

The financial assistance of WWF South Africa and the Leslie Hill Succulent Karoo Trust (as primary funder) towards this research is hereby acknowledged. Opinions expressed and conclusions arrived at, are those of the author and are not necessarily to be attributed to the above funders.

Table of contents

List of figures

List of tables

List of abbreviations

AIC	Akaike Information Criterion
AVHRR	Advanced Very High Resolution Radiometer
CHIRPS	Climate Hazards group Infrared Precipitation with Stations
COP12	Conference of the Parties 12
DDP	Dahlem Desertification Paradigm, later Drylands Development Paradigm
DEM	Digital Elevation Model
EIV	Ecological indicator value
EO	Earth Observation
ETM+	Enhanced Thematic Mapper Plus
EVI	Enhanced Vegetation Index
GEE	Google Earth Engine
GIS	Geographic information system
GIV	Grazing Index Value
GLADA	Global Assessment of Land Degradation and Improvement
GLADIS	Global Land Degradation Information Systems
GLASOD	Global Assessment of Soil Degradation
H-E	Human-Environment
IFOV	Instantaneous Field of View
IPBES	Intergovernmental Science-Policy Platform on Biodiversity and Ecosystem Services
L.Bare	Landsat SMA bare ground cover estimate
L.EVI	Landsat Enhanced Vegetation Index
L.MSAVI	Landsat Modified Soil Adjusted Vegetation Index
L.NDVI	Landsat Normalised Difference Vegetation Index
L.OSAVI	Landsat Optimised Soil Adjusted Vegetation Index
L.Rock	Landsat SMA bare rock cover estimate
L.SAVI	Landsat Soil Adjusted Vegetation Index
L.Veg	Landsat SMA perennial plant cover estimate
LADA	Land Degradation Assessment in Drylands
LCA	Latent Class Analysis
LDN	Land Degradation Neutrality
LDSF	Land Degradation Surveillance Framework
MESMA	Multiple Endmember Spectral Mixture Analysis
MSAVI	Modified Soil Adjusted Vegetation Index

MSI	Multispectral Instrument
MSS	Multispectral Scanner
NBA	National Biodiversity Assessment
NDVI	Normalised Difference Vegetation Index
NPP	Net Primary Productivity
NRCS	United States Natural Resource Conservation Service
NRLD	National Review of Land Degradation
OSAVI	Optimised Soil Adjusted Vegetation Index
PACD	Plan of Action to Combat Desertification
PLS	Partial least squares
PLSr	Partial least squares regression
RESTREND	Residual trend analysis
RMSE	Root Mean Square Error
RUE	Rain Use Efficiency
SANBI	South African National Biodiversity Institute
SAVI	Soil Adjusted Vegetation Index
SDG's	Sustainable Development Goals
SHCS	Subjective habitat condition score
SKk10	Southern Namaqualand Quartzite Klipkoppe Shrubland
SKn1	Namaqualand Klipkoppe Shrubland
SKn2	Namaqualand Shale Shrubland
SKn3	Namaqualand Blomveld
SKn4	Namaqualand Heuweltjieveld
SKn5	Platbakkies Succulent Shrubland
SKn6	Kamiesberg Mountain Shrubland
SMA	Spectral Mixture Analysis
SRTM	Shuttle Radar Topography Mission
SWIR	Shortwave Infrared
TIRS	Thermal Infrared Sensor
TM	Thematic Mapper
UAV	Unmanned Aerial Vehicle
UN	United Nations
UNCCD	United Nations Convention to Combat Desertification
UNCOD	United Nations Conference on Desertification
UNEP	United Nations Environment Programme
USGS	United States Geological Survey

VEGMAP	National Vegetation Map
VIP	Variable Importance for Projection
VNIR	Visible Near Infrared
WAD3	Third World Atlas on Desertification
WWF	World Wide Fund for Nature

Chapter 1:

1. Introduction

1.1. Problem statement

Climate change and a continually expanding human presence across the globe are putting more pressure on natural resources than ever before. This pressure is arguably greatest in the dryland environments of the world where water and other natural resources are already limited, and human populations are generally poorer and less buffered from changes to their natural environment (Dougill et al., 2010; Fraser et al., 2011; Huang et al., 2016; Reynolds et al., 2011, 2007). Land degradation in these regions, often referred to as desertification, not only results in the loss of biodiversity and a decline in ecosystem health but also impacts on the sustainability of mostly rural livelihoods (Scholes and Biggs, 2005; Stavi and Lal, 2015; Easdale, 2016). Because of this, there is consensus that desertification needs to be addressed globally. This is evidenced by the 197 nations that have ratified the United Nations Convention to Combat Desertification (UNCCD, 1994).

Even though some researchers challenge the concept of desertification and dispute its value in dryland studies (e.g. Behnke and Mortimore, 2016b; see section 1.2), desertification remains a problem of global significance (Cherlet et al., 2018). However, one of the difficulties associated with the concept is that there still exists no universal method to assess and map desertification at local and regional scales. While a range of different approaches such as the TRENDS.EARTH Quantum GIS plugin (Conservation International, 2018) have been proposed, such methods seldom include specific details within the local context and are less applicable at local and regional scales. This is largely because land degradation processes differ in different geographic locations necessitating the use of different methodologies to measure it (Cherlet et al., 2018; Gillson and Hoffman, 2007; Jones, 2000; Middleton, 2018). Therefore, despite the significant amount of work that has been dedicated to the subject globally, the need for a universal method to assess desertification persists.

1.2 Background and context

Land degradation and desertification have a deep and complex scientific, socio-economic and political history. The ideologies that impact land degradation today have been of global significance since at least the 15th century (Davis, 2016). Various authors provide global accounts of the history, causes of, and potential solutions to desertification (e.g. Conacher 2004, 2009; Sterk et al. 2016). Behnke and Mortimore's *The End of Desertification: Disputing Environmental Change in the Drylands* (2016) covers much of this history, primarily through chapters 2 (Toulmin and Brock, 2016) and 8 (Davis, 2016), with a specific focus on Africa and the Sahel in particular. Dahlberg (1994) provides the context for southern Africa, while various authors including Hoffman et al. (1999), Meadows and Hoffman (2002) and, more recently, von Maltitz et al. (2018) focus exclusively on the South African context. I will draw on some of the key themes from this literature in order to provide specific context for the assessment of land degradation and desertification in South Africa, and Namaqualand in particular. Numerous definitions of land degradation have been suggested by scientists of different disciplines, development and government agencies, as well as international organisations. Although these definitions have all, to a greater or lesser extent, been guided by observations of the natural environment, important differences occur as a result of the diverse perceptions of the various actors (Dahlberg, 1994). Much of the confusion has arisen because of the seemingly interchangeable understanding of related processes such as drought, desiccation and desertification (Toulmin and Brock, 2016).

1.2.1 Brief history

Early views & the emergence of a desiccation ideology

Prior to the 15th century, when Europeans began their widespread exploration of the globe, deserts and drylands were generally considered as naturally dry areas that, although not favourable for crop production, were not seen as 'bad' or degraded (Davis, 2016) (Table 1.1). This perception changed, however, over the next two to three centuries due largely to two main factors. The first was an upsurge in allegations that deforestation and overgrazing were resulting in desiccation and environmental degradation across Europe and within France in particular (Davis, 2016). Desiccation

theory suggests that humans can impact the climate through both the clearing and planting of trees. Deforestation is therefore thought to result in less moisture in the atmosphere and less rain (Grove, 1995). The second factor that influenced the colonial perception of drylands was the discovery of lush tropical islands in the Caribbean, South Pacific and Indian Oceans. These landscapes came to represent optimal environmental conditions and, compared to these verdant utopias, deserts were seen as harsh and unnatural wastelands (Grove, 1995). Since local inhabitants were seen to be the cause of the apparent desiccation, a top-down institutional response to the problems was generally promoted. This was achieved through government led reforestation projects as well as the enforcement of rules designed to limit both the movement, and natural resource use, of local people (Toulmin and Brock, 2016). The desiccation ideology shaped much of the European response to the deserts that they were to encounter over the next several centuries and continues to persist in the policies of dryland country governments today (UNCOD 1978; FAO 2013; Toulmin & Brock 2016).

Colonial views on desertification and the role of nomadic pastoralists

When France occupied Algeria in 1830 they did so with the expectation of finding the fertile landscapes that had been described in ancient classical sources (Davis, 2016). They were therefore disappointed upon discovering that most of their newly appropriated land was in fact desert. Driven by the environmental thinking of the time they concluded that the desert conditions that prevailed were caused by nomadic pastoralists who would cut down trees and allow their livestock to graze indiscriminately (Davis, 2008) (Table 1.1). This narrative spread across the region, becoming dominant by the 1870s and resulting in the fear that the Sahara was spreading northwards across French Algeria (Davis, 2016). When similar conditions were later observed south of the Sahara in the Sahel region, by both French and British colonists, the same narrative was used to describe a southward spread of the desert. The fears of an expanding Sahara ultimately drove much of the colonial policy around land and natural resource management of the time, and continues to impact strategies today (Aubréville, 1949; Jiang, 2016; Lamprey, 1975; Stebbing, 1935).

Table 1.1. Timeline of selected important events in the global desertification narrative.

Date / period	Description of major events
Pre-15th century	Deserts seen as naturally occurring dry areas (Davis, 2016).
15th-18th century	Deforestation and overgrazing in Europe leads to the development of desiccation theory (Grove, 1995).
1800s	Colonists occupy areas north and south of the Sahara and blame desert-like conditions of local nomadic pastoralists (Davis, 2008).
1927	The phrase 'desertification' is coined by Lavauden (1927) to refer to the creation of desert-like conditions through improper land use.
1968-1974	Humanitarian crisis in the Sahel with catastrophic loss of life and natural assets (Berg, 1976).
1977	United Nations Conference on Desertification (UNCOD) and plan of action to combat desertification (PACD).
1984	United Nations Environment Programme (UNEP) conclude that desertification has continued at the same rate as in 1977.
1992	Desertification is included as a key issue at Rio Earth Summit.
1992	World atlas of desertification published by UNEP (UNEP, 1992)
1994	United Nations Convention to Combat Desertification (UNCCD) initiated with 197 signatories to the convention.
1997	Second World Atlas of Desertification (Middleton & Thomas, 1997).
2002	Dahlem workshop on desertification develop the Dahlem Desertification Paradigm, later the Drylands Development Paradigm (DDP) (Reynolds et al. 2007).
2011	Special Issue of Land Degradation & Development journal within which the Global Drylands Observing System (GDOS) is proposed (Winslow et al., 2011).
2016	Challenge to the desertification paradigm and suggestion that the term be abandoned (Behnke & Mortimore, 2016)
2017	New DDP is proposed to deliver novel scientific insights and development impact (Stringer et al., 2017).
2017	UNCCD shifts its focus to Land Degradation Neutrality (LDN).
2018	Intergovernmental Science-Policy Platform on Biodiversity and Ecosystem Services (IPBES) assessment report on land degradation and restoration (IPBES, 2018).
2018	Third World Atlas of Desertification (Cherlet et al., 2018).
2019	Special issue on LDN published in the Environmental Science and Policy Journal (Metternicht et al. 2019).

The policies that emerged out of the apparent crisis had two main objectives. The first was to reforest the land that was thought to have been degraded by limiting tree felling in the region and promoting the planting of new trees. The second objective was to

halt the historically nomadic lifestyle of many pastoralists, as it was this lifestyle that was seen as the main cause of degradation (Davis, 2016, 2008). While the primary objective of this approach may have been to limit the impact that nomads had on the land, it also provided the colonial powers with greater control of the subjugated local populations (Davis, 2016). This tool has subsequently been used by post-colonial African states with large pastoral populations to more easily govern these populations, primarily through registration and taxation. The sedentarisation of historically mobile people has also made it easier for governments to provide such communities with the essential goods and services associated with modern states (Fratkin, 2001). The centralised administration of natural resources as well as the top-down approach of implementing projects has also continued to guide policy in many former African colonies, particularly in the Sahel region (Toulmin and Brock, 2016).

The desiccation and spreading desert narrative persisted throughout the 19th century but it was the droughts of the 1920s that firmly rooted the idea in both the scientific literature as well as in colonial policy (Chevalier, 1932). It was this period of drought that led to the first recorded use of the word desertification. Although French forester André Aubréville is often credited as the first to use the word (e.g. Sterk et al. 2016), he, in fact, cited another French colonial forester, Louis Lavauden, who first published the word 'desertification' in 1927 (Davis, 2016; Lavauden, 1927) (Table 1.1). Lavauden blamed nomadic pastoralists for the changes that he observed in the environment and asserted that the nomads had created what he referred to as a pseudo-desert zone (Lavauden, 1927). This set the trend for the desertification paradigm that gained momentum throughout the 20th century and continues to dominate global environmental policy in drylands today (Chevalier, 1932; Davis, 2016).

The Desertification paradigm and the UNCCD

The new desertification narrative was used extensively throughout the 1930s and 1940s but started to lose momentum during the 1950s and 1960s as a result of a period of generally wetter years (Swift, 1996). Severe drought, however, returned to the Sahel region towards the end of the 1960s and into the 1970s. It peaked between 1972 and 1974 and resulted in a catastrophic humanitarian crisis (Toulmin and Brock, 2016). As part of a worldwide increase in awareness of the role that humans were having on the environment, ideas about desertification began to dominate the discourse especially with reference to the degradation of the Sahel region (Toulmin

and Brock, 2016). This culminated in the United Nations Conference on Desertification (UNCOD) in 1977, from which emerged the Global Plan of Action to Combat Desertification (PACD) (UN General Assembly, 1977) (Table 1.1). The Desertification Branch of the UN Environment Programme (UNEP) was charged with the implementation of the PACD but, despite their project activities, a UNEP review in 1984 concluded that desertification was continuing at the same rate as reported in 1977 (UNEP, 1984). Several African states, therefore, proposed a UN convention on desertification in the build up to the 1992 Earth Summit in Rio de Janeiro (Stringer, 2006). As a result the United Nations Convention to Combat Desertification (UNCCD) was created in 1994 with the primary objective of combatting desertification and mitigating the effects of drought, particularly in Africa (United Nations, 1994). Importantly, the phrasing of this objective has changed over the years with the current objective being "*to forge a global partnership to reverse and prevent desertification / land degradation and to mitigate the effects of drought in affected areas in order to support poverty reduction and environmental sustainability*" (UNCCD, 2007, p.16). This change in objective has accompanied a change in the understanding of desertification. In preparation for the 1992 Rio Summit, UNEP defined desertification as "*land degradation in arid, semi-arid and dry sub-humid areas (drylands) resulting mainly from adverse human impact*" (UNEP, 1991, p.2). Already, the idea that desertification results in desert-like conditions had been removed and sole blame had been taken away from humans (Dahlberg, 1994). As evidence began to shift the primary blame for desertification away from humans, the definition was revised to read "*land degradation in arid, semi-arid and dry sub-humid areas resulting from various factors, including climatic variations and human activities*" (UNCCD 2013, p.6). The UNCCD has subsequently shifted its focus from defining and dealing with desertification specifically to focussing more on land degradation and using both terms interchangeably. Evidence of this shift can be seen in the latest agreement emerging from the twelfth UNCCD Conference of the Parties (COP12) which aims to achieve what is referred to as Land Degradation Neutrality (LDN, Orr et al. 2017).

1.2.2 Land Degradation Neutrality (LDN)

LDN is defined as "*a state whereby the amount and quality of land resources necessary to support ecosystem functions and services and enhance food security remain stable or increase within specified temporal and spatial scales and ecosystems*" (UNCCD 2016, p.9) (Table 1.1). The emergence of the Land Degradation Neutrality paradigm has reinvigorated land degradation research and policy. Because signatory countries need to report on the extent of land degradation, new methods of measuring land degradation have been developed. Also, national policies around land degradation are being revised and improved, and methods to begin to implement action on LDN have been proposed (Akhtar-Schuster et al., 2017). A special issue of the *Environmental Science and Policy* journal, which describes the LDN framework and associated policies, was published in 2019. Contributors to the special issue focussed on country and researcher experience in implementing the LDN framework and outlined policy opportunities that exist within the framework (Metternicht et al., 2019).

Land Degradation Neutrality aims to balance the losses of 'new' degradation in any given area with the gains obtained by reversing 'past' degradation through restoration (Orr et al., 2017). LDN emerged from the concept of zero net land degradation and was first introduced at the Rio+20 conference of the United Nations (UN, 2012). It was subsequently included as an overall target of the UNCCD at COP12 in 2015 and is included within the UN Sustainable Development Goals (SDGs). Specifically, target 15.3 of SDG goal 15 sets out to, "*by 2030, combat desertification, and restore degraded land and soil, including land affected by desertification, drought and floods, and strive to achieve a land-degradation neutral world*" (UN, 2015, p.24). LDN is considered a policy instrument to balance the processes of land degradation with the practices of restoration, rehabilitation and reclamation at different spatial scales, from global to local (Kust et al., 2017).

In order to monitor progress towards achieving target 15.3, the UNCCD, along with several international groups and partners, proposed SDG indicator 15.3.1 which is the "*proportion of land that is degraded over total land area*" (Sims et al., 2017, p.7). This indicator will be reported at the national level as either degraded or not degraded and will be calculated by assessing changes in a set of three biophysical sub-indicators,

which are land-cover / land-use change, land-productivity change, and change in soil organic carbon (Orr et al., 2017). These sub-indicators are proposed to capture the minimum collection of land attributes that can be compared globally (Kust et al., 2017). The methodology suggested by the UNCCD through their *Good Practice Guidance* document is intended to allow countries to select those datasets most appropriate to their context, and to determine the best process to derive each indicator (Sims et al. 2017).

In an effort to produce a method for all UNCCD signatory countries to report on SDG indicator 15.3.1, Conservation International's Land Degradation Monitoring Project developed the TRENDS.EARTH platform (Conservation International, 2018). This is an innovative tool that takes advantage of the Google Earth Engine (GEE) platform and the best available global and national datasets to calculate SDG indicator 15.3.1 and its sub-indicators (Sims et al., 2019). It has been proposed as a unified reporting method and structure for all UNCCD signatories. Changes in land productivity, land-cover change, and soil organic carbon can all be calculated using the tool (Conservation International, 2018). However, the land-cover change calculation is limited by the accuracy of land cover maps used, while the soil organic carbon measurements are largely limited by the lack of accurate data available globally. Changes in land productivity are calculated using the normalised difference vegetation index (NDVI) as a proxy for productivity. However, as will be discussed later, the use of vegetation indices alone do not provide sufficient support for reporting on the SDG 15.3.1 indicator, or assessing land degradation in all geographic contexts (Prince, 2019).

1.2.3 What is land degradation?

In compiling the third edition of the World Atlas of Desertification (WAD3), Cherlet (2018) describes the early preoccupation of the gathered experts simply with attempting to establish consensus on a definition of land degradation that allows it to be assessed at a global scale. Various authors provide early reviews of the definitions of land degradation and desertification, and the contexts in which the terms have been used (e.g. Dahlberg 1994; Nicholson et al. 1998; Herrmann & Hutchinson 2005). The definitions that are generally used have long been criticised for being too general and too vague (Thomas and Middleton, 1994). This is partly because land degradation is

context-specific and definitions that attempt to be less general will undoubtedly discount some key land degradation processes in certain locations. The criticism also arise partly as a result of disagreement about certain theoretical issues, including whether or not land degradation is reversible, whether grassroots or top-down approaches to defining and combating land degradation are more appropriate, and how to measure the amount of degraded land both locally and globally (Cherlet et al., 2018; Reynolds et al., 2003). From an ecological perspective, land degradation has been described as resulting from the disruption of the hydrological and ecological processes of an area, which in turn impact on the area's water, soil and vegetation characteristics (Hoffman et al., 1999). Desertification is, therefore, often referred to simply as land degradation in arid, semi-arid and dry sub-humid environments (drylands) (UNCED, 1992). This definition provides for multiple potential factors that may disrupt the hydrological and ecological processes of an area, leaving the potential cause of land degradation open to interpretation within a specific context.

Even though it is now widely accepted that desertification refers to land degradation in drylands, the term itself still causes concern, and the suggestion has been made that it is no longer analytically useful (Behnke and Mortimore, 2016a). This is partly because, for many, the word desertification invokes the original image of deserts expanding across the landscape and replacing formerly fertile land (Cherlet et al., 2018; Prince and Podwojewski, 2019; Reynolds et al., 2003). It is also because desertification research has historically occurred in disparate disciplines without an overarching framework. In response to this particular concern, a Dahlem workshop on Global Desertification was held in 2001 (Reynolds and Stafford Smith 2002). At this meeting, researchers from different disciplines developed a framework for desertification research. The Dahlem Desertification Paradigm (Reynolds and Stafford Smith 2002; Reynolds et al. 2003), later renamed the Drylands Development Paradigm (DDP) (Reynolds et al. 2007), emerged from this meeting (Table 1.1). This framework identifies important research, management and policy priorities in dryland environments with a significant emphasis on evaluating coupled human-environment (H-E) systems (Reynolds et al., 2011). The UNCCD definition of desertification is accepted within the DDP, although land degradation is not defined. Rather, the suggestion is made that land degradation be defined by the factors which can be observed and measured at the local scale (Reynolds et al., 2007; Reynolds and

Stafford Smith, 2002). This framework has subsequently been updated after a review of more recent research in dryland sciences in order to deliver insights that are in line with the objectives of the 2030 SDGs (Table 1.1) (Stringer et al., 2017). Within the context of a more human-centred approach to defining land degradation, Scholes (2009) provides a conceptual model based on the persistent net reduction of ecosystem services within the southern African context (Table 1.2). In this conceptualisation, land degradation is understood within a non-exhaustive group of syndromes that are related to drivers and symptoms of change that are known to impact natural resources and ecosystem services (Scholes, 2009)

Table 1.2. Conceptual grouping and description of land degradation syndromes for southern Africa (Scholes, 2009).

Degradation syndrome	Short descriptions
Plant species change	Bush encroachment
	Alien species invasion
	Less palatable mix
	Less productive cover
Non-optimal harvesting	Undergrazing
	Overgrazing
	Forest degradation
Hydrological change	Infiltration reduction
	Falling water table
Soil and nutrient loss	Soil erosion
	Nutrient depletion
Climate change	Greenhouse gas induced
	Land cover induced

Scholes' (2009) emphasis on ecosystem services is echoed in the latest Intergovernmental Science-Policy Platform on Biodiversity and Ecosystem Services (IPBES) Assessment Report on Land Degradation and Restoration (Table 1.1) (IPBES, 2018). The IPBES define land degradation as referring to "*the many processes that drive the decline or loss in biodiversity, ecosystem functions or services, and includes the degradation of all terrestrial ecosystems*" (IPBES, 2018, p.ix). In chapter four of the report, the status and trends of land degradation and restoration are explored with particular emphasis on the fact that degradation is not a single phenomenon, and that

land degradation processes can be both location-specific or driven by global processes (Prince et al., 2018).

The open-ended nature of the IPBES definition, as well as those more recently proposed by the DDP and institutions including the UNCCD, acknowledges that the term ‘land degradation’ needs to be defined as it manifests in the specific context of any given region of interest. This does not mean, however, that the condition of the vegetation in Namaqualand, South Africa, the area of interest in this study, cannot be influenced by global drivers. Rather, it suggests that this influence needs to be understood within the context of the specific local drivers that may also be important for the region. Land degradation in this thesis is, therefore, described as it is predicted to manifest within the specific context of the project area, taking into account the region’s ecology, topography, climate and different land-use practices. The uncertainty and inherent subjectivity in assessing land degradation is acknowledged and incorporated into both how land degradation is defined, as well as how it is ultimately mapped.

1.2.4 Competing paradigms

The more recent definitions for desertification, and the shift in objectives of institutions like the UNCCD, can largely be ascribed to a growing amount of research that emerged after the findings of the UNEP review in 1984 (Behnke and Scoones, 1993; Toulmin and Brock, 2016). Although the desertification narrative was met with scepticism by some scientists prior to the 1980s, their research made little headway when it came to policy decisions in areas such as the Sahel. As Horowitz (1982) contends, the complicity of pastoralists in the degradation of the Sahel had “*the status of a fundamental truth, so self-evident that marshalling evidence in its behalf is superfluous*” (Horowitz 1982, p.67). Evidence against the desertification narrative was largely ignored. This, however, has changed as the number of researchers challenging the desertification narrative has grown through the 1980s and 1990s (Toulmin and Brock, 2016). Desertification, as it was first described by Lavauden (1927), and as it was subsequently understood for decades thereafter, has been challenged from two main perspectives (Toulmin and Brock, 2016). The first has pointed to the lack of evidence implicating indigenous nomadic pastoralists in the conversion of fertile

landscapes into deserts. The second perspective has questioned the quality of the data used to conclude that landscapes were in fact being transformed into deserts, and that this process was occurring at the rate suggested in the literature (Swift 1996). What has emerged from this is a counter-narrative to the desertification paradigm which is perhaps best described in the chapters of Behnke and Mortimore's (2016) recent book entitled "*The End of Desertification? Disputing Environmental Change in Drylands.*"

The advancement of climate models, created to explain the Sahel drought of the 1970s, was pivotal to the desertification debate of the 1980s and 1990s. The debate can be summarised by two competing ideas. The first, which describes the desiccation narrative (Charney et al., 1977, 1975), is that local, human-induced vegetation loss causes an increase in the amount of exposed bare soil, an increase in surface albedo, less evaporation and therefore less rain. In contrast, the second hypothesis proposed that the Sahelian droughts were caused by global shifts in oceanic temperatures. Although subtle, the suggestion was that these shifts were significant enough to create a substantial reduction in rainfall supplied by the main rain-bearing systems to the region such as the West African monsoon (Folland et al. 1986; Palmer 1986; Rowell et al. 1995). Various climate models and observations produced by the end of the 1990s demonstrated that a combination of factors, including vegetation cover loss and global sea surface temperatures, could best explain the observed reduction in rainfall over the Sahel (Hoffman and Todd 2013). There was disagreement, however, over which factors were most important, with evidence pointing to both. Some research suggested that vegetation cover loss, which had occurred as a direct result of anthropogenic factors, was primarily responsible for the reduction in rainfall (Charney et al., 1975; Chen et al., 2005; Diedhiou and Mahfouf, 1996; Xue, 1997; Zeng et al., 1999). Others, however, favoured the view that changes in sea surface temperature were primarily responsible for the drought in the Sahel (Folland et al., 1986; Hulme et al., 1999; Lamb, 1978; Myneni et al., 1996; Nicholson et al., 1998; Nicholson and Kim, 1997; Rowell et al., 1995). Observations of deforestation and forest tree species loss south of the Sahel supported the vegetation cover loss narrative as fewer trees would result in less evapotranspiration which is essential for the maintenance of the West African monsoon (Gonzalez, 2001).

As more sophisticated models were developed throughout the 2000s, the debate began to shift more significantly towards the impact of global climate change. Changes in sea surface temperature were seen as the driving factor behind the Sahel drought, and this impact was only amplified by the anthropogenic reduction in vegetation cover (Gonzalez et al., 2012). Although local climate models were able to explain the process described by desiccation theory, that local land use can impact precipitation in an area, these models could never fully explain the full extent of the Sahel droughts. Only once the scale of the models was broadened to look at global climate patterns could researchers draw a link between changing ocean temperatures and the Sahel droughts (Giannini, 2016). The interaction between land surface change and atmospheric conditions has, therefore, played a secondary, and potentially amplifying, role to the primary driver of drought in the Sahel which is sea surface temperature anomalies (Giannini, 2016).

As blame for degradation in the Sahel shifted away from local pastoralists, a counter-narrative began to take shape. This new narrative encompasses the inherent complexity of dryland ecosystems in acknowledging the multifaceted interactions between climate, socio-economic systems, and the physical environment that drive land degradation in drylands (Behnke and Scoones, 1993). Fundamental to this shift is an increased emphasis on understanding the adaptive capacity of indigenous human populations who have passed on centuries of local knowledge regarding methods and livelihood strategies to cope with living in the dynamic Sahel environment (Mortimore, 2016). This new degradation paradigm has been described as the 'resilience' paradigm, and recognises that natural dryland social-ecological ecosystems are not at equilibrium and that local human populations have had to adapt to the uncertainty of these systems (Mortimore, 2016). Earth observation based analyses of changes in vegetation production in semi-arid areas across the globe, including within the Sahel, support this new narrative as the notion that land degradation is pervasive in these areas has been challenged (Fensholt et al., 2012). The very notion that land degradation is ongoing in many semi-arid areas around the world is not supported by Earth observation-based analyse of changes in vegetation productivity since the early 1980s (de Jong et al., 2011; Fensholt et al., 2015, 2013, 2012).

The DDP, described above, provided context for this narrative shift which has been further bolstered by various publications in the recent decade (e.g. Behnke and Mortimore, 2016b; Reynolds et al., 2011; Stringer et al., 2017). A more holistic and integrated approach to land degradation assessment and monitoring is, for example, proposed in a special issue of the journal *Land Degradation & Development* (Table 1.1) (Winslow et al., 2011). In this publication, the authors argue the need for a comprehensive monitoring and assessment programme that integrates social and environmental perspectives (Reynolds et al., 2011; Winslow et al., 2011), and this is ultimately delivered through the proposal of the Global Drylands Observing System (GDOS) (Verstraete et al., 2011). This shift in narrative is also evidenced by the latest *World Atlas of Desertification* (WAD3) (2018), which contends that although land degradation is a global problem, it involves complex interactions between social, economic and environmental systems which are not mappable at a global scale (Cherlet et al., 2018). The intention of WAD3 is to make global datasets available that can be interpreted at the local scale to produce land degradation assessments for those specific contexts. Analogous to the resilience paradigm, and informing the presentation of WAD3, is the idea that land degradation be described through a series of syndromes (Downing and Lüdeke, 2002). Syndromes describe dynamic, archetypal groups of interactive processes and symptoms which tend to repeat in many different contexts in typical combinations and patterns (Hill et al., 2008). Local level quantitative assessments of land degradation / desertification can be placed within the context of broader syndromes, which in turn can be adapted with new information from the assessment (Stellmes et al., 2013).

1.2.5 The South African context

The history of desertification described above outlines the different approaches that have been developed to understand desertification globally, and how these have influenced perceptions and policies around land degradation and desertification, particularly in the Sahel. It is important to understand the thinking behind these approaches as these ideas persist in the literature for far longer than any practical application. Perceptions of habitat condition are key to understanding the complexity of land degradation and to producing a map of desertification for any region that will

be useful and agreeable to a wide range of potential end users. Below, I provide a brief history of the desertification / land degradation debate in South Africa and Namaqualand and draw primarily on the earlier syntheses of Dean et al. (1995), Hoffman (1995), Hoffman et al. (1999), Hoffman & Meadows (2002) and Hoffman & Rohde (2007).

Brief history of human settlement

Southern Africa has a unique geo-political and socio-environmental history. This has influenced the natural environment, how it has been managed and how it has changed over the centuries (Carruthers, 2006). The region has a rich history of human occupation and is widely regarded as the birthplace of modern humans (Compton, 2016). Hunter-gatherers are believed to have occupied South Africa for at least the last 1.5 million years but, from an environmental perspective, it is the arrival of Khoe-khoen herders and Bantu-language speaking African agro-pastoralists about 2000 years ago that is likely more significant (Table 1.3) (Denbow and Wilmsen, 1986; Hoffman, 1997; Lander and Russell, 2018; Pleurdeau et al., 2012; Smith, 1992). The Khoe-khoen were nomadic pastoralists who would have historically led their sheep herds around the region in search of pasture that generally emerges following good rains. While the Bantu-language speaking African agro-pastoralists also had herds of sheep and cattle, they were less nomadic and would generally settle in areas for long enough to cultivate the soil and grow crops such as sorghum and millet. The Bantu-language speaking African farmers are likely to have entered the southern Africa region after the emergence of the Khoe-khoen herders in about 250 AD (Maggs and Whitelaw, 1991; Wright, 1977). In order to understand the history of environmental change and the extent of land degradation in southern Africa it is necessary to have some knowledge of early human settlement patterns in the region. However, it is recognised that the movement and labelling of different group identities and associated subsistence types is not without its difficulties and contestations (Lander and Russell, 2018).

Table 1.3. Selection of important events in the South African desertification narrative

Date / period	Description of major events
Before 2000 BP	People with hunter-gatherer lifestyles present across southern Africa with limited environmental impact.
± 2000 BP	First evidence of the emergence of pastoralist lifestyles in southern Africa and arrival of Nguni agro-pastoralists in eastern parts of the region.
1652	Arrival of Dutch settlers to the Cape and subsequent inland exploration results in skirmishes over land.
1830s	Movement of Dutch settlers away from the Cape as part of 'the great trek'.
1913	Following legislation dating back to the late 19th century, the Natives Land Act formally restricted black ownership of land to 7% of the country (Von Maltitz et al., 2018).
1914	Formation of the Drought Select Committee in response to severe drought across the country.
1919	Schwarz Kalahari Redemption Scheme proposes the flooding of the Kalahari to reverse desiccation in the region (Schwarz, 1919).
1923	Drought Investigation Commission (1920) report found that overstocking and kraaling of livestock was responsible for 'veld' degradation (du Toit et al., 1923).
1953	In Veld Types of South Africa, Acocks' suggests the that the Karoo is expanding into the rest of South Africa and desert will fill the vacuum in its place (Acocks, 1953).
1950s – 1990s	Apartheid era concentration of rural population into villages to make infrastructure provision easier and to ensure agricultural land was not lost to development ('Betterment').
1995	South Africa sign United Nations Convention to Combat Desertification (UNCCD) and commit to developing a National Action Plan to combat desertification.
1999	First national synthesis of Land Degradation in South Africa (Hoffman et al., 1999).
2000s	Several studies map land degradation / desertification at different spatial scales, and used different methodologies (Bai and Dent, 2007; Meadows and Hoffman, 2002; Thompson et al., 2009, 2005; Wessels et al., 2011, 2007b, 2004)
2010	Mapping land degradation and conservation in South Africa (Lindeque, 2009) is released as a contribution to the global LADA project (Biancalani et al., 2011).
2017/18	South Africa undertake national Land Degradation Neutrality (LDN) target setting process (Von Maltitz et al., 2019).

The first Europeans to settle in South Africa were the Dutch in 1652, in what is now Cape Town (Table 1.3). European exploration into the interior of the subcontinent began almost as soon as they had settled in the Cape (De Wet, 1979; Valentyn, 1971; Waterhouse, 1932). At first, relations between European explorers and the local inhabitants were relatively peaceful although there was competition for land and livestock, which led to skirmishes in the form of cattle raids (Penn, 1995). As Europeans, and later Dutch-speaking farmers (Boers), continued to expand into the interior, this competition for land intensified between all parties and continued into the 20th century. At first, a combination of disease, war and the expansion of the colonial frontier dispossessed black people of their land. During the late 19th century and much of the 20th century, however, land was forcibly removed from black people as a direct result of the legislation of the time (Benjaminsen et al., 2006; Kostka, 2004; Von Maltitz et al., 2018; Walker and Cousins, 2015; Webley, 2007).

Various legislative Act's from about the mid-1880's not only restricted the amount of land that black people could own in South Africa but also demanded the forced removal of black people from their land (Table 1.3). Although land dispossession had already largely taken place beforehand, the Native Lands Act of 1923 formally restricted black ownership of land to only 7% of the country (Beinart and Delius, 2015). As a consequence, many former black farmers were forcibly removed to village settlements in the black 'homelands' where they had little access to land for farming or for the grazing of their livestock. In contrast, individual white settler farmers and their families occupied large areas on which they were able to develop commercial-scale farming operations. Human and livestock population densities were therefore far greater in the former homelands than on white-owned farms in South Africa (Hoffman, 2015). The impact that these settlement patterns have had on South African people and the environment persists to this day as many of the former homelands constitute today's communal areas while much of the privately-owned land in the country is still owned by white farmers (Hoffman et al., 1999; Hoffman and Todd, 2000; Shackleton and Shackleton, 2015).

Desertification / land degradation in South Africa

From the end of the 19th century and well into the 20th century, several attempts were made to raise awareness about, and address, the land degradation issue in South Africa (Table 1.3). These efforts focussed primarily on the white-owned farms in the

country and comparatively little attention was paid to areas within the black homelands (Hoffman et al., 1999). During the early 20th century there was a pervasive notion among South African politicians, as well as the public, that the land governed by the Union of South Africa was likely to expand beyond its 1910 borders to include areas such as Basutoland (Lesotho), Swaziland and Bechuanaland (Botswana). Some even included South West Africa (Namibia) and Southern Rhodesia (Zimbabwe) in their expansionist visions (Hyam, 1972; Keppel-Jones, 1951). One of the primary motivations for these ideas, as argued by McKittrick (2015), was the need for water by white South African farmers. The idea was that water could be obtained from the large rivers which occur north of the country, and that white South African farmers would then have the right to access this water.

As desiccation theory had fuelled early policy around desertification in the Sahel, so too did it influence the thinking of many South Africans during the early 1900's. Ernest Schwarz, a geology professor at Rhodes University College (now Rhodes University), famously proposed the diversion of both the Chobe and Kunene rivers into the Kalahari desert in order to avoid the desertification of the region (Table 1.3) (Schwarz, 1919). Schwarz argued that much of the Kalahari had been laid waste by the local inhabitants but that if it was flooded it could become a fertile landscape on which white farmers could live and farm (Thomas and Shaw, 1991). Guided by this desiccation theory, Schwarz proposed that flooding the Kalahari would return moisture to the atmosphere and thus result in more rainfall for the region as a whole, and bring an end to desertification in South Africa (Schwarz, 1919; McKittrick 2015). Although Schwarz's desiccation theory received very little scientific support in South Africa, and his scheme was deemed impractical by the government of the time, he received a large amount of support from the South African public. The popularity of his idea was such that the Schwarz Kalahari Thirstland Redemption Society was formed in 1933 even though Schwarz had died five years earlier, in 1928 (McKittrick, 2015).

As with the persistence of the desertification paradigm in the Sahel, the desiccation narrative gained most traction in South Africa during years of severe drought (e.g. Dean et al., 1995; McKittrick, 2015; Meadows and Hoffman, 2002). There was little doubt among many South Africans that the region was drying up, and that this process threatened their livelihoods. The state of pastures in the country was a fundamental concern among farmers and researchers, particularly in the eastern margins of the

Nama-Karoo. Here, the belief was that poor grazing management, overstocking, trampling and kraaling (i.e. corralling) were decimating historically good grazing areas leading to a drying climate and further loss of vegetation cover (e.g. Shaw, 1875; Bradfield, 1908). Although interest in land degradation waned somewhat during several wet decades at the end of the 19th century, drought and related losses in livestock returned from about 1911. This brought the issue to the fore once again and resulted in the establishment of the Drought Select Committee in 1914 and the Drought Investigation Commission in 1920 (Critchley and Netshikovhela, 1998; Hoffman *et al.*, 1999; Beinart 2018; von Maltitz 2018). The Final Report of the Drought Investigation Commission emphasised the point that land-use practices, and not changing rainfall amounts and patterns, were resulting in an increase in the severity and frequency of drought conditions in South Africa (Table 1.3) (du Toit et al., 1923). Good rainfall, however, returned in the 1920s which may partly explain a lack of any response from the South African government, and public alike, to the 1923 report (Hoffman et al., 1999).

Research into desertification continued, however, with perhaps the most influential work in the South African desertification debate of the 20th century being completed by John Acocks in the 1940s and 1950s (Table 1.3). Acocks (1953) clearly and very effectively depicted the desertification of the eastern Karoo, and the north-eastern expansion of the arid Karoo shrublands, through a series of detailed maps. The first two maps represented the vegetation types of South Africa as they might have appeared before European colonisation (i.e. the pristine state), and as they were in 1950 when Acocks prepared his analysis. In a third map, Acocks predicted the future state of the vegetation in 2050 if desertification was not controlled (Acocks, 1953). In keeping with the narrative of the time, it was the farmers of the semi-arid eastern Karoo who were blamed for these changes. The main message repeated throughout Acocks' work was that poor land management by commercial small-stock farmers had degraded the environment and caused the eastward spread of the Karoo (Hoffman and Cowling, 1990; Meadows and Hoffman, 2002). Acocks also served on the Desert Encroachment Committee which released a report in 1951 that, unsurprisingly, concluded that vegetation loss had occurred as a result of historical land-use practices and not changing rainfall patterns (Government of South Africa, 1951). Acocks' 'expanding Karoo' hypothesis, as with the expanding Sahara narrative in North Africa,

continued to influence the desertification debate in South Africa for most of the latter half of the 20th century and as a result very little original research into desertification was undertaken (Hoffman, 2018). More recent literature has, however, challenged this popular narrative and has broadened the scope and increased the complexity of the debate across the country (Masubelele et al., 2015). Land degradation continues to be discussed within a broader range of scientific disciplines and within geographic contexts outside of the Karoo.

South Africa and the UNCCD

The UNCCD has defined five global aridity categories based on a comparison between a region's mean annual precipitation and its potential to lose water through evaporation and transpiration, otherwise known as the MAP: PET ratio. Hyper-arid zones have a MAP: PET ratio of less than 0.05, while humid zones have ratios greater than 0.65. The three categories that lie between these two zones are arid, semi-arid and dry sub-humid. These are the drylands that the UNCCD are concerned with (Hoffman and Ashwell, 2001; UNCCD, 2017; Von Maltitz et al. 2018). Ninety one percent of South Africa is comprised of drylands, while a further 8% is considered hyper-arid and only 1% humid. Understanding where, and for what reasons, land degradation occurs in the country is therefore of importance from both an environmental, and a socio-economic, perspective.

South Africa signed the UNCCD in June 1995 and ratified it in September 1997, thus obligating the country to produce a National Action Programme to combat desertification (Table 1.3) (Hoffman et al., 1999; Von Maltitz et al., 2018). The first step for the then Department of Environmental Affairs and Tourism, which was tasked with facilitating the process, was to commission a study of the land degradation debate in South Africa. This study had the overall objective of conducting an assessment of the desertification issue in South Africa, and specific objectives around conducting literature reviews, creating maps and bibliographies, outlining a monitoring programme, and contributing to the writing of the White Paper on desertification (Hoffman et al., 1999). A final report was compiled by Hoffman et al. (1999) entitled "*Land Degradation in South Africa*" which was followed by a popular book on the theme (Hoffman and Ashwell, 2001). Through a participatory process, including workshops in 367 magisterial districts in South Africa, the report details the level of soil and veld degradation in South Africa, as well as providing a combined index of degradation for

the country (Hoffman et al., 1999). A similar approach, though this time following the Land Degradation Assessment in Drylands (LADA) questionnaire (Lindeque, 2009), was conducted for the country as a contribution to the global LADA project (Biancalani et al., 2011; IIASA, 2009). At the same time, several authors have attempted to address the land degradation issue at different spatial scales and using a variety of different methodologies and techniques, from remote sensing methods to coupling expert and local knowledge (Bai and Dent, 2007; Meadows and Hoffman, 2002; Thompson et al., 2009, 2005; Wessels et al., 2011, 2007a, 2007b, 2004; Wessels and Prince, 2007), and these are expanded on in chapter 2 of this thesis.

While there has been significant debate around the extent of land degradation in the country, there is broad consensus that degradation has been generally more severe in communal versus private land (Hoffman et al., 1999; Hoffman and Todd, 2000; Meadows and Hoffman, 2002; Todd and Hoffman, 2009, 1999; Wessels et al., 2007a; Wessels and Prince, 2007). Communal land in South Africa refers generally to the former Apartheid homelands which are characterised by higher human and animal population densities and a history of neglect by the South African government (Hoffman and Ashwell, 2001). Commercial areas on the other hand are largely the former white-owned farms and are generally large enough for livestock farmers to rotate animals within paddocks in order to allow the land to rest and recover (Meadows and Hoffman, 2002).

South Africa and LDN

As part of the incorporation of target 15.3 into the SDGs at COP12 of the UNCCD, countries were invited to develop voluntary LDN targets. This process took place in South Africa between 2016 and 2018 (Table 1.3) and resulted in the setting of two national targets (Table 1.4). These are to have no net loss in productivity, and to achieve a 5% gain in productivity, by 2030 as compared to 2015 levels (Von Maltitz et al., 2019). These nationwide targets may carry little meaning for practical management objectives, however, without consideration of biome level or landscape process-based targets. An increase in productivity in a South African grassland, for example, may be related to bush encroachment or an increase in alien invasive species. This is indicative of a degraded landscape and not an improvement as would be suggested if only productivity was considered. A more stratified approach, at least at the biome level, is therefore needed to understand degradation in the country. As a result, the

South African LDN target setting process determined both sub-national and specific targets to avoid, minimise and reverse land degradation (DEA, 2018). Another concern with LDN in South Africa is that the sub-indicators suggested by the UNCCD have not been found to correlate well with perceived land degradation in the country. The results of two highly participative, stakeholder-based studies into the extent of land degradation across the country's 367 district municipalities disagreed with the location and extent of land degradation, as indicated by the measures of productivity, land cover change, or soil organic carbon suggested by the LDN framework (Von Maltitz et al., 2019).

Table 1.4. LDN targets for South Africa to be achieved by 2030. Adapted from DEA (2018) and von Maltitz et al. (2019).

National targets	Net gain is achieved by 2030 as compared to 2015 with an additional 5% of the national territory having improved.
Sub-national targets	No net loss in the grassland biome by 2030 as compared to 2015.
	No net loss in the thicket biome by 2030 as compare to 2015.
Specific targets	Improve productivity and SOC stocks in 6 000 000 ha of cropland.
	Rehabilitate and sustainably manage 1 809 767 ha of "forest".
	Rehabilitate and sustainably manage 1 349 714 ha of fynbos.
	Rehabilitate and sustainably manage 87 621 ha of thicket.
	Rehabilitate and sustainably manage 2 436 170 ha of grassland.
	Rehabilitate and sustainably manage 2 646 069 ha of savanna.
	Rehabilitate and sustainably manage 149 877 ha of Succulent Karoo.
	Rehabilitate and sustainably manage 528 632 ha of Nama Karoo.
	Rehabilitate and sustainably manage 76 525 ha of desert.
	Rehabilitate 61 900 ha of wetlands.
	Clear 1 063 897 ha of alien invasive species.
	Clear 633 702 ha of bush encroached land.
	Rehabilitate 350 000 ha of artificial areas.

Chapter 2:

2. Theory and application

2.1 Theoretical basis of the desertification debate

Attempts to explain the nature and extent of land degradation are often contextualised within two competing paradigms in rangeland ecology, which may be divided broadly into equilibrium and non-equilibrium views of how dryland resources respond to herbivory and rainfall (Herrmann and Hutchinson, 2005).

Central to the development of the desertification paradigm is the view that ecosystems are in a state of equilibrium with climate. According to this view, ecosystems respond to natural disturbances by reverting back to an equilibrium state over time. Unnatural (e.g. deforestation, cultivation, overgrazing) or extreme events (e.g. extended drought), however, cause irreversible damage and degradation. In his study of plant succession Frederic Clements (1916) articulated how, after a disturbance, plant communities develop through a series of states from a pioneer state, dominated by weedy, fast-growing species to a final 'climax' state which is in equilibrium with the prevailing environment. He further described the plant community as being a 'living organism', developing over time from an 'infant stage' to a state of 'maturity' (Clements, 1916). Part of the reason that the theory of succession has dominated ecological thinking for so long, despite very early opposition to the idea from authors such as Gleason (1917), is that the narrative has an identifiable protagonist, or potential endpoint, in the form of the climax plant community. Huntsinger (2016) suggests further that forces which result in the degradation of this climax state, as well as the degraded state itself, may be viewed as the antagonists of the story. Advocates of desertification, therefore, often contrast the expected lush vegetation which should exist under prevailing climatic conditions with the barren wastelands that are observed in some degraded dryland environments, and consider nomadic pastoralists as adversaries in the 'natural' process of succession (Huntsinger, 2016).

Equilibrium theory formed the core of ecological thinking for several decades and succession theory was used as a guide in the management of rangelands and forests across the world. Ideas around carrying capacity, which prescribe sustainable limits to

maximum population size, also influenced the management of domestic livestock populations of both commercial ranchers and nomadic pastoralists alike (Scoones, 1999). The view was that different management practices could be used to shift rangelands from one desired state to another depending on the intended use of the landscape (Dahlberg, 1994). The study of rangelands and the process of land degradation are, therefore, very closely linked to the practical management of landscapes. As a result, several range management models, developed for different environments under a broad range of circumstances have emerged (Briske et al., 2017). Clements' theories of plant succession, in particular, drove the development of early range management models which were universally accepted (Briske, 2017; Westoby et al., 1989).

It was only from the 1970s, following a proliferation of studies using both mathematical models and observations of real ecosystems, that equilibrium theory was widely challenged and the key concepts of non-equilibrium theory were developed (Westoby et al. 1989; Herrmann & Hutchinson 2005). Non-equilibrium theory describes ecosystems that respond non-linearly to key drivers such as rainfall and herbivory and usually have high levels of spatial and temporal variability (DeAngelis and Waterhouse, 1987). The emergence of non-equilibrium theory has resulted in the development of a new ecological lexicon, with terms such as resilience, persistence, reversibility and stability being used to describe the dynamics of different ecosystems and how they respond to biotic and abiotic influences (Dahlberg, 1994; Scoones, 1999). Drylands, in particular, have received significant attention with the idea emerging that they are not in equilibrium but rather shift over time between different community assemblages or states, which are driven primarily by changing rainfall patterns and different soil and topographical types.

In the same way that assumptions around equilibrium theory influenced the development of models based on plant succession, so too have non-equilibrium ideas resulted in the adoption of new models which can be used for management purposes (Dahlberg, 1994). One of the most influential of these is the state-and-transition model described by Westoby et al. (1989). Assuming that ecosystems are not in equilibrium, the state-and-transition model characterizes landscapes into groups of disparate states and a set of possible transitions between these states (Westoby et al. 1989). In order for a landscape to transition from one state to another, it requires an action that

is usually a combination of environmental factors and management practices. For any given landscape, a number of different states can be identified, and knowledge of transitional drivers can help to promote or avoid certain states (Milton and Hoffman, 1994). Management for any given area ultimately becomes less rigid and more dynamic and flexible in how it is implemented (Dahlberg, 1994). Degradation studies can also benefit from state-and-transition theory by identifying potentially degraded states as well as the factors that may influence the transition both into and out of that state.

State-and-transition theory has been built on with the development of additional concepts and methodologies that serve specific purposes based on local conditions. For example, having observed that environmental change, and transitions between ecosystem states can be discontinuous, Friedel (1991) developed the concept of thresholds of environmental change. The suggestion is that once a threshold is crossed it may not be possible for the ecosystem to revert back to the previous state without significant management intervention (Dahlberg, 1994; Friedel, 1991). Milton et al. (1994) present a stepwise model of arid or semiarid rangeland degradation in which rangelands can occur in one of five steps. Each step is described by the abiotic or biotic factors thought to maintain the rangeland in that step, and management options are suggested based on these descriptions (Milton et al., 1994). Rangeland ecologists can therefore use multivariate analyses to determine where thresholds are likely to exist in a landscape and use these findings to guide management toward preventing ecosystems from crossing a threshold into a degraded state (Bosch and Gauch, 1991; Bosch and Kellner, 1991; Friedel, 1991). Turnbull et al. (2008) offer a similar conceptual framework specifically for understanding semi-arid land degradation. Their cusp catastrophe model, however, uses an eco-hydrological framework to consider both the potential for a linear and reversible transition to a more degraded state, as well as for transitions to occur across ecosystem thresholds (Turnbull et al. 2008). Similar thinking is applied by Prince et al (2018) in their conceptual representation of the states and processes of degradation which illustrates the potential contributions of both human and natural environmental stress in dryland environments.

Vegetation dynamics, however, are rarely explained entirely by either equilibrium- or non-equilibrium-based models. In reality the two theories, and the models that emerge from them, are seldom mutually exclusive. In a review of the paradigms used to explain

vegetation dynamics on rangelands, Briske et al. (2003) suggest that so-called equilibrium and non-equilibrium systems are generally not distinguished on the basis of differences in fundamental processes and functions, but rather by their evaluation within different spatial and temporal scales (Briske, 2017). Equilibrium models also typically emphasise the importance of biotic feedbacks such as plant competition and the impact of livestock on vegetation parameters, while non-equilibrium models focus on abiotic drivers such as rainfall patterns (Vetter, 2005). The vegetation dynamics of a particular landscape may, for example, be best described by rainfall patterns at the annual or decadal time scale, and intra-specific plant competition at the seasonal scale. This suggestion builds on the assessment by Wiens (1984) that, instead of a rigid dichotomy between the two theories, there exists a continuum of ecosystem behaviour from equilibrium to non-equilibrium type responses (Wiens, 1984). The proposal is that ecosystems be conceptualised with models that incorporate both equilibrium and non-equilibrium dynamics at a range of different spatial and temporal scales (Briske, 2017; Briske et al., 2003).

2.2 Mapping landscapes across space and time

Landscape maps usually emphasise either a bio-ecological or a geo-ecological perspective (Moss, 2000). The bio-ecological perspective is driven by the need to understand the spatial component of species at the plant population and community scale. The geo-ecological perspective, on the other hand, tries to represent the relationships that exist between factors such as vegetation, soils, human land use and topography which together produce potentially distinct landscape units (Cullum et al., 2016a; Moss, 2000). State-and-transition models will, for example, classify a landscape into distinct states that can then be mapped as separate landscape units (e.g. Milton and Hoffman, 1994). To do this, units are generally classified according to certain measurable characteristics, and boundaries are identified based on the general range for any given unit. For example, for a landscape unit to be classified as grassland, boundaries may be set for parameters such as dominant growth forms, maximum tree cover or maximum tree height (Dixon et al., 2014). If these variables do not fall within the specified boundary constraints, then the area will not be classified as grassland and will rather fall into some other pre-determined class. Units in different

locations that have the same characteristics can be mapped together allowing land managers to develop regional management plans. A core assumption that allows for the extrapolation between locations is that the processes that shape landscape units, and their associated drivers, will be the same across locations (Cullum et al., 2016a). This assumption, of course, will not be equally true for all units mapped together and it is up to the researcher or end user of the map to determine whether the potential error created by this assumption is acceptable or not. In general, the mapping of landscapes is achieved through the application of a typical statistical classification method which assigns each pixel in an image to a pre-specified class. In this case, any given pixel can only ever be either one of the specified classes (e.g. land cover type) or not, and can never fall somewhere in between (Foody, 1996).

2.2.1 Fuzzy classification in theory and application

More recently in the practice of mapping landscapes, and particularly since the advent of remote sensing technology, attempts have been made to take into account the inherent complexity of these landscapes through the use of fuzzy classification techniques (Cullum et al., 2016a; Oldeland et al., 2010; Rocchini and Ricotta, 2007). Fuzzy classifications, based on fuzzy systems and fuzzy set theory, provide an alternative to more traditional hard classification techniques, which require defined set membership (Zadeh, 2008, 1965). The philosopher Plato laid the initial foundation for what is now referred to as fuzzy logic by demonstrating that there exists a grey area to any thesis or logic (McBratney & Odeh 1997). In traditional or Boolean logic, any given number of elements will either belong to a set or not. That is to say that membership function values can only be 0 (does not belong to the set) or 1 (belongs to the set) (Nickel and Schröder, 2017). Fuzzy logic, on the other hand, allows for membership function values to range between 0 and 1. Thus, an element can belong partly to one or more sets simultaneously (Zadeh 1965; McBratney & Odeh 1997; Nickel & Schröder 2017). Mathematically, fuzzy set theory is a generalisation of traditional set theory where the ‘fuzziness’ stems from imprecision or uncertainty. One of the most important outcomes of this idea is that individuals may be grouped into classes that do not have sharply defined boundaries (Kandel, 1986).

Fuzzy classification has been used in a number of different scientific contexts, most notably in the soil sciences (e.g. Burrough et al., 1997; McBratney and De Gruijter, 1992; McBratney and Odeh, 1997; Nickel and Schröder, 2017). There are also, however, several examples of fuzzy classification within remote sensing (e.g. Foody 1996; Benz et al. 2004), and vegetation mapping applications (e.g. Roberts 1996; Tapia 2004). These techniques have greatest utility in instances where the unit of observation (i.e. the pixel) is mixed in terms of its class attribution (Tong et al., 2017). Hard classifications are inappropriate for mixed pixels, which may contain two or more land-cover classes, thus necessitating the use of a fuzzy classification approach (Myint et al., 2009). For example, in a comparison between traditional 'hard' classification techniques of land cover, and classification approaches based on fuzzy set theory, Foody (1996) showed that the fuzzy classifications enabled a more accurate representation of land cover in a study site in the United Kingdom. Fuzzy classification techniques have particular utility for land degradation studies in that a landscape may be highly heterogeneous in terms of its condition, with relatively small degraded areas occurring adjacent to more natural areas. This may be the case, for example, in subsistence farming areas where small cultivated areas of land are likely to occur within a larger rangeland landscape. In this case, the fuzzy classification technique can pick out the proportion of a mixed pixel that is cultivated. A hard classification technique would either over estimate the amount of cultivation by classifying the whole pixel as cultivated, or underestimate the amount of cultivation by classifying the whole pixel as natural rangeland (Tong et al., 2017). Spectral mixture analysis (SMA) techniques, which are expanded on in section 5.1.2 of this thesis, are an example of a fuzzy classification method applied to remote sensing data.

2.3 Mapping land degradation

Accurate data on the causes and impacts of land degradation are needed in order to produce reliable assessments of the extent of degradation across an area (Verstraete et al., 2011). These data can be obtained at different taxonomic, geographic and temporal scales, and can also be collected both *in situ* and remotely (Chapin et al., 2010). The different scales at which the data can be sourced provide opportunities for generating accurate and informative assessments, but also provide challenges

associated with linking data from different scales (Vogt et al., 2011). There is rarely a single scale of measurement that is able to account for how specific processes influence the patterns that are observed at multiple spatial and temporal scales (Hutchinson, 1953). The impact of local environmental drivers may, for example, become negligible at greater spatial scales. Data on degradation is also influenced heavily by the subjective assessments of experts, and may not be replicable in either the same or in different areas by different observers (Prince, 2016).

Historically, four broad approaches have been used to quantify the extent of land degradation in an area. These include the opinions of experts, satellite-derived measurements of net primary productivity, the application of biophysical models and the mapping of abandoned cropland areas. Although each approach is able to offer some insight into the problem of land degradation in an area, none, on its own, has been able to explain the issue in its entirety (Gibbs and Salmon, 2015). Numerous maps of degradation at the global scale have been developed (e.g. UNEP, 1992, 1997; Cherlet *et al.*, 2018), yet only four have arguably been completed with a high enough spatial resolution for use at regional scales (Prince, 2016). These are the Global Assessment of Soil Degradation (GLASOD) (Oldeman et al. 1991), the United States Natural Resource Conservation Service (NRCS) Global Major Land Resource Stresses Map (Beinroth et al., 2001), the Global Assessment of Land Degradation and Improvement (GLADA, Bai et al. 2008), and the Global Land Degradation Information Systems (GLADIS) (Nachtergaele et al., 2011). These four suites of maps differ significantly in the input data and the methodologies used. As a result, the global estimates of total degraded area from these and other assessments vary from under 500 million hectares to in excess of six billion hectares (Gibbs and Salmon, 2015; IPBES, 2018). These products have, therefore, been criticised not only for their lack of agreement but also for their inability to be applied, especially at regional and local scales, to prevent and control land degradation (Verón et al., 2006; Wessels, 2009). There is growing consensus, however, that although desertification is a phenomenon that may not be amenable to being mapped at the global scale (Cherlet et al., 2018), maps showing global trends or patterns of vegetation change (e.g. Fensholt *et al.*, 2015) can be used as a primary guide to identify areas at the regional and local scale which may require more in depth land degradation assessment and monitoring.

Much of the difficulty associated with global assessments is that land degradation or desertification is not a single phenomenon and is not easily or simply measured. A number of factors at different spatial and temporal scales may result in land degradation, and even the same factor at the same scale may have a significantly different impact in two different environments. For example, livestock grazing at the same intensity may have a far greater impact on an area with slightly less rainfall than a similar, wetter environment. A further complication with global assessments is related to the definition that is used for land degradation, and specifically, what aspect of the land degradation process is being illustrated. Some maps, for example, illustrate what could be considered the end condition of the land, or the condition of the land at the time of the assessment (Bai et al., 2008a). Other maps represent a trend in the productivity of the land over a pre-determined time period, while still other assessments are representative of ongoing processes of land degradation, or the perceived risk of degradation (Fensholt et al., 2015; Gibbs and Salmon, 2015; Prince, 2016; Symeonakis et al., 2016). Another significant challenge in mapping land degradation is that land with naturally low productivity is often erroneously described as degraded (Gibbs and Salmon, 2015).

In chapter four of the IPBES assessment report on land degradation and restoration, Prince et al. (2018) summarise these issues and present six different degradation states (Table 2.1) (see also Prince, 2016). States A and C are commonly mistaken for degraded land, particularly in more large-scale assessments, but are not actually degraded. Land in these states may erroneously increase estimations of land degradation, thus inflating the perceived extent of the crisis. State B, on the other hand, is often mapped as non-degraded as the degradation has already taken place before monitoring efforts have been made. Long-term ground-based field data on land condition is patchy and generally only goes back as far as the 1970s, when desertification and land degradation started to become a genuine concern (Thomas, 1997). Satellite data provide an alternative to field data, but has also have a relatively limited time scale, only being available from about 1980 through the Landsat programme. States E and F are arguably the only truly degraded states as it is not possible for their condition to naturally improve or recover in an acceptable time scale, even once the processes that have resulted in their degradation have been removed. In order to recover, land in this state needs external intervention in the form of

restoration or rehabilitation efforts. State D is probably the state most focussed on, as land in this state has the greatest potential for recovery. If stressors on this land are removed, the land is likely to return to a non-degraded state without any further, potentially costly intervention (Milton *et al.* 1994; Prince *et al.*, 2018). If the stressors are not removed, however, the potential exists for the land to further degrade into states E and F. The identification of the state of a piece of land almost always requires a comparison to a reference condition, or baseline. The identification of an appropriate baseline is key to land degradation assessments but has proven to be profoundly difficult to achieve in practice. In chapter six of this thesis I expand on the types of baselines that have been used in land degradation mapping, and outline the potential problems associated with these baselines.

Table 2.1. The characterisation of six degradation states as described by, and adapted from, Prince et al. (2018) p. 230.

Degradation state	Comment
(A) Appearance of degradation	Land with low resource availability. In its natural state, often appears superficially similar to degraded land.
(B) Degraded in the past	Assumed to be in a natural state, but actually degraded. Lack of baseline prevents correct interpretation.
(C) Susceptible to degradation	Susceptible land owing to its natural properties and its environment, but not actually degraded.
(D) Land recovers when stressors removed	Land apparently degraded, but within its range of resilience. When stressors are removed, the land returns to its initial, non-degraded condition.
(E) Temporal trend of increase in degradation	The degradation persists when stressors are removed – and there is a temporal trend of increasing degradation.
(F) Stable, degraded state	Degraded land in static condition that changes little when stressors are removed, but never recovers to a non-degraded condition.

Due partly to the lack of confidence in global assessments, as well as to the specific context of many land degradation processes, considerable effort has been made to assess land degradation at local and regional scales (eg. Frederiksen 1993; Mambo & Archer 2007; Stringer & Reed 2007; Thompson et al. 2009; Vogt et al. 2011; Pandey et al. 2013; Ibrahim et al. 2015; Vågen et al. 2016; Hoffman & Ashwell 2001; Hoffman et al. 2018). These assessments are used to guide regional and local land degradation policy. Finer scale assessments rely on similar data inputs and methodologies as

global assessments but differ in that the scale of observation better matches the scale of application. These more localised assessments are also able to take into account the specific processes that are likely to cause land degradation at the local and regional scale, and the observable and measurable patterns that are likely to result from these processes. The literature on local and regional land degradation assessments that have been undertaken around the world is vast. As a result, only the assessments of land degradation that have been undertaken in southern Africa are detailed below.

2.3.1 Mapping land degradation in South Africa

In section 1.2.5 of this thesis an account of the history of the land degradation debate in South Africa is provided, and the importance of Acocks' 'expanding Karoo' theory, which was dominant during the first half of the twentieth century, is highlighted. The maps produced by Acocks were first investigated by Hoffman & Cowling in 1990 and again towards the end of the century by the National Review of Land Degradation (NRLD) in South Africa (Hoffman et al. 1999). In the latter investigation, which was based primarily on expert opinion, the former homelands (communal areas) emerged as the locations in the country where land degradation was considered most severe. The idea proposed in this report, and also by Hoffman & Ashwell (2001) and others (Anderson and Hoffman, 2011; Hoffman and Todd, 2000; Meadows and Hoffman, 2002; Todd and Hoffman, 1999), was that increased human and animal populations in communal areas resulted in overgrazing and the loss of plant cover and biomass which, in turn, led to increased levels of soil erosion and soil degradation.

Subsequent to the NRLD, several different attempts have been made to map land degradation at different spatial scales in the country. In keeping with global land degradation mapping trends, the majority of these efforts have been based on changes in remotely sensed vegetation indices. The most popular of these indices is the normalised difference vegetation index (NDVI), which is considered a good proxy of primary productivity, and has been utilised for a variety of different ecological applications including land degradation (e.g. Bai et al., 2008b; Del Barrio et al., 2016; Fensholt et al., 2012; Symeonakis and Drake, 2004; Tong et al., 2017). NDVI measures the difference between an image's red and near-infrared wavelengths, taking advantage of the fact that live, green vegetation strongly absorbs radiation in

the visible red wavelength while strongly reflecting radiation in the near-infrared wavelengths (Rouse et al., 1973; Wessels et al., 2007b). NDVI values range between -1 and 1, where negative values generally indicate water, values closer to zero indicate no, to very little, green (live) vegetation, and larger positive values approaching one indicate increasing density or biomass of live green vegetation (Pettorelli et al., 2005).

In a comparison between known degraded and non-degraded areas in the northeast of the country, Wessels et al. (2004) found that seasonally summed Advanced Very High Resolution Radiometer (AVHRR) NDVI values were significantly lower for degraded areas in savanna landscapes with similar soil and climatic conditions. Wessels and his co-authors have also investigated the potential of using methods such as rain-use efficiency (RUE) and residual trend analysis (RESTREND) to determine the extent of land degradation, predominantly in the north and northeast of the country in the summer rainfall zone (Wessels et al., 2007a, 2006, 2004). Thompson et al. (2009) developed habitat-specific degradation models to map grazing-related degradation in the Little Karoo region of South Africa's Cape Floristic Region. Their method created a model for how specific habitats are likely to respond to degradation, and then linked these models to time series NDVI data. Degraded areas may, for example, have higher NDVI values than adjacent non-degraded areas after a rainfall event as a result of the proliferation of annual (disturbance-tolerant) plant species. Incorporating expert knowledge of specific habitats was found to improve the accuracy of mapping assessments over methods that simply used the sum of NDVI over an area (Thompson et al. 2009).

In areas with sparse vegetation cover, the reflectance of bare soils dominates the radiation signal making the interpretation of NDVI in terms of vegetation cover difficult and far less accurate (Chabrillat, 2006). As a result, a number of soil-adjusted vegetation indices have been developed for arid areas to reduce the influence of soil background noise on the vegetation signal (Chabrillat, 2006; Washington-Allen et al., 2004). These include, amongst others, the soil adjusted vegetation index (SAVI), developed by Huete (1988), the modified soil adjusted vegetation index (MSAVI) (Qi et al. 1994), and the optimised soil adjusted vegetation index (OSAVI) (Rondeaux et al., 1996).

2.3.2 Limitations of using single vegetation indices

Vegetation indices calculated from satellite data have been used to successfully study vegetation productivity and phenology since the early 1970s, but have been found to be somewhat limited when vegetation cover is naturally low (McGwire et al., 2000). On their own, none of the satellite-derived vegetation indices have been able to resolve the challenge of separating areas that have been degraded by human impact from those areas of naturally low vegetation productivity, or sparse vegetation cover (Okin and Roberts, 2002). A number of studies have however demonstrated the utility of these indices under certain environmental conditions, and particularly for broad analyses of changes in vegetation productivity (e.g. Boschetti et al., 2007; Fensholt et al., 2012, 2013, 2015; González-Dugo and Mateos, 2008; Liaqat et al., 2017; Qi et al., 1994; G. Rondeaux et al., 1996; Symeonakis et al., 2016; Wu et al., 2007; Yengoh et al., 2014). Similarly, several studies have shown that the indices are less useful in other locations, and specifically where vegetation cover is low (e.g. Lawrence & Ripple 1998; Elmore & Mustard 2000; McGwire et al. 2000; Ren et al. 2011; Kong et al. 2015; Ren et al. 2018). The most popular indices, or techniques developed to manipulate satellite data for vegetation mapping and monitoring, have exploited the infrared and red wavelength bands. Variations of the NDVI calculation include other bands such as the blue band but very seldom do indices incorporate the entire spectral signal of the satellite data. More recent techniques, however, have begun to take advantage of more of the available bands in multi- and hyper-spectral imagery, using techniques such as linear mixture modelling and spectral mixture analysis, which are discussed in chapter 5.

2.3.3 Limitations of hard boundaries for mapping desertification classes

Mapping desertification using hard classification techniques requires the *a priori* development of known land cover classes. This enables the grouping and mapping of landscape units into one of the predefined classes. For hard classification, however, membership can only be defined with a membership value of 0 (does not belong to the class) or 1 (belongs to the class). This technique presupposes that hard, well-defined boundaries exist in the landscape, and units cannot belong to more than one

class at any given time. Popular classes that have been used to map land degradation, for example, are natural, near-natural, moderately modified, severely modified, and irreversibly modified (Driver et al., 2011). Classifying land units into these classes quickly becomes problematic because of the inherent subjectivity that is involved in the process. Separating landscapes into natural and near natural classes is on its own filled with potential pitfalls, let alone defining the level of modification. The problem lies not as much with units that clearly fit into a specific class, but rather with those that are closer to the boundary of a class than the middle of any given class. Two pieces of land may, for example, be very similar in all respects except one has vegetation cover of 50% and the other has cover of 49%. If the boundary between classes is set at 50% then these two landscapes will be given different classifications, say moderately modified for the land with 49% cover and near-natural for the land with 50% cover. This could ultimately result in two different management strategies being applied to the two landscapes where the same strategy may have been more appropriate.

2.4 Towards a new approach - Archetypes

Despite the widespread application of landscape mapping projects, which range from efforts to map global patterns and processes, to the production of very specific local maps, no standard approach exists for the delineation of different landscape units (Cullum et al., 2016a). Different categorisations are based on the scale of observation, both spatially and temporally, as well as the widely accepted norms within specific institutions and scientific disciplines. The use of archetypes has, therefore, been proposed as a method to standardise the mapping procedure across diverse applications (Cullum, 2014). Archetypes are abstract constructs which represent a typical example or appropriate model for any given class or landscape unit (Cullum et al., 2016a). The notion of the archetype has been adapted by Cullum et al. (2016) from the discipline of cognitive psychology, and specifically from work by Eleanor Rosch on prototypes (1975, 1978). Rosch developed prototype theory to explain how humans associate typical examples, or prototypes, with specific categories or classes, and how there is a gradient within a class from examples most associated with the class to those least associated with the class (Rosch, 1975). Prototypes are described in

cognitive classification as exemplars of an idealised class member and the degree of class membership is determined by the degree of similarity to one or more class exemplar (Cullum et al., 2016a). Prototype theory suggests that natural categories exist that we are able to learn more rapidly and, therefore, choose more often (Rosch, 1973). Archetypes differ from the prototypes described by Rosch in that they are not derived from unconscious thought and learning but can be constructed, refined and adapted for local applications (Cullum et al., 2016a). Archetypes draw heavily on the fuzzy logic and fuzzy classification approaches discussed earlier in this chapter. These approaches which can be quantitative and statistically testable if necessary have been developed to address the inherent vagueness and imprecision of the natural world.

2.4.1 Using archetypes to map degradation

This study proposes to extend the application of archetypes in landscape mapping (Cullum et al. 2016) to the assessment of land degradation in the arid Namaqualand region of the Succulent Karoo Biome in South Africa's Northern Cape Province. A method to assess land degradation in Namaqualand is developed that can be adapted to other dryland environments, and particularly to the globally-renowned Succulent Karoo. The use of archetypes in landscape mapping initially requires agreement on the conceptualisation of the landscape. This involves identifying the key aspects and processes in the landscape, as well as the different scales at which they exist (Cullum *et al.* 2016). The two approaches to the construction of a landscape archetype are the process-based approach and the phenomenological approach. The process-based approach would describe a conceptual model for a class that links hypothesised processes and drivers with the observed features and patterns that they may generate. The model may be based on a well-established conceptual framework for the landscape, or can be constructed from a combination of local knowledge and scientific theory (Cullum et al., 2016a). The phenomenological approach, on the other hand, describes a real example that is carefully selected to be the best representative of a pre-determined class. This archetype will display all the features and properties most commonly associated with the class (Cullum et al., 2016a). In practice, the approaches overlap, as a conceptual model may point to a particular landscape which proves to be, through statistical analysis, the best example of a particular class (Cullum et al.,

2016a). This is likely to be the case when assigning archetypes in the assessment of habitat condition in Namaqualand.

2.5 Research questions and objectives

This study has two main emphases. The first was to produce a map of desertification for the Namaqualand Hardeveld Bioregion that can be used immediately and directly by conservation practitioners working in the region. This map illustrates the habitat condition of the project area in relation to known drivers of desertification and is presented in the form of a habitat condition archetype. The need to develop this map is the objective for which this research has been funded. The second emphasis of this thesis was to present the methodology to be used as a technique to understand and map land degradation regionally. This methodology will help countries in delivering on LDN targets, while contextualising the inherent uncertainty and complexity in the mapping procedure (Figure 2.1). By combining field sampling data with Landsat and Sentinel satellite data, as well as data on the potential drivers of desertification, this thesis will address the following research objective and underlying research questions:

2.5.1 Overall research objective

Investigate a more appropriate method to map land degradation at a regional scale in dryland environments.

Question 1 (Chapter 4)

What are the most appropriate field measures of habitat condition for the Namaqualand Hardeveld Bioregion that can be measured rapidly in the field?

Objectives

- Develop a conceptual diagram of the potential drivers of land degradation in Namaqualand;
- Identify the measures of land degradation that can be collected in the field, and collect field data related to habitat condition from a representative sample of plots across the extent of the project area;

- Determine whether the data collected from the field cluster into groups that can be associated with different levels of habitat condition.

Question 2 (Chapter 5)

What is the most appropriate method to measure habitat condition using available Earth observation data?

Objectives

- Derive remote sensing variables based on Earth observation data for the location of each field plot through Google Earth Engine;
- Develop a multivariate model to determine the remote sensing variables that correspond best with the condition of the veld, as determined from the field data.

Question 3 (Chapter 6)

Develop an approach to map habitat condition for the project area that can be repeated for similar dryland environments.

Objectives

- Develop multivariate models to measure the relative influence of potential drivers of desertification on the habitat condition of the project area determined through question 2 (chapter 5);
- Develop an archetype for habitat condition, based on the results from chapter 5 and the influence of the drivers determined here, against which the rest of the project area can be compared;
- Create a GIS spatial layer incorporating the archetype information and display the condition of the Hardeveld bioregion according to this archetype.

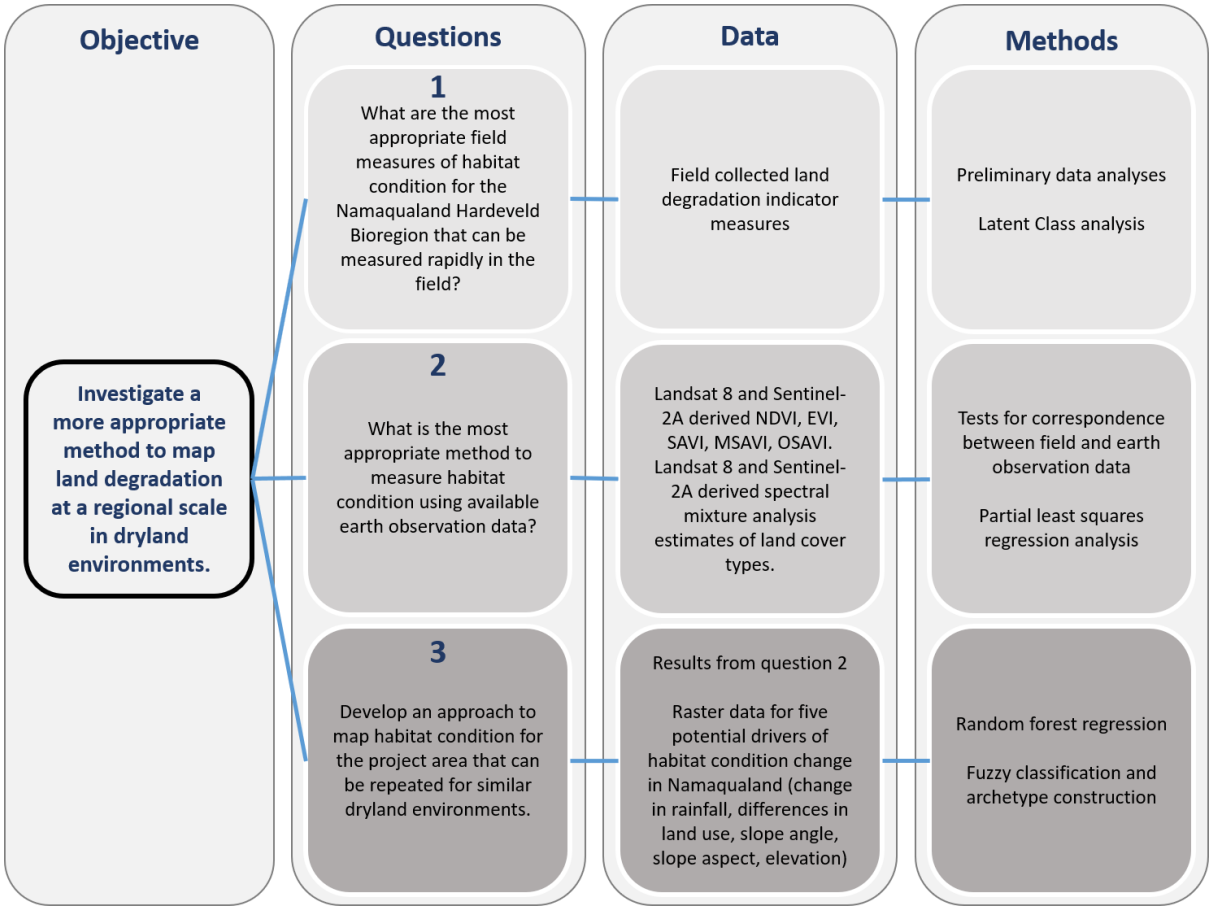

Figure 2.1. Flow chart of the key research questions posed, and the data and methods used, to address the overall objective of this thesis.

2.6 Conceptual framework of the drivers of land degradation in Namaqualand

Any attempt to map the extent of land degradation over a given geographical area needs to be underpinned by a sound conceptual framework. This needs to be developed through the incorporation of known ecological principles, expert knowledge, and assumptions about the processes driving land degradation in the landscape as well as the patterns that are likely to manifest as a result. Inherent in the desertification debate over of the last three to four decades is the idea that both climate and humans are potential drivers of land degradation and that it is important to be able to separate the impact of each in order to determine what can be done to mitigate or reverse their effects (del Barrio et al., 2016; Evans and Geerken, 2004; Ibrahim et al., 2015; Wessels et al., 2007b).

As with most natural regions around the world, a combination of biotic and abiotic factors, that incorporate both equilibrium and non-equilibrium dynamics at a range of spatial and temporal scales (Briske et al. 2003), likely drive changes in habitat condition in Namaqualand (Figure 2.2). The potential impact of any given driver depends on many factors, including the long-term history of the timing and severity of the driver's impact, and the adaptability of the ecosystem and the species that live in it. The relationships between potential drivers, between drivers and the ecosystem, and between individual ecosystem components also play an important role in the overall impact on the landscape or ecosystem (e.g. Kiage, 2013). Although several factors may be universally important, the level of impact is often dependent on the specific region in question. It is therefore important to develop a sound conceptual framework for land degradation in the region of interest.

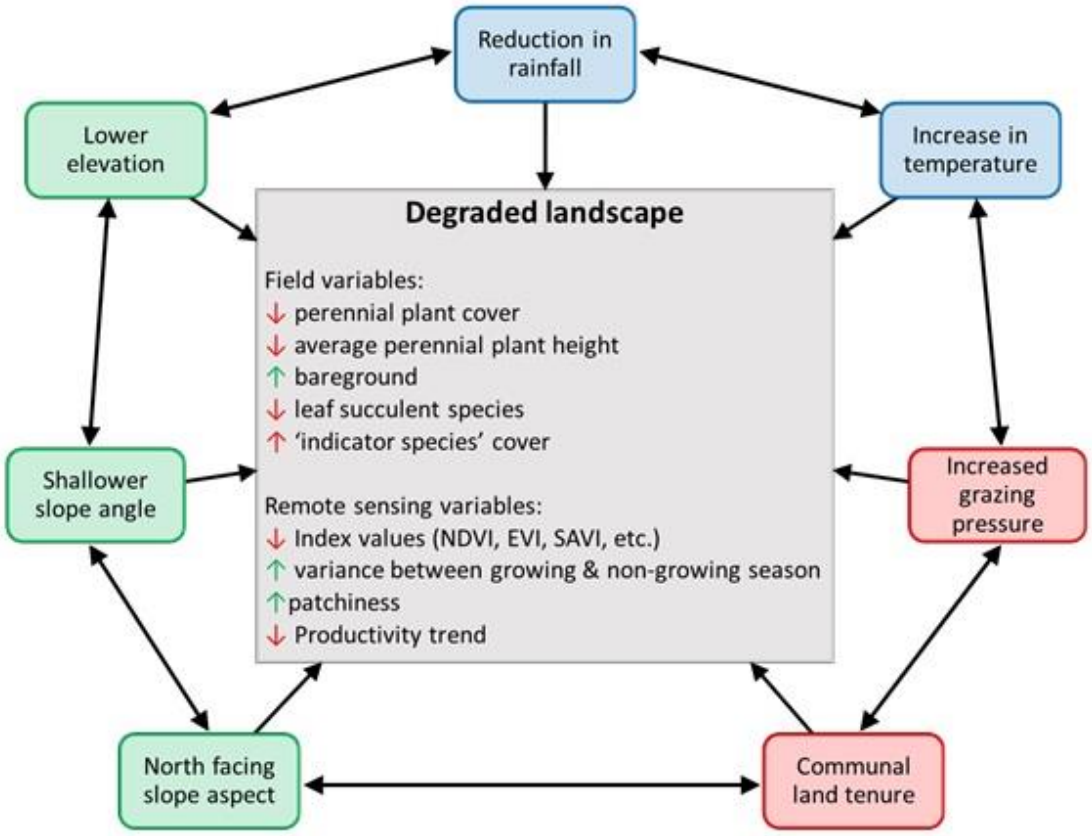

Figure 2.2. Conceptual model for land degradation in Namaqualand. Blue, green and red shaded boxes represent the climatic, topographic and land use related potential land degradation drivers respectively. The central box represents the field and remote sensing measures that are hypothesised to be associated with a degraded landscape in Namaqualand.

Climate change over time frames of years to millennia is likely to have influenced the vegetation of Namaqualand (Chase and Meadows, 2007). Being a hot and dry region, changes in temperature and rainfall are likely to have a major impact on certain species that may already be at the limits of their distribution. For example, Namaqualand has experienced an increase in minimum temperatures of 1.4 °C, and an increase in maximum temperatures of 1.1 °C, over the last century (Davis et al., 2016). This is likely to first affect those species that are adapted to slightly cooler temperatures, species that are adapted to more sheltered niches, or those species that occur at higher altitudes. Although recent and historical rainfall patterns exhibit no clear statistical trends, predictions for the region are for a general reduction in total rainfall (Davis et al., 2016). Although plant species in Namaqualand are adapted to small and sporadic rainfall events, a reduction in rainfall is likely to impact species that require fairly consistent moisture input, as well as those species that require rainfall as a primary mode of seed dispersal (Davis et al., 2017; Parolin, 2001; van Rheede van Oudtshoorn and van Rooyen, 1999).

The predominant land use in Namaqualand is small stock farming (Desmet, 2007). Sheep and goats have been farmed in Namaqualand for over 2000 years, but with very different levels of intensity in different locations. As discussed in chapter one, in general, communal areas in South Africa are perceived as having far greater levels of land degradation than comparable privately owned areas as a result of higher human and animal populations per unit area (e.g. Todd and Hoffman, 1999). It is therefore expected that differences in land tenure in the project area will result in differences in both plant cover and biodiversity attributes. Previously cultivated land, as well as land associated with current or past mining activity, is also likely to be more strongly associated with most measures of land degradation in the project area. This is primarily a result of the loss of topsoil, and the resulting depletion of the soil bank, that is associated with these two extractive land uses. Abandoned mining areas, where limited active restoration efforts have taken place, have been found not to recover their natural indigenous perennial vegetation cover irrespective of the amount of time since mining has been abandoned (Carrick and Krüger, 2007; le Roux and Odendaal, 1992; Schmidt, 2002). The rate of recovery of previously cultivated land varies depending on the history and extent of cultivation, and the restoration efforts that have taken place since the abandonment of cultivation. In general, the longer old crop land has been

left to rest the more likely it will be to recover its natural vegetation, though the rate of recovery likely depends on the existence and diversity of the underlying seed bank (Allsopp, 1999; Botha et al., 2008; Schmiedel et al., 2010).

Differences in certain topographic features, such as slope aspect, slope steepness and elevation, are also likely to be associated with differences in habitat condition across the project area. North-facing slopes in the southern hemisphere are, for example, considerably warmer than south-facing slopes, increasing the risk that temperatures may exceed the thresholds of certain plant species (Suggitt et al., 2011). The gradient of the slope is also likely to impact the potential level of degradation in Namaqualand. Although sparsely vegetated steep slopes are likely to be more prone to erosion in certain regions, erosion is not a major environmental concern in Namaqualand due largely to limited rainfall. Rather, steep slopes are less likely to be accessed by grazing livestock and are therefore expected to be less degraded than shallower slopes (Anderson and Hoffman, 2007).

Topographic features, in fact, are likely to impact habitat condition largely through their interaction with the two other drivers of desertification, changing climate and differences in land use. For example, warmer north-facing slopes are generally more attractive for herders and their livestock in the cooler winter months. As a result, north-facing slopes in Namaqualand are likely to be grazed more heavily than south-facing slopes. Although upland areas are generally grazed less than lowland areas in Namaqualand, they have been found to be used as grazing reserves during and immediately after periods of drought, particularly in the region's communal areas (Samuels, 2006; Samuels et al., 2007). The prevalence of stock posts or kraals in Namaqualand has also been found to be associated with lowland areas, thus potentially increasing the impact on the vegetation in these areas (Samuels, 2013). Shallower slopes in Namaqualand have also predictably been more extensively cultivated than steeper slopes, and thus the impact of previous land use practices on habitat condition may be exacerbated by the general topography of the area. The potential drivers of desertification in Namaqualand are likely to interact across the region resulting in differing levels of habitat condition change in different area.

In general, the potential drivers can be grouped into three main categories. The first are climatic factors such as an increase in temperature and a reduction in rainfall. The

second are land use factors such as increased grazing intensity and a communal land tenure regime, while the third group are topographic features relating to a gentler slope angle, north-facing slope aspect, and a lower relative elevation. These drivers are likely to result in a more degraded landscape through a reduction in perennial plant cover and plant height, an increase in the cover of bare ground, a reduction in leaf succulent species diversity and cover, and an increase in land degradation indicator species (Figure 2.2). These variables can be easily measured in the field, but they need to be related to remote sensing variables in order to map desertification over the entire extent of the project area. The conceptual model therefore includes hypothesised changes in remote sensing variables that are predicted to be related to changes in the field variables.

2.7 Thesis outline

This thesis is divided into 7 chapters. **Chapter 1** provides historical background to the desertification/land degradation debate before describing the theoretical context within the ecological literature. Thereafter the emphasis is on the South African context of land degradation, with a specific focus on Namaqualand. The main methods used thus far to map land degradation, both globally and at regional to local scales, are described in **chapter 2**, and their limitations highlighted. The potential of using archetypes, after Cullum (2014) and Cullum et al. (2016a and 2016b), to map land degradation is then introduced as a novel method to address the complexity of the exercise. **Chapter 3** describes the procedure followed to determine the project area and plot locations, before describing the general biophysical characteristics of the region. This includes a description of the region's climate, topography, vegetation and land use. **Chapter 4** focusses on the development of a habitat condition model for the project area based on field data which are related to habitat condition (Figure 2.3). In **chapter 5**, remote sensing data, collected through Google Earth Engine (Gorelick et al., 2017), is analysed with respect to the field data from chapter four to determine what remote sensing measures correspond best with field-based assessments of habitat condition. In **chapter 6** the remotely-derived habitat condition measures are then evaluated with respect to potential drivers of habitat condition change. The change in the remote sensing measure over the past three to four decades is also evaluated to determine

areas that have potentially become degraded over this time period. Chapter 6 also includes the development of the land degradation archetype for the project area in order to map the differences in vegetation condition. **Chapter 7** then provides a general discussion for the thesis and places the methodology used and maps produced within the conceptual framework of land degradation in South Africa and globally. Limitations to both the methodology and the resulting outputs are also discussed before the thesis is brought to a conclusion.

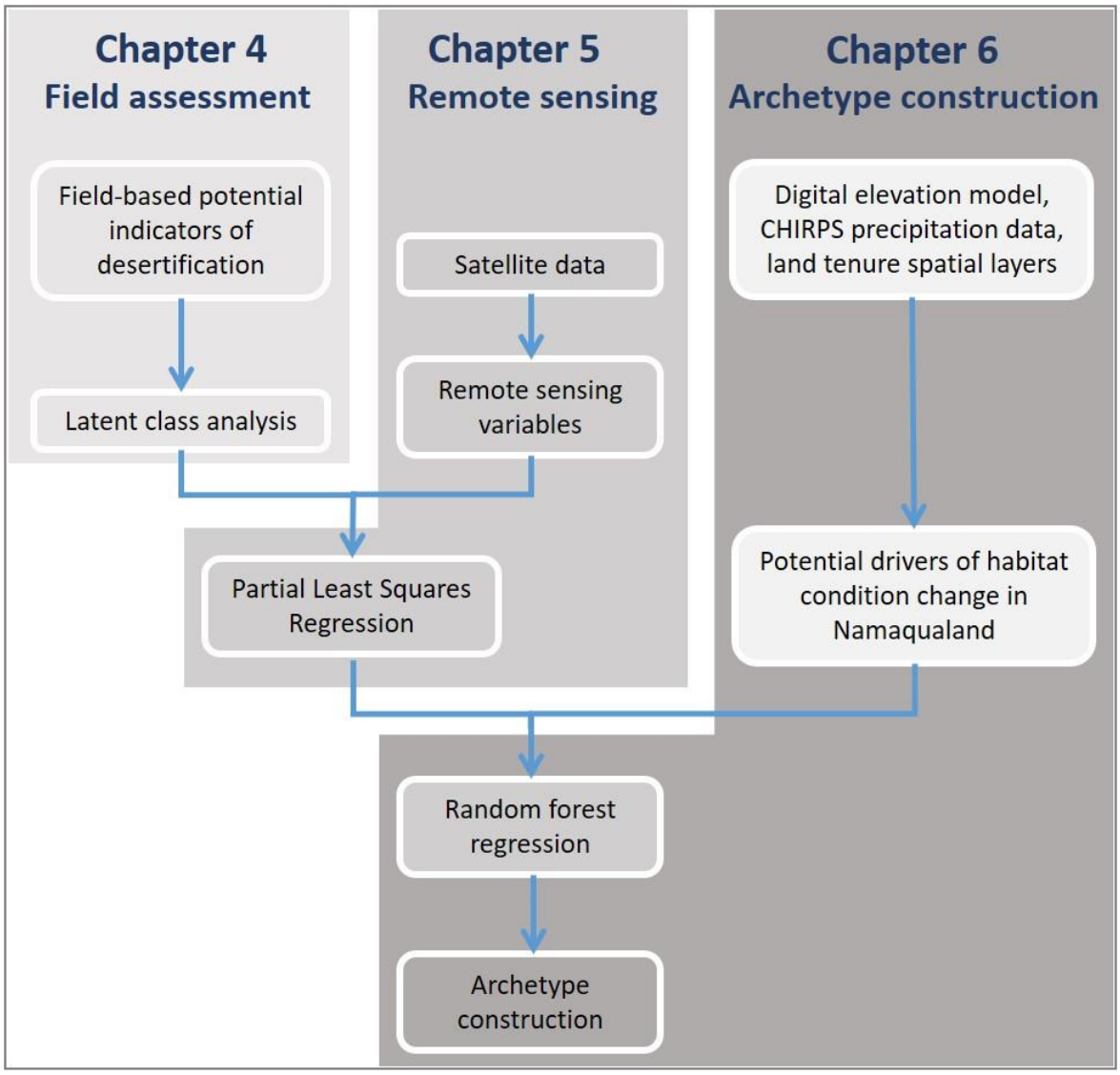

Figure 2.3. Flow diagram illustrating the broad methodology of the thesis used in chapters four to six to ultimately map land degradation across the project area.

Chapter 3:

3. Biophysical description of the study area

Namaqualand is a distinct bio-geographical region that makes up the north western section of the Succulent Karoo biome in South Africa, an area of approximately 50 000 km2 (Cowling et al., 1999c) (Figure 3.1). It occurs between the Orange and Olifants Rivers in the north and south respectively, and between the Atlantic Ocean to the west and the Bushmanland plains to the east (Desmet, 2007). An early overview of the physical and biological environment of Namaqualand is provided in volume 142 of the journal *Plant Ecology* (Cowling et al., 1999a), while a special issue in the Journal of Arid Environments, on *Sustainable Land Use in Namaqualand* (Hoffman et al., 2007a) provides further context and detail. This study focusses on the Namaqualand Hardeveld bioregion (Mucina and Rutherford 2006), which covers nearly 50% of the total land area of Namaqualand. A brief description of the topography, geology and soils, climate, land use and vegetation of this bioregion is outlined below.

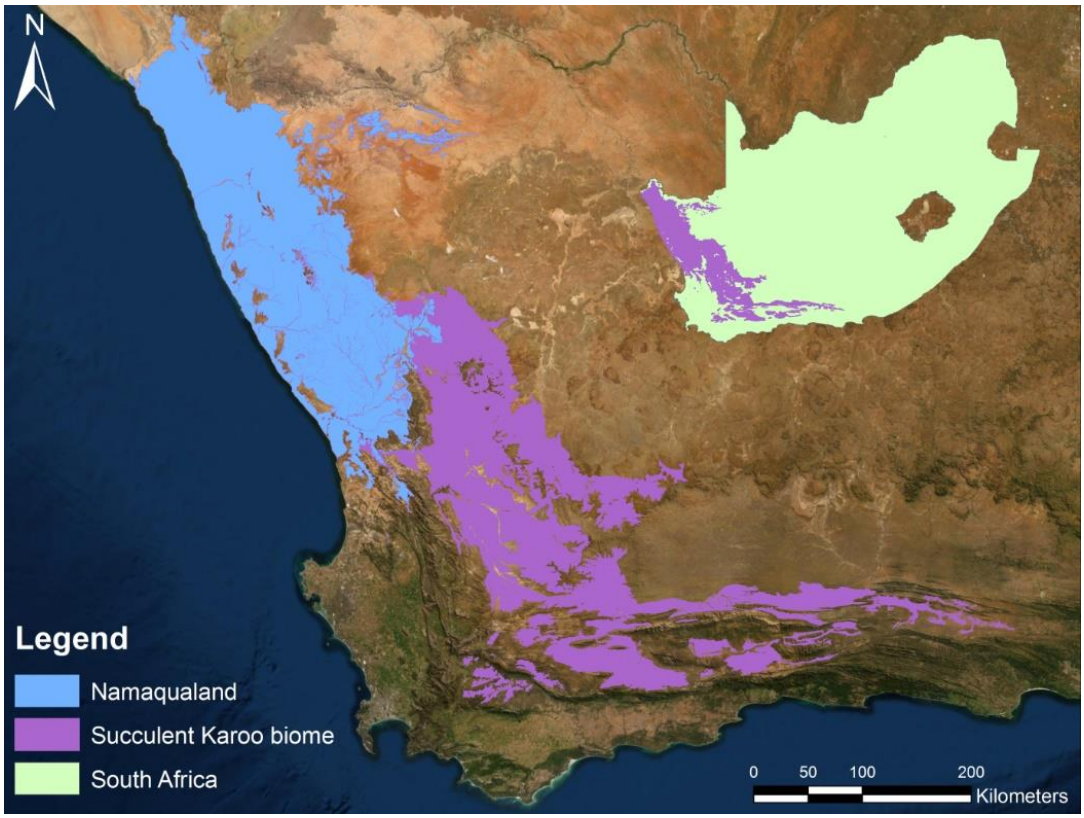

Figure 3.1. The location of Namaqualand and the Succulent Karoo biome. Inset depicts the location of the Succulent Karoo relative to South Africa as a whole. Details of the location of the Namaqualand Hardeveld bioregion can be found in Figure 3.2.

3.1 Topography, geology and soils

Dean and Milton's 1999 book on the ecological patterns and processes of the Karoo provides a detailed synthesis of Karoo ecosystems as a whole. A thorough description of the topography, geology and soils of the Karoo, including Namaqualand, can be found in this volume (Meadows & Watkeys 1999; Watkeys 1999). More recently, Francis et al. (2007), have described the main characteristics of different soils in Namaqualand, while Mucina et al. (2006) detail the topography, geology and soils of each vegetation type in the bioregion (Francis et al., 2007; Mucina et al., 2006a). Central Namaqualand is dominated by large intrusions of chiefly granitic igneous rocks that form the Kamiesberg Mountains. These comprise the highest peaks in Namaqualand, reaching between 1 400 and 1 700 metres above sea level. North of the Kamiesberg is the Richtersveld, characterised by a diversity of pre-Gondwanan rocks intruded by granite and gneiss as well as exposed sedimentary rocks (Meadows & Watkeys 1999). To the east of the Kamiesberg lie the Bushmanland plains which form the boundary of Namaqualand and the start of the high interior plateau of the country. The west and southwest of the Kamiesberg is characterised by the low gneiss foothills of the Hardeveld which give way to the gently undulating coastal plains (Cowling et al., 1999b; Desmet, 2007). Underlying much of the Hardeveld and coastal plains are hardpans consisting of either siliceous (dorbank) or calcareous (calcrete) material (Cowling et al. 1999). The Knersvlakte, a broad flat landscape characterised by expanses of quartz gravel beds, extends southeast of the Kamiesberg (Desmet, 2007).

Namaqualand soils are complex and diverse but can be broadly categorised into three main groups (Desmet, 2007). The first are those soils which form much of the coastal plain, as well as Bushmanland, and generally have very low clay contents of less than 3%. The second and most common soils are red and yellow sandy to loamy soils with 6 – 15% clay content. These soils are derived from the weathering of the surrounding granitic parent material. The last group of soils are found in the Hardeveld bioregion and represent the soils of the study area. These soils are generally red, base-rich colluvial soils which also derive from the surrounding granite (Francis et al., 2007). Hardeveld soils are also commonly associated with heuweltjies. These are circular mounds up to 50 metres in diameter which, because of their association with termite nests (Esler and Cowling, 1995; McAuliffe et al., 2019), have soils with significantly

higher nutrient status than the surrounding matrix (Desmet, 2007; Midgley and Musil, 1990; Moore and Picker, 1991). Soils in Namaqualand are generally free from waterlogging and have neutral to high pH levels (Davis, 2013; Desmet, 2007; Watkeys, 1999).

3.2 Climate

Namaqualand is a semi-arid winter rainfall region, where over 60% of the rain falls between the months of May and September with the wettest months occurring between June and August (Cowling et al. 1999; Desmet and Cowling, 1999). The climate of Namaqualand, and indeed much of southern Africa, is determined primarily by two pressure systems. These are the southern subtropical high-pressure belt which sits over the sub-continent, and the circumpolar westerly airstream to the south (Desmet and Cowling, 1999; Schulze, 1965). Local scale climate and weather patterns are also influenced by the cold Benguela current of the Atlantic Ocean to the west, the centrally located Kamiesberg mountains, as well as the mountains of the escarpment to the east (Davis, 2013).

Although much of Namaqualand receives less than 150 mm per annum, this ranges from about 50 mm in the northwest to nearly 500 mm in the Kamiesberg mountains, and generally increases from north to south (Cowling et al., 1999b; Desmet, 2007; Desmet and Cowling, 1999). Mean annual precipitation (MAP) is between 100 mm for the Platbakkies Succulent Shrubland (a third of which falls in summer) and the Namaqualand Heuweltjieveld, and about 145-160 mm for the other vegetation types in the study area (Mucina et al., 2006a). Despite generally low rainfall amounts across Namaqualand, the climate of the region is characterised by relatively predictable rainfall when compared to other arid regions with similar mean annual precipitation (Desmet, 2007). As a result, severe, prolonged droughts are relatively infrequent (Desmet and Cowling, 1999). The generally low winter rainfall is ameliorated by the presence of fog and dew throughout the year, and particularly in the otherwise dry summer months. Namaqualand receives dewfall and coastal fog on about 75 days of fog in the year, with the amount of fog exceeding rainfall amounts in some areas (Davis et al., 2016; Desmet and Cowling, 1999; Schmiedel et al., 2012). Fog plays a significant role in reducing water stress for desert adapted plants allowing for greater

survival of individual plants as well as year-round recruitment (Desmet and Cowling, 1999; Schmiedel et al., 2012).

Temperatures across Namaqualand are generally mild throughout the year. Mean annual temperatures (MAT) for the study area range between 16-18°C while mean maximum summer temperatures are usually less than 30°C. South-westerly sea breezes blowing off the cold Atlantic Ocean moderate summer temperatures (Desmet, 1996) although maximum daily temperatures of up to 40°C are sometimes recorded in the winter months. These temperature peaks occur as a result of warm subsiding air that sweeps down the escarpment from the interior plateau of the country as katabatic or 'berg' (lit. mountain) winds (Cowling et al., 1999b). Platbakkies Succulent Shrubland has the greatest range between mean monthly maximum and minimum temperatures, which are 37°C and -3°C respectively. This vegetation type experiences between 20 and 40 frost days a year while the rest of the study area experiences eight to 13 days of frost. Namaqualand Heuweltjieveld is the only vegetation type in the study area that experiences virtually no frost days, with temperatures that rarely go below 5°C (Mucina et al., 2006a).

Observed changes in the Namaqualand climate reveal several general patterns that are described in MacKellar et al. (2007), Haensler et al. (2010) and Davis et al. (2016). There has been a general increase in temperatures across the region, as well as an increase in the frequency of hot extremes over the last century, with minimum and maximum temperatures having increased by 1.4 and 1.1°C respectively (Davis et al., 2016). These changes are in line with observed increases in regional temperatures across the globe (Davis et al., 2016). Rainfall patterns analysed by MacKellar et al. (2007) between 1950 and 1999 reveal spatial partitioning with generally increased precipitation in the central coastal belt and northeast section of Namaqualand, and a general drying of the escarpment (MacKellar et al., 2007). Davis et al. (2016) found that although rainfall between 1901 and 2009 decreased over the eastern parts of Namaqualand during winter, and over the central and southern parts during spring, these patterns were not statistically significant. The trends in increasing temperature observed for Namaqualand are expected to persist into the future. Rainfall, on the other hand, is expected to decrease overall, despite an increase in late summer convective precipitation in the northeast (Davis et al., 2016; MacKellar et al., 2007). More frequent and severe drought periods, such as the drought experienced by the

region as a whole between 2015 and 2018, are likely to exacerbate the impact of a generally worsening climate on people and the environment (Davis-Reddy, 2018).

3.3 Land use

Hoffman and Rohde (2007) provide an overview of how changes in land-use practices have impacted on the Namaqualand environment. The region's complex socio-economic and political context (Botha et al. 2008, Kelso and Vogel, 2015) as well as the implementation of land reform policies have had a significant effect on the natural resources of the region (Benjaminsen et al., 2006; Lebert and Rohde, 2007; May and Lahiff, 2007).

Hoffman and Rohde (2007) describe the environmental history of Namaqualand through a series of three distinct 'ecological revolutions', which is a term first conceived by Merchant (1987) and defined as "major transformations in human relations with non-human nature" (Merchant 1987, p.265; Hoffman & Rohde 2007). The first ecological revolution is referred to as the pastoral ecological revolution, which took place as a result of the introduction of livestock to Namaqualand approximately 2000 years ago (Hoffman and Rohde, 2007; Webley, 2007). Although evidence of the first humans in Namaqualand has been dated to the Early Stone Age, the first people to settle in the region for an extended period did so around 50 000 years ago toward the end of the Middle Stone Age (Dewar, 2006; Dewar and Stewart, 2017). Subsisting by hunting and gathering, and migrating to and from the coast in response to favourable environmental conditions, these early colonists would not have had a significant impact on the environment. Nomadic Khoe-Khoen herders, however, began to rear livestock around 2000 BP, a practice which likely changed the relationship between people and their environment (Webley, 2007). The total human population, and the livestock they kept, during this time probably never exceeded a few thousand individuals. This, along with a nomadic way of life, is likely to have limited the impact these early pastoralists had on the natural environment (Hoffman and Rohde, 2007). There are, however, suggestions that both San hunter-gatherers and Khoe-Khoen herders may have caused soil erosion and local changes to plant communities through the repeated use of preferred campsite and kraal (corral) locations and alterations to the fire regime (Sampson, 1986; Sugden, 1989) (Samson 1986; Sugden 1989).

The second ecological revolution is described as the colonial ecological revolution. This, it is proposed, commenced as early as 1713 with the spread of smallpox from the Cape Colony into Namaqualand, which decimated the human pastoral population (Hoffman and Rohde, 2007). From this time onwards, the local Namaqualand population was forced into smaller and smaller areas of less favourable habitat by continued land appropriation and forced sedendarisation by both colonial and apartheid governments. The Nama, which is the local name given to the group of Khoe-Khoen herders living in Namaqualand at the time of colonial settlement, were increasingly confined to smaller areas within regions such as the Kamiesberg and Richtersveld. White farmers, however, were permitted access to more extensive areas in which to graze their herds. In 1878, white farmers were, for the first time, allowed to purchase land privately, allowing them to fence their land and demarcate fixed boundaries. The creation of service villages by the apartheid government in the first half of the 20th century, the subsidisation of white farmers, and a shift to the commercial exploitation of sheep that required less farm labour all led to an increase in the number of rural households, and increasing pressure on natural resources in communal areas (Hoffman and Rohde, 2007). Mining has also taken place in Namaqualand since the late 17th century when copper ore was 'discovered' near present-day Springbok. Since the 1680s, copper ore and diamonds have been the primary exports from the region. Mining has had a significant impact on the natural environment, both because of the mining activities themselves but also as a result of the construction of transportation infrastructure (Carrick and Krüger, 2007).

The third and contemporary ecological revolution in Namaqualand, as described by Hoffman and Rohde (2007), is the post-agrarian ecological revolution. Various factors, including increased urbanisation, improved transport, the modernisation and development of agricultural technology, an end to agricultural subsidies, as well as increased land reform activities have resulted in an overall reduction in agriculture and mining in Namaqualand since about 1950. This has coincided with a greater emphasis on conservation initiatives in the region, particularly those associated with the promotion of tourism, and the expansion of protected areas such as the Namaqua and Richtersveld National Parks, and the Goegap and Knersvlakte Nature Reserves (Hoffman and Rohde, 2007). The predominant land use in Namaqualand, however, remains the farming of small livestock, especially sheep. As a result, overgrazing,

particularly in communal areas, has been singled out as the biggest threat to biodiversity (Todd and Hoffman, 1999).

3.4 Vegetation

Early attempts to map the vegetation of South Africa were on a relatively coarse scale with only a maximum of 21 vegetation types being described across the country (Adamson, 1938; Pentz, 1945; Pole Evans, 1936). A more comprehensive map was developed by Acocks in the *Veld types of South Africa* (Acocks, 1953). Acocks mapped 70 veld types and 75 variations across eleven broad groups which are similar to today's biomes. A veld type is defined as "a unit of vegetation whose range of variation is small enough to permit the whole of it to have the same farming potentialities" (Acocks, 1953, p.1).

Acocks' veld types underpinned much of the understanding of vegetation distribution in South Africa for half a century. Improved spatial information and mapping technologies, however, led to both the need and the capability of developing an updated vegetation map for the country. This responsibility fell to the South African National Biodiversity Institute (SANBI) who, through a direct parliamentary mandate via the 2004 Biodiversity Act, are required to report on the country's biodiversity, the conservation status of species and ecosystems, and the impacts they face. As a result, SANBI require a detailed vegetation baseline for the country against which trends can be observed and changes reported on (Mucina and Rutherford, 2006).

The VEGMAP project, which was initiated in 1996 was finally published in 2006 as *The Vegetation of South Africa, Lesotho and Swaziland* (Mucina and Rutherford, 2006; SANBI, 2006). SANBI have continued to improve the vegetation map through several VEGMAP projects (VEGMAP 2009; 2012). The most recent update is the Vegetation Map 2018 (VEGMAP 2018) which was released in June 2019 (SANBI, 2019). VEGMAP 2018 describes a total of 459 vegetation types within South Africa. The vegetation types, which are the finest scale unit within the VEGMAP context, are grouped into 41 bioregions. The bioregions are, in turn, grouped within the nine major biomes of South Africa. A vegetation type is defined as "a complex of plant

communities ecologically and historically (both in spatial and temporal terms) occupying habitat complexes at the landscape scale" (Mucina et al. 2006, p.16).

Nearly 6 500 plant species occur in the sixty-four vegetation types of the Succulent Karoo biome, which is one of only two global biodiversity hotspots that occur in a dryland environment (Myers et al., 2000). Covering about half of the area of the Succulent Karoo, the four Succulent Karoo bioregions of Namaqualand contain 47 of the biome's vegetation types (Figure 3.2). This region is home to approximately 3 500 plant species, of which about 25% are endemic (Desmet 2007; SANBI 2018). The vegetation types of Namaqualand have been largely described as shrublands that are dominated by predominantly leaf-succulent of deciduous-leafed woody perennial shrubs or sub-shrubs. Trees are rare to absent across much of the area (Desmet, 2007).

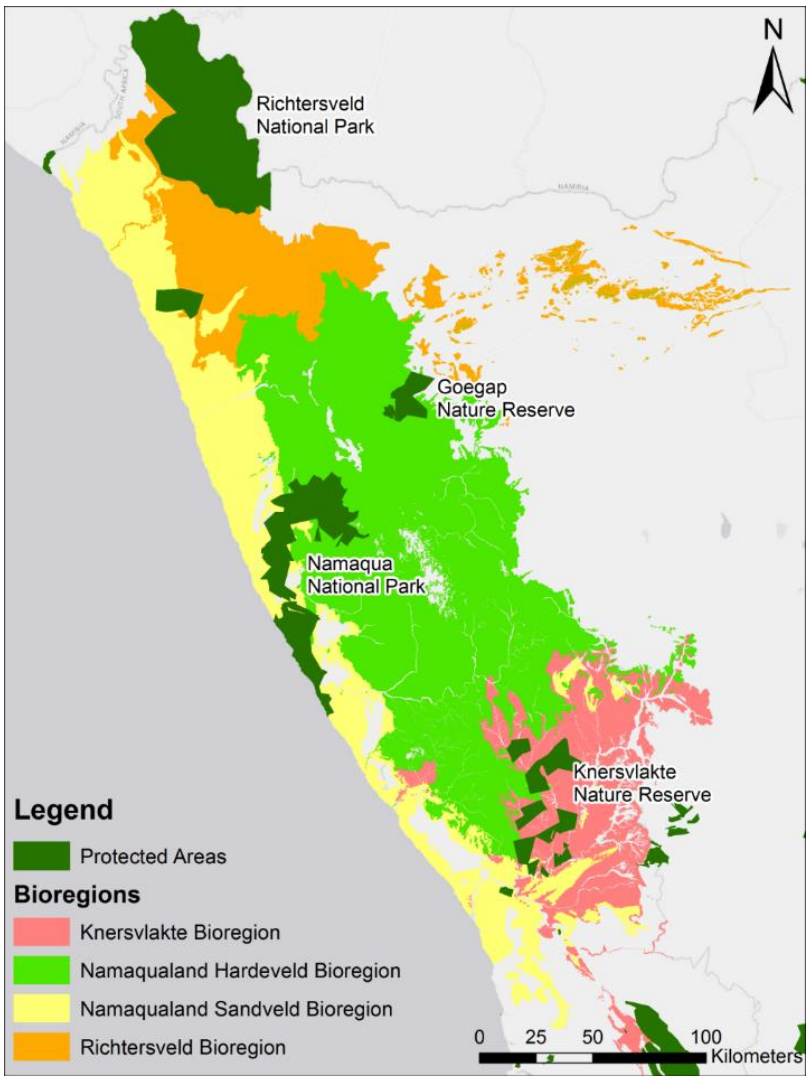

Figure 3.2. The four bioregions that comprise Namaqualand, and the protected areas that occur within the region.

3.4.1 Project area selection

To map the condition of vegetation and extent of degradation across an area, the underlying ecological and anthropogenic processes and drivers need to be broadly consistent, and the measurable response in vegetation characteristics need to be largely similar. As an extreme example, mapping differences in tree cover between a forest and a savanna may help to distinguish the two vegetation units but will not aid in drawing any conclusions about the condition of the two different landscapes. Expectations of broad vegetation patterns, therefore, need to be similar across the project area. It would not be possible to sample all the Namaqualand bioregions due to the number of replicates required, the amount of data that would be collected at each sample site, as well as the relative inaccessibility of many areas within Namaqualand. Therefore, a subset of representative vegetation units has been selected which cover a large proportion of the region, encompass much of the diversity present and are relatively accessible for field monitoring purposes. The relative protection afforded to each potential vegetation unit, through their inclusion in protected areas, was also considered. Units with a significant percentage of land already included in protected areas were not considered for this project as one of the broader aims of the project is to contribute to future conservation through aiding protected area expansion efforts, which will be more useful for vegetation units that are poorly protected by the current protected area network.

Although pockets of the Namaqualand Cape Shrublands Bioregion fall within the geographic extent of the Namaqualand area, this bioregion forms part of the Fynbos biome and is not of interest for this project. The Richtersveld and Knersvlakte bioregions are well represented by the protected area network through the Richtersveld National Park and the recently proclaimed Knersvlakte Nature Reserve (Figure 3.2). The Knersvlakte Nature Reserve emerged as a result of a comprehensive regional biodiversity plan which continues to contribute to the expansion of the protected area. Namaqualand Sandveld units have been subject to extensive mining and many of these areas are so severely degraded as to prove unhelpful in the development of the land degradation assessment method. Of those areas that have not been severely degraded, a significant proportion is already conserved within the Namaqua National Park. The Namaqualand Hardeveld bioregion is a relatively contiguous area which forms nearly half the total area of Namaqualand, and covers

about the same extent as the other three bioregions together. Formal conservation protection of the Hardeveld bioregion is in the form of the Goegap Nature Reserve and a relatively small section of the Namaqualand National Park (Figure 3.2) while the majority of the area is not formally conserved. The Hardeveld bioregion is also bisected by the National N7 highway which runs north-south, and several regional roads that run east-west across the project area. These roads, and the small to large towns that occur along it, make access to the bioregion more possible than some of the other bioregions. As a result, the Namaqualand Hardeveld bioregion is the focus of this project, with the view of developing a method that will be transferrable to similar regions within Namaqualand, the Succulent Karoo biome and globally.

3.4.2 Vegetation types

The Hardeveld Bioregion is comprised of seven vegetation types covering a total area of 18 318 km^2 (Figure 3.3). These vegetation types are the Namaqualand Klipkoppe Shrubland (SKn 1), Namaqualand Shale Shrubland (SKn 2), Namaqualand Blomveld (SKn 3), Namaqualand Heuweltjieveld (Skn 4), Platbakkies Succulent Shrubland (SKn 5), Kamiesberg Mountain Shrubland (SKn 6), and the Southern Namaqualand Quartzite Klipkoppe Shrubland (SKk 10) (SANBI 2018). Of these, the Southern Namaqualand Quartzite Klipkoppe Shrubland is a recent addition following the publication of VEGMAP 2018. Although the six other vegetation types are original to the initial VEGMAP project, the extent and boundaries of these types have changed and, in some cases, certain portions have been reclassified as different vegetation types in entirely different biomes. This is important to note as it points to the adaptability which needs to be built into mapping procedures and products, and further supports the use of archetypes introduced in chapter two. A land degradation assessment technique, for example, needs to be adaptable to a change in project area as a fixed final product would only be useful for as long as the current VEGMAP exists.

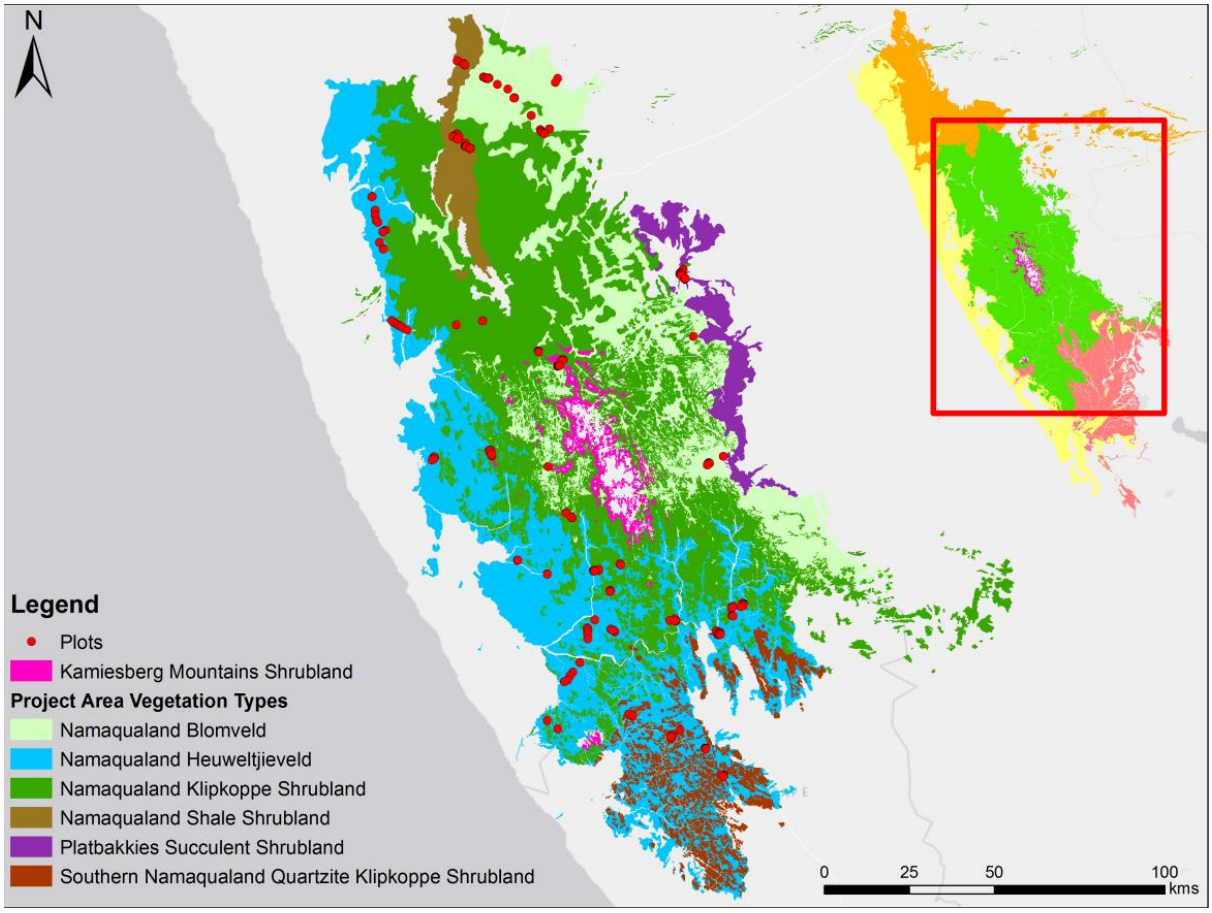

Figure 3.3. The Namaqualand Hardeveld bioregion comprising seven vegetation types, six of which make up the project area for this thesis. Inset depicts the location of the bioregion with respect to Namaqualand as a whole.

A comprehensive description of the six original Hardeveld bioregion vegetation types is provided in chapter five of Mucina and Rutherford (2006) (Mucina et al., 2006a). A description of the newly classified Southern Namaqualand Quartzite Klipkoppe is available on the SANBI Biodiversity GIS website (http://bgis.sanbi.org/), and is based on a report by Desmet and Dayaram (2016). Namaqualand Klipkoppe Shrubland (SKn 1) makes up the central region of Namaqualand and is the largest of the project area vegetation types (Figure 3.3). The area is characterised by open shrubland up to 1 m tall on a landscape of granite and gneiss domes, with only a few *Aloe dichotoma* trees scattered on some slopes. Shrubs typically display ericoid or succulent foliage. Although SKn 1 is the largest vegetation type in the study area, its extent has nearly halved following its reclassification in VEGMAP 2018. This reclassification has occurred primarily to the south of its former extent, which is now classified as either

Namaqualand Heuweltjieveld (SKn 4) or the newly assigned Southern Namaqualand Quartzite Klipkoppe Shrubland (SKk 10). Namaqualand Heuweltjieveld (SKn 4) is distributed in the foothills of the escarpment, largely to the west of the Klipkoppe Shrubland and inland of the coastal plains, but now also makes up a significant part of the southern extent of the region. The area covered by SKn 4 is nearly 50% larger in VEGMAP 2018 as compared with VEGMAP 2012. The diagnostic feature of this low shrubland landscape is the leaf-succulent dominated mosaic of heuweltjies in a matrix of surrounding vegetation (Mucina et al., 2006a). The Southern Namaqualand Quartzite Klipkoppe Shrubland (SKk 10) also occurs to the south of the project area but only covers about 5% of the bioregion. A distinction has now been made between the SKk 10 and SKn 1 based primarily on the underlying geology. SKk 10 occurs on quartzite hills and koppies, and not the granite and gneiss domes typical of SKn 1 (Desmet and Dayaram, 2016). Although there are large structural and floristic similarities between SKn 1 and SKk 10, there are many species endemic to SKk10. There is also floristic overlap with the quartz patches of the northern Knersvlakte. This makes SKk 10 a distinct unit in some ways, and transitional between northern Knersvlakte and typical Namaqualand Klipkoppe Shrubland (Desmet and Dayaram, 2016).

Occurring to the north, and covering only about 3% of the region, Namaqualand Shale Shrubland (SKn 2) is characterised by smooth undulating country typically supporting relatively dense shrubland (Figure 3.3). Parts of the former extent of the vegetation type to the south and west have been reclassified as Renosterveld, thus falling within the Fynbos biome. Namaqualand Blomveld (SKn 3) occurs in scattered patches across much of the region but predominantly to the east. A large portion has been reclassified in VEGMAP 2018 as Bushmanland Arid Grassland (Nama Karoo biome), and only covers about 60% of its former extent. SKn 3 predominantly occurs on sedimentary surfaces between the rocky granitic hills and mountains of the Kamiesberg. The Blomveld is characterised by sparse dwarf shrubs with succulent or ericoid leaves. Large areas of the former Platbakkies Succulent Shrubland (SKn 5) have also been reclassified as Bushmanland Arid Grassland resulting in a 50% reduction in its overall extent. SKn 5 represents a transition zone between the Succulent Karoo vegetation types and those of the Nama-Karoo. The area is mainly flat plains with some low koppies and hills where low succulent shrubs dominate loamy

colluvial and rocky soils, and grasses dominate more sandy soils (Mucina et al., 2006a). Kamiesberg Mountains Shrubland (SKn 6) occurs on predominantly steep south to east facing slopes towards the peaks of the Kamiesberg Mountains. It Is characterised by tall shrubland consisting of both non-succulent and succulent shrubs, and has been categorised as transitional to Renosterveld (Mucina et al., 2006a). It is therefore difficult to access for rapid field assessment and is not necessarily representative of the general vegetation of Namaqualand. Kamiesberg Mountains Shrubland has therefore not been included in the project area. The remaining six vegetation types cover nearly half of the total area of Namaqualand and also account for a large proportion of the region's biodiversity. As a result, these six vegetation types form the extent of the project area.

Chapter 4:

4. Field-based assessment of habitat condition

4.1 Field-based assessment of land degradation

The primary aim of this project is to map the extent and severity of land degradation across Namaqualand. This was achieved through adopting some of the methodology applied in similar arid and semi-arid regions by authors such as Thompson et al. (2005), Todd (2009), Oldeland et al. (2010), and many others. These methods were extended to incorporate the use of archetypes, as proposed by Cullum (2014) and Cullum et al. (2016a and 2016b). This approach resulted in the creation of a versatile land degradation map that incorporates the inherent uncertainty in the mapping procedure. A fundamental component of this methodology was to first obtain an ecological understanding of the vegetation types to be mapped, as well as to identify the range of habitat condition possible within the study area.

Habitat condition has been defined as the difference between one dynamic ecological state resulting from an understood natural regime of disturbance and recovery, and the other consisting of modified states thought to result from anthropogenic disturbance (Harwood et al., 2016). Habitat condition can be thought of as the broader framework within which land degradation processes act. Thus, a potentially degraded landscape will fall on one side of the spectrum of possible condition for an area, while a landscape that has been less impacted upon will fall on the other side. Land degradation can be defined, in this case, as either a decrease or deterioration in habitat condition over time, or by a condition state that is known to be degraded. In order to create a spectrum of possible habitat condition for a landscape it is important to include quantitative measures of condition that can be applied continuously across the project area. These measures can then be combined to provide a range of condition scores for the region (Harwood et al., 2016).

For this project, field measures were chosen for two main purposes. The first group was used to create a spectrum of possible condition for the Namaqualand Hardeveld bioregion. The second group of indicators was used to interpret the results of the mapping procedure within the context of known anthropogenic and abiotic drivers of

change, and ultimately to construct a land degradation archetype for the project area (see chapter six). Due to the relatively large size of the study area, at nearly 20 000 km^2, and the relative inaccessibility of some areas as a result of inevitable time and other logistical constraints, a sample of reference sites first needed to be identified for field work.

Field-based assessments of habitat condition and land degradation are commonplace and, as a result, a variety of different techniques and sampling methods have been developed (e.g. Stocking and Murnaghan, 2000; Todd, 2009; Vågen et al., 2013b). These techniques vary depending on the overall objectives of the study, the relative expertise of the sampling team, and the amount of time and resources that are available. Another important factor in the development of field sampling techniques is the scale of the project area (Anderson, 2018). The sampling technique as well as the selection of attributes to sample is largely dependent on the overall size of the project area. Relatively small farms may, for example, be sampled extensively in order to cover as much of the farm as possible. In these instances, a larger number of variables may be measured at a finer spatial scale. Larger areas, on the other hand, may require a fewer number of variables that can be scaled up to the extent of the project area (Marvin and Asner, 2016).

4.2 Land degradation indicators

Field-based land degradation assessment approaches rely on a set of indicators that are thought to characterise both observed characteristics in the field, and the processes potentially associated with these characteristics. Various lists of indicators for measuring desertification have been developed (Table 4.1). These indicators are generally grouped within a hierarchy where broad, globally applicable indicators make up the higher levels and more regionally- or locally-specific indicators are associated with lower levels of the hierarchy (e.g. Berry et al. 2009). This approach allows for a larger list of potential indicators to be available for local and regional studies that can describe desertification in each specific context, and which can then be grouped within the broader indicator categories at the global scale (Sommer et al., 2011). Such an approach is particularly useful within the context of UNCCD reporting and, therefore, remains a priority for the convention (UNCCD, 2009).

Table 4.1. Timeline of the different approaches and the broad set of indicators proposed for land degradation field assessments

Publication summary	Broad indicator categories (with selected examples)
Guidelines for Field Assessment (Stocking and Murnaghan, 2000)	Indicators of soil loss (rills, gullies); indicators of production constraints (crop yield, nutrient deficiencies).
Land Degradation Assessment in southern Africa (Stringer and Reed, 2007)	Agricultural (declining livestock condition, decreased milk production); vegetation (decreased grass cover, decreased abundance of trees); soil (increased soil looseness, decreased soil organic matter); wild animals and insects (decreased abundance of birds / game).
Manual for Describing Land Degradation Indicators (DESIRE, 2008)	Physical and ecological (rainfall, slope aspect, plant cover); economic (farm size, grazing intensity, land use type); social (population density); institutional (protected areas).
Selected Global Indicators of Land Degradation (IIASA, 2009)	Land cover (cultivated land, forest, pastures); soil and terrain (erodibility, slope); management (crop management index).
Field-Based Assessment of Degradation (Todd, 2009)	Plant functional type percentage cover; ecological indicator value (EIV).
UNCCD Recommended Minimum set of Impact Indicators (Berry et al., 2009)	Water availability per capita; change in land use; percentage of population above poverty line; level of land degradation; plant and animal biodiversity; aridity index; lands under sustainable land management; land cover status.
Local Level Assessment of Land Degradation and Sustainable Land Management (Bunning et al. 2011)	Vegetation (decline in vegetation cover, decline in species / habitat diversity, reduced vegetation productivity); soil (description of soil sample, pH, organic carbon).
Application of Indicator Systems for Monitoring and Assessment of Desertification form National to Global Scales (Sommer et al., 2011)	High level indices (natural capital loss, land at risk, Human Appropriation of Net Primary Production, human wellbeing, biodiversity index); themes (water, soil, vegetation, animals, biodiversity); fundamentals (precipitation, slope, land cover, livestock, protected areas, etc.).
Identifying Best Land Management Practices for Combating Desertification (Kosmas et al., 2012)	Physical environment (annual rainfall, aridity index, soil drainage, slope aspect / gradient); socio-economics (farm ownership, population density, farm subsidies); land management (major land use, plant cover, land use intensity).
The Land Degradation Surveillance Framework (Vågen et al., 2013b)	Land form (position, slope gradient); vegetation (type, structure, cover); land use (current use, conservation status, impact of uses); soil (visible erosion, infiltration, texture).
Evaluation and Selection of Indicators for Land Degradation and Desertification Monitoring (Kairis et al., 2014)	Water erosion (water storage, land terracing); tillage erosion (tillage direction, policy implementation); soil salinisation (ground water exploitation, water demands); water stress (land abandonment, soil erosion control); forest fires (grazing intensity); overgrazing (soil water conservation).

One of the first comprehensive sets of guidelines for the field assessment of land degradation published following the establishment of the UNCCD was compiled by Stocking and Murnaghan (2000). This publication brought together knowledge and expertise gained through two internationally funded projects to provide a range of indicators of soil loss and production constraints (Table 4.1). Guidance is also provided as to how indicators can be combined to provide a clearer picture of land degradation for any given area. This publication is also significant in that it illustrates the changing perspective within the desertification narrative in that the assessment is viewed through the lens of the farmer and land user (Stocking and Murnaghan, 2000). Another globally significant attempt to establish a comprehensive list of land degradation indicators was conducted through the European Union funded Desertification Mitigation and Remediation of Land (DESIRE) project. The first report produced through this project lists a total of 72 indicators related to causes or processes of land degradation and desertification shown to be important in 18 degradation and desertification hotspots around the world. These indicators were determined through engagement with scientists and various stakeholder groups. (DESIRE, 2008).

Under the umbrella of the DESIRE project, Kosmas et al. (2012) provide a list of indicators for identifying suitable land management practices for combatting desertification (Table 4.1). These indicators reflect a reduced subset of those presented by the original DESIRE document (Kosmas et al., 2012). Kairis et al. (2014) further evaluate which indicators in the DESIRE database are best related to several specific land degradation processes, such as erosion and overgrazing. They found that, among a long list of both biophysical and socio-economic indicators, rainfall seasonality, slope gradient and water scarcity were found to be the most important indicators of land degradation globally (Kairis et al., 2014). At a similar scale to the DESIRE project, the UN FAO's Land Degradation Assessment in Drylands (LADA) project has developed several field manuals for local land degradation assessment as well as a compilation of a selection of global indicators of land degradation (Bunning et al., 2011; IIASA, 2009). These various publications, along with previous work by the UNCCD and other organisations, formed the basis of the UNCCD recommended minimum set of impact indicators published in 2009 (Berry et al., 2009). This set of 11 indicators was primarily established to help identify the impact of the UNCCD in implementing their 10 year strategic plan that emerged from the 8th conference of the

parties (UNCCD, 2007). Although national and regional indicators can subsequently be fed into land degradation assessments where appropriate, the reproducibility of the framework is limited by its objective of measuring the UNCCD's impact. Sommer et al. (2011), therefore, provide a framework for selecting indicator sets for land degradation or desertification assessments at all spatial scales. Their framework includes three levels of data organisation with several hundred fundamental indicators grouped initially into five major themes, which are nested within five high level indices. This approach allows for indicator-based monitoring and assessment to be rooted within a specific broader desertification framework (Sommer et al., 2011).

These global indicator lists and systems provide a good framework for land degradation assessment at the regional or local scale, but require good national and regional data that in many cases, and particularly within the African context, does not exist. As a result, several regional level indicator lists and frameworks have been developed from as early as the establishment of the UNCCD. For example, continuing with the more participatory approach promoted by Stocking and Murnaghan (2000), but within the narrower spatial scale of southern Africa, Stringer and Reed (2007) provide a list of land degradation indicators obtained through workshops with local communities (Table 4.1). Vågen et al. (2013), on the other hand, collate several years of land degradation research in Africa to produce the Land Degradation Surveillance Framework (LDSF) which allows for the development of a baseline assessment of a landscape for monitoring land degradation processes and recovery over time.

The indicators that have been used in land degradation studies in other arid areas around the world provide useful guidance in developing a list of potential indicators for Namaqualand. These indicators, however, need to be chosen through specific knowledge of the ecology and socio-economic conditions of Namaqualand, as well as through detailed analysis of land degradation studies in South Africa, and particularly the more arid regions of the country. Todd (2009) completed a field-based assessment of degradation in the Namakwa district as part of the Degradation Mapping Project (Table 4.1). This assessment included six vegetation types that fall within both the Nama-Karoo and Succulent Karoo biomes (Todd, 2009), one of which is shared with this project: the Namaqualand Heuweltjieveld vegetation type. The field methodology and measures implemented by Todd (2009) were, therefore, used as a starting point for this project.

4.3 Methods

4.3.1 Plot selection

In order to ensure that sampling occurs across the entire range of potential habitat conditions, plot locations should either be based on known conditions, or a random distribution of plots across the area if the habitat condition is not known (Todd, 2009). Ideally, the range of potential conditions should be uniformly sampled across the different vegetation types such that all condition types are equally represented. Using a random distribution of plots was not possible for this study because of the relative inaccessibility of some plots, and the excessive amount of time it would take to sample the plots. If sampled randomly, the plots would be distributed across many different land owners and land users each of whom would have to be consulted in order to obtain permission to sample on their land. Other plots would be distributed in near inaccessible steep and mountainous terrain. Another potential flaw of a random sampling method is that the full range of possible conditions is unlikely to be adequately sampled resulting in ecologically important but less widespread areas being excluded (Hirzel and Guisan, 2002). For example, the highest grazing impact in the project area generally occurs in small and isolated areas around water points and kraals. These areas would likely be underrepresented in a randomly assigned set of plots. As a result of these factors, a more targeted approach was employed for this study in order to document the full range of habitat condition across the project area.

Google Earth Pro™ was used to determine the most appropriate zones within the project area on which to focus the sampling efforts. This initial desktop reconnaissance was based on locating a range of relatively accessible vegetation types as close as possible to primary and secondary roads. Data collection at each plot was kept to between 15 and 20 minutes in order to sample as many plots in a day as possible and collect all the data in the same growing season. A data sheet was developed to allow for swift and consistent field data collection and to make it easy for future practitioners to rapidly assess the habitat condition of areas of interest (Figure 2.1).

SHCS:	1	2	3	4	5	6	7	8	9	10
Site:				Photo ID:			Latitude:			
Date:				Elevation (m):			Longitude:			
Plot ID:										
Average perennial shrub height (cm):						No. of leaf succulent species:				
Annual	Lf Su	St Su	Non Su	G.a/ind	Grass	Biocr	Baregr	Rock	Litter	Total
Dominant biocrust type:								Cyano	Lichen	Bryo
Land form:					Azonal	Pedi	Toe-sl	Mid-sl	Ridge	Plateau
Slope aspect:			N	NE	E	SE	S	SW	W	NW
Dominant land use:										
Slope(°):	0 – 5	5 – 10	10 – 15	15 – 20	20 – 25	25 – 30	30 – 35	35 – 40	40 – 45	> 45
Distance to nearest water point (m):						or kraal (m)				
Dung counts:										
Notes:										

Figure 4.1. Data sheet created for recording plot characteristics and collecting field data. (SHCS – subjective habitat condition score; Cover estimates (annual – annuals, Lf Su – leaf succulent plant species, St Su – stem succulent plant species, Non Su – non-succulent perennial plant species, G.a/ind – Galenia Africana / degradation indicator species, grass – perennial grasses, Biocr – biological soil crust, Baregr – bare ground, Rock – bare rock, Litter – dead organic matter); Cyano – cyanobacteria; Bryo – bryophytes; Pedi – pediment; Toe-sl – toe-slope; Mid-sl – mid-slope).

The primary objective of the field work phase was to sample the entire range of habitat conditions possible for the Namaqualand Hardeveld bioregion. As such, piospheres and fenceline contrasts, where a difference in habitat condition was observed, were sought out during the desktop reconnaissance phase, as well as while driving through the potential sampling zones. Lange (1969) determined that the impact of grazing sheep decreased radially away from water points and coined the term piosphere to describe this observation. Washington-Allen et al. (2004, p.136) extended the definition to “include any concentrated animal or anthropogenic impact that radiates from an area of concentration”. The sampling of piospheres is useful in the assessment of degradation in drylands as it allows for a range of potential habitat condition, from ‘degraded’ to ‘non-degraded’, to be sampled over a relatively small area and short space of time (Figure 4.2). The study of piospheres has also allowed for the separation of grazing impacts from climatic effects, which is an issue of particular concern in drylands (Pickup et al., 1994; Wessels et al., 2007b). As a result, piospheres or grazing gradients have been used extensively as indicators of

desertification and land degradation in arid areas (Andrew, 1988; Bastin et al., 1993; Beukes and Ellis, 2003; Dougill et al., 1999; Hanan et al., 1991; Jafari et al., 2008; Kotzé et al., 2013; Pickup and Chewings, 1994; Riginos and Hoffman, 2003; Sternberg, 2012; Thrash, 2000; Washington-Allen et al., 2004). The analysis of piospheres in this study was useful in determining a range of possible conditions within an area while controlling for abiotic drivers such as differences in climate or soils. Piosphere sampling also allowed for a greater number of plots to be sampled at any given time as several plots could be sampled in one area.

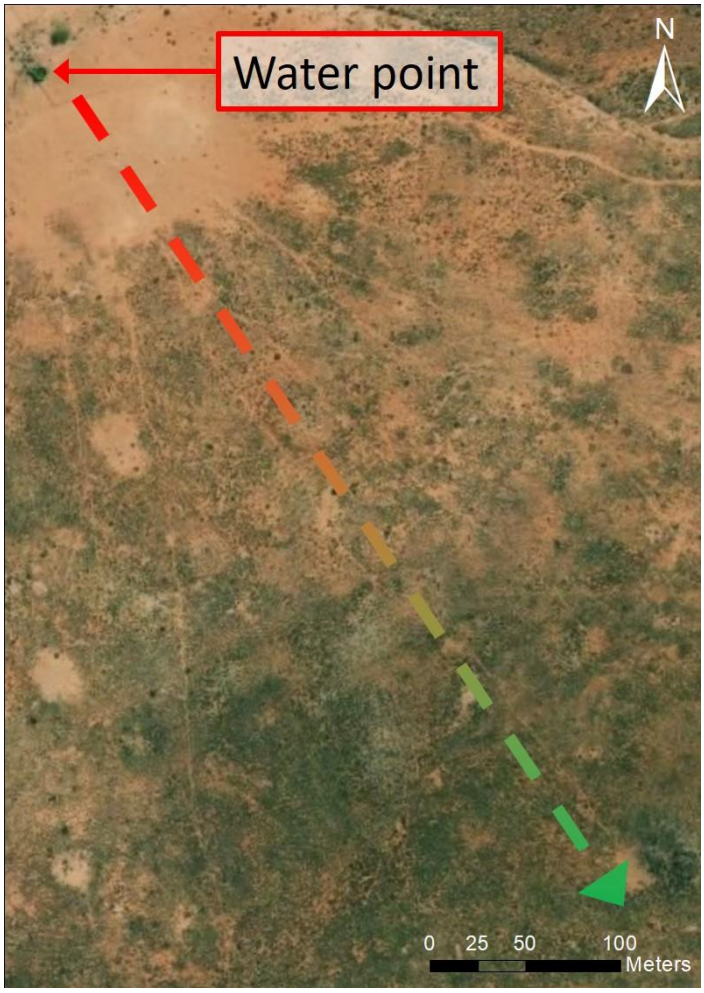

Figure 4.2. Example of a piosphere located within the project area (30.70403°S; 18.46500°E), with illustrations indicating the location of the water point away from which there is a gradient of decreasing grazing pressure (red and green arrow).

Differences in vegetation cover and composition across fence lines are useful for the same reason as piospheres in that the observed differences are likely a result of different land use or management practices, and not differences in abiotic drivers (Todd and Hoffman, 2009) (Figure 4.3). Fenceline contrasts allow for noticeably

contrasting habitat conditions to be sampled in a small geographic area, thus saving time and resources during field sampling. They have been analysed mostly to explore differences in livestock grazing practices in communal versus private land, and to evaluate the consequences of heavy gazing on plant species richness and community composition (Todd and Hoffman, 1999, 2009; Nenzhelele et al. 2018). For the purposes of this study, fenceline contrasts were identified in order to improve field sampling efficiency by sampling a range of different habitat conditions in as short a time as possible and in a relatively small geographic area.

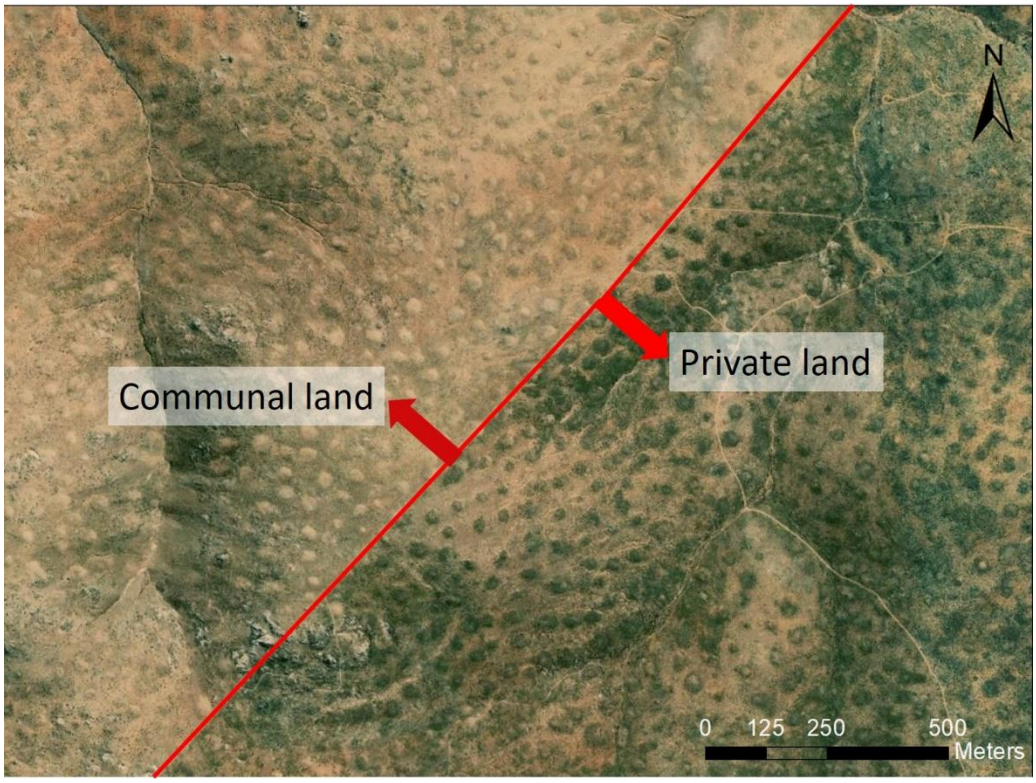

Figure 4.3. Example of a fenceline contrast located within the project area (30.52950°S; 17.62722°E), with illustrations indicating the fenceline between communal land in the north-west and privately-owned land in the south-east.

4.3.2 Data collection

During a four week period between September and October 2017, a total of 317, 5 m x 5 m plots were sampled across the six vegetation types of the Hardeveld bioregion, with a minimum of 50 plots for each vegetation type (Figure 4.4). The location of these plots was based on the vegetation types depicted in VEGMAP 2012 as this was the latest available resource at the time of field sampling. Subsequent to the completion of the field work, VEGMAP 2018 was released. Forty of the original 317 field plots

occur outside the boundaries of the Namaqualand Hardeveld bioregion as defined by VEGMAP 2018. The exclusion of these plots did not, however, alter the results of the analyses and, therefore, 277 field plots from the six vegetation types of the project area were sampled. The 40 plots that were excluded, along with an additional 20 plots sampled during an earlier reconnaissance trip were used to ground truth the results obtained in chapter five (see section 5.2.2). Using the field data sheet (Figure 4.1), quantitative and qualitative data, relating to the biophysical condition of the area were collected, and each plot was assigned a subjective habitat condition score (SHCS). This score was based on a subjective assessment of the plot that considered the various indicators included in the data sheet as well as expert knowledge of the biophysical characteristics of the area. The scores range between one and ten, with a score of one indicating a very degraded landscape and a score of ten indicative of a non-degraded landscape. These scores were later compared with the more quantitative measures of land degradation to investigate their degree of correspondence.

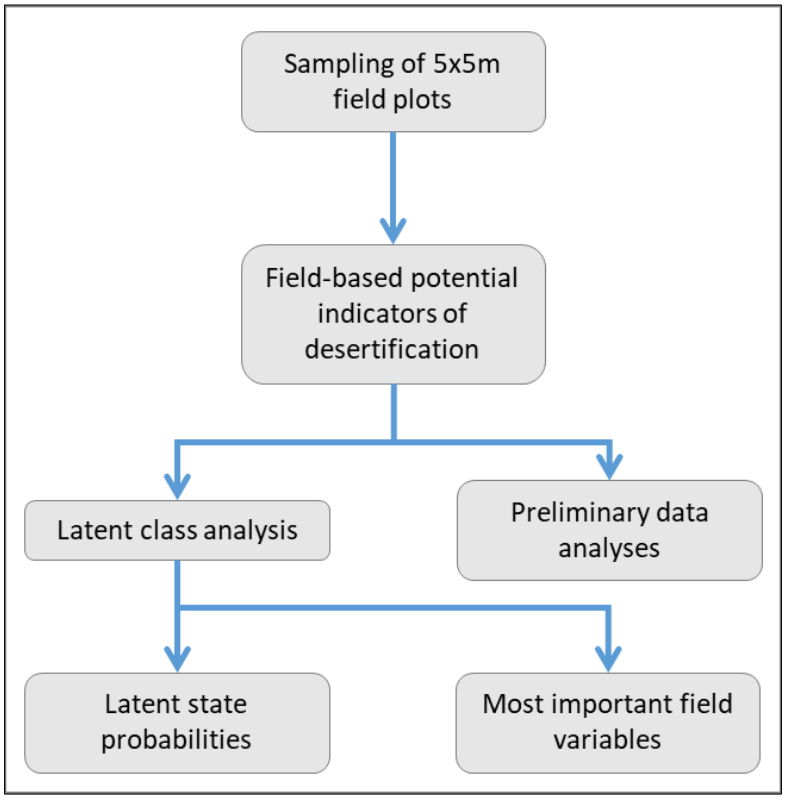

Figure 4.4. Flow diagram illustrating the methodology employed to collect and analyse the field data.

The location of each plot was recorded both on a handheld GPS as well as on the data sheet (Figure 4.1). This was important both for ensuring the satellite data matched the plot location as accurately as possible, as well as to allow for potential future replication and monitoring. Elevation was also recorded from the GPS and was later verified through a digital elevation model (DEM) created in Google Earth Engine (Appendix A). Average perennial shrub height (cm) was estimated using a two-metre measuring pole. The height for a range of shrubs was estimated and the average was calculated from these estimates. The number of leaf succulent species was then determined. This step required knowledge of the dominant growth forms only and not a detailed knowledge of the species themselves. The vegetation of the area was divided in the data sheet into six functional groups: annuals (Annual), leaf succulent shrubs (Lf Su), stem succulent shrubs (St Su), non-succulent shrubs (Non Su), land degradation indicator species - namely *Galenia africana* (G.a/ind), and perennial grasses (Grass). The cover of these groups, along with the estimated cover of biological soil crust (Biocr), bare ground (Baregr), rock, and litter, were estimated such that the sum of all ten parameters equalled 100 percent for each plot (Figure 4.1 - Total). The dominant biocrust type (cyanobacteria, lichen, bryophyte) was also recorded. The dominant landform on which the plot was located, as well as the approximate slope aspect and angle, were also recorded. More accurate values for the slope characteristics were later determined using the DEM from GEE. Land tenure was recorded in the field and later verified using geospatial layers obtained from SANBI, as well as national cadastral information. The distance to the nearest kraal and / or water point was estimated in metres. Lastly, a 0.5 m x 0.5 m quadrat was randomly positioned in five different locations within the plot and the number of livestock dung droppings was recorded in each quadrat and summed to get an overall dung count for each plot.

Variables used in field-based analysis

Prior to creating a model of the field data, a preliminary visual assessment of the data was completed to determine the distribution of the variables, and how they were related to each other (Figure 4.4). The data were divided into potential measures of habitat condition, and potential drivers of change in habitat condition. The potential measures of habitat condition were used in the analyses for this chapter while the drivers were used to evaluate the final habitat condition assessment in chapter six.

Elevation, slope angle and aspect, land tenure, and landform were, therefore, not included in the development of the field-based assessment methods. The variables referring to the distance to the nearest water point or kraal were excluded as these measures were difficult to obtain in the field without prior knowledge of the location of all existing kraals and water points, and therefore contain too many missing values. Of the growth form cover estimates, perennial leaf succulents, stem succulents, and non-succulents were summed to determine an overall value for perennial vegetation cover. Perennial leaf and stem succulent cover estimates were summed to obtain a perennial succulent cover estimate. Estimated cover of annuals, biological soil crust, bare ground, bare rock and litter were summed to obtain an estimate of the percentage of the plot that was not vegetated. Lastly, the estimated cover of annuals was added to the estimate for bare ground cover to obtain an estimate for a total bare ground cover. This is because annual plants often grow during a very brief period in bare or degraded landscapes. The cover of annuals was also generally very low at the time of the field work.

4.3.3 Data analyses

All data analyses were performed in R statistics (R Core Team 2019).

Distribution of the field data

Histogram charts were initially created to determine the general distribution of the data with respect to the subjective habitat condition score, as well as the other field measures.

In order to determine whether there were differences across the subjective habitat conditions scores for each of the field-based measurements, a series of Kruskal-Wallis rank sum tests were performed. This was accomplished with the kruskal.test() function available in base R (R Core Team, 2019). Kruskal-Wallis is a non-parametric alternative to the one-way ANOVA test where there are more than two groups, and the assumptions of the one-way ANOVA are not met. If the Kruskal-Wallis tests returned a significant result, suggesting a difference between one or more subjective habitat condition scores (SHCS), then a multiple pairwise comparison test was performed to determine which groups differed from each other. This was accomplished using the pairwise.wilcox.test() function, also available in base R (R Core Team, 2019). The pairwise comparison output is a table of p-values for each pair in the SHCS groups.

Latent class analysis

To determine whether the field sites clustered into distinct groups related to different levels of habitat condition, the depmixS4 package, which was developed to fit dependent mixture models on mixed categorical and continuous data, was used (Visser and Speekenbrink, 2010). Mixture models are probabilistic models that are used to make inferences about the properties of potential sub-populations within a broader population, with only observations of the pooled population. Examples of dependent mixture models include standard and hidden/latent Markov models, finite mixture distribution models, and latent class models (Visser and Speekenbrink, 2010). Latent class analysis (LCA) is a method for finding subtypes of related cases (latent classes) from multivariate data and can be performed using the depmixS4 package. LCA is similar to other clustering techniques but is more flexible in that it allows for the possibility that groups recovered from the data are uncertain (Oberski, 2016). LCA is considered an appropriate method for determining whether the Namaqualand field data cluster into any groups associated with habitat condition, while allowing for the fact that uncertainty exists within the designated clusters.

LCA allows for a choice in the number of classes that are thought to exist in the dataset. In order to avoid any associated subjectivity, the model can be run several times with differing numbers of classes (nstates) to determine the number resulting in the best model fit. The model used in this analysis was run starting with nstates = 1, and then with an increasing number of classes until the model did not run successfully. The Akaike information criterion (AIC) for each successful run was compared, with a lower AIC indicating a better model fit. Once the ideal number of classes was determined, the posterior probabilities were extracted from the model output. Posterior probabilities are the probability that each sample (plot) belongs to a specific class. The relative importance of the various field variables in distinguishing the latent states, as well as the distribution of the field plots relative to their assigned states are determined, and the results are used as response variables in a model predicting field cover from Earth observation data.

4.4 Results

4.4.1 Field data

Distribution of plots

The distribution of the field plots relative to their assigned subjective habitat condition score (SHCS) was normal with most plots being assigned an SHCS of between three and six, and fewer plots with very low (most degraded) or very high (least degraded) scores (Figure 4.5A). There were, however, fewer plots with scores of eight or more than with scores of one to two, with only one plot with an SHCS of nine or above. Estimated perennial plant cover (Figure 4.5B) and estimated mean perennial plant height (Figure 4.5C) were both skewed to the right indicating low overall perennial plant biomass across the sampled plots. Estimated cover of bare ground (Figure 4.5D) as well as the cover estimate of everything in the plot apart from perennial vegetation (non-vegetated cover) were approximately normally distributed (Figure 4.5E). The estimated cover of succulent plant species was skewed heavily to the right indicating a predominance of plots with no succulent plant species cover (Figure 4.5F). The number of leaf succulent species was also skewed to the right with between zero and two succulent species recorded for most plots (Figure 4.5G). Dung count, too, was skewed to the right indicating a high proportion of plots with zero to very little dung, and only a small number of plots with a high dung count (Figure 4.5H).

Differences between SHCS

There were significant differences across the subjective habitat condition scores (SHCSs) for all seven field variables ($p < 0.001$). As a result of there being only one plot with a SHCS of nine, this plot was excluded from the graphs represented in Figure 4.6. Estimated perennial plant cover (Figure 4.6A) and estimated mean perennial plant height (Figure 4.6B) increased with increasing SHCS ($p < 0.05$). Estimated bare ground (Figure 4.6C) as well as the estimated area of the plot not covered with perennial plant cover (Figure 4.6D) decreased with increasing SHCS ($p < 0.05$). Estimated succulent species plant cover (Figure 4.6E) and the recorded number of leaf succulent species (Figure 4.6F) increased between a SHCS of one and five before levelling out, and even decreasing with a SHCS of eight ($p < 0.05$). Lastly, recorded livestock dung count (Figure 4.6G) decreased significantly with increasing SHCS ($p < 0.05$).

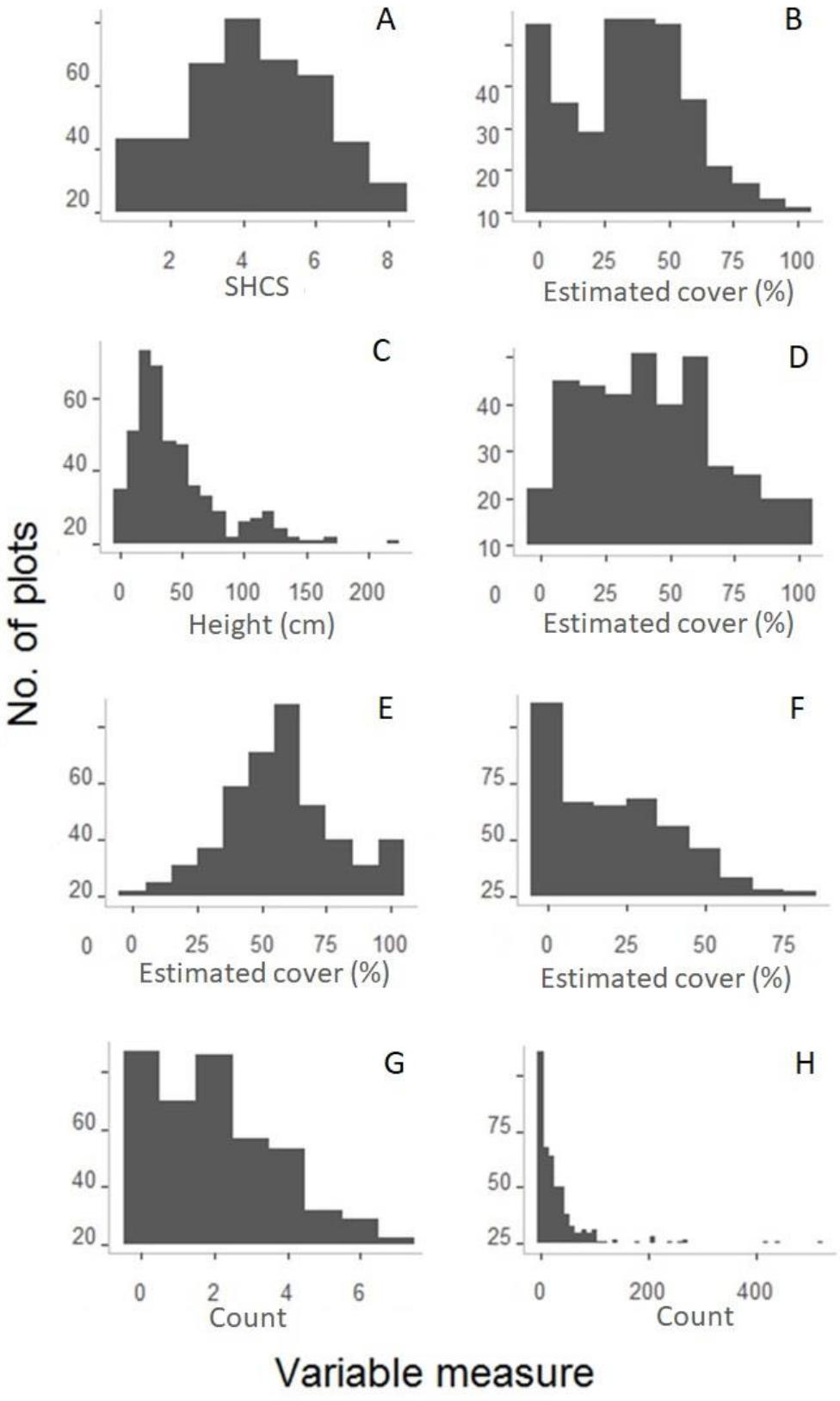

Figure 4.5. Distribution of the field plots relative to the field variables measured: A – Subjective Habitat Condition Score (SHCS); B – estimated perennial plant cover (%); C – estimated mean perennial plant height (cm); D – estimated bare ground cover (%); E – cover of plot that is not perennial plant cover (%); F – estimated succulent plant cover (%); G – recorded number of leaf succulent species; H – recorded dung count.

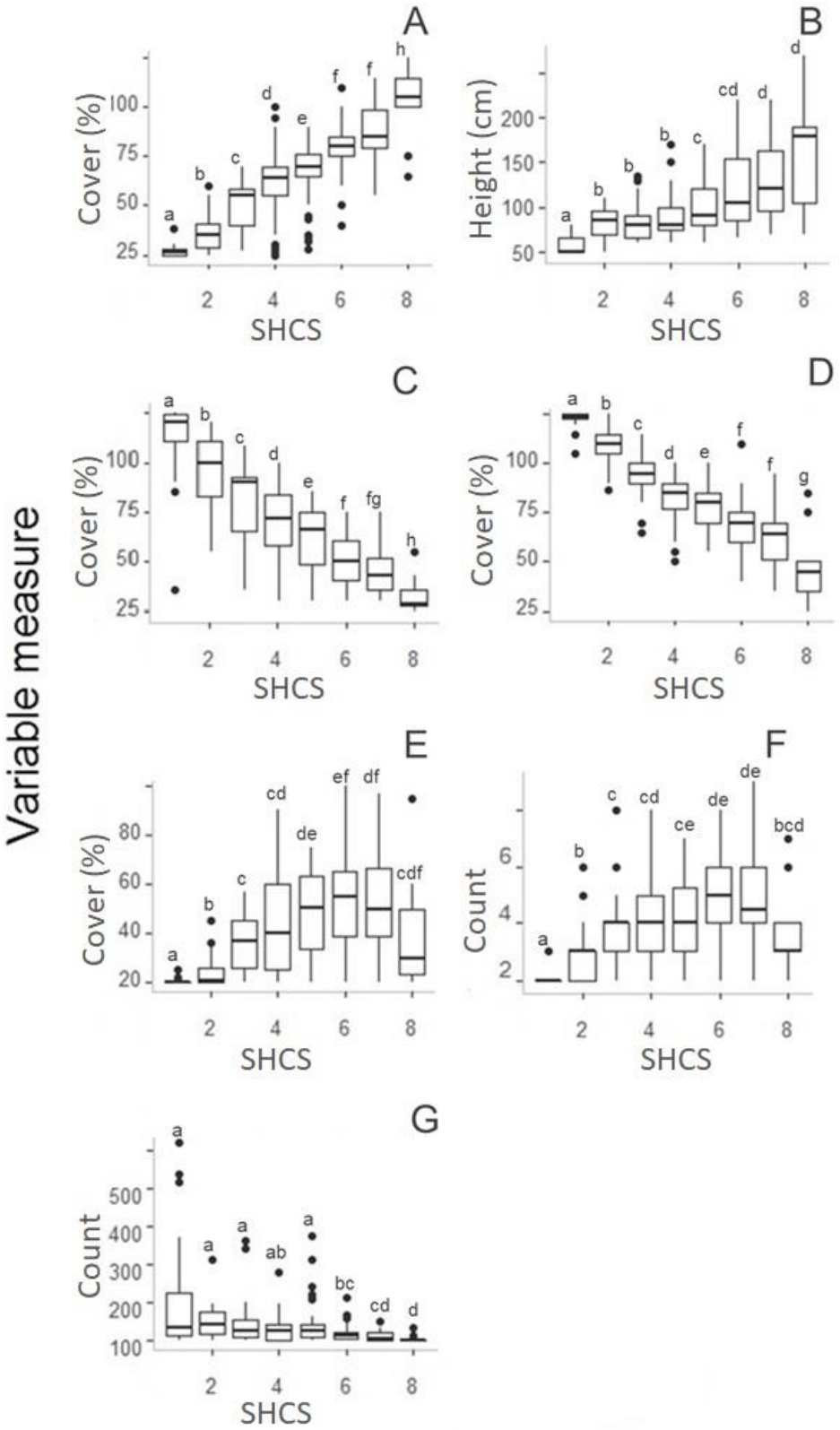

Figure 4.6. Variables used in the latent class analysis relative to the Subjective Habitat Condition Score (SHCS) where 1 = most degraded and 8 = least degraded. A – estimated perennial plant cover (%); B – estimated mean perennial plant height (cm); C – estimated bare ground cover (%); D – cover of plot that is not perennial plant cover (%); E – estimated succulent plant cover (%); F – recorded number of leaf succulent species; G – recorded dung count.

4.4.2 Latent Class Analysis

Best model

A latent class model with three latent classes (nstates = 3) returned the lowest AIC value for the field data (Table 4.2). This model was chosen to determine the grouping of the field plots with respect to the measured field variables, as well as the most important variables in distinguishing between these groups.

Table 4.2. Series of latent class analysis (LCA) models with increasing number of latent states (nstates). Akaike information criterion (AIC) values used to determine model quality are reported along with variables used in the models.

Model	nstates	AIC	Variables
LCAmod1	1	19487.13	Mean perennial plant height, number of leaf succulent species, perennial plant cover, succulent species cover, cover of non-vegetation, cover of annuals and bare ground, dung count
LCAmod2	2	18313.44	
LCAmod3	3	17841.34	
LCAmod4	4	Error	

Distribution of plots according to latent states

The latent class analysis allows for each field plot to be assigned to one of the three latent states (S1, S2, and S3) (Table 4.3). The number of plots per state was relatively evenly distributed but there were fewer plots in S1 and S3 than in S2. More plots with a lower SHCS are found in S1, while plots with a median SHCS are more associated with S2, and plots with higher SHCS are in S3. The relationship between latent class assignment and SHCS was found to be significant using a Chi-square test (Chisq = 254.19, df = 16, $p < 0.001$).

Table 4.3. The number of plots assigned to each latent class (state) according to their subjective habitat condition score (SHCS).

		Subjective Habitat Condition Score (SHCS)									Total number of plots
		1	2	3	4	5	6	7	8	9	
State	S1	28	24	16	12	15	1	0	0	0	96
	S2	0	4	33	41	28	21	4	1	0	132
	S3	0	0	1	13	16	27	21	10	1	89

The probability of a plot belonging to S1 is highest with a low SHCS, while the probability of belonging to S3 is highest with a high SHCS, and the probability of belonging to S2 is highest with a median SHCS (Figure 4.7). Though the probability of a plot being in S2 is never zero for any given SHCS, the probability of being in S1 is zero for an SHCS of six or above, and the probability of a plot being in S3 is zero for an SHCS of three and below.

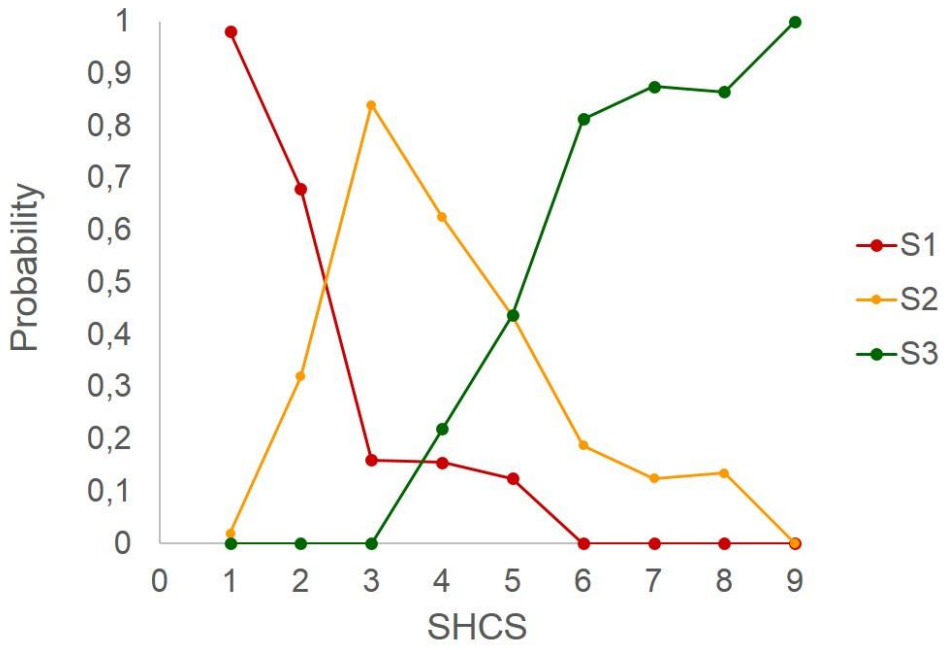

Figure 4.7. Mean probability of being assigned to each latent class (S1, S2 & S3) plotted against the subjective habitat condition score (SHCS).

Distribution of plots according to field variables

Plots with high perennial plant cover are generally grouped into S3 while plots with low perennial plant cover are in S1 (Figure 4.8A). Correspondingly, most of the plots with high bare ground cover are associated with S1, and most of the plots with low bare ground cover are grouped into S3 (Figure 4.8B). A similar pattern was evident for the percentage of the plot not covered in perennial vegetation (Figure 4.8C). More plots in S1 have zero leaf succulent species (Figure 4.8D) and zero estimated succulent cover (Figure 4.8E). Plots with taller perennial shrubs are associated with S3, while there are more plots with shorter mean perennial plant height estimates in S1 (Figure 4.8F). S1 is associated with plots with very high dung count, while a large proportion of the plots with no recorded livestock dung are grouped into S3 (Figure 4.8G).

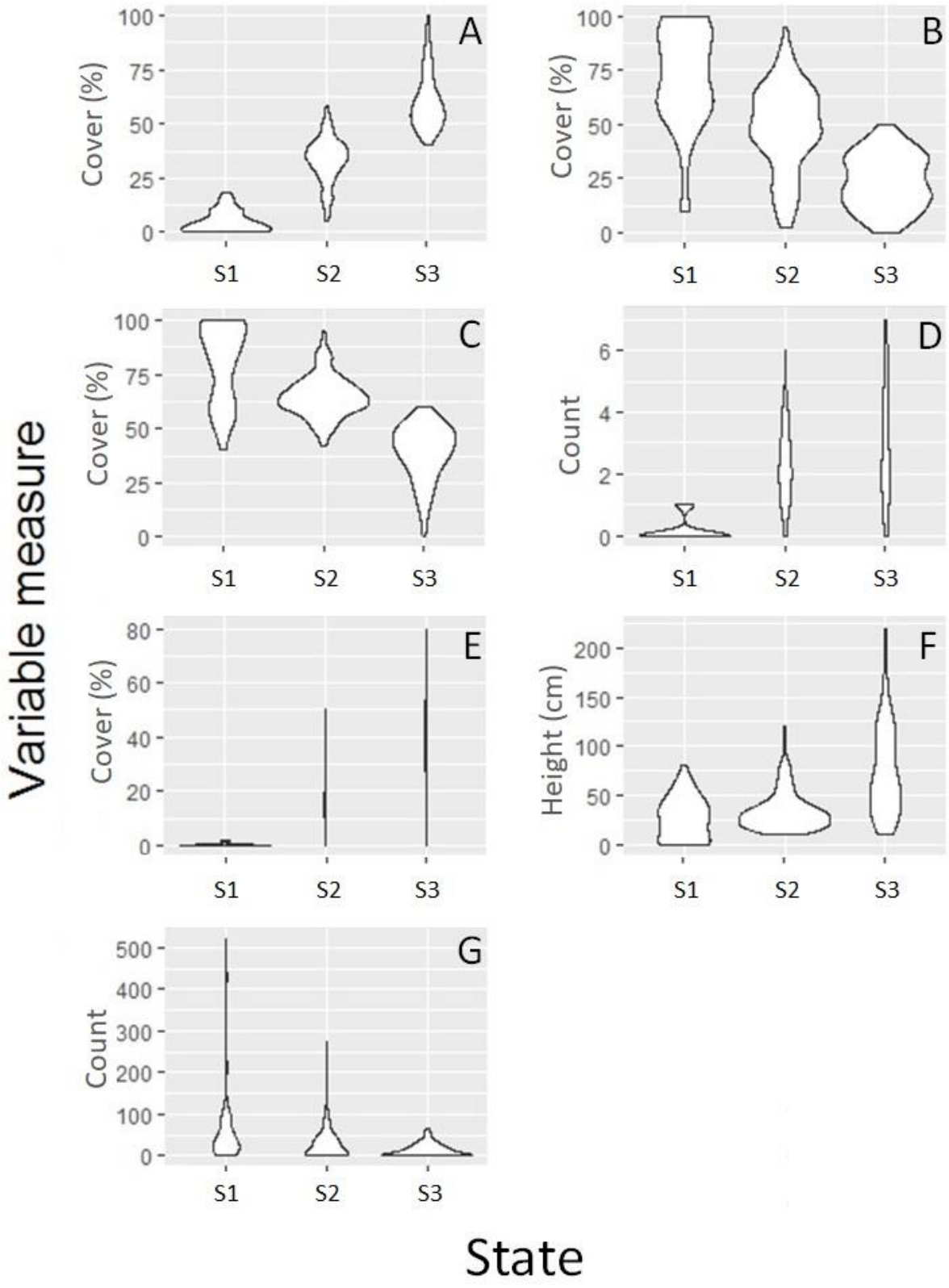

Figure 4.8. Distribution of each field variable measure relative to the three latent class states (S1, S2, S3). A – estimated perennial plant cover (%); B – estimated bare ground cover (%); C – cover of plot that is not perennial plant cover (%); D – recorded number of leaf succulent species; E – estimated succulent plant cover (%); F – estimated mean perennial plant height (cm); G – recorded dung count.

Variables that most influence latent class determination

Standardised scores are used in LCA to evaluate the relative contribution that each variable in an analysis has in separating the data into the respective latent classes. The bigger the difference in standardised scores between latent classes, the more important the variable is. For our model, the difference in standardised score between states one and two is greatest for non-vegetation cover, followed by perennial plant cover and succulent species cover. Perennial plant cover, bare ground cover, and non-vegetation cover have the greatest difference in standardised scores between states one and three, while non-vegetation cover, perennial plant cover, and bare ground cover have the greatest difference in standardised scores between states two and three (Figure 4.9).

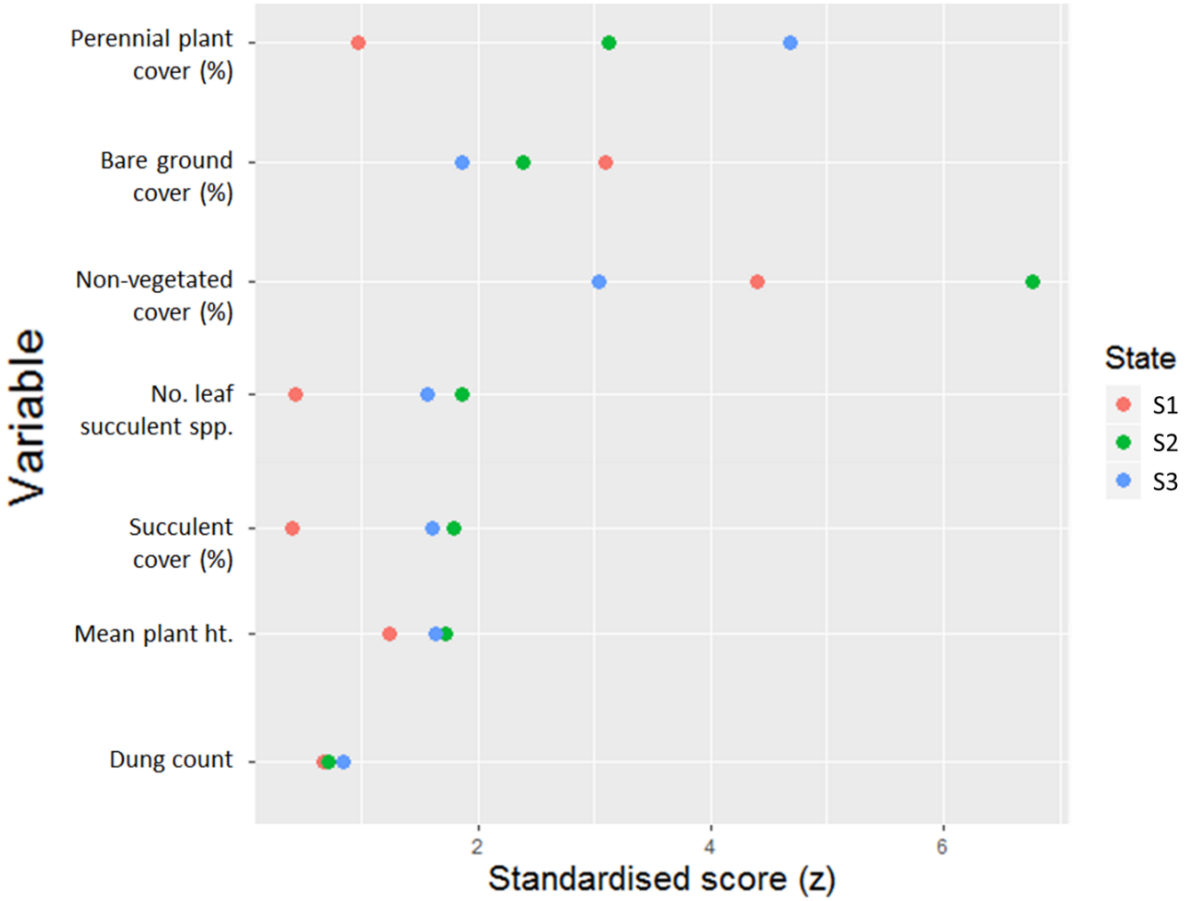

Figure 4.9. Standardised scores (z) for each variable in the latent class model LCAmod3 according to latent class state. Variables have been sorted by the differences between states one and three such that the variable with the greatest difference is at the top of the graph.

4.5 Discussion

The 277 plots sampled for this project provide an excellent indication of the range of habitat condition for the project area, from completely bare areas (e.g. Figure 4.10A) to areas with higher perennial plant cover, more succulent plant cover and diversity, and taller perennial shrubs (e.g. Figure 4.10B). The value of expert knowledge is also emphasised through the positive correlation between the various field measures and the subjective habitat condition scores. Importantly, the sampled plots group well into three different states that are related to the habitat condition of the project area. Potentially degraded plots are almost exclusively associated with S1, while plots that may be considered 'pristine' are generally associated with S3. As expected, the majority of plots fall between these two extremes, and are associated with S2. Estimated perennial plant cover and bare ground cover were found to be the two most important variables in distinguishing between the three latent states.

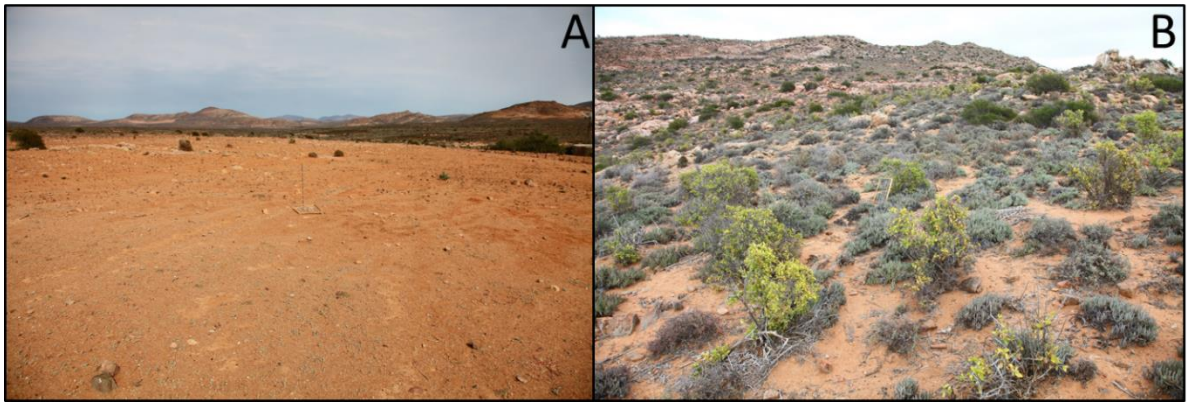

Figure 4.10. Examples of two field plots sampled between September and October 2017 that could represent degraded (A) and 'pristine' (B) extremes in habitat condition for the project area.

4.5.1 Indicator selection

Several potential indicators were identified in this project based on whether they reflect the condition of the veld, as well as whether they can be measured easily in the field. Potentially useful indicators suggested by the various publications listed in Table 4.1 were not included if their measurement was either too time consuming, or too technical for the purposes of a rapid field assessment. Indicators were also not considered if they were deemed inappropriate for the specific conditions of the Namaqualand

Hardeveld bioregion. As the overall aim of this project was to map the condition of the veld in the project area through the use of satellite imagery, another consideration for indicator selection was whether the measure is likely to correspond with the satellite data. If the aim of using satellite data was to map cover for the project area then field-based cover estimates are likely to be important measures with which to test the accuracy of the satellite data (Lausch et al., 2016). It is therefore useful that the field estimates of perennial plant cover and bare ground emerge as the most important variables from the latent class analysis. Although some of the other variables, including the succulent plant cover and diversity, the mean perennial plant height, and the dung count for each plot, were less important than the cover estimates, their association with the three latent states remains important. This is because any relationship between the satellite data and the latent states, or the field estimates of cover, that is investigated in chapter five of this thesis are also indicative of a relationship between the satellite data and these other variables.

4.5.2 Habitat condition of the Namaqualand Hardeveld bioregion

The distribution of the measured field variables illustrate what may be expected for a dryland environment, and the Namaqualand Hardeveld bioregion in particular, with a large proportion of the area sampled having lower overall plant biomass represented by relatively low overall plant cover, and short to medium sized shrubs (Luther-Mosebach et al., 2012; Mucina et al., 2006a). The mean perennial plant cover across the field plots was about 35% which would be considered normal for this dryland environment. The average mean perennial plant height of about 48 cm was also consistent with expectations (Luther-Mosebach et al., 2012). Although species diversity was not considered in this project, the number of leaf succulent species, and the estimated cover of succulent plants, also correspond well with what has been found previously. Alpha (within community) diversity has been found to be very high across Namaqualand, and particularly in the Hardeveld where a mean of between 90 and 115 species have been recorded at the 0.1 hectare scale (Cowling et al., 1989). A linear extrapolation of this ratio would result in around two to three species per 5 m x 5 m plot, as was found in the field data (see Figure 4.5G). Although the relationship between plot size and species diversity may not be linear (Crist et al., 2003), this

comparison serves to illustrate that the mean number of leaf succulent species across the field plots is more or less expected for the Hardeveld bioregion. As a result, an occurrence of more than two leaf succulent species in the project area could illustrate higher than average succulent diversity, and be indicative of veld in above average condition. The field data therefore appears to represent the broad vegetation characteristics of the Hardeveld bioregion and provides a good approximation of the range of condition possible in this environment.

4.5.3 Variables for comparison with Earth observation data

Posterior probabilities

The archetypal approach to mapping requires the development of a group of models for the area that represent a conceptual understanding of the landscape under different ecological conditions (Cullum, 2014; Cullum et al., 2016a). It is advantageous that the field plots across the project area are grouped statistically into three states that could represent three different potential condition classes for the bioregion. State one (S1) includes plots with indicator measures predicted to characterize a potentially degraded landscape (low plant cover, few or no succulent species present, high bare ground cover (Todd, 2009)), and has the potential to be used to approximate the 'degraded' side of a habitat condition continuum for the project area. State three (S3), on the other hand, was characterised by indicator measures more associated with a non-degraded landscape (high plant cover, higher succulent species cover and diversity, less bare ground (Bunning et al., 2011; Todd, 2009; Vågen et al., 2013b)), and could be used to approximate the 'non-degraded' end of the same continuum. There is very little overlap in the probabilities of a plot belonging to both S1 and S3. S1 and S3 could represent two sides of a potential spectrum in habitat condition, against which the rest of the project area can be compared. State two (S2) generally falls between states one and three with regard to the variables measured, and represents the larger group of plots in the project area that fall between the two extremes of potential condition. In order to categorise these plots at a finer scale, they can be classified by their degree of similarity to both ends of the habitat condition spectrum, represented by S1 and S3. Thus, information is not lost in the classification of the landscape as a whole.

Field variables

At the level of the field assessment, the number of leaf succulent species, the mean perennial plant height and dung count are important variables for establishing the habitat condition of the project area. Plots with no succulent plant species cover are associated with a potentially degraded landscape, and are important in separating S1 from both S2 and S3 (Figure 4.9). The mean perennial plant height increased from S1 to S3 with no mean estimates lower than 10 cm for either S2 or S3 (Figure 4.8F). Dung count also appears to be an important predictor of habitat condition in that many more plots in S3 have no livestock dung than in the other two states, while S1 has plots with the highest livestock dung counts (**Error! Reference source not found.**G). While a low dung count may not be indicative of the condition of the veld, a very high dung count suggests a potentially degraded landscape. This suggests that factors other than overgrazing may result in a degraded landscape in the project area, but that overgrazing is almost certainly an important driver of desertification in some locations. One potential factor that will impact the contribution of dung count to the separation of the three latent states is long-term legacy effects. Areas that have been ploughed, mined, or heavily grazed in the past are likely to have low perennial plant cover, and are unlikely to be heavily grazed in the present. These areas would therefore have low dung counts despite being degraded.

These variables are, however, unlikely to correspond well with the Earth observation data. The habitat condition archetype created in chapter 6 of this thesis is developed by considering both the variables which were found to be the most important in describing each condition extreme, as well as by the variables which best highlight the differences between these two extremes. Estimated perennial plant cover and the estimated cover of bare ground were the two most important variables in distinguishing between states one and three (Figure 4.9). This is unsurprising as these are the two variables most associated with the subjective assessment of the condition of most vegetated landscapes (e.g. Todd, 2009). Although there is significant overlap, in terms of the cover of bare ground, between S2 and S1 and S3 respectively, there was very little overlap between S1 and S3. Some of the plots in S1 had relatively low bare ground cover estimates of between 10 and 50% but this is likely a result of these plots having significant bare rock cover, and not high perennial plant cover. This would explain the relatively low cover of bare ground despite the plots being grouped into S1.

This observation is corroborated by the fact that there are no plots in S1 with less than 40% non-vegetation cover. There is no overlap in perennial plant cover between S1 and S3 as no plots in S1 have more than 20% perennial plant cover, and no plots in S3 have less than 35% perennial plant cover (**Error! Reference source not found.**A).

Vegetation cover has been found to be significantly related to the condition of the veld in Namaqualand (Todd, 2009). In a field-based assessment of degradation in the Namakwa District, Todd (2009) developed an Ecological Indicator Value (EIV) for each species in his study based on the South African Department of Agriculture's Grazing Index Values (GIVs). GIVs are an indication of a species productive value for livestock and are derived from an understanding of the species nutritional value, its ability to provide palatable fodder, and its ability to hold and bind soil (du Toit, 2000; du Toit et al., 1995). Despite being a good predictor of the agricultural productive potential of vegetation, GIVs are not always a good predictor of the overall condition of the vegetation. Thus, Todd (2009) developed EIVs to take into account the broader ecological value of the species and provide a better predictor of veld condition more generally. He found a significant positive relationship between total plant cover and EIVs across the different communities within the Namakwa District (Todd, 2009). This suggests that, as vegetation cover increases, so too does the condition of the veld. This relationship can, however, be skewed by the presence of land degradation indicator species such as *Galenia africana*. This species has been found to colonise disturbed areas after clearing or overgrazing, forming a relatively homogenous composition for the area. *G. africana* is not only unpalatable, and sometimes toxic, to livestock but has also been found to potentially change the soil conditions where it grows, preventing the establishment of other species (Allsopp, 1999). Thus, high percentage cover of this species would indicate a potentially degraded landscape, and would not correlate with an increase in veld condition. As a result, cover of this species was excluded from the perennial plant cover field estimates, and included as a variable on its own in the original data sheet used for this project's field work phase.

4.6 Conclusion

The condition of the veld in the Namaqualand Hardeveld bioregion of the Succulent Karoo biome can be reliably estimated by considering a handful of important indicators

related primarily to the cover types present in the area, the presence of leaf succulent species, and the potential differences in grazing pressure to which different areas have been subjected. These indicators all contribute to the classification of each plot into one of three latent states. Importantly, for the purposes of comparing these latent states to Earth observation data, the probabilities of each plot belonging to each latent state have been determined. This provides continuous variables which are subsequently predicted by the Earth observation data in chapter five of this thesis. In the case where these probabilities did not result in a good model fit, the most important field variables from the latent class analysis (bare ground cover, non-vegetated cover and perennial plant cover) were used as response variables in their place. As a result, the probabilities of belonging to S1, S2 and S3, as well as estimated perennial plant cover, non-vegetated cover, and estimated bare ground cover, are used in chapter five to determine what remote sensing derived measure best corresponds to the condition of the veld in the project area.

Chapter 5:

5. Correspondence of Earth observation data with field data

5.1 Introduction

The use of remote sensing technology, and its applications, for land degradation and desertification assessment and monitoring have long been considered a useful alternative to often costly, labour-intensive, and spatially- and temporally-limited field measures of plant biophysical variables (Alavipanah et al., 2010; Chikhaoui et al., 2005; Liaqat et al., 2017; O'Connor et al., 2015; Okin et al., 2001; Salih et al., 2017; Somers et al., 2010). Remote sensing techniques are most often based on a quantification of vegetation density or productivity as a proxy for the complex dynamics that take place in a degrading landscape (Chabrillat, 2006). They take advantage of the diverse spectral reflectance values that different land-cover types exhibit across a number of spectral wavelength bands. The number of spectral bands used, and the manipulation of band values into meaningful productivity estimates, depends both on the remote sensing technique that is considered, as well as the known land cover dynamics in the area of interest. Calculated from only two spectral bands, the normalised difference vegetation index (NDVI), for example, has often been used as a proxy for primary productivity in savanna ecosystems (e.g. Diouf and Lambin, 2001; Wessels *et al.*, 2006; Hoscilo *et al.*, 2015; Georganos *et al.*, 2017). In ecosystems where soil reflectance may influence the spectral signal, however, indices such as the soil adjusted vegetation index (SAVI) have been developed (Huete, 1988). Various three band indices have also been developed in an attempt to enhance the sensitivity to vegetation change and reduce the impact of noise from both atmospheric condition and soil. Among these, the enhanced vegetation index (EVI) has often been used for more densely vegetated areas such as tropical rainforests (e.g. Samanta et al., 2012; Zhou et al., 2014). While initial calculations for the determination of various vegetation indices made use of two or three spectral bands only (usually red, infrared and blue) more recent techniques, such as spectral mixture analysis (SMA), have been developed to take advantage of the full spectral signal derived from satellite imagery.

Such approaches are thought to be more sensitive to vegetation changes on the ground (Caixeta, 2016).

5.1.1 Satellite imagery

Resolution

Understanding the resolution of available satellite imagery is key to determining the imagery that is best suited to the study aims (Dalsted et al., 2003; Nagendra, 2001). The four types of resolution that are important when discussing satellite imagery are radiometric resolution, spatial resolution, spectral resolution, and temporal resolution (Lefsky and Cohen, 2003). Radiometric resolution describes the sensitivity of the imagery to differences in electromagnetic energy. The finer the radiometric resolution of satellite imagery the better it is at discerning small differences in reflected or emitted energy. Radiometric resolution is recorded as the bit depth of the imagery, which ranges from 0 to any selected power of 2 and represents the number of brightness levels available (Lefsky and Cohen, 2003). 2-bit imagery therefore has four potential brightness values ($2^2 = 4$), while 8-bit imagery has 256 potential values ($2^8 = 256$). The brightness values can be thought of as the varying shades of any given band (Alavipanah et al., 2010). Each pixel in a 2-bit panchromatic (black and white) image will, for example, be one of four shades of grey. The blue band in an 8-bit multispectral image, on the other hand, could be represented by 256 different shades of blue.

Spatial resolution of satellite imagery is defined as the pixel size of the image, representing the size of the surface area being measured on the ground (Nagendra, 2001). For example, the pixels from Advanced Very High Resolution Radiometer (AVHRR) data are approximately one kilometre long by one kilometre wide, while the pixel size of GeoEye-1 satellite imagery is only 41 x 41 centimetres, representing one of the highest spatial resolution datasets available from commercial satellites today (www.digitalglobe.com). The spatial resolution of imagery impacts on the level of detail that can be observed. It is recommended that the spatial resolution of the chosen imagery corresponds reasonably closely with the sampling area and plot size of field-based assessments, or ground-truthing exercises (Alavipanah et al., 2010; Dalsted et al., 2003). Imagery with one-kilometre spatial resolution is, for example, inappropriate where field plot size is one square metre as details in the field will be lost in the satellite

imagery. Equally, however, imagery with 41 centimetre spatial resolution data may not correspond well with field data taken from 10 m^2 plots (Anderson, 2018).

Spectral resolution is determined by the number of spectral bands, and the width of each band, in the satellite imagery (Campbell, 1996). Panchromatic imagery, for example, only has one band which would allow for only a black and white display. Normal colour images use the three bands within the visible spectrum (red, green and blue), while multispectral imagery includes four or more bands. Hyperspectral imagery has the highest spectral resolution of satellite imagery and utilises hundreds of distinct spectral bands. All ground-based objects have a spectral response curve, or unique spectral signature, which can be improved if multiple bands are used (Alavipanah et al., 2010). While it might not be possible to separate bare ground from a parking lot in a panchromatic image, for example, once more bands are included the two land cover types will become more easily distinguishable.

The last type of resolution to consider is temporal resolution. This is the time interval between two identical flights over the same area (Lefsky and Cohen, 2003). It is, therefore, the time interval between exact repeat images, taken from the same position and angle, of an area on the ground (Nagendra, 2001). A higher temporal resolution allows for more short-term changes on the ground to be detected, while a lower temporal resolution may only allow for more long-term change to be observed. Landsat satellites, for example, have a temporal resolution of 16 days which allows for an almost bi-monthly assessment of an area (Xie et al., 2019). This allows for seasonal vegetation change to be detected, as well as more sporadic change resulting from isolated rainfall events. SPOT images, on the other hand, have a revisit interval of only two days allowing for very specific vegetation change detection in response to rainfall or land use change (Dalsted et al., 2003).

Measuring change

One of the fundamental difficulties in land degradation monitoring and reporting, or any attempt to establish the ecological condition of an area, is that field data collected at one point in time can only provide a snapshot of the condition of that particular landscape at that time. As a result, condition assessments need to consider both the long- and short-term historical changes that have occurred in any given landscape. There are, however, very few reliable long-term monitoring projects globally from

which to estimate changes on a larger scale (Prince et al., 2018). As a result, changes in measures derived from remote sensing imagery have been used to develop an idea of the potential changes in vegetation that have taken place on the Earth's surface over the past forty years or so (Burrell et al., 2017; de Jong et al., 2011; Holden and Woodcock, 2016; Jönsson and Eklundh, 2004; Wessels et al., 2004). The amount of time that can be assessed is limited by how long the specific satellite programme or platform has been operational, with the longest continuous satellite record of the Earth's land surface, the Landsat Program, dating back to 1972 (NASA, 2020). Changes to the Earth's surface that occurred before 1972, therefore, cannot be monitored directly through the use of remote sensing imagery (Xie et al., 2008). Even Landsat data from the 1970s, 80s and 90s is problematic in that is doesn't cover the entirety of the Earth's land surface. The life span of individual satellites, and the history of different satellite programmes therefore needs to be considered when choosing satellite data for any Earth observation analysis (Cherlet et al., 2018).

Choosing appropriate imagery

The different types of resolution in satellite imagery are not independent of each other and, as a result, trade-offs need to occur in the development of a satellite image sensor (Kennedy et al., 2009). For example, a small instantaneous field of view (IFOV) is needed to produce imagery with high spatial resolution. The small IFOV, however, limits the amount of energy that can be detected and thus results in a lower radiometric resolution. Although it is possible to produce imagery with high spatial and radiometric resolutions, this can only be accomplished by broadening the wavelength range for particular bands, and therefore reducing the spectral resolution of the imagery (NRCAN, 2016). Different satellites also travel in different orbits around the Earth, some closer to the Earth's surface, and others further out. This not only impacts the spatial resolution of the imagery, but also the temporal resolution as the orbit path of a satellite affects how long it takes to orbit the Earth, and therefore how often it can take an image of the same point on the Earth's surface (Sabins, 1987). The compromises that are made in the development of satellite sensors and the orbits the satellites take influences the selection of which satellite platform to use for any given study (Kennedy et al., 2009; Lefsky and Cohen, 2003).

Another limitation on the use of satellite imagery is the availability of the imagery. Much high-resolution satellite data collected largely by privately owned satellite platforms

needs to be purchased and is not available within the budgetary constraints of most research programmes, especially those from developing country institutions. Several platforms have provided data free of charge but the costs of downloading, processing and storing the data have historically been costly both in terms of time and digital space. The recent development of Google Earth Engine has, however, eliminated many of the issues associated with downloading and processing satellite data. This freely available and widely used tool consists of a multi-petabyte satellite data catalogue with over 350 raster datasets, along with a computation service to access and manipulate the data (Gorelick et al., 2017). The data catalogue includes a wide variety of sources for climate and weather data, satellite imagery (Landsat, Sentinel, Modis, etc.), and geophysical data. Data acquisition and manipulation is performed using Python or JavaScript coded scripts. These scripts 'outsource' computations to the Google cloud, which run commands externally before returning a result that can then be printed or exported for display or further analysis. Google Earth Engine saves an unprecedented amount of time, computer processing power and storage compared to more traditional satellite data acquisition and processing techniques that generally require large datasets to be downloaded and processed on one's own computer (Xie et al., 2019).

5.1.2 Remote sensing measures of vegetation cover

Normalised difference vegetation index

As discussed earlier in chapter two, the vast majority of remotely sensed land degradation assessments, as well as attempts to either map cover type or estimate plant percentage cover in arid and semi-arid environments, have utilised a vegetation index of some form or other. A range of vegetation indices have been developed from different wavelength (band) combinations. The normalised difference vegetation index (NDVI), as discussed in Chapter 2, is the most commonly used example (**Error! Reference source not found.**), where NIR = reflectance in near infrared band, RED = reflectance in red band.

$$NDVI = \frac{NIR - RED}{NIR + RED} \quad (1)$$

In arid and semi-arid areas, however, calculations based on NDVI do not always correlate well with field-based measures of plant biomass or production (Chabrillat,

2006). This is partly because bare ground (or bare rock) has the potential to distort the spectral reflectance values of the area and alter the NDVI reading. It is also partly a result of NDVI being sensitive to the amount of chlorophyll present, and if chlorophyll amounts are generally low then NDVI may not be able to distinguish differences in the amount of vegetation or biomass present (Chabrillat, 2006).

Alternative indices

As a result of the limitations associated with NDVI, several alternative indices have been developed. Although many of these indices continue to rely on the normalised difference between the red and infrared wavelengths, they include modifications to the NDVI calculation that attempt to reduce much of the signal noise associated with either atmospheric or soil conditions.

The enhanced vegetation index (EVI) is one such example that has been developed to improve on NDVI, and predict vegetation cover more accurately. This index was specifically designed to be more sensitive to changes in vegetation in areas with high biomass, to reduce the influence of atmospheric conditions, and to correct for canopy background signals. EVI has been found to be more responsive to canopy features such as leaf area index and canopy type than chlorophyll (Gao et al., 2000). This may be beneficial in Namaqualand where canopy features may differ more significantly across the project area than the amount of chlorophyll. The EVI equation therefore contains several important differences when compared to the NDVI equation (**Error! Reference source not found.**), where NIR = reflectance in near infrared band, RED = reflectance in red band, Blue is the reflectance in the blue band, C1 and C2 are coefficients of the aerosol resistance term, and L is the canopy adjustment factor (Huete et al. 1994; Huete et al., 1997).

$$EVI = G \times \frac{NIR - RED}{(NIR + C1 \times RED - C2 \times Blue + L)} \quad (2)$$

The soil adjusted vegetation index (SAVI) was developed specifically to reduce the impact that the soil background effect has on NDVI (Huete 1988). In order to accomplish this, a soil-adjustment factor was added to the NDVI equation (**Error! Reference source not found.**), where NIR = reflectance in near infrared band, RED = reflectance in red band, and L = soil adjustment factor (0.5) (Huete, 1988).

(3)

$$SAVI = NIR - \frac{NIR - RED}{NIR + RED + L} \times (1 + L)$$

Huete (1988) found the optimal soil-adjustment factor (L) to vary with vegetation density between 0 and 1, but ultimately suggested using a constant L = 0.5 to reduce soil noise considerably over a wide range of vegetation densities. If, however, one has prior knowledge of vegetation cover for the area or the ability to develop an iterative function, a more accurate value for L can be determined for any given study area. Huete (1988) found the optimal value to decrease with increasing vegetation density and cover. Subsequent authors have made further adjustments to either the NDVI or SAVI equations, including the optimised soil adjusted vegetation index (OSAVI – **Error! Reference source not found.**) ((Rondeaux et al., 1996)) and the modified soil adjusted vegetation index (MSAVI - **Error! Reference source not found.**5), where NIR = reflectance in near infrared band, and RED = reflectance in red band (Qi et al., 1994; Rondeaux et al., 1996). MSAVI was developed under the premise that L should vary inversely with the amount of vegetation present so the L constant in the SAVI equation has been replaced with a variable L function ((Qi et al., 1994)).

$$OSAVI = NIR - \frac{NIR - RED}{NIR + RED + 0.16} \quad (4)$$

$$MSAVI = \frac{2NIR + 1 - \sqrt{(2NIR + 1)^2 - 8(NIR - RED)}}{2} \quad (5)$$

Spectral mixture analysis: An alternative approach to vegetation indices

The use of vegetation indices relies on the assumption that spectral reflectance values of live green vegetation, soil and other potential land-cover types differ to the same extent across different regions with highly variable plant cover and type. Spectral mixture analysis (SMA) is seen as an alternative approach to the use of vegetation indices where, instead of using specific bands, SMA uses the full spectral signal available in the visible near infrared to shortwave infrared (VNIR-SWIR) range (Chabrillat, 2006; Thorp et al., 2013). Underlying SMA is the assumption that all the pixels within a given image of a landscape are a linear combination of a finite number

of dominant features, referred to as endmembers (Okujeni et al., 2013). These endmembers are assumed to have relatively constant spectral properties which allows for an unmixing analysis to calculate the percentage cover of each endmember in each pixel (Yang et al., 2012). Thus, the designation of accurate endmembers is fundamental to a useful SMA, as is the inclusion of endmember values for all cover types likely to be present within a given pixel, e.g. shade, soil, live vegetation, dead vegetation, paving, rock, etc. (Okin and Roberts, 2002).

The sparse vegetation cover present in arid and semi-arid areas around the world can make the use of SMA and related techniques problematic. Okin et al. (2001), for example, showed that the use of SMA in areas where vegetation cover is less than approximately 30% was nearly impossible, and suggested an alternative approach: multiple-endmember spectral mixture analysis (MESMA) (Okin et al., 2001; Okin and Roberts, 2002; Roberts et al., 1998). One of the major limitations of the SMA approach is that all the pixels in an image are unmixed using the same endmembers. This can become problematic when a feature is only present in certain portions of the image and is not an appropriate endmember for every pixel, or when a feature (e.g. live vegetation) exhibits significant spectral variation which cannot be well represented by one endmember observation (Thorp et al., 2013). MESMA addresses these potential pitfalls by testing multiple combinations of endmembers and endmember spectra for each pixel in the image (Roberts et al., 1998). MESMA is a modified SMA approach where a library is developed containing the spectra of all possible cover types for the image. Including more than one spectral endmember for a potential cover type in an image allows for the considerable spectral variability often found in arid- adapted vegetation and soils. This, therefore, highlights the potential of the approach to address the many difficulties associated with remote sensing applications in arid and semi-arid areas (Okin and Roberts, 2002; Okin et al., 1999). Work conducted through the Humboldt University of Berlin's Earth Observation Lab, in particular, has highlighted the benefits of adopting a spectral unmixing approach for land cover mapping in different environments (Higginbottom et al., 2018; Hostert et al., 2003; Senf et al., 2020; Sonnenschein et al., 2011).

Endmember spectral values can be obtained from field or from laboratory measurements (reference endmembers), or from the image itself (image endmembers), provided each plausible cover type is represented at least once (Okin

et al., 1999; Roberts et al., 1998). The designation of reference endmembers is considered to be the optimal approach for MESMA (Wu and Murray, 2003). However, image endmembers are considered a viable alternative, and are associated with several advantages over reference endmembers. Image endmembers, for example, contain the same systematic errors due to image processing (atmospheric correction, etc.) as the image which is to be unmixed (Settle and Drake, 1993). Image endmembers are also derived at the same scale as the original image, negating potential scaling errors (Myint et al., 2009). Various studies have highlighted the benefits of using a spectral unmixing approach with multiple endmembers for vegetation mapping over the use of broadband vegetation indices like NDVI (de Jong and Jetten, 2007; Elmore and Mustard, 2000; Mcgwire et al., 1992; Okin and Roberts, 2002; Sonnenschein et al., 2011; Yang et al., 2012).

5.2 Methods

5.2.1 Data collection: remote sensing

All remote sensing data for this project were obtained through the Google Earth Engine cloud-based platform (Figure 5.1) (Gorelick et al., 2017). A number of filters were applied to all the satellite data, depending on the type of computation performed (see Appendices B-E). All data were subject to a cloud masking algorithm which removed those pixels likely to reveal the presence of significant cloud cover, and therefore not be representative of the ground surface reflectance. From the start, all data were filtered to the geographic extent of the project area to reduce the amount of computing power required to perform each calculation. At this time, it was also possible to select the specific bands within the satellite image that were to be used for each computation (Appendices B-E).

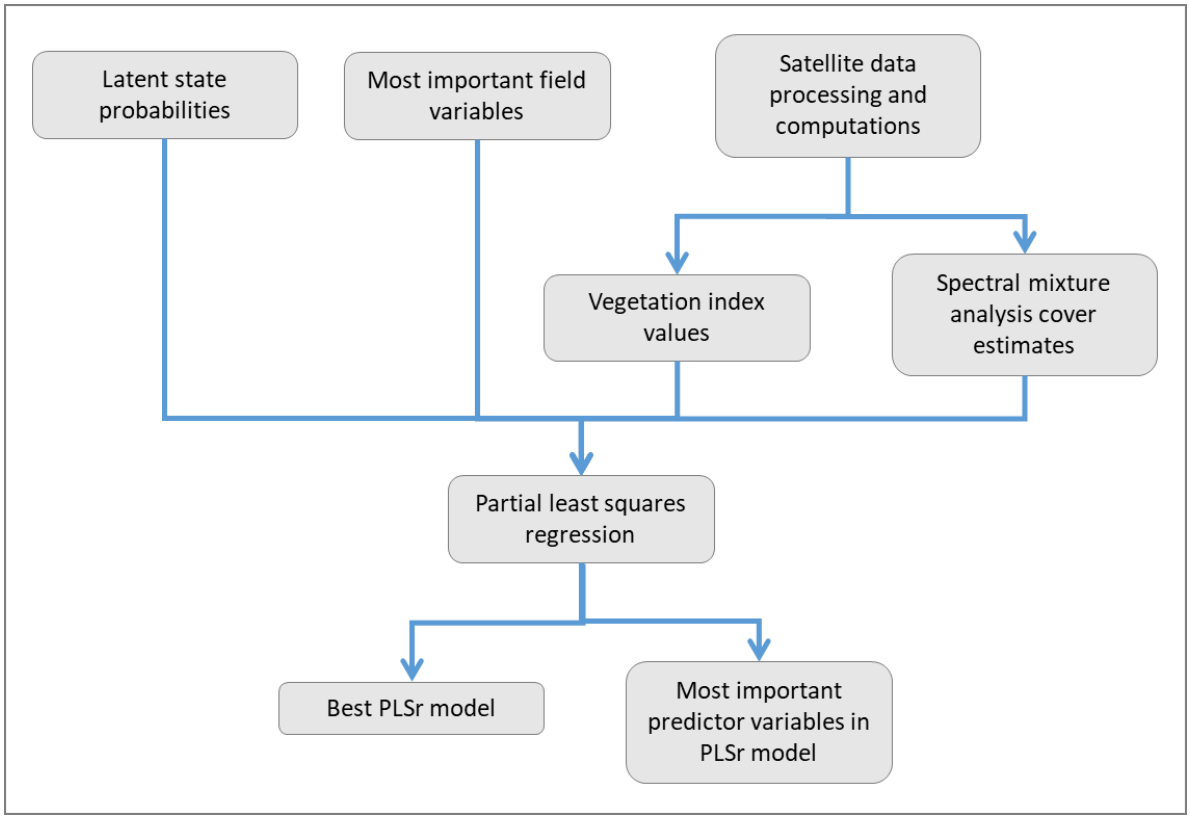

Figure 5.1. Flow diagram illustrating the methodology employed to collect and analyse the satellite data and test correspondence with the field data.

Satellite platforms

As discussed above, the choice of satellite platform for any given project needs to take into account several factors including the desired resolution of the satellite imagery. In order for the methods developed here to be useful and adaptable within the wider context of the world's drylands it was decided that the satellite imagery used needs to be freely available. The spatial resolution of the imagery should correspond as closely as possible with the 5 x 5 m field plots sampled, and the temporal resolution must allow for at least seasonal vegetation change in the project area to be detectable. The spectral resolution should at least include those bands used in the development of the various vegetation indices, while the radiometric resolution must be fine enough to pick up relatively subtle differences in reflected electromagnetic energy that are likely in an arid environment like Namaqualand. Landsat and Sentinel-derived Earth observation data were therefore used for this project (Table 5.1), along with topographic data obtained from the Shuttle Radar Topography Mission (SRTM) digital elevation dataset.

Table 5.1. Four resolution types for both Landsat and Sentinel satellite data.

Satellite platform		Radiometric resolution	Spatial resolution	Spectral resolution	Temporal resolution	Availability
Landsat	1-4	4-bit	30 – 60 m	4 bands (0.5-1.1 µm)	16 days	1972 – 1978
	5	10-bit	30 m	7 bands (0.45-0.60, 0.63-0.69, 0.76-0.90, 1.55-1.75, 2.08-2.35, 10.4-12.5 µm)	16 days	1984 – 2012
	7	10-bit	30 m	8 bands (0.45-0.60, 0.63-0.69, 0.77-0.90, 1.55-1.75, 2.08-2.35, 10.4-12.5 µm)	16 days	1999 – 2020
	8	12-bit	15 – 30 m	11 bands (0.43-0.90,1.36-1.38, 1.57-1.65, 2.11-2.29, 10.60-11.19, 11.50-12.51 µm)	16 days	2013 - 2020
Sentinel-2		12-bit	10 – 60 m	12 bands (± 0.4-2.2 µm)	5 days	2015 – 2020

The Landsat programme provides some of the most widely used satellite imagery across scientific disciplines, and particularly within the ecological sciences (e.g. Brown De Colstoun et al., 2003; Mandanici and Bitelli, 2016; Midekisa et al., 2017; Vågen et al., 2013a; Xie et al., 2019; Yang et al., 2012; Zhu and Liu, 2015). The low spectral and spatial resolution of Landsats 1 – 3, relative to the later platforms, resulted in only imagery from the last four Landsat satellites being considered for this project. Landsats 4 and 5 were launched in 1982 and 1984 respectively, and both carried the Landsat MSS as well as the Landsat Thematic Mapper (TM). The Landsat TM produces imagery consisting of six spectral bands at a 30 m spatial resolution. Landsat 6 failed to launch in 1993 which means that Landsat 7 is the next available platform from the programme. Landsat 7 carries the Landsat Enhanced Thematic Mapper Plus (ETM+), producing seven spectral band imagery with a spatial resolution of 30 m, as well as a panchromatic band with a spatial resolution of 15 m. Although the Scan Line Corrector

on Landsat 7 failed in 2003, data from the platform is still useful for Earth observation. For Landsat 8, Operational Land Imager (OLI) and Thermal Infrared Sensor (TIRS) imagery consists of nine spectral bands with a spatial resolution of 30 m, a panchromatic band with a 15 m spatial resolution and two thermal bands with a spatial resolution of 100 m. Landsat 4, 5, 7 and 8 data therefore provide the best opportunity to gather time series information at a spatial resolution that corresponds well with the field plots in this study (Table 5.1). An added advantage of these Landsat data is that they have a relatively good temporal resolution of 16 days for many parts of the Earth's surface. Scenes are repeated between 22 and 23 times a year, and the timing of changes in the Earth's ground reflectance can be monitored (NASA, 2020).

The Sentinel missions, which form part of the Copernicus programme under the European Space Agency, are much younger than Landsat, with the first Sentinel satellite (Senitnel-1A) launched in April 2014 (ESA, 2020). Sentinel-1 is, however, a radar imaging mission, while Sentinel-2 provides multi-spectral high-resolution imaging for Earth observation. Sentinel-2A was launched in June 2015 while Sentinel-2B was launched in March 2017. Both satellites carry a single multi-spectral instrument (MSI) with 13 spectral bands in the visible/near infrared (VNIR) and short wave infrared spectral range (SWIR). Spatial resolution of Sentinel-2 data is 10 m for bands 2, 3, 4 (visible) and 8 (near infrared), which are the bands most used for vegetation mapping (Table 5.1). Sentinel does not currently provide useful data for long-term time-series analysis, but it does have the advantage of having a higher spatial resolution than Landsat. Index values from both satellite platforms can, therefore, be compared as to how well they correspond to the current condition of the veld, and the best index values can be used to determine the trajectory of change from 1984 for Landsat, and from 2015 for Sentinel.

Index values

Generally, vegetation mapping projects, including habitat condition and land degradation assessments, tend to choose or develop one index that is considered the best proxy for vegetation productivity for that location. By using this approach, the advantages of incorporating information from other indices are lost. NDVI may, for example, be found to be the best proxy for vegetation biomass over an entire project area but it may be the case that SAVI proves to be a better proxy for pockets of land with relatively sparse vegetation cover. As a result, while most of the area will be

relatively well mapped, those areas with low cover may not be. The vegetation index values derived for this thesis were calculated to reflect the habitat condition of the landscape at the time the field data was collected. Generally, this would require the generation of data from a satellite scene obtained as close to the same time as the field data was collected. However, a median value can also be derived over a longer time period provided that the landscape has not changed significantly over that period. If comparing productivity between growing season and non-growing season, for example, a median value could be derived from each season and compared. Since the data collection for this thesis took place during a drought year, a median value could be obtained for a longer time period as the value would not have fluctuated significantly. The benefit of deriving a median value, as opposed to calculating an averaged or blended value, is that the median is generally robust against extremes and avoids potential outliers in the data (Xie et al., 2019). A value for each plot for each of the five indices, NDVI, EVI, SAVI, OSAVI and MSAVI, was therefore determined by calculating the median index value for the period between 1 January 2017 and 31 October 2017, for both Landsat 8 and Sentinel-2 data (Appendices B & C). The time period was limited to 2017 so as not to incorporate any values that were uncharacteristically high as a result of previous rainfall events prior to the drought. Although the spatial resolution of 30 m of Landsat 8 imagery is larger than the size of the field plots (5 x 5 m), efforts were made to sample plots in the field in relatively homogenous landscapes such that the spectral signal of the Landsat imagery was representative of the ground cover of the individual plot. Vegetation index values calculated from Sentinel-2 data, however, may provide a better proxy for vegetation productivity of the plot due to this satellite's smaller spatial resolution at 10 m.

Spectral unmixing

Spectral unmixing is an example of a spectral transformation method. A predetermined number of endmembers, represented by pixels corresponding to different land-cover types, are used to determine the proportional area occupied by each land-cover type in all other pixels. This method relies on the assumption that the spectra of all the land-cover types in a pixel combine linearly. The weighting coefficients of each spectral endmember, which sum to one for each pixel, are interpreted as the proportional area occupied by each land-cover type in a pixel (Okin and Roberts, 2002). In order to optimise the accuracy of the analysis, models must include all land-cover types likely

to be present in a pixel. Endmember values were, therefore, determined for three broad categories within the project area: bare ground, bare rock, and vegetation cover.

Endmember selection

Endmember values were derived directly from the available satellite imagery. In order to locate areas with as close to 100% cover for each of the three land-cover types, the field data described in chapter four were used to initially guide where endmembers should be located. The field data were sorted by each of the land-cover types and the plots with the highest percentage cover estimates were noted. These were then used to locate areas that appeared visibly homogenous on Google Earth imagery. Polygons were drawn around observably homogeneous areas and classified as one of the three land-cover types. Several polygons were drawn to represent each land-cover type, and the mean spectral value for all the polygons of each type was used as the spectral endmember. These values were then used in the unmix() function available in Google Earth Engine to determine the proportional estimate of each cover type for each pixel in the project area (Appendices D & E). The relevant arguments were applied in order to constrain the outputs to both be non-negative and to sum to one.

5.2.2 Data analyses

Preliminary correspondence with field data

Vegetation index and spectral mixture analysis (SMA) values for the 277 field plots were exported from Google Earth Engine for analysis in R (R Core Team 2019). Posterior probability values for latent class states S1, S2, and S3, as well as the values of the three most important field variables from the LCA in chapter four were joined with the Earth observation data. From this exercise each plot could then be assigned a designated state, a value representing the probability of belonging to each of the three states, and a value for each field variable and for each remote sensing variable. A multivariate approach to analysing the data was needed due to the large number of predictor variables, as well as the multiple response variables. Before the multivariate analysis was performed, however, a series of Kruskal-Wallis rank sum tests were carried out to determine whether the values of the remote sensing variables differed significantly across the designated latent class states. If a significant difference was

found, then, as with the analysis in chapter four, a multiple pairwise comparison test was performed to determine where this difference lay. In order to visualise the relationship between the field-based cover estimates and the remote sensing indices and SMA cover estimates, a series of scatterplots were created. The statistical significance of these relationships was determined through the multivariate analysis described below.

Partial Least Squares Regression

Partial least squares (PLS) methods were first developed primarily to address issues of collinearity in multivariate analyses (Wold et al., 1984). The methods have been used subsequently as an alternative to other regression methods in ecology (Abdi, 2010; Carrascal et al., 2009; Serbetar, 2012). Partial least squares regression (PLSr) is an extension of multiple regression analysis which allows for the effects of linear combinations of several predictor variables on one or more response variables to be analysed (Carrascal et al., 2009). PLSr, therefore, has several advantages over multiple regression in that it can be used on multicollinear data. Also, a large set of predictor variables can be used, and more than one response variable can be included in the same model (Nash and Chaloud, 2011; Serbetar, 2012; Wold et al., 1984). Collinearity has been found to be an issue in the analysis of multiple remote sensing vegetation indices as these indices are often highly correlated (Zhu and Liu, 2015). This could be particularly problematic in Namaqualand as not only is there the potential for different index values (e.g. NDVI and SAVI) to be highly correlated, but the same index values calculated from different satellite platforms (Sentinel and Landsat) are also likely to be correlated. The use of PLSr circumvents this potential limitation. The response variables in this project were either the respective probabilities of belonging to any one of the three states from the latent class analysis, or the field variables found to be most important in predicting these states. The advantage of being able to include more than one response variable in the PLSr model was of considerable benefit to this analysis.

Partial least squares regression was performed in R (R Core Team, 2019) using the plsdepot package (Sanchez, 2012). The aim of the analysis was to determine which remotely derived variables best predict either the probabilities of belonging to S1 and S3 or the percentage cover estimates of the three most important variables as determined from the Latent Class Analysis (LCA) outlined in chapter four (bare ground,

non-vegetated cover, perennial plant cover). The plsdepot package provides a general framework for partial least squares (PLS) analysis in R, with the plsreg2 function allowing for multiple response variables. A series of models were run with different response and predictor variables to determine which combination of variables produced the best model fit. Model fit for each run was determined by the model's Q^2cum (cumulative Q^2) value, while the model's predictive accuracy was determined by the cumulative explained variance of the predictor variable (R^2Ycum). Explained variance was used to evaluate the accuracy (goodness of fit) of the model and represented the amount of variance explained for either the dependent variables (R^2X) or the independent variables (R^2Y) (Hair et al., 2014; Xiaosong and Lai, 2012). Chin (1998) proposed R^2Y values of 0.67, 0.33, and 0.19 as being substantial, moderate, and weak respectively (Chin, 1998; Xiaosong and Lai, 2012), while others suggest a rough rule of thumb of 0.75, 0.50, and 0.25 respectively describing substantial, moderate, and weak levels of model accuracy (Henseler et al. 2009; Hair et al. 2011; Hair et al., 2014). Q^2 is a measure of the difference between the predicted and original values of the response variables (i.e. the predictive accuracy of the model), with a higher Q^2 being indicative of a smaller difference between these values (Hair et al., 2014). If $Q^2 > 0$ then the model is viewed as having predictive relevance, while if $Q^2 < 0$ this indicates a lack of predictive relevance (Henseler et al., 2009; Xiaosong and Lai, 2012). Although a Q^2 value greater than zero indicates that an endogenous construct can be predicted, it does not necessarily point to the quality of the prediction (Hair et al., 2014; Rigdon, 2014; Sarstedt et al., 2014). The cumulative Q^2 value (Q^2cum) represents the predictive accuracy of the model across all the components in the model.

Model selection

Model selection was performed by initially determining the best response variables and then the best predictor variables. The first model included the 16 remote sensing variable values for each plot as predictor variables and the respective probabilities of each plot belonging to each of the three latent states as response variables. The next iteration had the same predictor variables but only included the probabilities of belonging to S1 and S3 as the response variables. To determine whether the actual field estimates of cover are better predictors of the various remote sensing variables, the next model included the same predictor variables with the three field estimates as

response variables. The next model only included the field estimates of bare ground and perennial plant cover as response variables. Once the model with the highest Q^2cum and R^2Ycum values was established, the least important remote sensing variables were removed from subsequent iterations to determine if this improved overall model performance. The importance of the individual predictor variables was established by considering their respective standardised coefficient values as well as their variable importance for projection (VIP) values. The greater these values are for each variable relative to the other variables in the model, the more important the variable is in predicting the response variables (Serbetar, 2012). Variables with low standard coefficient and VIP values were therefore excluded from the next model run. If this exclusion resulted in a better model fit and accuracy, then the new model was retained.

Projection of PLSr model to the project area

Once the best model was selected, it was then used to predict the response variables over the project area. The plsdepot package does not include the R predict() function that is often used for this purpose. Thus, the model regression coefficients and intercept values of the predictor variables were exported from R for each of the response variables. These were then mapped over the project area in Google Earth Engine and ground truthed with data from 61 field plots that were excluded from the original field data used for chapter four (Appendix G). This allows for a comparison between the individual variables and the final model prediction to determine whether individual variables are able to predict the condition of the veld better than the model, or vice versa.

5.2.3 Time series trend and variation

As Sentinel-2 data are only available from 23 June 2015, the platform is inappropriate for exploring more medium to long term change. Therefore, the Landsat-derived remote sensing variable that was found to correspond best with the condition of the veld was then analysed over time. This was accomplished by collating Landsat 5, 7 and 8 TOA (top of atmosphere) reflectance (Orthorectified) imagery to get an idea of change in the project area from 1984 to 2019 (Appendix F). Landsat 5 imagery was filtered to between 1 January 1984 and 1 January 1999, while Landsat 7 imagery from

1 January 1999 and 11 April 2013, and Landsat 8 imagery from between 11 April 2013 and 31 July 2019. The images from the three satellites were merged, using the ee.ImageCollection function in GEE, and sorted into chronological order from 1 January 1984 to 31 July 2019 to form an image collection of variable values. A linear fit reducer was applied to the image collection in GEE to determine the trend in condition in the project area since 1 January 1984. A raster image, which represents the value of the slope, was then exported from GEE.

5.3 Results

5.3.1 Preliminary correspondence with field data

The differences between the latent class states for each of the remote sensing variables were significant for all but two of the variables. These are Landsat 8 and Sentinel-2A SMA proportional estimates of rock cover (Figure 5.2 – L.Rock and S.Rock respectively). The Landsat 8 and Sentinel 2-A spectral mixture analysis proportional estimates of bare ground (L.Bare and S.Bare respectively) and vegetation (L.Veg and S.Veg respectively) were significantly different across all pairs of latent states ($p < 0.001$). All the Landsat 8 and Sentinel-2A 2017 index values had significant differences for all pairs of latent states ($p < 0.05$), except for the difference between S2 and S3 for Sentinel EVI (Figure 5.2 – S.EVI) ($p = 0.175$).

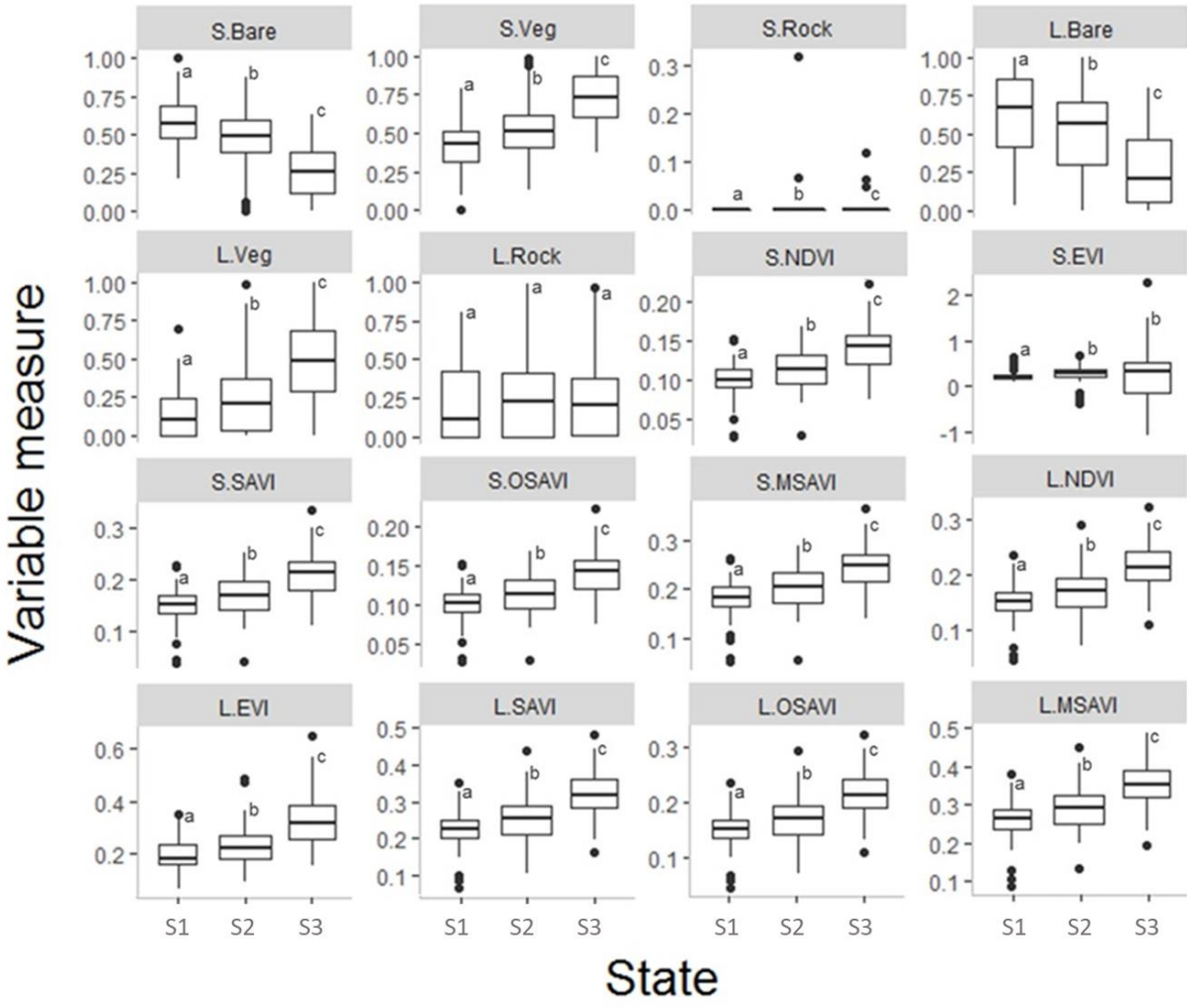

Figure 5.2. Satellite data-derived remote sensing variable measures grouped into the three latent states (S1, S2, S3) with letters indicating significant differences between states. L refers to Landsat 8 derived variables, S refers to Sentinel-2A derived variables; Bare, Veg, and Rock refer to spectral mixture analysis estimates of bare ground, perennial plant cover, and bare rock respectively; NDVI, EVI, SAVI, OSAVI, and MSAVI refer to the five vegetation indices mentioned in the methods section.

Scatterplots with regression lines reveal the general relationship between the 16 remote sensing variables included in the initial PLSr model and the three most important field variables determined from the latent class analysis in chapter four. As expected, many of the index-based remote sensing variables increase linearly with field-estimated perennial plant cover (Figure 5.3) and decrease linearly with both estimated bare ground cover (Figure 5.4) and estimated non-vegetated cover (Figure 5.5). The strength and significance of these relationships are determined through the PLSr analysis results presented below.

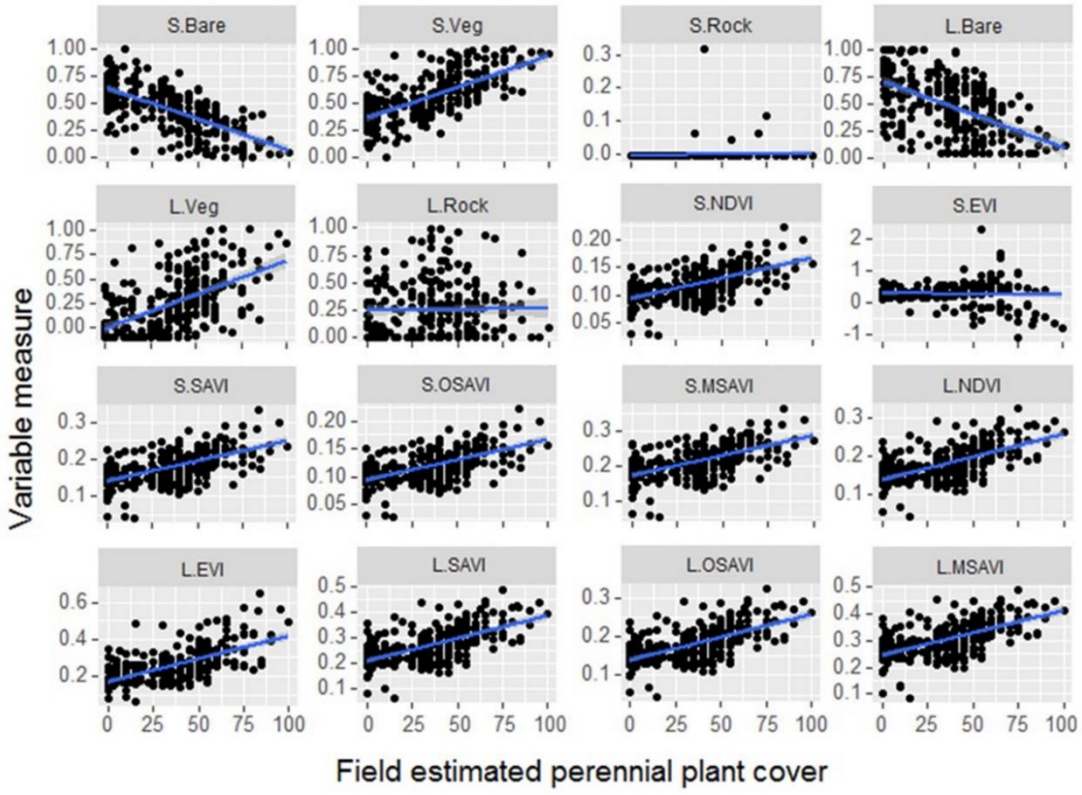

Figure 5.3. Remote sensing variable measures plotted against field-estimated perennial plant cover.

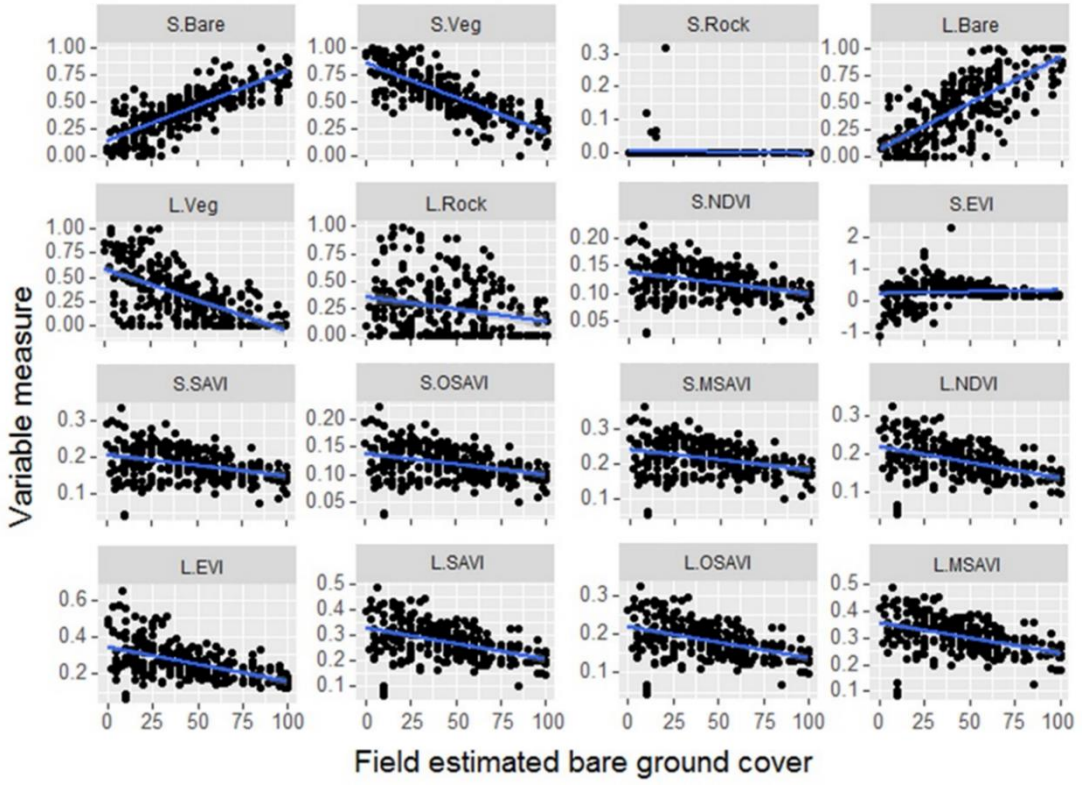

Figure 5.4. Remote sensing variable measures plotted against field-estimated bare ground cover.

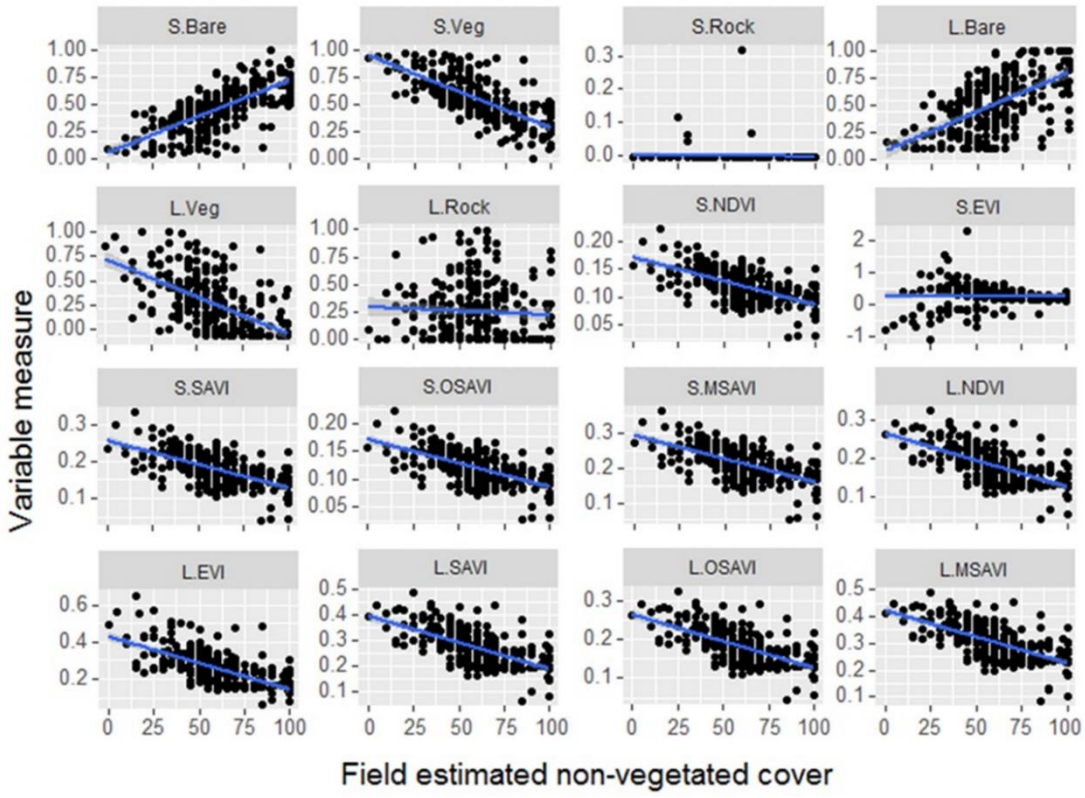

Figure 5.5. Remote sensing variable measures plotted against field-estimated non-vegetated cover.

5.3.2 Partial least squares regression

Variable determination and model selection

Model selection was performed as described in the approach and research design section, starting with a model with all 16 predictor variables and the three latent class variables as the responses (pls1 – Table 5.2). Field-estimated perennial plant and bare ground cover emerged as the best response variables (pls4). For the subsequent models, the least important remote sensing variables (as determined by standardised coefficient and VIP scores) were removed to determine if this improved model performance. For example, the least important predictor variables from pls 4, for both response variables, were Landsat and Sentinel SMA estimates of bare rock cover (L.Rock and S.Rock respectively), and Sentinel EVI (S.EVI) (Figure 5.6). These variables were removed for pls5. The least important variables, Landsat SMA estimate of perennial plant cover (L.Veg) and Landsat EVI (L.EVI), were removed for pls6 resulting in slightly improved model performance. Removing Sentinel MSAVI (S.MSAVI) slightly improved the performance of pls7. Further elimination of predictor

variables for pls8-11 did not improve model performance (Table 5.2). Pls7 was therefore chosen as the best model for predicting both perennial plant cover and bare ground cover for the project area. The most important variables for predicting field-estimated perennial plant cover are the Sentinel SMA estimates of perennial plant cover (S.Veg) and bare ground (S.Bare), followed by the remaining Sentinel vegetation indices (S.NDVI, S.OSAVI, S.SAVI). The most important variables for predicting field-estimated bare ground cover are the Sentinel SMA estimates of bare ground (S.Bare) and perennial plant cover (S.Veg), followed by the Landsat SMA estimate of bare ground cover (L.Bare) (Figure 5.7).

Table 5.2. Model fit (Q^2cum) and accuracy (R^2Ycum) for partial least squares regression models with various combinations of response and predictor variables. The row with the best fit model (pls7) is shaded in green.

Model	Response variables (excluded variables)	Predictor variables	Explained variance (R^2Ycum)	Predictive accuracy (Q^2cum)
pls1	All 16	Probabilities for S1, S2, S3	0.229	0.203
pls2	All 16	Probabilities for only S1 and S3	0.317	0.280
pls3	All 16	Perennial plant cover, non-vegetated cover, bare ground cover	0.580	0.531
pls4	All 16	Perennial plant cover, bare ground cover	0.580	0.538
pls5	13 (L.Rock, S.Rock, S.EVI)	Perennial plant cover, bare ground cover	0.589	0.540
pls6	11 (L.Rock, L.Veg, L.EVI, S.Rock, S.EVI)	Perennial plant cover, bare ground cover	0.592	0.548
pls7	10 (L.Rock, L.Veg, L.EVI, S.Rock, S.EVI, S.MSAVI)	Perennial plant cover, bare ground cover	0.592	0.554
pls8	9 (L.Rock, L.Veg, L.EVI, S.Rock, S.EVI, S.MSAVI, S.SAVI)	Perennial plant cover, bare ground cover	0.592	0.544
pls9	8 (L.Rock, L.Veg, L.EVI, S.Rock, S.EVI, S.MSAVI, S.SAVI, S.NDVI)	Perennial plant cover, bare ground cover	0.591	0.550
pls10	7 (L.Rock, L.Veg, L.EVI, S.Rock, S.EVI, S.MSAVI, S.SAVI, S.NDVI, S.OSAVI)	Perennial plant cover, bare ground cover	0.564	0.547
pls11	L.Bare, S.Bare, S.Veg	Perennial plant cover, bare ground cover	0.535	0.510

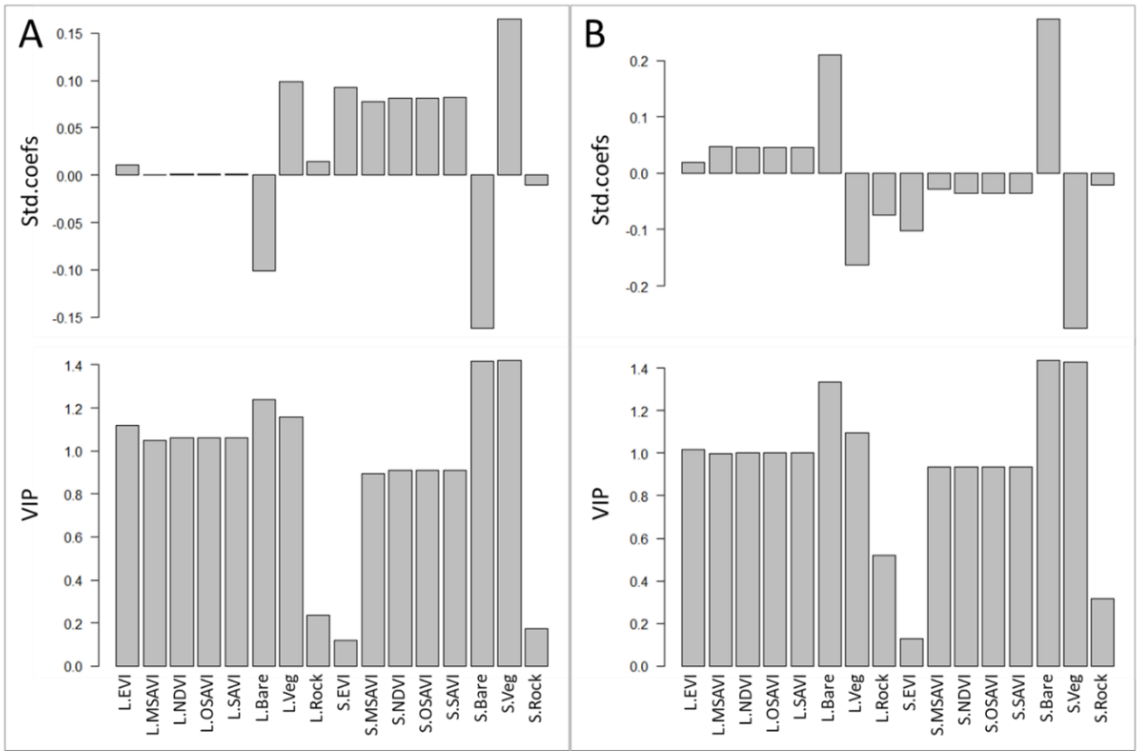

Figure 5.6. Relative importance of the 16 predictor variables of pls4 illustrated by standardised coefficient and variable importance for projection plots for field-estimated perennial plant (A) and bare ground cover (B).

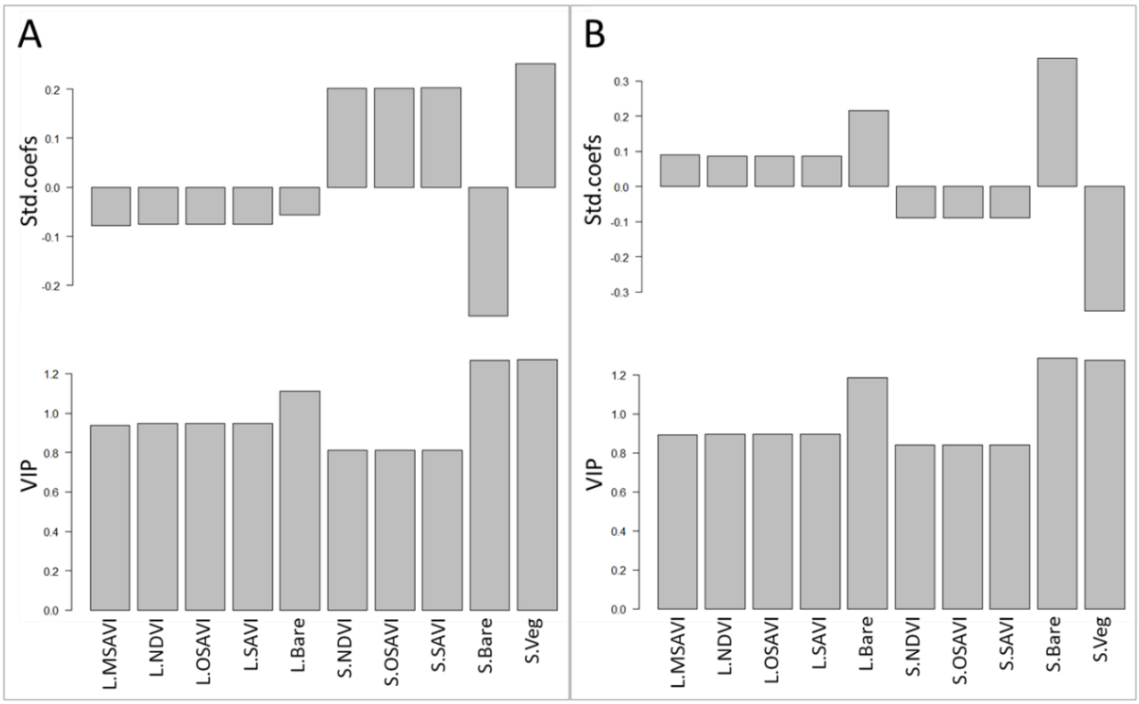

Figure 5.7. Relative importance of the 10 predictor variables of pls7 illustrated by standardised coefficient and variable importance for projection plots for field-estimated perennial plant (A) and bare ground cover (B).

5.3.3 Projection of PLSr model to project area

Accuracy test

The partial least squares regression models of bare ground and perennial plant cover were able to reliably estimate field cover for the project area. Associations between model predictions and field estimates of cover were tested using data from 61 test plots that were not included in the initial analyses in chapter four, or the PLSr model development earlier in this chapter.

There was a strong and significant relationship between all pls7 cover predictions and the field estimates of cover for the 61 test plots (Table 5.3). The strongest correlation was between pls7 predicted bare ground cover and field-estimated bare ground cover ($r = 0.827$, $p < 0.001$). While the association between pls7 predicted perennial plant cover and field-estimated perennial plant cover was not as strong ($r = 0.706$), it was still significant ($p < 0.001$). Pls7 predicted bare ground and perennial plant cover are therefore projected over the project area (Figure 5.8A & B).

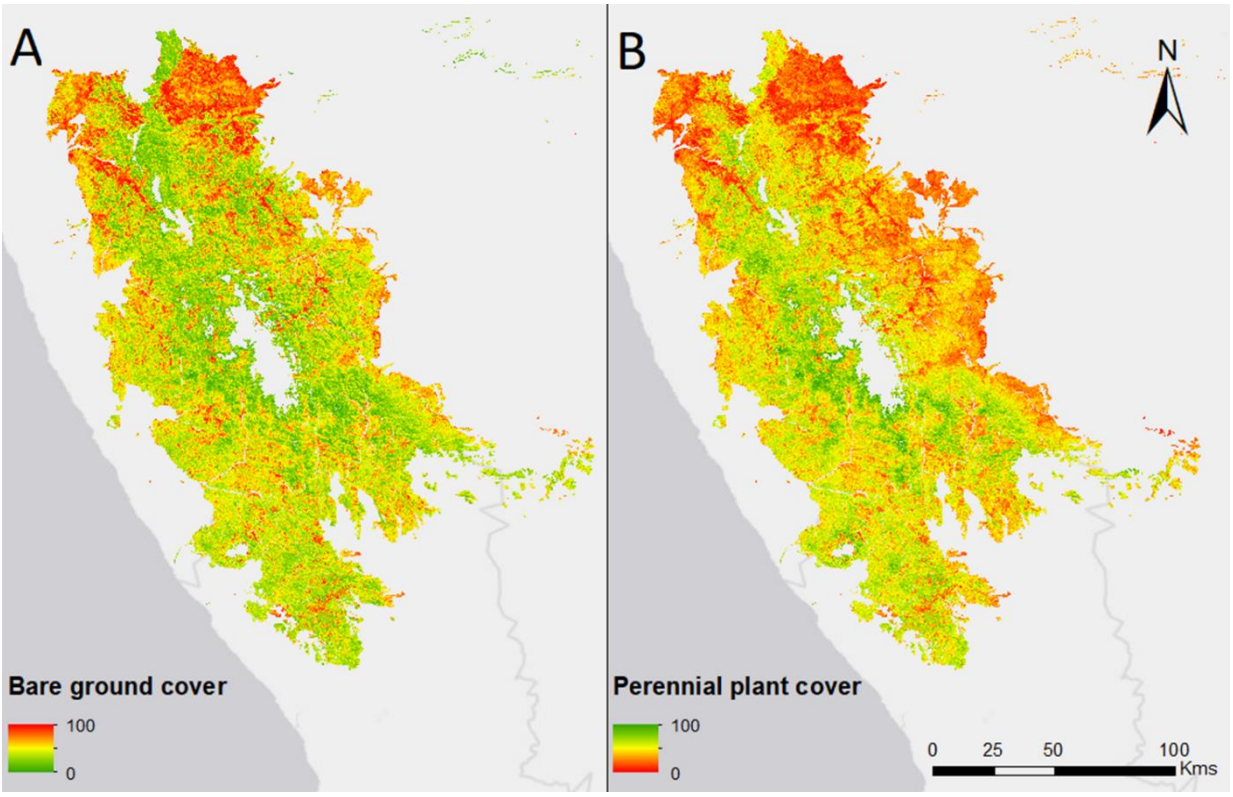

Figure 5.8. Partial least squares regression predicted bare ground cover (A) and perennial plant cover (B) for the Namaqualand Hardeveld bioregion.

Table 5.3. Correlations between the perennial plant and bare ground cover pls7 predictions and field estimates for the 61 test plots. Correlation coefficients, confidence intervals, and p-values are reported.

pls7 cover predictions	Field estimates of cover	Correlation coefficient (r)	Confidence intervals	p-value
Perennial plant cover	Perennial plant cover	0.706	0.552; 0.813	< 0.001
	Bare ground cover	- 0.753	- 0.844; - 0.618	< 0.001
Bare ground cover	Perennial plant cover	- 0.750	- 0.842; - 0.614	< 0.001
	Bare ground cover	0.827	0.727; 0.893	< 0.001

5.3.4 Variable selection for observing change

The level of importance attributed to each remote sensing variable in predicting the two response variables is corroborated by a circle of correlations plot, which illustrates the relative correlation between the predictor variables and the response variables in the model (Figure 5.9). The closer the variables are together the higher the correlation between them. The vegetation indices from each satellite platform were highly correlated to each other. Sentinel vegetation indices have been grouped into the variable S.Indices, while the Landsat vegetation indices have been grouped into the variable L.Indices. Because Sentinel data covers the period from 2015 onwards, only the correlations between the Landsat variables and the field-based cover estimates are considered for this section which addresses medium to long term changes in the landscape. The Landsat vegetation indices (L.Indices) are positively correlated with field-estimated perennial plant cover (field.Veg), although the strongest relationship is between the Landsat SMA estimate of bare ground cover and field-estimated bare ground cover ($r = 0.748$, $p < 0.001$, CI [0.691, 0.796]). As such, the slope of the trend line showing the change in L.Bare since 1984, as well as the difference between the 95th and 5th percentiles (percentile range), were determined for the project area (Figure 5.10A & B).

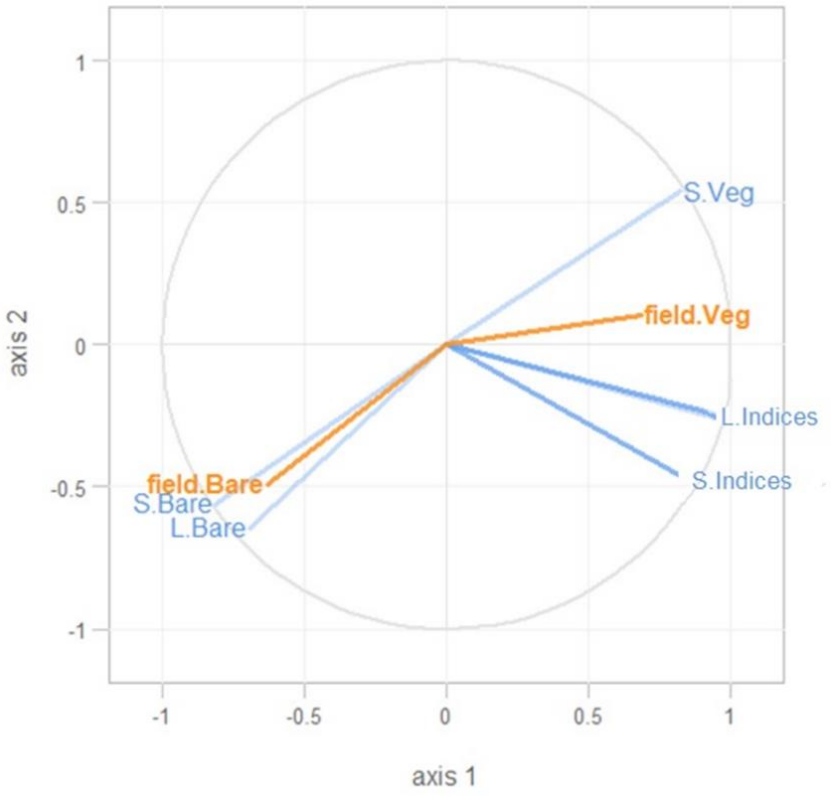

Figure 5.9. Predictor (blue) and response (orange) variables used in pls7. Variables that are closer together are more highly correlated to one another. Variable codes are described in Figure 5.2.

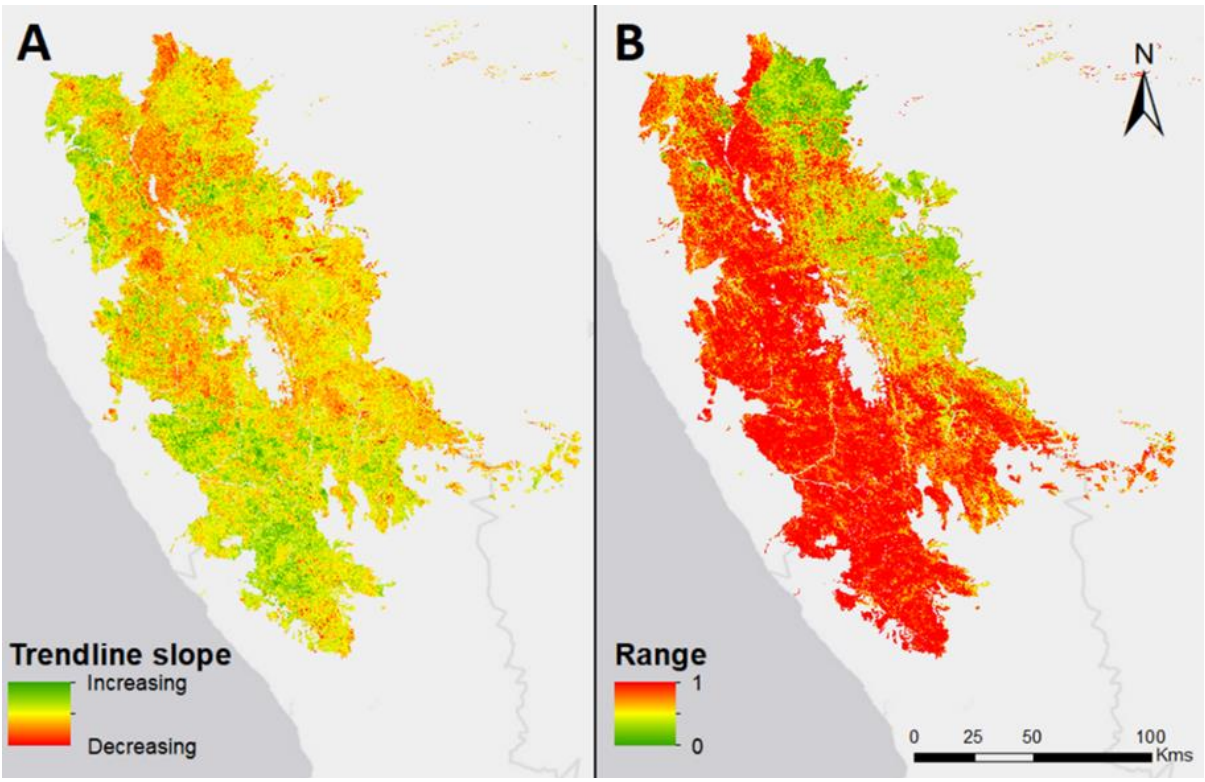

Figure 5.10. The trendline slope of the Landsat spectral mixture analysis estimated bare ground cover from 1984 to 2019 (A), and the difference between the 95th and 5th percentiles (percentile range) bare ground estimate values from between 1984 and 2019 (B).

5.4 Discussion

The results of this chapter show that field-based estimates of cover can be more accurately predicted through a multivariate analysis of remote sensing data than through the more traditional means of using one or a few vegetation indices. Bare ground cover, in particular, can be accurately predicted for the project area ($r = 0.827$, $p < 0.001$, CI [0.727, 0.893]). The accuracy of this prediction seems largely a result of the use of spectral mixture analysis (SMA), as opposed to vegetation indices, in estimating field cover. There is greater correspondence between SMA estimates and field-based estimates than between any of the vegetation indices and field-based estimates (Figure 5.9). SMA estimates provide a quantitative measure of cover as opposed to providing a proxy for primary productivity making it possible to discern changes in different cover types across landscapes (Elmore and Mustard, 2000; Yang et al., 2012). These findings support the results of similar analyses which have compared SMA estimates to several vegetation indices in different ecological contexts (e.g. Elmore and Mustard, 2000; McGwire et al., 2000; Wessman et al., 1997; Yang et al., 2012).

5.4.1 Variable selection

The latent class states S1 and S3 (see chapter 4) represent the two extremes on a continuum between a potentially 'degraded' landscape and a 'non-degraded' landscape and the difference between these two states formed the basis for determining differences in the remote sensing variables in this chapter. The difference between S1 and S3 was significant for 14 of the original 16 remote sensing variables (Figure 5.2). A PLSr model with only probabilities of belonging to S1 and S3 as the response variables (pls2) did not perform particularly well, however, despite performing better than a model with all three states as the responses (pls1). Since field-estimated perennial plant cover and bare ground cover were found to be the most important variables in distinguishing between S1 and S3 in chapter four (Figure 4.9), these variables were then used as response variables in place of the latent class probabilities. Model performance increased substantially with the field estimates as responses (Table 5.2), with the best performing model including the two field estimates

of cover as the responses and 10 of the original 16 remote sensing variables as predictors (pls7).

Of the six variables that were excluded from the final model, the SMA estimates of bare rock cover (L.Rock and S.Rock) were the least surprising. These estimates were derived for the purposes of ensuring all potential cover types were included in the SMA process and were not expected to influence model development (Figure 2.2). Perhaps more interestingly, was the exclusion of both the Sentinel and Landsat EVI variables (S.EVI and L.EVI) in the final model. EVI was specifically developed to be more sensitive than NDVI to changes in vegetation productivity in areas of high plant biomass. It is, therefore, not surprising that it was found not to be a good predictor of cover in this low plant biomass environment. It is, however, surprising that Sentinel MSAVI (S.MSAVI) was found not to be a good predictor of field-estimated cover, as this index was specifically developed for more arid landscapes (Qi et al., 1994). In general, however, the vegetation indices were found to be less important than the SMA estimates, and the relative importance of all indices was fairly even (Figure 5.6A & B, and Figure 5.7A & B). The results of the PLSr analysis highlight the importance of the spectral mixture analysis proportional cover estimates (Figure 5.7). These estimates were consistently better at predicting field cover, and particularly bare ground, than the vegetation indices included in this project.

Change in bare ground cover

The change in bare ground cover represented by the trendline slope value (Figure 5.10A) and the percentile range (Figure 5.10B) illustrate a potential change in habitat condition across the project area but require further investigation for any meaningful interpretations to be made. Though beyond the scope of this analysis, a thorough time series analysis of the bare ground estimates from 1984 to 2019 could reveal the extent and nature of change over this time period. This would be useful for determining the impact of fairly recent changes in potential drivers across the project area but cannot consider any of the change that took place prior to 1984, when much land degradation occurred in South Africa (Von Maltitz et al., 2019). For the purposes of this project, these values are used to support the construction of the habitat condition archetype by contributing to the calculation of the archetype membership values in chapter 6.

5.4.2 Vegetation indices

The normalised difference vegetation index (NDVI) has not only been used widely in land degradation and desertification studies, but has been used extensively by ecologists in general as a proxy for vegetation productivity (Pettorelli et al., 2005). Whether in relation to measures such as net primary productivity (e.g. Hunt, 1994; Schloss et al., 1999; Wang et al., 2017), leaf area index (e.g. Liu et al., 2010; Wu et al., 2007), evapotranspiration (e.g. González-Dugo and Mateos, 2008b; Ibrahim et al., 2015), plant biomass (e.g. Santin-Janin et al., 2009; Xue et al., 2017), or various other measures of plant production, the use of NDVI is largely accepted as the most appropriate method of observing vegetation on the Earth's surface remotely (Gonzalez-Roglich et al., 2019). The inclusion of NDVI in various UNCCD desertification indicators and parameters, which need to be reported on by all 197 member states, supports this view (UNCCD, 2016, 2013).

A primary concern with the institutionalisation of NDVI is that results obtained from NDVI mapping procedures, particularly at the national scale, are seldom ground truthed (Herrmann and Sop, 2016). NDVI has been found not to correspond well with primary productivity when vegetation cover is low (Chabrillat, 2006; Dawelbait and Morari, 2008; Eisfelder et al., 2012; Higginbottom and Symeonakis, 2014). This is concerning since low vegetation cover is a principal characteristic of many dryland environments which are the focus of desertification monitoring and research initiatives. Adjustments to the standard NDVI formula, developed predominantly to take into account the influence of soil on the reflectance of an area, have also had limited success in mapping primary productivity in naturally dry areas (McGwire et al., 2000). In this project, the various indices calculated from both Landsat 8 and Sentinel-2A data were moderately well correlated with the field-estimated perennial plant cover but were outperformed by the proportional estimates of cover calculated from the spectral mixture analyses (Figure 5.9). SMA therefore presents a potentially more appropriate method for mapping cover in the Hardeveld bioregion than the more traditional use of vegetation indices. This method is, however, heavily reliant on the accurate determination of endmember values for all possible cover types in the landscape being analysed (Okin et al., 2001).

5.4.3 Spectral mixture analysis

In this project, endmember values for bare ground were far easier to obtain than endmember values for perennial plant cover. This is because areas with 100% bare ground cover are far easier to locate than 100% vegetated areas within the project area. Bare ground areas are locations that have either been heavily grazed or have been previously cultivated, and the perennial plant cover has not returned. Endmember values were generated for the year that the field data were collected (2017). Namaqualand, along with most of the country, was experiencing a severe drought during this time period. As a result, proliferations of annual plants, which would impact the endmember values for bare areas, were highly unlikely. Endmember values for perennial plant cover are far more difficult to obtain for dryland areas in general because it is difficult to locate areas in drylands where perennial plant cover is at, or near, one hundred percent. In order for an endmember to truly reflect the spectral signature of the target land cover type, the area from which the endmember is calculated (either a polygon representing a group of pixels, or a set of individually located pixels) needs to be covered entirely by that land cover type. This is likely why the correlations between the Landsat 8 and Sentinel-2A spectral mixture analysis and field-based estimates of bare ground are greater than the correlations between the estimates of perennial plant cover (Figure 5.9).

These results suggest that future work should focus on developing better endmember values (spectral signatures) for perennial plant cover in drylands, and particular plant cover types in specific drylands. Similar work has already commenced globally through the United States Geological Survey Spectroscopy Lab that have compiled and measured over 2 500 spectra of various materials including plants. These spectra are measured with field, laboratory and airborne spectrometers, and already include several plant types and species (Kokaly et al., 2017). Field- and laboratory-based spectral measures of plant species and types in the context of Namaqualand, and other dryland systems, will greatly enhance the potential of mapping these regions more accurately.

5.5 Conclusion

Understanding and mapping the extent of bare ground in Namaqualand will go a long way toward mapping the overall condition of the area because extensive bare areas in Namaqualand do not occur naturally and are indicative of a degraded landscape. It is, however, important to consider the potential drivers of land degradation in the area to place the observed prevalence and extent of bare ground into context. In the next chapter, predicted cover for the project area has been related to habitat condition drivers, for which data are available. This helps to contextualise the observed habitat condition of the project area within a framework related to the potential drivers of change for the region. This information is then used to create and evaluate the final archetype for habitat condition in the Namaqualand Hardeveld bioregion.

Chapter 6:

6. Habitat condition archetype construction with cover estimates and desertification drivers

6.1 Introduction

Any illustration of the biophysical world relies, to an extent, on the interpretation of observations, measurements, and incorporated knowledge of the biophysical characteristics of the area (Cullum et al., 2016a). Therefore, the foundation of many maps will commonly be based on a conceptual model of the landscape. This model is likely influenced by various factors acting at multiple scales, which need to be reduced into a two-dimensional representation of the world. This generalisation results in a provisional conceptualisation that is subject to revision (Cullum et al., 2016a). In many cases, however, the creation of a map is based on a hard or fixed classification of the landscape which doesn't allow for uncertainty and is not open to future revision.

The use of archetypes and fuzzy classification is particularly useful for addressing this lack of certainty and is ideal for the purpose of mapping land degradation and habitat condition (Xie et al., 2008). The rangelands of Namaqualand exist within a spectrum of potential habitat condition from 'degraded' to relatively 'pristine' or 'non-degraded' land (Figure 5.8). An archetype that represents each of these two extremes can be constructed and the habitat condition for any area can be illustrated relative to both extremes. This spectrum of habitat condition is influenced by numerous biotic and abiotic drivers, measures of which can be incorporated into the archetype description and construction. Each map unit will be represented by its degree of similarity to both extremes of the habitat condition archetype. The inherent uncertainty involved in the assessment of land degradation in Namaqualand can be retained and the archetype can be represented by the set of specific drivers that are thought to affect habitat condition in the area (Cullum et al., 2016a). The relative importance of each driver can also be included in the archetype construction. As a result, if certain drivers are found to be more important in future studies, or studies focussed on different ecological areas, flexibility is included in the archetype approach to accommodate these differences (Cullum, 2014).

6.1.1 Baselines in mapping landscapes

As discussed in chapter two of this thesis, land degradation can be mapped in different ways and can occur in different states. In almost all cases, land is assessed in comparison with what may be considered the 'natural', 'non-degraded' or 'pristine' state (Prince et al., 2018). This state is generally referred to as the baseline, or reference state, against which current conditions can be compared and assessed. Baseline or reference states have been used in ecological monitoring for decades and have emerged out of the need to understand and measure the impacts that humans, and changing environmental conditions, have had on ecosystems and landscapes (e.g. Holling, 1973; Jenkins and Bedford, 1973a; Tully et al., 2015). Determining an appropriate reference state is, therefore, a fundamental step for most land degradation assessments, but it is also one of the most challenging. As a result, a number of different types of baseline states have been used to compare against current conditions (Table 6.1).

Table 6.1. Selected types of baselines developed for the detection of trends in degradation. Adapted from Prince et al. (2018).

Baseline type	Meaning	Data sources
Natural	Pre-modern (≤10,000 yr. BCE)	Palaeontological and archaeological data
	Pre-Anthropocene (+/- 1850-1950)	Early descriptions; traveller's records, images / maps; historical photographs; archival records; recent archaeology; land use assessments.
Historical	Typically, mid-19th century, 1950s, and early 21st century.	Ecological data: information on environmental events and trends (e.g. meteorological variables, CO2, land use).
Target	The state that is most desirable to the land user.	Land managers, farmers, foresters, biodiversity experts, environmentally-aware public, policy documents.

The three primary baseline types are natural, historical and target baselines (Table 6.1), although baselines based on current conditions or the maintenance of ecological integrity have also been developed (Prince et al., 2018). All these methods are, however, dependent to some extent on an underlying notion of what the assessor may

consider a natural or non-degraded condition (Prince, 2016). Natural baselines can be considered the optimal condition of the land prior to human influence. This may be considered the state of the environment before the existence of modern humans (≤10,000 BCE), estimated through the use of palaeontological or archaeological data, or a time period that is deemed to pre-date significant environmental change associated with human occupation (Prince et al., 2018). In Namaqualand, for example, evidence suggests that early hunter-gatherers had very limited impact on the environment, and arguably it was only until about 2000 years ago, with the arrival of Khoe-Khoen herders, that humans begun to have a significant impact on the land (Hoffman et al., 2007b) (Chapter 3). It could also be argued, however, that the transhumance patterns practiced by these herders followed a relatively natural cycle of grazing, which mimicked indigenous wild ungulate herds, and that they too had only a negligible impact on the environment when compared, for example, to later farming practices employed by colonial Europeans from the 1700s (Hoffman and Rohde, 2007). In the Namaqualand context, therefore, a natural baseline may be based on the state of the environment either before the arrival of modern humans, before the advent of pastoralism in the area, or before the arrival of European settlers. The choice of a natural baseline, therefore, does not escape the subjectivity associated with the assessment of land degradation, but does provide a useful benchmark for degradation studies, provided suitable data can be obtained. Information from repeat photography has been used to determine natural baselines in Namaqualand for the pre-Anthropocene (+/- 1850-1950) (Table 6.1). Historical photographs from the early 20th century have been analysed to determine the nature, extent and rate of environmental change in different habitats over time. These habitats include rangelands under both communal (Rohde and Hoffman, 2008) and private (Hoffman and Rohde, 2007) land tenure as well as ephemeral rivers (Hoffman and Rohde, 2011). Even though historical photographs help in the development of natural baselines they often show landscapes that have been grazed by large numbers of domestic livestock for decades or even longer.

Historical baselines differ from natural baselines in that they are the measured condition of a site in the past, based on actual ecological data collected at the time. Historical baselines are useful in providing an objective assessment of the changing condition of a site. Provided the same measurement techniques are used and

repeated during each assessment, data from the past can be compared to current data using appropriate statistical methods. Unfortunately, there are very few long-term monitoring sites available globally, which limits the use of historical baselines for mapping the nature, extent and rate of environmental change (Prince et al., 2018). Also, the start dates, and the time period being assessed, often differ between sites. This makes it difficult to compare degradation trends between sites. In addition, some of the same problems with establishing natural baselines emerge for the setting of historical baselines in that degradation may have occurred long before the historical baseline data were collected (Fisher et al., 2018).

While the use of natural and historical baselines is based on the condition of the land at some time in the past, preferably prior to significant human impact, the development of target conditions reflects the 'desired' condition of the land (Table 6.1). This desired state is grounded entirely on choices made in relation to the productivity, value and desired outputs of, or services provided by, the land (Bliss and Fischer, 2011; Perrings et al., 2010; Wunder and Bodle, 2019). The target condition desired by a livestock farmer in Namaqualand may, for example, be based on land that can provide sustained forage for sheep which optimises lamb production and growth. Such a target is less likely to be influenced directly by concerns over biodiversity conservation. Target conditions are, therefore, especially beneficial in multiple-use areas, or areas where different stakeholders have vested interests (Vogler et al., 2015; Willemen et al., 2018). For example, the development of a target condition which foregrounds concerns over biodiversity would be more appropriate for a farmer who both raises livestock and promotes ecotourism activities, such as hiking. In this context, the target condition may be land that continues to support livestock production while improving biodiversity conservation for aesthetic purposes. While the amount of biodiversity may never reach historical levels, important biodiversity can be conserved without severely limiting the primary livelihood of the farmer. Target baselines do not require universal agreement but should represent the desires of important stakeholders in any given landscape (Kohler et al., 2018).

6.1.2 Baseline to archetype link

The use of archetypes could address some of the issues associated with determining traditional baselines. This is because the baseline can be adjusted as new information becomes available. Archetypes can be viewed as dynamic and adaptable baselines, which are ideally based on a holistic understanding of the condition of the landscape (Cullum et al., 2016a). The use of field and Earth observation data, along with expert knowledge of an area, can all feed into the construction of archetypes for a landscape. This is particularly important in the remote sensing context where new data becomes available regularly, technologies improve dramatically in a short period of time, and the capacity to deal with complex ecological questions improves exponentially with time (Pettorelli et al., 2014). To have such adaptability within mapping procedures is especially important for dryland environments where there is a general lack of consensus over what constitutes land degradation. Within the remote sensing context, baselines have been established by developing models of potential vegetation index values based on biophysical factors, and then examining deviations in actual index values in response to the impact of different land use practices (Paruelo and Lauenroth, 1995; Stoms and Hargrove, 2000). A similar approach can be applied to archetypes in that archetype membership values can be compared under management regimes, or climatic conditions.

6.1.3 Incorporating desertification drivers into archetype construction

In chapters four and five of this thesis, the condition of the project area with respect to field and Earth observation data, has been mapped. It is important, however, that data on different cover classes across the project area is contextualised with reference to how habitat condition has changed over time and with respect to the potential drivers of this change. In this chapter, data on the possible drivers of change in habitat condition are used to evaluate the potential impact of each of these drivers, and a habitat condition archetype is then constructed incorporating this information.

Habitat condition in Namaqualand has been found to be related to both biotic and abiotic factors including differences in climate, topography and land-use (Figure 2.2). Spatial and temporal changes in climate and land-use directly result in differences in

habitat condition in the project area, across both space and time (Davis-Reddy, 2018; Davis et al., 2017, 2016; Hahn et al., 2005; Midgley and Thuiller, 2007; Nenzhelele et al., 2018; Schmiedel et al., 2012; Schmiedel and Oldeland, 2018; Todd and Hoffman, 2009). Topographical features, on the other hand, have a predominantly indirect or secondary impact on habitat condition in that the impact of changes in climate and land-use are influenced by differences in topography across the project area (Anderson and Hoffman, 2011, 2007; Samuels et al., 2007). A model was created in order to determine the most important desertification drivers in relation to the predicted perennial plant and bare ground cover derived from chapter five. These drivers, along with fuzzified versions of the PLSr predictions and the change in the estimated cover of bare ground, were then used to construct a habitat condition archetype for the project area.

6.2 Methods

Predicted perennial plant and bare ground cover represent two extremes of a potential habitat condition spectrum for the project area. These two variables, as well as the trendline slope value and the percentile range of Landsat SMA estimated bare ground cover estimate from 1984 to 2019 (Figure 5.10), were used to construct the habitat condition archetype (**Error! Reference source not found.**).

6.2.1 Drivers of habitat condition

The five potential drivers of desertification (**Error! Reference source not found.**) are in no way an exhaustive list of the factors that may result in a degraded landscape in the project area. Instead, they are a sample of factors for which freely available data could be collected across the project area, primarily through the Google Earth Engine platform. These drivers are likely to not only interact with one another in impacting habitat condition, but also with other drivers not mentioned here. The purpose of analysing these drivers is to inform the construction of the habitat condition archetype for the project area, which can later be adapted as more information and data becomes available.

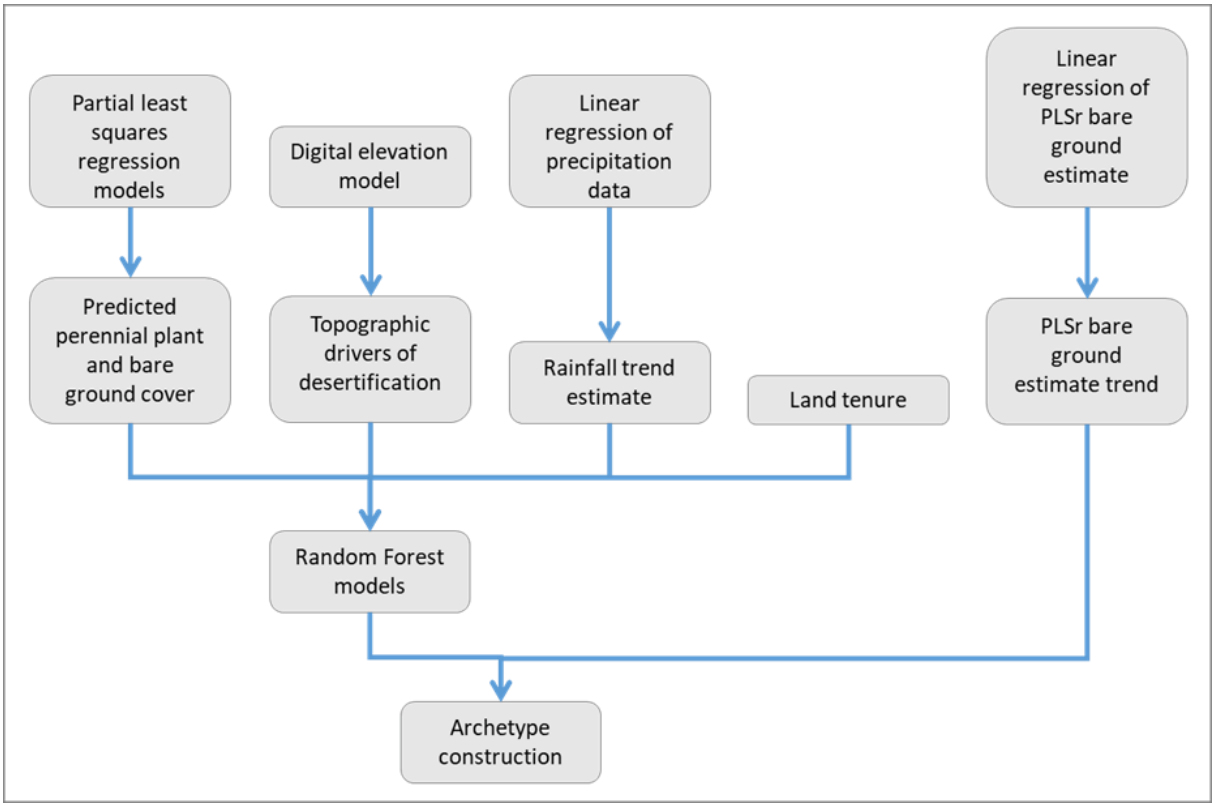

Figure 6.1. Flow diagram illustrating the methodology employed to collect and analyse the desertification drivers' data and construct a habitat condition archetype for the project area. PLSr refers to partial least squares regression analysis.

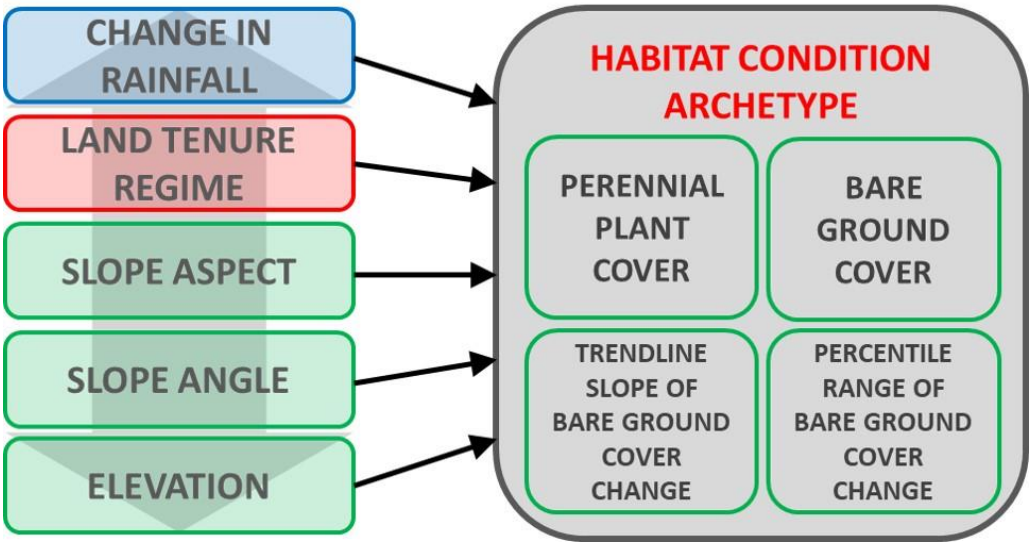

Figure 6.2. Factors influencing the construction of the habitat condition archetype. The four primary variables (predicted perennial plant cover, predicted bare ground cover, trendline slope of bare ground cover change and percentile range of bare ground cover change) are used to determine the fuzzy membership values, while the five external drivers (change in rainfall, land tenure regime, slope aspect, slope angle, elevation) provide an additional layer of information to the final archetype.

Topographic features

Variations in topography across landscapes are thought to have both a direct and an indirect effect on vegetation in Namaqualand (Desmet, 2007; Francis et al., 2007). In general, a decrease in slope steepness, a more northerly slope aspect, and lower elevation habitats are related to an increase in bare ground cover, and a decrease in perennial plant cover (**Error! Reference source not found.**) (Anderson and Hoffman, 2007; Samuels, 2006; Samuels et al., 2019, 2007).

Measures of slope angle, slope aspect, and plot elevation were derived from a digital elevation model (DEM) in Google Earth Engine (Appendix A). The Shuttle Radar Topography Mission (SRTM) digital elevation data were used to derive these values. SRTM provide DEMs for nearly the entire globe at a resolution of approximately 30 metres (Farr et al., 2007). This ensures that not only are most areas of interest likely to be covered by the data, but that the data are also at a similar spatial scale to other satellite imagery likely to be used, particularly Landsat data. Elevation in metres above sea level were derived along with values for both slope angle and aspect. The values for elevation were derived directly from the SRTM dataset. Slope angle values measured in degrees and ranging from 0° (completely flat landscape) to a maximum of 90° (vertical cliff face) were derived from the SRTM dataset using ee.Terrain.slope() function in GEE. Slope aspect values were initially derived from the SRTM dataset using the ee.Terrain.aspect() function, which produces values between zero and 360 degrees. Values of zero and 360 are problematic, however, in that they represent the same aspect but are statistically very different numbers. As a result, the degree values were converted to range between -1 to 1 such that a value of -1 represents a south-facing slope while a value of 1 represents a north-facing slope (**Error! Reference source not found.**, where AspectNS = slope aspect between -1 (south) and 1 (north), Aspect = original aspect in degrees). East and West are represented by values of zero meaning the entire landscape is represented on a linear scale from -1 to 1 irrespective of whether the slope is more west or east facing.

$$AspectNS = cos\left(\frac{Aspect \times \pi}{180}\right) \quad (5)$$

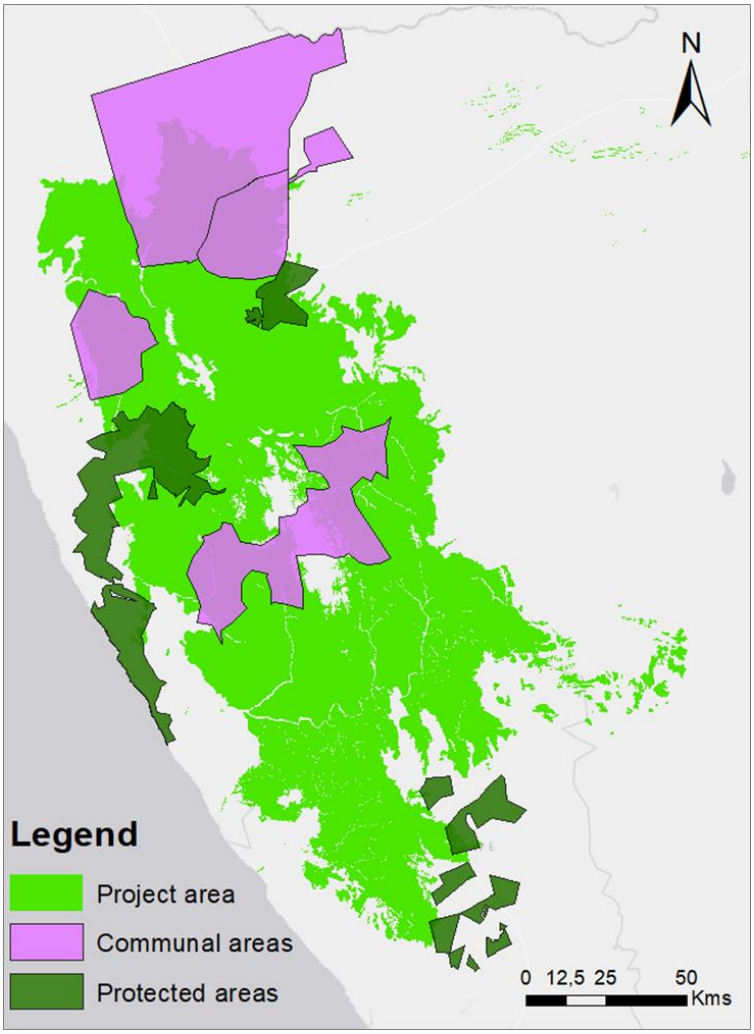

Figure 6.3. The three land tenure regimes considered for this project area. The extent of the project area that does not belong to either communal tenure or one of the official protected areas has been classified as privately owned despite incorporating small portions of state (municipal) land.

Rainfall trend

Even though the interaction between vegetation and a changing climate is complex, it is generally expected that a historical decrease in rainfall across the project area will result in higher bare ground cover and lower perennial plant cover (**Error! Reference source not found.**) (Davis-Reddy, 2018; Davis et al., 2017). The sporadic nature of rainfall patterns and the sparse spatial distribution of weather stations in Namaqualand results in limited accurate rainfall data for the extent of the project area (Davis et al., 2016). The isolated nature of many rainfall events also means that rainfall data from a weather station in one location may not represent the rainfall received in a geographically adjacent area. Another constraint on obtaining rainfall data for the project is the fact that the methods need to be replicable for similar dryland areas, and

for the Succulent Karoo in particular. It is therefore important that the rainfall data used in the model be available through the Google Earth Engine platform. As a result, the Climate Hazards group Infrared Precipitation with Stations (CHIRPS) dataset was used to determine the trend in rainfall across the project area from 1984 to 2019 (Appendix H). This dataset is based on an algorithm that blends satellite-derived cold cloud duration observations with station data to produce precipitation estimates on a global scale (Funk et al., 2015). A value representing the trendline slope of the linear rainfall trend from 1984 to 2019 was determined using the ee.Reducer.linearFit() function in Google Earth Engine. This function computes the slope and offset (intercept) for a linear regression of two inputs, precipitation and time in the case of this thesis.

Land tenure

In general, communal areas in Namaqualand have been reported to contain a higher proportion of degraded areas than privately owned land (Nenzhelele et al., 2018; Todd and Hoffman, 2009, 1999). Communal land tenure is predicted to be related to higher bare ground cover and lower perennial plant cover for the project area (**Error! Reference source not found.**). The extent of three different land tenure regimes were derived from various geographic information systems (GIS) spatial layers. The project area was divided into land under communal tenure, private tenure, or land belonging to the country's official protected area network. The protected areas network in South Africa is continually changing and it is difficult to obtain the latest spatial extent of protected areas in the country. For this project, a protected area GIS spatial layer was obtained from the South African Biodiversity Institute (SANBI) and represents the extent of both formal and informal protected areas in the country as of the National Biodiversity Assessment 2011 (NBA 2011). Three protected areas occur within the extent of the project area: Namaqua National Park, Goegap Nature Reserve, and Knersvlakte Nature Reserve (**Error! Reference source not found.**).

Spatial layers of land tenure for the country are difficult obtain as tenure is relatively fluid with respect to recent land reform, and spatial layers are not often updated by government agencies. The purpose of looking at land tenure in this context is to see if historically different land use practices have resulted in differences in habitat condition within the project area. As a result, recent changes in land tenure are not of particular interest and the historical extent of private versus communal land can be used.

Published maps of communal areas in Namaqualand (Benjaminsen et al., 2006; Lebert, 2004; May and Lahiff, 2007) as well as spatial layers shared by colleagues, were used to create a spatial layer in ArcMap 10.4 of farm portions belonging to communal areas in the project area. Land tenure is therefore presented as a categorical factor in the analysis with three potential classifications (communal, private and protected area).

6.2.2 Data analysis

The purpose of the analyses in this chapter was to explore the relationship between the cover estimates developed in chapter five (response variables), and the five potential habitat condition drivers of change determined for the project area, i.e. elevation, slope aspect, slope angle, rainfall trend, land tenure (predictor variables). To accomplish this, a seven-band raster image was created in GEE, with each band representing each of the response and predictor variables (Table 6.2). The spatial resolution of the raster was set at 30 m x 30 m to remain consistent with the majority of the individual data inputs (SRTM topographic measures and PLSr estimates). This results in a raster image with 19 888 566 pixels and seven bands. The raster was then imported into R using the Raster package, and an appropriate multivariate method for evaluating raster data was used.

Table 6.2. A description of the bands making up the raster image used in the random forest model.

Band	Variable type	Description
Elevation	Predictor	The elevation (in metres) of the project area, calculated from the DEM.
SlopeAspect	Predictor	The slope aspect of the project area, calculated from the DEM (-1 = South, and 1 = North).
SlopeAngle	Predictor	The slope angle (in degrees) of the project area, calculated from a Digital Elevation Model (DEM).
RainfallTrend	Predictor	Trend in rainfall from 1984 to present using CHIRPS modelled climate data.
LandUse	Predictor	Three different broad land tenure categories: private, communal, protected area.
BarePred	Response	PLSr predicted perennial plant cover.
VegPred	Response	PLSr predicted bare ground cover.

The raster was initially converted into a data frame in order to perform the analyses. The resulting data frame of nearly 20 million rows and seven columns was too large for computations to succeed and thus the stratified() argument from the splitstackshape package in R (Mahto, 2019) was used to sample the data in a random but stratified manner. The sample was stratified proportionally according to the land tenure variable such that the number of points analysed in each land tenure type (private, communal, or protected area) was proportional to the number of points in each type in the original raster. Different sample sizes were evaluated to determine the largest potential sample size that could be used without resulting in a computational error. The different sample sizes were chosen such that the area covered by each unit of the sample represented an intuitive spatial resolution on the ground.

Preliminary analysis

Two Kruskal-Wallis rank sum tests were performed for each of the response variables to determine whether there was a significant difference in bare ground and perennial plant cover across the three land tenure categories. Once again, if a significant difference was found then a pairwise comparison was performed to determine where this difference occurred.

Random forest

The random forest algorithm is an ensemble method within machine learning that has been used successfully for both classification (categorical response variable) and regression (continuous response variable). Random forest models are an extension of single decision tree models in that they average the results of several randomised decision trees (the forest) (Breiman, 2001). This method has been shown to both improve prediction accuracy and avoid the problem of overfitting, which is often associated with single decision trees (Hengl et al., 2018). Randomness is introduced in the model first by sampling a random number of points from the original data, and secondly by subsetting the number of predictors used to generate the best split at each tree node (mtry) (Liaw and Wiener, 2002).

A common problem with various spatial analyses, and multivariate statistical methods in general, is the issue of collinearity. Collinearity, often synonymous with multicollinearity, occurs when predictors in a multiple regression are highly correlated

and cannot independently predict the value of the response variable, thus reducing their statistical significance (Dormann et al., 2013). It has been suggested that the random sampling of a subset of predictor variables at each tree node in a sufficiently large forest will reduce the problem of collinearity in random forest models (Afanador et al., 2016). Despite this suggestion, tree-based models have been found to be no less tolerant of collinearity than regression-based approaches (Dormann et al., 2013), thus necessitating an evaluation of potential collinearity in this project. The correlation between the predictor variables in the data was determined and potential collinearity assessed following the general rule of thumb which is not to use variables correlated at $r > 0.7$ (Dormann et al., 2013).

The two main parameters that can be tuned in a random forest model using the randomForest package are the number of trees used for the final model (ntree), and the number of predictors chosen at each tree node (mtry) (Liaw and Wiener, 2002). The trainl() function from the caret package (Kuhn, 2019) was used to perform K-fold cross validation in order to determine the optimum values for both ntree and mtry. Once these values were determined, the data were split into a training and a test set with 70% of the data becoming the test set. Random forest models were then run with the training set. Different models were run with different combinations of predictor variables in order to determine the model that explains the most amount of variance in the data, as determined by the percent of the variance in the training data explained ('%Var explained'). Once the best model was selected for each response variable (PLSr bare ground and perennial plant cover estimates), the predict() function was used to predict the random forest model on the test set, and the accuracy of the model was determined by looking at the Root Mean Square Error (RMSE) value. The importance of the individual predictor variables was then determined by the %IncMSE, which is the percentage increase of the mean squared error (Breiman, 2001). The larger this value for each variable, the more important the variable is in the model.

6.2.3 Habitat condition archetype construction

The PLSr cover estimates, as well as the Landsat SMA bare ground trendline slope and percentile range values, were used to construct the habitat condition archetype for the project area. This was accomplished by initially converting the variables to values between zero and one using the Fuzzy Membership tool in ArcMap 10.4 (ESRI, 2011). A membership value of one represents 100% similarity to the non-degraded extreme of the habitat condition archetype while a value of zero represents 100% similarity to the degraded extreme. Different membership type options are available with the Fuzzy Membership tool that specify the algorithm used in the fuzzification of the input raster, i.e. how the range of values in the raster data are converted to a range between zero and one. The outputs of each type were investigated to determine which type resulted in the best approximation of the habitat condition. The values of the fuzzified bare ground cover and bare ground trend and percentile range images were inverted such that a high membership value represents high perennial plant cover, and corresponds with the habitat condition archetype. The new images, which represent fuzzy approximations of bare ground cover, perennial plant cover and the trend and percentile range of the Landsat SMA bare ground estimate, were then combined using the Fuzzy Overlay tool. This tool combines membership raster data together based on a selected overlay type. The overlay type specifies the method used to combine the membership data. The most appropriate overlay type for the project area was used such that the final layer represents the similarity of each pixel in the project area to the habitat condition archetype. The raster layers representing the five potential desertification drivers were then combined with the fuzzy overlay raster to form a new multi-band raster representing the habitat condition archetype for the project area. Membership values can therefore be interpreted within the context of the desertification drivers.

Interpretation

To improve the utility of the habitat condition map and produce estimates of the extent of desertification over the study area it is necessary to develop a classification system for the range of habitat condition membership values observed in the field. As such, the membership values for each pixel within the project area were evaluated with respect to a range of subjective thresholds. The proportion of the project area that falls within a set of predetermined membership value ranges is reported. One common

method of interpreting such data is to classify the values into groups that have been established based on the mean ± two standard deviations away from the mean (Prince et al., 2009). This approach allows for the groups to be based on a classification of the data and thus eliminates the subjectivity inherent in many classification approaches. An advantage of the archetype approach is that these groups can then be viewed within the context of the potential desertification drivers for the project area.

6.3 Results

6.3.1 Stratified sampling

The original raster image contains 19 888 556 pixels with a spatial resolution of 30 metres. Only the models representing a spatial resolution of 500 m x 500 m and 1 km x 1 km, and containing a sample of less than 100 000 pixels, were able to run. Only 0.09% of the full dataset was sampled at a 1 km x 1 km spatial resolution, while a 500 m x 500 m resolution image represented 0.36% of the number of pixels of the full dataset. This sample was therefore chosen to represent the data for further analyses.

Table 6.3. The number of pixels sampled in order to determine the maximum sample size with which to perform the random forest regression.

Proportion sampled	Ground resolution (m)	No. of pixels	Result
1	30 x 30	23 060 974	Fail
0.09	100 x 100	2 075 487	Fail
0.0144	250 x 250	332 078	Fail
0.0036	500 x 500	83 019	Success
0.0009	1 000 x 1 000	20 754	Success

6.3.2 Drivers of habitat condition

Preliminary analysis

Both the PLSr estimated perennial plant cover and bare ground cover were significantly different across the three land tenure categories ($p < 0.001$) (Figure 6.4). Estimated bare ground cover did not differ significantly between private land and land within official protected areas ($p = 0.31$). Bare ground cover in communal lands, on the other hand, was significantly different from both private and protected areas ($p <$

0.001). The same pattern was evident for estimated perennial plant cover in that there was no difference between private land and protected areas (p = 0.64), but there was a significant difference between communal land and both private and protected areas (p < 0.001).

Variance was very high for the four continuous predictor variables of bare ground cover (**Error! Reference source not found.**) and perennial plant cover (**Error! Reference source not found.**). The correlations between the cover estimates and the four potential drivers were generally low to moderate, though they were all significant (Table 6.4). The low p values simply indicate the confidence in the stated correlation coefficient. The strongest correlations were between the cover estimates and slope angle with higher bare ground cover being related to a gentler slope (r = - 0.419), and higher perennial plant cover being related to a steeper slope (r = - 0.309).

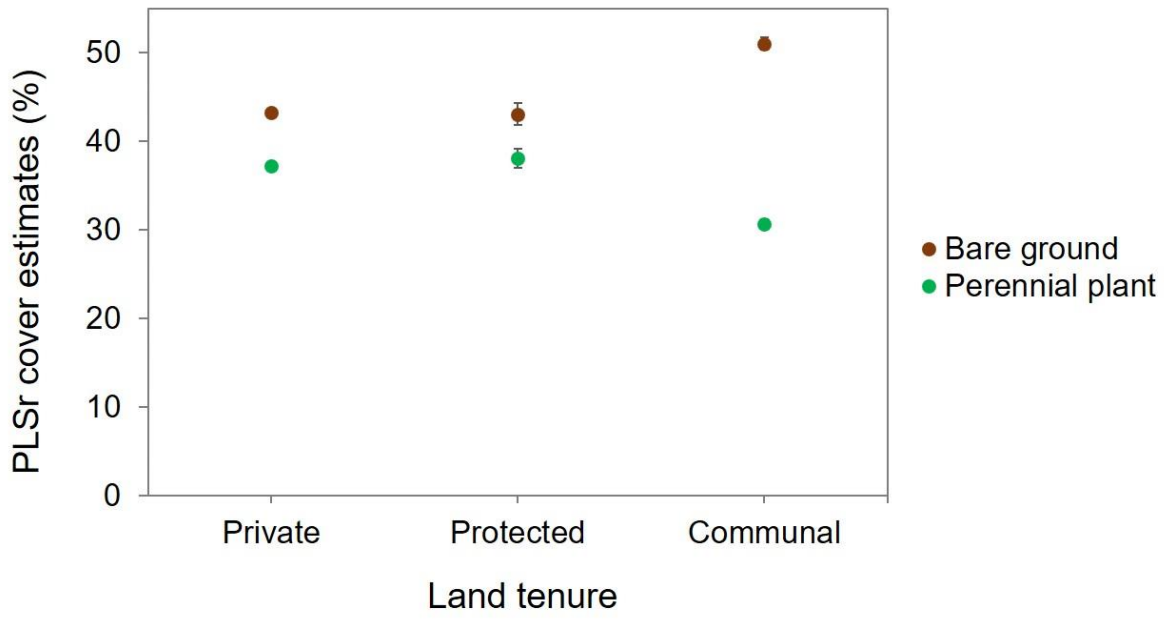

Figure 6.4. Mean partial least squares regression estimates and 0.95 confidence intervals of bare ground cover and perennial plant cover across the three land tenure regimes.

Table 6.4. Correlations between the perennial plant and bare ground cover pls7 predictions and the four continuous predictor variables.

pls7 cover predictions	Desertification drivers	Correlation coefficient	Confidence intervals	p-value
Bare ground cover	Rainfall	0.168	0.155, 0.181	< 0.001
	Angle	- 0.419	- 0.430, - 0.408	< 0.001
	Aspect	0.283	0.271, 0.296	< 0.001
	Elevation	- 0.062	- 0.075, - 0.048	< 0.001
Perennial plant cover	Rainfall	- 0.297	- 0.309, - 0.284	< 0.001
	Angle	0.309	0.297, 0.321	< 0.001
	Aspect	- 0.204	- 0.217, - 0.191	< 0.001
	Elevation	- 0.126	- 0.140, - 0.113	< 0.001

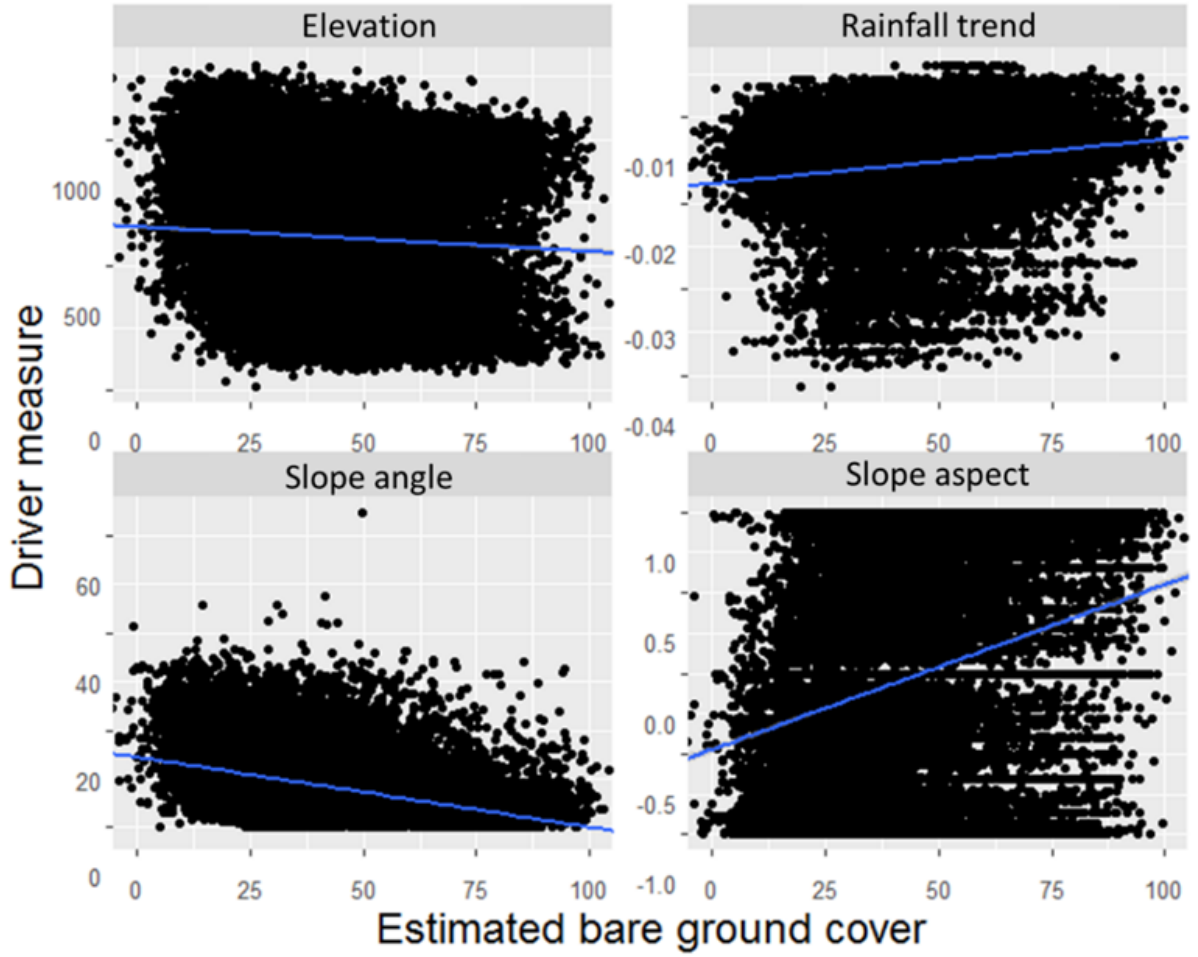

Figure 6.5. The four continuous predictor variables and partial least squares regression estimated bare ground cover for a sample of 20 754 points.

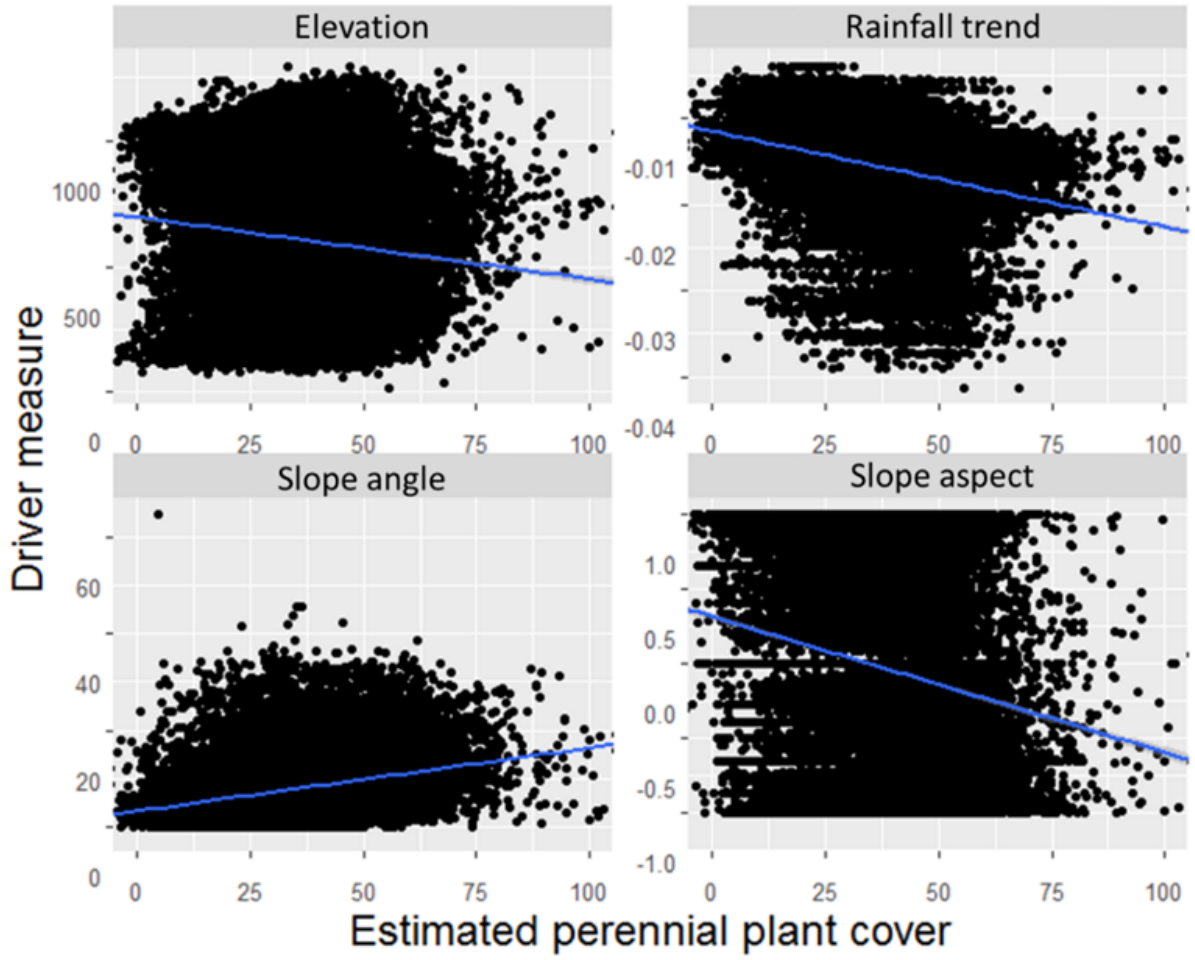

Figure 6.6. The four continuous predictor variables and partial least squares regression estimated perennial plant cover for a sample of 20 754 points.

Random forest

Before using all four potential predictors of bare ground and perennial plant cover in a random forest model, the degree of collinearity was assessed among these predictors. The results showed that Pearson's correlation coefficients were never higher than the r = 0.7 rule of thumb threshold for collinearity to be an issue (Table 6.5).

Table 6.5. Correlations (r) between the four continuous predictors to be used in the random forest models.

	Slope angle	Slope aspect	Elevation
Rainfall trend	0.211	-0.009	-0.040
Elevation	0.118	0.012	
Slope aspect	-0.052		

Model evaluation

The final number of variables randomly sampled as candidate predictors at each split in the random forest trees was two (mtry = 2), and the number of trees making up the final random forest model for bare ground was 500 (ntree = 500). The bare ground model managed to explain 43.1% of the variance in the training data set while the perennial plant cover model had a similar level of performance in that it explained 41.77% of the variance in the training set. The correlation between the random forest model predicted bare ground and the PLSr predicted bare ground was acceptable (r = 0.67), while the RMSE for the model was 14.33. The correlation between the random forest model predicted perennial plant cover and the PLSr predicted perennial plant cover was also acceptable (r = 0.68), while the RMSE for this model was 11.41. If the least important variables were removed from the two models, then the model performance decreased slightly for both the bare ground model (% variance explained = 40.7%) and the perennial plant cover model (% variance explained = 40.68).

Variable importance

Slope angle was the most important variable in predicting estimated bare ground (%IncMSE = 269.58). Slope aspect (%IncMSE = 156.09), elevation (%IncMSE = 153.83), and rainfall trend (%IncMSE = 140.56) all had similar levels of importance, while land tenure was the least important variable (%IncMSE = 89.81) in predicting bare ground (Figure 6.7A). With respect to predicting perennial plant cover, slope angle was again the most important variable (%IncMSE = 174.04), although rainfall trend was almost as important (%IncMSE = 172.38). Elevation was the next most important variable (%IncMSE = 126.81), while slope aspect (%IncMSE = 96.73) and land tenure (%IncMSE = 93.05) were the two least important variables in predicting perennial plant cover (Figure 6.7B).

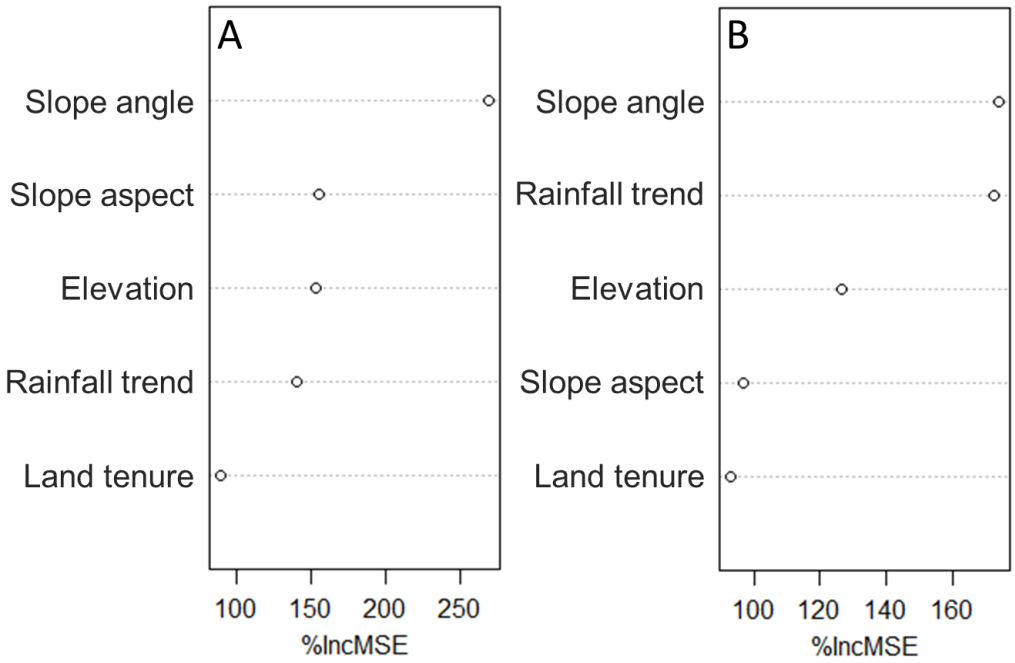

Figure 6.7. Predictor variable importance for the two random forest models predicting bare ground cover (A) and perennial plant cover (B) respectively. %IncMSE refers to the percentage increase of the mean squared error as a result of the variable being permuted (Breiman, 2001).

6.3.3 Habitat condition archetype

The different overlay type options available through the Fuzzy Overlay tool in Arcmap 10.4 resulted in different ranges in the membership values calculated for the habitat condition archetype. The 'AND' option chooses the minimum of the memberships from the input rasters resulting in membership values that are generally lower than desired, while the 'OR' option chose the maximum membership value of the input rasters resulting in a left-skewed range of high values. 'PRODUCT' is defined as a 'decreasive' function which de-emphasizes the importance of input rasters having similar values, while the 'SUM' option is an additive function that emphasizes the effect of multiple evidence. These two options therefore respectively result in membership values that are lower and higher than desired. Lastly, the 'GAMMA' option combines the 'SUM' and 'PRODUCT' values algebraically and produces a more appropriate range of values for the project area (**Error! Reference source not found.**). This raster was then combined in GEE with the raster layers of the five desertification drivers to produce a multi-band raster layer representing the habitat condition and the drivers

that have been found to impact on this condition (**Error! Reference source not found.**).

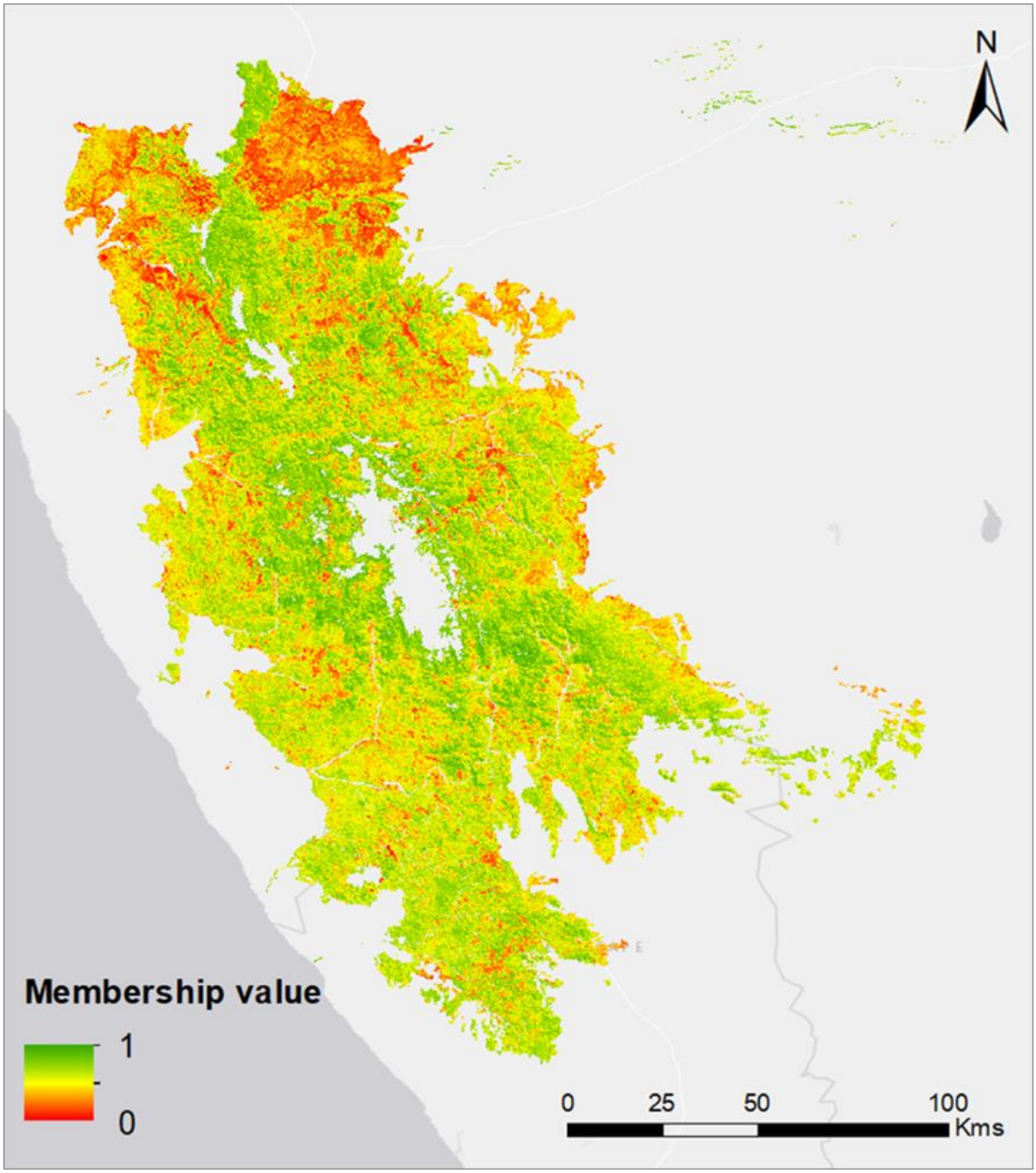

Figure 6.8. Habitat condition archetype map of the project area using the GAMMA overlay type option of the fuzzy overlay tool in ArcMap 10.4 to combine raster images representing estimated bare ground and perennial plant cover, and the trendline slope and percentile range of Landsat SMA estimated bare ground cover from 1984 to 2019 (ESRI, 2011).

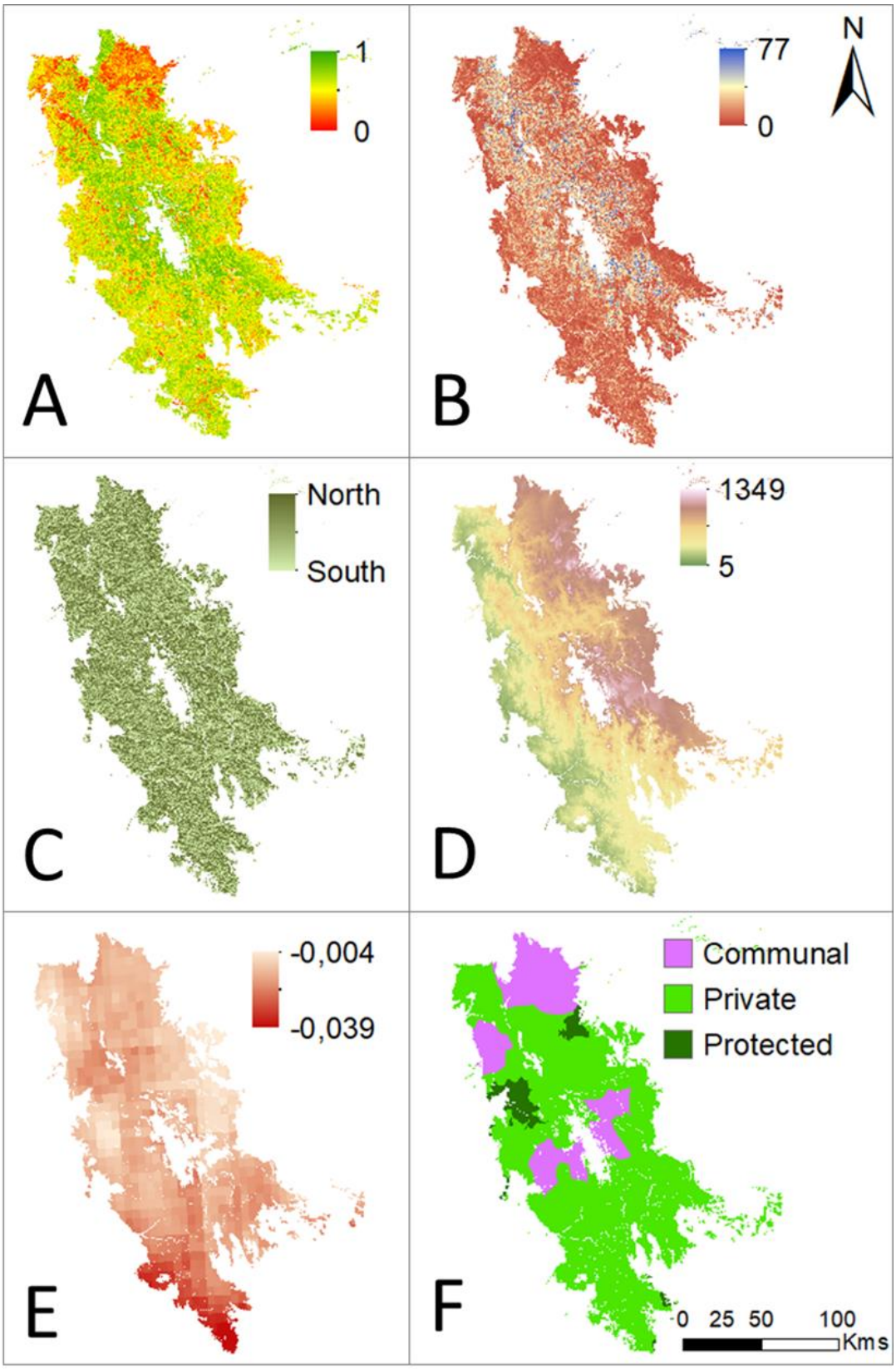
A
1
0
B
77
0
N
C
North
South
D
1349
5
E
-0,004
-0,039
F
Communal
Private
Protected
0 25 50 100
Kms

Figure 6.9. The six layers that constitute the final habitat condition archetype raster for the project area. Archetype membership values (A) can be evaluated relative to slope angle (B) in degrees, slope aspect (C), elevation (D) in metres, rainfall trendline slope (E), and land tenure (F).

Interpretation

The 'GAMMA' option was used to generate the raster representing the habitat condition membership values for the project area. The membership values were normally distributed across the project area (Figure 6.10) with a mean value of 0.55 and a standard deviation of 0.19. A large proportion (65.52%) of the project area had membership values that fell between 0.4 and 0.7, with 23% having membership values greater than 0.7, and 11% having values lower than 0.3 (Table 6.6). Six groups are generated through an evaluation of the mean ± two standard deviations for the membership values (Table 6.7), with the majority of the project area falling within one standard deviation either side of the mean (Table 6.7).

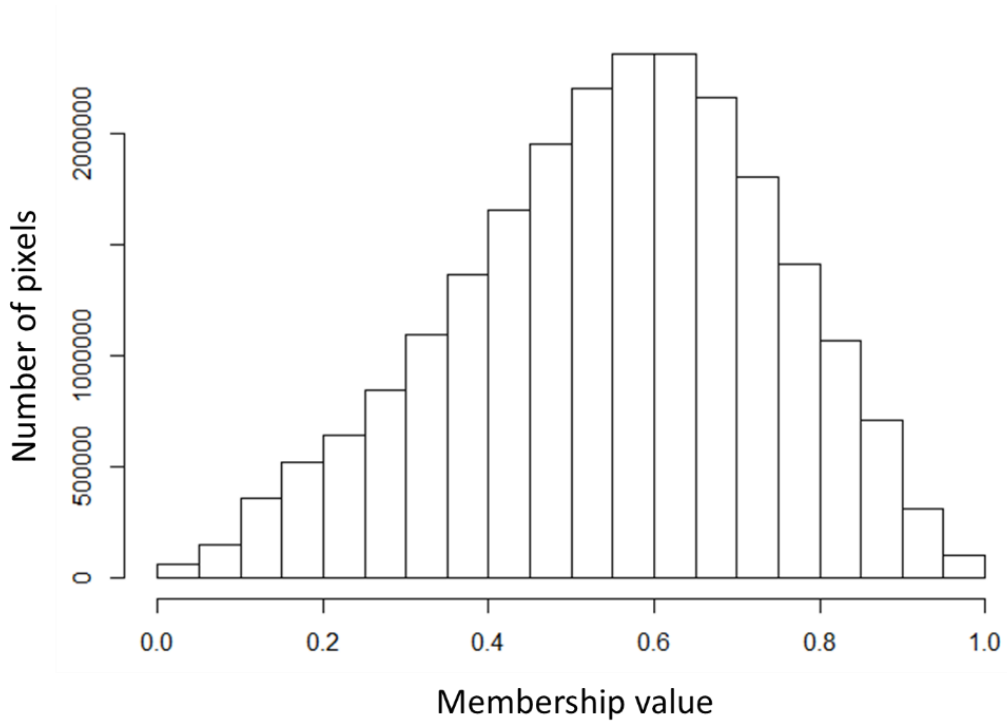

Figure 6.10. Distribution of habitat condition archetype pixels relative to their membership values.

Table 6.6. Proportion of the total project area within specified ranges of habitat condition archetype membership values.

Membership value range	Number of pixels	Percentage of the project area	Cumulative percentage of the project area
0 - 0.1	208026	0.90	0.90
0.1 - 0.2	876834	3.79	4.69
0.2 - 0.3	1484922	6.42	11.11
0.3 - 0.4	2458130	10.63	21.74
0.4 - 0.5	3611119	15.62	37.36
0.5 - 0.6	4560956	19.72	57.08
0.6 - 0.7	4520379	19.55	76.63
0.7 - 0.8	3220448	13.93	90.56
0.8 - 0.9	1775881	7.68	98.24
0.9 - 1	407754	1.76	100

Table 6.7. Proportion of the total project area within ranges specified by the mean and standard deviation of the habitat condition archetype membership values (mean = 0.55, S.D = 0.19).

Descriptive statistic range	Potential desertification class	Membership value range	Number of pixels	Percentage of the project area
Between 0 and two SD less than the mean	Severely degraded	0 - 0.17	764728	3.31
Between one and two SD less than the mean	Moderately degraded	0.17 - 0.36	3146181	13.61
Between the mean and one SD less than the mean	Stable	0.36 - 0.55	6931884	29.98
Between the mean and one SD greater than the mean	Stable	0.55 - 0.74	8354177	36.13
Between one and two SD greater than the mean	Slightly above average	0.74 - 0.93	3745384	16.20
Between two SD greater than the mean and 1	Significantly above average	0.93 - 1	182095	0.79

6.4 Discussion

Maps linking Earth observation data to various aspects of the Earth's surface, including vegetation cover, productivity and biodiversity, are useful for a wide range of ecological, conservation and management applications (Corbane et al., 2015; O'Connor et al., 2015; Pettorelli et al., 2016, 2014; Turner et al., 2015). Being able to interpret changes in these cover types over time, and within the context of potential drivers of change, is particularly useful within the context of desertification (Stellmes et al., 2013). The habitat condition archetype presented here provides a quantitative measure of desertification for the project area derived from accurate estimates of cover, the relative change in the amount of bare ground cover since 1984, and within the context of five potential desertification drivers. Habitat condition can, therefore, begin to be explained through the lens of potential desertification syndromes for the project area (Scholes, 2009).

6.4.1 Importance of desertification drivers

The relative importance of rainfall trend and slope aspect were the primary differences between the two random forest models predicting bare ground and perennial plant cover, with rainfall trend emerging as a better predictor of perennial plant cover than aspect (Figure 6.7). Land tenure was found to be the least important variable for both estimated bare ground and perennial plant cover. This is surprising considering the focus that has occurred over the last 25 years on the impact of different land tenure regimes on the vegetation of Namaqualand (Hoffman et al., 2007b). Removing this variable from the random forest models, however, reduced the performance and accuracy of the models suggesting that all five drivers are important for predicting cover in the project area. This is evidenced by the fact that there was a significant difference in cover estimates between the different land tenure groups (**Error! Reference source not found.**). Although rainfall trend was an important variable in predicting perennial plant cover, this needs further investigation as the nature of the relationship was contrary to what one might expect. An increase in perennial plant cover is expected to be related to an increasing precipitation trend (Davis et al., 2016), but this was not the case. A number of factors could be responsible including the potential lack of accuracy of the precipitation data. CHIRPS precipitation data for the

project area is modelled on data from a limited number of weather stations (Davis et al., 2016). Due to the highly variable topography of the area which influences rainfall patterns across short distances, it would be inappropriate to extrapolate this station data to even adjacent areas (MacKellar et al., 2007). This factor has resulted in poor correlations between the weather station data and actual rainfall events in similar locations in the Western Cape region of South Africa (Maswanganye, 2018). The relatively poor relationship between rainfall trend and perennial plant cover could also be due to the differences in spatial scale between the cover estimates and the rainfall data. CHIRPS data has a spatial resolution of approximately five kilometres (0.05°), which is much larger than the 30 m resolution of the cover estimate data, and probably too large to take into account the highly variable rainfall of the Namaqualand Hardeveld bioregion (van Rooyen et al., 2015). More accurate rainfall data with better spatial coverage and resolution would certainly improve the predictive strength of this variable in determining the condition of the veld in the project area.

The importance of slope angle for predicting both bare ground and perennial plant cover suggests that different drivers of desertification interact with each other. For example, grazing pressure in Namaqualand has been found to be higher in lower lying areas with gradual slopes that are more easily accessible to grazers (Anderson and Hoffman, 2007). Livestock either avoid steep slopes or are unable to access very steep areas and thus prefer more flat plateaus and lowlands (Samuels et al., 2007). Previously cultivated land in Namaqualand, which has subsequently been abandoned, is also generally found in flatter areas as these areas are more easily accessed and ploughed. These old fields have been shown to have limited ability to recover their vegetation layer without active intervention and often remain bare for decades after abandonment (Carrick and Krüger, 2007; Schmiedel et al., 2010). The presence of old fields and higher relative grazing pressure are, therefore, likely to contribute to the relationship between the cover estimates and slope angle in the random forest model. Slope aspect was also found to be important in predicting bare ground and has a similar level of importance to elevation in the models. This suggests that low lying, north-facing slopes are likely to have more bare ground than higher altitude, south-facing slopes.

Overall improvement to the random forest models is likely to materialise either through the addition of data related to other potential desertification drivers, or an improvement

in the accuracy or resolution of the data related to the five predictors used (Hill et al., 2008; Reynolds et al., 2011; Stellmes et al., 2013; Václavík et al., 2013). These predictors were never presented as an exhaustive list of the potential desertification drivers for the project area but rather comprise a snapshot of the potentially complex interactions between social, economic and environmental factors that influence desertification (Cherlet et al., 2018; Prince and Podwojewski, 2019).

6.4.2 Archetypes for land degradation mapping

The complexity of desertification processes across the world at a range of scales has contributed to a fundamental shift in mapping desertification. Attempts to create deterministic maps, particularly at the global scale, have largely been replaced with the presentation of desertification syndromes (Cherlet et al., 2018; del Barrio et al., 2016; Hill et al., 2008; Scholes, 2009; Stellmes et al., 2013). These syndromes are synonymous with archetypes in that they are based largely on attempts to integrate knowledge of diverse human-environment systems using a variety of methods, and resulting in a more nuanced general understanding of desertification (Hill et al., 2008; Stellmes et al., 2013; Václavík et al., 2013). A primary example of this shift is illustrated by the third World Atlas on Desertification (WAD3) (Cherlet et al., 2018). Instead of presenting a prescribed model for desertification at the global scale, WAD3 rather presents a variety of different global datasets, that represent global change issues, from which users can choose the most appropriate for their context. A final map is then presented that illustrates the level of convergence between these global change issues and suggests the potential for land degradation in any given area (Cherlet et al., 2018). This potential can then be evaluated by individual users within the local or regional context.

The syndromes approach was developed within global change research to address the inherent complexity in understanding and modelling global change (Cassel-Gintz and Petschel-Held, 2000; Lüdeke et al., 2004; Petschel-Held et al., 1999; Schellnhuber et al., 1997), and was first applied to the desertification issue in a paper presented to the Dahlem Workshop on Desertification (Downing and Lüdeke, 2002). Within the southern African context, Scholes (2009) has developed five dryland degradation syndromes which represent the broad mechanisms through which natural

capital in drylands is lost. These syndromes, whether at the global or regional scale, provide a framework within which local to regional-scale studies can be done. The desertification drivers presented here can be viewed within the context of Scholes' (2009) syndromes while incorporating the quantitative approach to archetype construction proposed by Cullum (2014, 2016).

The proportion of the project area that is degraded can be determined through various interpretations of the habitat condition archetype membership values. One potential interpretation of the data is for the user to set a membership value threshold for what they consider to be degraded land. This threshold could be decided upon arbitrarily, it could be based on expert knowledge of the area and its underlying patterns and processes, or it could be chosen based on the desertification driver data available in the archetype spatial layer. If, for example, it is decided that the threshold for land to be considered severely degraded is a membership value of 0.2 then this would constitute nearly 5% of the project area, while a threshold of 0.3 would include over 11% of the project area (Table 6.6). The areas that fall below this threshold can then be analysed in terms of the underlying desertification drivers to determine if the low membership value is related to potentially 'natural' (i.e. decreasing precipitation trend) or anthropogenic (different land tenure regimes) causes. The other potential classification method presented here is to distinguish degradation classes according to the descriptive statistics of the membership values. In this case, the data is grouped into six classes to which descriptions can be assigned (Table 6.7). According to these subjective class descriptions, nearly 17% of the project area could be classified as being somewhat degraded and, of this, only about 3% could be considered severely degraded.

Chapter 7:

7. General discussion and conclusions

7.1 Introduction

Even though desertification has been an issue of global concern for centuries, there is still no approach to measuring desertification that is generally accepted and universally appropriate (Cherlet et al., 2018). This is due to various issues starting with the terminology used, and how desertification is defined. The history of the desertification debate has been highly politicised and, as such, has resulted in much contention around the use of the word itself (Toulmin and Brock, 2016). The original image of the improper use of landscapes by local land users resulting in desert-like conditions persists in some scientific and policy domains today (Prince and Podwojewski, 2019). This is despite the emergence of a more nuanced contemporary understanding that the drivers and symptoms of desertification are considerably more complex and dynamic than originally thought (e.g. Reynolds *et al.*, 2011). The persistence of the original desertification narrative is, therefore, not only a result of the significant momentum that it gathered during the mid to late 1990's, but also a result of this complexity. However, when simple ideas are replaced with increased complexity, particularly within institutional structures, the simple idea will tend to persist as it is easier to understand, and is perceived to be easier to measure, and manage (Behnke and Mortimore, 2016b; Prince and Podwojewski, 2019).

Various authors dispute the value of using the term desertification (Behnke and Mortimore, 2016a). This argument is based on several issues including the pre-scientific and inaccurate origins of the term itself (Davis, 2016), the fact that desertification cannot easily be defined or quantified (Prince, 2016), the proposed need to integrate desertification into a broader global change framework (Giannini, 2016), and the ongoing realisation that the contemporary understanding of rangeland dynamics contradicts several key notions embedded within desertification theory (Huntsinger, 2016). Despite this opposition, the use of the term desertification continues both in the scientific literature, and especially within global and national institutions (Behnke and Mortimore, 2016b). Today, however, desertification is primarily understood as land degradation in the world's drylands. This shifts the

emphasis onto defining what is meant by land degradation. Consensus seems to be settling on the suggestion that land degradation be defined within the context in which it is measured (Reynolds et al., 2003), with a focus on measuring loss in both natural capital and ecosystem services (IPBES, 2018), and placing land degradation into broader frameworks known as syndromes or archetypes of change (Downing and Lüdeke, 2002; Prince and Podwojewski, 2019; Reynolds et al., 2011; Scholes, 2009). These global frameworks help to provide direction for desertification studies at smaller spatial scales, and emphasise the utility of multiple perspectives and classifications based on fuzzy, and not hard, approaches (Hill et al., 2008; Stellmes et al., 2013). Though the UNCCD has shifted its focus since its inception, member states still need to report on the amount of degraded land in their countries. This requires a quantification of the extent of desertification in the country. This quantification can, however, occur with a more contextualised and nuanced understanding of the heterogeneous nature of desertification at all spatial and temporal scales, and within the conceptual framework of a coupled human-environment system (Cowie et al., 2011; Reynolds et al., 2003; Salvati et al., 2019; Symeonakis et al., 2016; Václavík et al., 2013; Verstraete et al., 2011).

7.2 Summary of contribution

7.2.1 Delivery on research objectives

The overall objective of this project was to investigate a more appropriate approach to the mapping of desertification. This objective was addressed through a local level desertification assessment of six of the seven vegetation types of the Namaqualand Hardeveld bioregion of the Succulent Karoo biome, South Africa. While the objective was to develop an approach that could be applied globally, a primary output of the project included the development of a user-friendly map of the project area that could be used by conservation practitioners working in the region. The main findings of this thesis are discussed briefly below within the context of the three questions posed in chapter two (Figure 2.1). This is followed by a summary of the proposed methodology and an evaluation of how effectively it could be used to assess desertification in similar dryland environments around the world.

Research questions:

1. What are the most appropriate field measures of habitat condition for the Namaqualand Hardeveld bioregion that can be measured rapidly in the field?
2. What is the most appropriate method to measure habitat condition using freely available Earth observation data?
3. What is the best approach to map desertification for the project area that can be repeated for similar dryland environments?

Question 1

The first question is related to the habitat condition of the project area as measured in the field. Various potential indicators of desertification or land degradation were investigated to determine which indicators would likely represent the range of potential habitat condition across the project area (Figure 4.1). The purpose of this section was to evaluate how these indicators cluster in relation to one another, and to provide field data with which to ground truth the Earth observation data collected for the analysis in chapter five.

Defining land degradation at the level of the landscape, or at least at the regional scale, requires a good understanding of the underlying ecology of the area. Thus, a conceptual model of the landscape becomes particularly important (Figure 2.2). Although it is important to minimize significant sources of bias and subjectivity in the classification of landscapes in order to make methods repeatable and more relevant at larger spatial scales, this cannot take place without expert input at the level of understanding the landscape (Cullum et al., 2016b). This expert knowledge can come from different sources, including scientific experts in ecology, geology and climate, for example, and practical experts in the form of farmers, conservation practitioners and government agents that have real ‘on the ground’ working knowledge of an area (Cherlet et al., 2018; Kong et al., 2014; van Haren et al., 2019). Information from such sources can be used to develop a conceptual understanding of a landscape which can then be tested against data collected both remotely and from the field. The conceptual diagram proposed in chapter two was developed to understand some of the potential factors that are likely to result in a degraded landscape in the project area, and how

this could be measured. This diagram was then updated in chapter six to only include data determined to be most important for the project area (**Error! Reference source not found.**).

The data collected in the field for this project clustered significantly into groups representing different potential habitat condition states for the project area (Figure 4.7). These states were primarily distinguished by the cover estimates of both perennial plant cover and bare ground cover (Figure 4.9). The analysis of the field data provides a good approximation of the range of habitat condition for the plots sampled and can, therefore, be used to determine the most appropriate Earth observation data for mapping this condition across the project area.

Question 2

The second question addressed in this thesis was to determine the most appropriate method to assess habitat condition using Earth observation data. In order for Earth observation data from satellite imagery to be useful for assessing and monitoring desertification it needs to be related to what is happening on the Earth's surface, both from the perspective of vegetation cover and productivity, and through the lens of ecosystem functioning and ecosystem services (Fensholt et al., 2015; Herrmann and Sop, 2016; Higginbottom and Symeonakis, 2014; O'Connor et al., 2015).

The normalised difference vegetation index (NDVI) has been widely and successfully used for this purpose (e.g. Symeonakis and Drake, 2004; Thompson et al., 2009; Wessels et al., 2016), although various other methods have also been proposed (e.g. Huete, 1988; Knyazikhin et al., 1998; Qi et al., 1994) One of these alternative methods is spectral mixture analysis (SMA) which, in considering the full electromagnetic spectrum of the data collected, is suggested to improve correspondence with field data, particularly in arid areas (e.g. Okin and Roberts, 2002; Clasen *et al.*, 2015). SMA is a fuzzy classification method that is particularly useful for classifying mixed pixels, as is often the case in arid areas where a Landsat pixel, for example, will rarely be covered by only one cover type (Somers et al., 2010). A selection of vegetation indices, as well as SMA-derived estimates of cover, were therefore investigated in chapter five in relation to the field data collected in chapter four.

A model was produced through a partial least squares regression (PLSr) analysis which accurately predicted both perennial plant and bare ground cover for 61

independent test field plots across the project area (Table 5.3). Further interrogation of this model revealed that the SMA estimates of cover were better predictors of field-based cover in this specific context than any of the five vegetation indices tested (Figure 5.7). This confirms the finding that the use of vegetation indices for vegetation mapping may be less useful in certain contexts, and particularly when vegetation cover is low (Chabrillat, 2006; McGwire et al., 2000; Okin and Roberts, 2002). Personal communication with biodiversity assessment practitioners in South Africa suggests that products and maps that have relied too heavily on NDVI are not trusted to represent vegetation cover for the arid regions of the country. As a result, spectral mixture analysis is presented as a better predictor of cover for the Namaqualand Hardeveld bioregion studied here. The need to assess desertification for national and international institutions often results in there being no time for ground truthing of findings derived from remotely sensed data. It is therefore important that ground truthing of the Earth observation proxies used by these institutions is carried out regularly and in different geographical contexts to ensure that the most appropriate proxies are used in the different contexts (Higginbottom and Symeonakis, 2014).

Question 3

The final question posed to address the overall objective of this thesis was to use the data collected through the analyses in chapters four and five, along with new data related to potential desertification drivers in the project area, to produce a map of desertification for the Hardeveld region of Namaqualand. Random forest models were developed to investigate the impact of five potential desertification drivers on estimated cover for the project area. This information, along with a fuzzy classification of the PLSr findings, was then used to construct a habitat condition archetype for the project area (**Error! Reference source not found.**). This archetype presents a quantitative measure of desertification (Table 6.6 and Table 6.7) within the context of potential desertification drivers (**Error! Reference source not found.**). The archetype, and the accompanying conceptual diagram (**Error! Reference source not found.**), fit well into a broader conceptualisation of degradation syndromes for southern Africa (Table 7.1) proposed by Scholes (2009), and can be used to inform the specific and sub-national LDN targets reported by the South African Department of Environmental Affairs (Table 1.4) (DEA, 2018; Speranza et al., 2019). A simple classification of the archetype membership values, based on the mean and one or two standard deviations

from the mean (Canty and Nielsen, 2006; de la Barreda-Bautista et al., 2011; Prince et al., 2009; Zanchetta and Bitelli, 2017), suggests that the majority (± 66%) of the project area is in a stable condition, while about 17% is potentially degraded and about the same amount is in above average condition (Table 6.7; Figure 6.10). Of the area that is potentially degraded, only about 3% have membership values between zero and two standard deviations smaller than the mean, suggesting that only about 3% of the project area could be considered severely degraded.

The archetypal approach allows for different knowledge systems to contribute to the construction of the archetypes and, importantly, allows for future changes to the conceptual understanding of land degradation to be included in archetype design (Cullum et al., 2016a). These changes could be in the form of new knowledge regarding the importance of land degradation indicators and drivers, or improved data gathered through different acquisition techniques or through future improvements in available technologies.

Mapping landscapes into a series of distinct habitat condition classes tends to remove the inherent uncertainty in the mapping procedure. Mapping membership values, on the other hand, allows users to determine their own thresholds for these values based on their own investigation and expectations (Oldeland et al., 2010). Information relating to the specific locations is also often lost in traditional maps. The archetypal approach allows for two areas that have the same archetype membership value to be analysed or managed differently if they are found to be influenced by different factors (Cullum et al., 2016b). Two areas may, for example, appear to be degraded to the same extent (equal membership values) but one of the areas may have experienced a decrease in annual rainfall for several decades, while the other area has experienced a change in management. The approaches to conserving or managing these areas will, therefore, differ as a result of the difference in the potential driver resulting in the observed habitat condition. These differences in response would not be possible with a traditional mapping approach (Cullum, 2014) .

7.2.2 Proposed approach

The habitat condition archetype presented here can be used to determine the extent of desertification in the Namaqualand Hardeveld bioregion through a quantitative assessment of ground truthed Earth observation data, and with an understanding of

the different potential drivers of change in the region. The general approach to adapt and replicate these findings, and construct habitat condition archetypes for similar dryland environments, involves the most relevant aspects of the approach used in this thesis (Table 7.1). Since the approach has been developed for replication within the more technical work environment of conservation and government institutions, the statistical analyses are not included. Instead, the approach focuses on a methodology that can be replicated in a relatively short time period using freely available software and technology.

Table 7.2. A proposed general approach to constructing habitat condition archetypes for dryland environments.

Step	Basic considerations
1. Spectral endmember determination	Determine endmember values for all possible cover types. Endmembers should ideally be determined in the field or laboratory but can also be determined from drone or Earth observation (EO) data. Cover types can be proposed and agreed upon by experts and relevant stakeholders.
2. Spectral mixture analysis	Run the .unmix() function in Google Earth Engine to derive the proportional estimates of cover for each pixel in the generated image.
3. Consider change over time	Use Landsat cover estimates from 1984 to determine and analyse the change in different cover types over time. Contextualise observed changes with known patterns and processes.
4. Collect data on potential drivers of change	Through Google Earth Engine, as well as other globally accessible data repositories (e.g. 3rd World Atlas of Desertification), collect spatial data related to the potential drivers of desertification in the area of interest.
5. Construct habitat condition archetype	Use fuzzy classification techniques in QuantumGIS or other GIS platforms to derive habitat condition membership values. Present membership values along with data on the factors which are most important in influencing the process of desertification.

Limitations

Unlike the use of vegetation indices, spectral mixture analysis methods require the designation of endmember values for the various land cover types across the area of interest. In order to produce optimal results, all elements that are likely to be present in any given pixel need to be included in the analysis (Okin and Roberts, 2002). In areas with highly heterogeneous soil and vegetation characteristics, this can be

problematic as certain cover types that cover relatively small areas may invariably be excluded. Although this concern is largely circumvented with the use of multiple endmembers (e.g. Caixeta, 2016; Hamada et al., 2013; McGwire et al., 2000; Okin et al., 1999), some important cover types may be missed during endmember determination. There was poor correlation between estimated rock cover and the spectral mixture analysis estimates of bare rock cover for this project. This could be due to the choice of endmembers representing bare rock, or the presence of lichens that may interfere with the bare rock spectral signal. The presence of biological soil crust (biocrust), particularly in dryland environments, has been shown to have a significant impact on the spectral response of different cover types, and this effect is enhanced by the rapid response of biocrust to even small amounts of available moisture (Rodríguez-Caballero et al., 2015). As a result of the drought experienced in the project area during the period for which the SMA estimates were determined, vegetation productivity is not expected to have changed significantly. The biocrust spectral signal may, however, have changed if water became available in the form of fog or mist at any point during the sampling period. This small amount of available moisture would likely impact the biocrust spectral signal to a larger extent than the vegetation signal, thus impacting on the proportional estimates obtained (Rodríguez-Caballero et al., 2015).

A limitation of this project, which also provides scope for future research, is the analysis of change in the Earth observation data over time. Obtaining field and Earth observation data on the condition of the Earth's surface from the past and how it has changed over time will always be a limiting factor in land degradation research. However, this limitation can be reduced by better understanding the potential drivers of habitat condition in any given context, and how the magnitude and trajectory of these drivers have changed. Understanding these changes through historical records, paleontological records, and personal accounts can help to predict how the condition of the veld has changed and alleviate the need for extensive field and Earth observation data.

7.2.3 Implications for conservation and management

Local level

The habitat condition map, and related GIS spatial layers, generated through this project will be presented directly to the WWF South Africa Land Programme for use by the programme and its' partners for conservation planning activities and protected area network expansion work in Namaqualand (WWF South Africa, 2019). Through the Leslie Hill Succulent Karoo Trust, and various other funding mechanisms, these conservation organisations utilise spatial information to make decisions on potential areas of interest for conservation activities. Although primarily involved with protected area expansion, these activities also include engagement with stakeholders around biodiversity stewardship opportunities and initiatives to maximise social-economic benefits for local communities living in and around protected areas and biodiversity hotspots (WWF South Africa, 2018). The spatial layers will be able to assist with decision making at the local and regional scale before site visits are made to areas of potential conservation interest. The GEE scripts will also be shared, and will allow for a more thorough evaluation of change through the generation of time series charts for specific points within the project area.

National level

Land degradation, or desertification, has been a concern in South Africa for over a century (see section 1.2.5 of this thesis), yet the extent of land degradation across the country is still unknown (Skowno et al., 2019). This is related to a number of issues already mentioned in this thesis, and has been flagged consistently as an area of concern in the three National Biodiversity Assessments that have been published for South Africa (Driver et al., 2011, 2004; Skowno et al., 2019). Although the map outputs that have been generated through this thesis will prove useful for the Namaqualand Hardeveld bioregion specifically, the methodology used to create these outputs will help to improve desertification mapping across the country as a whole. As shown in Table 1.4, South Africa has a list of thirteen specific targets to avoid, minimise and reverse land degradation (DEA, 2018). The creation of habitat condition archetype maps at the level of the bioregion or the biome, as suggested by von Maltitz et al. (2019), can help to pinpoint areas where these targets can be addressed. As mentioned in section 3.4 of this thesis, the latest iteration of the VEGMAP project

(VEGMAP 2018) classifies the vegetation of South Africa into 41 bioregions which are grouped into the country's ten major biomes (SANBI, 2019). A nationally led project which aims at producing individual maps for each bioregion in the country is entirely possible if the approach suggested here is followed. This will allow for more accurate reporting on the progress made towards addressing the agreed upon LDN targets, and will help to address the need for local level assessments, as suggested in NBA 2018 (Skowno et al., 2019).

International level

The methodology proposed here for mapping land degradation can be contextualised broadly within the growing narrative around syndromes of land degradation that has emerged in the literature as an alternative to the traditional desertification narrative (e.g. Cherlet et al., 2018; del Barrio et al., 2016; Prince et al., 2018; Reynolds et al., 2011, 2007; Stellmes et al., 2013). Habitat condition can be understood within agreed upon syndromes and quantified to allow for accurate reporting of desertification to international institutions like the UNCCD. The approach is based on a sound conceptual framework developed through extensive field work and expert knowledge of the project area. It is further bolstered by a rigorous statistical foundation that utilises various multivariate methods such as latent class analysis, partial least squares regression, and random forest regression. These analyses produce an accurate estimation of habitat condition on the ground. The method also takes advantage of the relatively recent advancements in Earth observation made possible through Google Earth Engine (Gorelick et al., 2017; Smith et al., 2019). Framing the methodology within the archetypes or syndromes research results in a robust and adaptable method for assessing the habitat condition of dryland environments that are characterised by sparse vegetation cover.

The designation of endmembers for all cover types across the world's terrestrial land surfaces is improbable at present. As a result, the method proposed here is unlikely to be currently viable for the production of a global desertification map. Rather, the method is proposed to produce improved land degradation assessments at the local and regional scale that can fit into a broader land degradation narrative (Cherlet et al., 2018). It is widely proposed that global land degradation maps that have been created through the use of vegetation indices like NDVI (e.g. Fensholt et al., 2015, 2012) are vital for pinpointing locations across the globe where regional and local assessments

need to be made. The methods suggested in this thesis can therefore be used at the secondary spatial scale in locations suggested by global assessments (Cherlet et al., 2018; Fensholt et al., 2015).

7.3 Future research

Where the use of vegetation indices may be less appropriate, spectral mixture analysis, and its analytical variants, have the potential to more accurately map dryland environments (Dawelbait and Morari, 2008; Rodríguez-Caballero et al., 2015). This potential will be improved through the designation and evaluation of endmember values for a greater variety of land surfaces, plant species, and plant functional types and communities (Clark, 2017; Roberts et al., 2015; Somers et al., 2011; Somers and Asner, 2013; Youngentob et al., 2011), both in the laboratory and in the field. If the development of a more complete spectral library coincides with the likely availability of higher resolution remote sensing data, from both unmanned aerial vehicles (UAVs) and satellite platforms, then the potential to accurately assess the state of drylands will be vastly improved (Greenville et al., 2017; Transon et al., 2018). The United States Geological Survey (USGS) are already addressing this limitation through establishing a high resolution spectral library which contains reflectance spectra for mineral, rock and soil samples, as well as spectra for various plants, vegetation communities, microorganisms and man-made materials (Kokaly et al., 2017). The inclusion of spectral signatures specific to dryland environments will improve the ability of dryland researchers to map land degradation, although these efforts need to take place within known archetypes of land degradation for the region of interest.

The emergence of UAVs (drones) fitted with high resolution multi-spectral camera equipment provides scope for significant improvement in land degradation mapping (Manfreda et al., 2018), particularly with the spectral mixture analysis approach (e.g. Chen et al., 2016; Duan et al., 2019; Mitchell et al., 2012; Sankey et al., 2018). UAVs allow for the delineation of endmember spectra at a finer spatial resolution than is possible with satellite data. Spectral signatures obtained through drone imagery can be used to inform spectral mixture analyses conducted with satellite imagery by acting as training data (Sankey et al., 2018). The approach to mapping vegetation cover using drone imagery has already shown great promise within the South African

drylands context in comparison with field surveys, and will only be improved with greater human and capital resources (Schumann et al., 2018). The spectral signals of individual species can be ascertained to determine accurate cover estimates at the species level across much larger geographic areas than is possible with field-based surveys (Hill et al., 2017; Lu and He, 2018, 2017; Manfreda et al., 2018; Michez et al., 2016; Rose et al., 2015). Future studies using unmixing estimates from drone imagery can therefore be incorporated into habitat condition archetypes at the local scale.

Improvements can be made to contextualising quantitative assessments of land degradation through the incorporation of data relevant to the particular land degradation syndrome (Cherlet et al., 2018; Prince et al., 2018). This includes improvement in spatial data related to rainfall, soils, land use and land management, but also includes the collation of data and information from various other contemporary and historical sources (Reynolds et al., 2011, 2007). The knowledge gained by local land users in dynamic dryland environments over generational time spans can greatly improve the understanding of local and regional land degradation syndromes. This knowledge can be obtained through formal stakeholder engagement and informal storytelling, and through an investigation of historical archives and records (Akhtar-Schuster et al., 2016; Chasek et al., 2011; Reed et al., 2011). The institutionalisation of such integrated knowledge transfer systems will improve the understanding of dryland dynamics, and inform the development of spatially explicit land degradation syndromes (Akhtar-Schuster et al., 2016, 2011).

As mentioned in the limitations section above, an analysis of the change in proportional estimates determined through the unmixing algorithm in GEE provides significant scope for future research. Comprehensive time series analyses of these estimates could provide significant insight into the state and direction of change across the project area. The utility of such an analysis over the use of vegetation indices has already been highlighted within the dryland context (Sonnenschein et al., 2011), and provides significant scope, particularly for more local, site-specific assessments.

7.4 Concluding remarks

The regional habitat condition map, and associated GIS spatial layers, that have been created through this project will directly inform conservation planning in the region by the WWF South Africa and its conservation and government partners. The method to create these regional outputs is presented as a tool to enhance efforts at the national level to assess land degradation in South Africa, and address the targets established through the LDN target setting process for the country (DEA, 2018; Skowno et al., 2019; Von Maltitz et al., 2019). The methods are also proposed to improve land degradation mapping more generally across the globe, particularly in dryland environments where the use of traditional vegetation indices may be inappropriate. The conceptualisation of land degradation in this project aligns with the paradigm shift in the desertification literature toward understanding land degradation globally through the lens of specific land degradation syndromes (Cherlet et al., 2018; Prince et al., 2018; Reynolds et al., 2011, 2007, 2003). The construction of a habitat condition archetype utilising a sound statistical approach that includes a quantitative measure of condition with reference to potential drivers of change for the region is unique, and provides opportunities for local and regional scale assessments to feed into broader understandings of land degradation at the national and global scale.

References

Abdi, H., 2010. Partial least squares regression and projection on latent structure regression (PLS Regression). Wiley Interdiscip. Rev. Comput. Stat. 2, 97–106. https://doi.org/10.1002/wics.051

Acocks, J.P.H., 1953. Veld Types of South Africa. Mem. Bot. Surv. South Africa 28, 1–192.

Adamson, R.S., 1938. The vegetation of South Africa. British Empire Vegetation Committee, London.

Afanador, N.L., Smolinska, A., Tran, T.N., Blanchet, L., 2016. Unsupervised random forest: A tutorial with case studies. J. Chemom. 30, 232–241. https://doi.org/10.1002/cem.2790

Akhtar-Schuster, M., Amiraslani, F., Morejon, C.F.D., Escadafal, R., Fulajtar, E., Grainger, A., Kellner, K., Khan, S.I., Pardo, O.P., Sauchanka, U., Stringer, L.C., Reda, F., Thomas, R.J., 2016. Designing a new science-policy communication mechanism for the UN Convention to Combat Desertification. Environ. Sci. Policy 63, 122–131. https://doi.org/10.1016/j.envsci.2016.03.009

Akhtar-Schuster, M., Stringer, L.C., Erlewein, A., Metternicht, G., Minelli, S., Safriel, U., Sommer, S., 2017. Unpacking the concept of land degradation neutrality and addressing its operation through the Rio Conventions. J. Environ. Manage. 195, 4–15. https://doi.org/10.1016/j.jenvman.2016.09.044

Akhtar-Schuster, M., Thomas, R.J., Stringer, L.C., Chasek, P., Seely, M., 2011. Improving the enabling environment to combat land degradation: Institutional, financial, legal and science-policy challenges and solutions. L. Degrad. Dev. 22, 299–312. https://doi.org/10.1002/ldr.1058

Alavipanah, S.K., Rafiei Emam, A., Khodaei, K., Hadji Bagheri, R., Yazdan Panah, A., 2010. Criteria of selecting satellite data for studying land resources. Desert 15, 83–102. https://doi.org/10.22059/jdesert.2011.23005

Allsopp, N., 1999. Effects of grazing and cultivation on soil patterns and processes in the Paulshoek area of Namaqualand. Plant Ecol. 142, 179–187.

https://doi.org/10.1023/A:1009826412617

Anderson, C.B., 2018. Biodiversity monitoring, earth observations and the ecology of scale. Ecol. Lett. 21, 1572–1585. https://doi.org/10.1111/ele.13106

Anderson, P.M.L., Hoffman, M.T., 2011. Grazing response in the vegetation communities of the Kamiesberg, South Africa: Adopting a plant functional type approach. J. Arid Environ. 75, 255–264. https://doi.org/10.1016/j.jaridenv.2010.10.012

Anderson, P.M.L., Hoffman, M.T., 2007. The impacts of sustained heavy grazing on plant diversity and composition in lowland and upland habitats across the Kamiesberg mountain range in the Succulent Karoo, South Africa. J. Arid Environ. 70, 686–700. https://doi.org/10.1016/j.jaridenv.2006.05.017

Andrew, M.H., 1988. Grazing Impact in Relation to Livestock Watering Points. Trends Ecol. Evol. 3, 336–339.

Aubréville, A., 1949. Climats, Forêts et Désertification de l'Afrique Tropicale;, 44th ed, Société des Editions Gelgraphiques, Maritimes et Coloniales. Paris, France.

Bai, Z.G., Dent, D., 2007. Land degradation and Improvement in South Africa 1: identification by remote sensing. Report 2007/03. ISRIC – World Soil Information, Wageningen.

Bai, Z.G., Dent, D., Olsson, L., Schaepman, M., 2008a. Global assessment of land degradation and improvement 1: identification by remote sensing. Report 2008/01. ISRIC – World Soil Information, Wageningen. https://doi.org/report 2008/01

Bai, Z.G., Dent, D.L., Olsson, L., Schaepman, M.E., 2008b. Proxy global assessment of land degradation. Soil Use Manag. 24, 223–234. https://doi.org/10.1111/j.1475-2743.2008.00169.x

Bastin, G., Pickup, G., Chewings, V.H., Pearce, G., 1993. Land degradation assessment in central Australia using a grazing gradient method. Aust. Rangel. J. 15, 190–216.

Behnke, R., Mortimore, M. (Eds.), 2016a. The End of Desertification? Springer Berlin Heidelberg, Berlin.

Behnke, R., Mortimore, M., 2016b. Introduction: The End of Desertification, in: Behnke, R., Mortimore, M. (Eds.), The End of Desertification: Disputing Environmental Change in the Drylands. Springer, pp. 1–34. https://doi.org/10.1007/978-3-642-16014-1

Behnke, R., Scoones, I., 1993. Rethinking range ecology: implications for rangeland management in Africa, in: Behnke, R., Scoones, I., Kerven, C. (Eds.), Range Ecology at Disequilibrium: New Models of Natural Variability and Pastoral Adaptation in African Savannas. Overseas Development Institute and IIED, Woburn, UK, pp. 1–30.

Beinart, W., 1984. Soil Erosion , Conservationism and Ideas about Development : A Southern African Exploration , 1900-1960. J. South. Afr. Stud. 11, 52–83.

Beinart, W., Delius, P., 2015. The Natives Land Act of 1913: A template but not a turning point., in: Cousins, B., Walker, C. (Eds.), Land Divided, Land Restored: Land Reform in South Africa for the 21st Century. Jacana Media, Cape Town, pp. 24–39.

Beinroth, F.H., Eswaran, H., Reich, P.F., 2001. Global Assessment of Land Quality, in: Scott, D., Mohtar, R., Steinhardt, G. (Eds.), Sustaining the Global Farm. International Soil Conservation Organization, pp. 569–574.

Benjaminsen, T.A., Rohde, R.F., Sjaastad, E., Wisborg, P., Lebert, T., 2006. Land reform, range ecology, and carrying capacities in Namaqualand, South Africa. Ann. Assoc. Am. Geogr. 96, 524–540. https://doi.org/10.1111/j.1467-8306.2006.00704.x

Benz, U.C., Hofmann, P., Willhauck, G., Lingenfelder, I., Heynen, M., 2004. Multi-resolution, object-oriented fuzzy analysis of remote sensing data for GIS-ready information. ISPRS J. Photogramm. Remote Sens. 58, 239–258. https://doi.org/10.1016/j.isprsjprs.2003.10.002

Berg, E., 1976. The Economic Impact of Drought and Inflation in the Sahel, in: Discussion Paper No. 51. Center for Research on Economic Development, Michigan, pp. 1–38.

Berry, L., Abraham, E., Essahli, W., 2009. UNCCD Recommended Minimum set of

Impact Indicators. Bonn, Germany.

Beukes, P.C., Ellis, F., 2003. Soil and vegetation changes across a Succulent Karoo grazing gradient. African J. range For. 20, 11–19. https://doi.org/10.2989/10220110309485793

Biancalani, R., Nachtergaele, F., Petri, M., Bunning, S., 2011. Land degradation assessment in drylands, LADA Project.

Black, M., 1937. Vagueness. An Exercise in Logical Analysis. Philos. Sci. 4, 427–455. https://doi.org/10.1086/286476

Bliss, J.C., Fischer, A.P., 2011. Toward a Political Ecology of Ecosystem Restoration, in: Egan, D., Hjerpe, E.E., Abrams, J. (Eds.), Human Dimensions of Ecological Restoration: Integrating Science, Nature and Culture. Island Press, Washington, pp. 135–148. https://doi.org/10.1017/CBO9781107415324.004

Bosch, O.J.H., Gauch, H.G., 1991. The use of degradation gradients for the assessment and ecological interpretation of range condition. J. Grassl. Soc. South. Africa 8, 138–146. https://doi.org/10.1080/02566702.1991.9648281

Bosch, O.J.H., Kellner, K., 1991. The use of a degradation gradient for the ecological interpretation of condition assessments in the western grassland biome of Southern Africa. J. Arid Environ. 21, 21–29. https://doi.org/10.1016/s0140-1963(18)30724-9

Boschetti, M., Bocchi, S., Brivio, P.A., 2007. Assessment of pasture production in the Italian Alps using spectrometric and remote sensing information. Agric. Ecosyst. Environ. 118, 267–272. https://doi.org/10.1016/j.agee.2006.05.024

Botha, M.S., Carrick, P.J., Allsopp, N., 2008. Capturing lessons from land-users to aid the development of ecological restoration guidelines for lowland Namaqualand. Biol. Conserv. 141, 885–895. https://doi.org/10.1016/j.biocon.2007.12.005

Bradfield, E.R., 1908. Erosion and Dessication of the Karoo. Agric. J. Cape Good Hope 33, 657–659.

Breiman, L., 2001. Random forests. Mach. Learn. 45, 5–32. https://doi.org/10.1007/978-3-662-56776-0_10

Briske, D.D. (Ed.), 2017. Rangeland Systems: Processes, Management and Challenges, First. ed. Springer Nature, Cham. https://doi.org/10.1007/978-3-319-46709-2_2

Briske, D.D., Fuhlendorf, S.D., Smeins, F.E., 2003. Vegetation dynamics on rangelands: A critique of the current paradigms. J. Appl. Ecol. 40, 601–614. https://doi.org/10.1046/j.1365-2664.2003.00837.x

Briske, D.D., Illius, A.W., Anderies, J.M., 2017. Nonequilibrium Ecology and Resilience Theory, in: Briske, D.D. (Ed.), Rangeland Systems: Processes, Management and Challenges. Springer Nature, pp. 197–227.

Brown De Colstoun, E.C., Story, M.H., Thompson, C., Commisso, K., Smith, T.G., Irons, J.R., 2003. National Park vegetation mapping using multitemporal Landsat 7 data and a decision tree classifier. Remote Sens. Environ. 85, 316–327. https://doi.org/10.1016/S0034-4257(03)00010-5

Bunning, S., McDonagh, J., Rioux, J., 2011. Manual for local level assessment of land degradation and sustainable land management, Land Degradation Assessment in Drylands Technical Report No. 11. Rome.

Burrell, A.L., Evans, J.P., Liu, Y., 2017. Detecting dryland degradation using Time Series Segmentation and Residual Trend analysis (TSS-RESTREND). Remote Sens. Environ. 197, 43–57. https://doi.org/10.1016/j.rse.2017.05.018

Burrough, P.A., Van Gaans, P.F.M., Hootsmans, R., 1997. Continuous classification in soil survey: Spatial correlation, confusion and boundaries. Geoderma 77, 115–135. https://doi.org/10.1016/S0016-7061(97)00018-9

Caixeta, F.F., 2016. An evaluation of Multiple Endmember Spectral Mixture Analysis applied to Landsat 8 OLI images for mapping land cover in southern Africa's Savanna . University of Louisville.

Campbell, J.B., 1996. Introduction to remote sensing., 2nd ed. Guilford Press, New York.

Canty, M.J., Nielsen, A.A., 2006. Visualization and unsupervised classification of changes in multispectral satellite imagery. Int. J. Remote Sens. 27, 3961–3975.

https://doi.org/10.1080/01431160500222608

Carrascal, L.M., Galván, I., Gordo, O., 2009. Partial Least Squares Regression as an Alternative to Current Regression Methods Used in Ecology. Oikos 118, 681–690.

Carrick, P.J., Krüger, R., 2007. Restoring degraded landscapes in lowland Namaqualand: Lessons from the mining experience and from regional ecological dynamics. J. Arid Environ. 70, 767–781. https://doi.org/10.1016/j.jaridenv.2006.08.006

Carruthers, J., 2006. Tracking in Game Trails: Looking Afresh at the Politics of Environmental History in South Africa. Environ. Hist. Durh. N. C. 11, 804–829. https://doi.org/10.1093/envhis/emq007

Cassel-Gintz, M., Petschel-Held, G., 2000. GIS-based assessment of the threat to world forests by patterns of non-sustainable civilisation nature interaction, in: 4th International Conference on Integrating GIS and Environmental Modeling (GIS/EM4): Problems, Prospects and Research Needs. Banff, pp. 1–23. https://doi.org/10.1006/jema.2000.0370

Chabrillat, S., 2006. Land Degradation Indicators : Spectral indices. Ann. Arid Zone 45, 331–354.

Chapin, F.S., Carpenter, S.R., Kofinas, G.P., Folke, C., Abel, N., Clark, W.C., Olsson, P., Smith, D.M.S., Walker, B., Young, O.R., Berkes, F., Biggs, R., Grove, J.M., Naylor, R.L., Pinkerton, E., Steffen, W., Swanson, F.J., 2010. Ecosystem stewardship: sustainability strategies for a rapidly changing planet. Trends Ecol. Evol. 25, 241–249. https://doi.org/10.1016/j.tree.2009.10.008

Charney, J., Quirk, W.J., Chow, S., Kornfield, J., 1977. A Comparative Study of the Effects of Albedo Change on Drought in Semi–Arid Regions. J. Atmos. Sci. 34, 1366–1385. https://doi.org/10.1175/1520-0469(1977)034<1366:ACSOTE>2.0.CO;2

Charney, J., Stone, P.H., Quirk, W.J., 1975. Drought in the Sahara: A Biogeographical Feedback Mechanism. Sci. New Ser. 187, 434–435.

Chase, B.M., Meadows, M.E., 2007. Late Quaternary dynamics of southern Africa's

winter rainfall zone. Earth-Science Rev. 84, 103–138.

Chasek, P., Essahli, W., Akhtar-Schuster, M., Stringer, L.C., Thomas, R., 2011. Integrated land degradation monitoring and assessment: Horizontal knowledge management at the national and international levels. L. Degrad. Dev. 22, 272–284. https://doi.org/10.1002/ldr.1096

Chen, J., Ming, Y.Z., Wang, L., Shimazaki, H., Tamura, M., 2005. A new index for mapping lichen-dominated biological soil crusts in desert areas. Remote Sens. Environ. 96, 165–175. https://doi.org/10.1016/j.rse.2005.02.011

Chen, J., Yi, S., Qin, Y., Wang, X., 2016. Improving estimates of fractional vegetation cover based on UAV in alpine grassland on the Qinghai–Tibetan Plateau. Int. J. Remote Sens. 37, 1922–1936. https://doi.org/10.1080/01431161.2016.1165884

Cherlet, M., Hutchinson, C.F., Reynolds, J.F., Hill, J., Sommer, S., Von Maltitz, G., 2018. World Atlas of Desertification, 3rd ed. Publication Office of the European Union, Luxembourg. https://doi.org/10.2760/9205

Chevalier, A., 1932. Les Productions végétales du Sahara et de ses confins Nord et Sud: Passé - présent - avenir. Rev. Bot. appliquée d'agriculture Colon. 12, 669–924.

Chikhaoui, M., Bonn, F., Bokoye, A.I., Merzouk, A., 2005. A spectral index for land degradation mapping using ASTER data: Application to a semi-arid Mediterranean catchment. Int. J. Appl. Earth Obs. Geoinf. 7, 140–153. https://doi.org/10.1016/j.jag.2005.01.002

Chin, W.W., 1998. The Partial Least Squares Approach to Structural Equation Modeling, in: Marcoulides, G.A. (Ed.), Modern Methods for Business Research. Lawrence Erlbaum Associates, London.

Clark, M.L., 2017. Comparison of simulated hyperspectral HyspIRI and multispectral Landsat 8 and Sentinel-2 imagery for multi-seasonal, regional land-cover mapping. Remote Sens. Environ. 200, 311–325. https://doi.org/10.1016/j.rse.2017.08.028

Clasen, A., Somers, B., Pipkins, K., Tits, L., Segl, K., Brell, M., Kleinschmit, B.,

Spengler, D., Lausch, A., Förster, M., 2015. Spectral Unmixing of Forest Crown Components at Close Range, Airborne and Simulated Sentinel-2 and EnMAP Spectral Imaging Scale. Remote Sens. 7, 15361–15387. https://doi.org/10.3390/rs71115361

Clements, F.E., 1916. Plant Succession. An Analysis of the Development of Vegetation. Carnegie Institution of Washington, Washington. https://doi.org/10.1126/science.45.1162.339

Compton, J.S., 2016. Human Origins: How Diet, Climate and Landscape Shaped Us. Earthspun Books, Cape town.

Conacher, A., 2009. Land degradation: A global perspective. N. Z. Geog. 65, 91–94. https://doi.org/10.1111/j.1745-7939.2009.01151.x

Conacher, A., 2004. Land Degradation and Desertification: History, Nature, Causes, Consequences, and Solutions, in: Sala, M. (Ed.), Theme 6.14 Geography, Encyclopedia of Life Support Systems (EOLSS). Developed under the auspices of the UNESCO, EOLSS Publishers, Oxford, UK, p. 10.

Conservation International, 2018. Trends.Earth Documentation (No. 0.57). http://trends.earth/docs/en/.

Corbane, C., Lang, S., Pipkins, K., Alleaume, S., Deshayes, M., García Millán, V.E., Strasser, T., Vanden Borre, J., Toon, S., Michael, F., 2015. Remote sensing for mapping natural habitats and their conservation status - New opportunities and challenges. Int. J. Appl. Earth Obs. Geoinf. 37, 7–16. https://doi.org/10.1016/j.jag.2014.11.005

Cowie, A.L., Penman, T.D., Gorissen, L., Winslow, M.D., Lehmann, J., Tyrrell, T.D., Twomlow, S., Wilkes, A., Lal, R., Jones, J.W., Paulsch, A., Kellner, K., Akhtar-Schuster, M., 2011. Towards sustainable land management in the drylands: Scientific connections in monitoring and assessing dryland degradation, climate change and biodiversity. L. Degrad. Dev. 22, 248–260. https://doi.org/10.1002/ldr.1086

Cowling, R.M., Esler, K.J., Rundel, P.W., 1999a. The Plant Ecology of Namaqualand, South Africa. Plant Ecol. 142, 1–187.

Cowling, R.M., Esler, K.J., Rundel, P.W., 1999b. Namaqualand, South Africa – an overview of a unique winter-rainfall desert ecosystem. Plant Ecol. 142, 3–21. https://doi.org/10.1023/A:1009831308074

Cowling, R.M., Gibbs Russell, G.E., Hoffman, M.T., Hilton- Taylor, C., 1989. Patterns of plant species diversity in southern Africa, in: Huntley, B. (Ed.), Biotic Diversity in Southern Africa. Concepts and Conservation. Oxford University Press, Cape Town, pp. 19–50.

Cowling, R.M., Pierce, S.M., Paterson-Jones, C., 1999c. Namaqualand: a succulent desert. Fernwood Press, South Africa.

Crist, T.O., Veech, J.A., Gering, J.C., Summerville, K.S., 2003. Partitioning Species Diversity across Landscapes and Regions: A Hierarchical Analysis of α, β, and γ Diversity. Am. Nat. 162, 734–743. https://doi.org/10.1086/378901

Critchley, W., Netshikovhela, E.M., 1998. Land degradation in South Africa: Conventional views, changing paradigms and a tradition of soil conservation. Dev. South. Afr. 15, 449–469. https://doi.org/10.1080/03768359808440024

Cullum, C., 2014. Integrating Stream Networks and Landscape Mosaics in a New Conceptualisation of Savanna Landscapes. University of the Witwatersrand.

Cullum, C., Brierley, G., Perry, G.L.W., Witkowski, E.T.F., 2016a. Landscape archetypes for ecological classification and mapping: The virtue of vagueness. Prog. Phys. Geogr. https://doi.org/10.1177/0309133316671103

Cullum, C., Rogers, K.H., Brierley, G., Witkowski, E.T.F., 2016b. Ecological classification and mapping for landscape management and science: Foundations for the description of patterns and processes. Prog. Phys. Geogr. 40, 38–65. https://doi.org/10.1177/0309133315611573

Dahlberg, A., 1994. Contesting views and changing paradigms : the land degradation debate in Southern Africa.

Dalsted, K., Paris, J.F., Clay, D.E., Clay, S. a, Reese, C.L., Chang, J., 2003. Selecting the Appropriate Satellite Remote Sensing Product for Precision Farming. Site-Specific Manag. Guidel. 40, 1–6.

Darkoh, M., 2019. The Nature, Causes and Consequences of Desertification in the Drylands of Africa. Hum. Impact Environ. Sustain. Dev. Africa 20, 199–235. https://doi.org/10.4324/9781315192963-10

Davis-Reddy, C., 2018. Assessing vegetation dynamics in response to climate variability and change across sub-Saharan Africa. Stellenbosch University.

Davis, C.L., 2013. Trends in vegetation productivity and seasonality for Namaqualand, South Africa between 1986 and 2011 : an approach combining remote sensing and repeat photography 1–147.

Davis, C.L., Hoffman, M.T., Roberts, W., 2017. Long-term trends in vegetation phenology and productivity over Namaqualand using the GIMMS AVHRR NDVI3g data from 1982 to 2011. South African J. Bot. 111, 76–85. https://doi.org/10.1016/j.sajb.2017.03.007

Davis, C.L., Hoffman, M.T., Roberts, W., 2016. Recent trends in the climate of Namaqualand, a megadiverse arid region of South Africa. S. Afr. J. Sci. 112, 1–9. https://doi.org/10.17159/sajs.2016/20150217

Davis, D., 2016. Deserts and Drylands Before the Age of Desertification, in: Behnke, R., Mortimore, M. (Eds.), The End of Desertification: Disputing Environmental Change in the Drylands. Springer, pp. 203–223. https://doi.org/10.1007/978-3-642-16014-1

Davis, D., 2008. Brutes, beasts and empire: veterinary medicine and environmental policy in French North Africa and British India. J. Hist. Geogr. 34, 242–267. https://doi.org/10.1016/j.jhg.2007.09.001

Dawelbait, M., Morari, F., 2008. Limits and potentialities of studying dryland vegetation using the optical remote sensing. Ital. J. Agron. 2, 97–106. https://doi.org/10.4081/ija.2008.97

de Jong, R., de Bruin, S., de Wit, A., Schaepman, M.E., Dent, D.L., 2011. Analysis of monotonic greening and browning trends from global NDVI time-series. Remote Sens. Environ. 115, 692–702. https://doi.org/https://doi.org/10.1016/j.rse.2010.10.011

de Jong, S.M., Jetten, V.G., 2007. Estimating spatial patterns of rainfall interception from remotely sensed vegetation indices and spectral mixture analysis. Int. J. Geogr. Inf. Sci. 21, 529–545. https://doi.org/10.1080/13658810601064884

de la Barreda-Bautista, B., López-Caloca, A.A., Couturier, S., Silván-Cárdenas, J.L., 2011. Tropical Dry Forests in the Global Picture: The Challenge of Remote Sensing-Based Change Detection in Tropical Dry Environments, in: Carayannis, E. (Ed.), Planet Earth 2011 - Global Warming Challenges and Opportunities for Policy and Practice. InTech, Rijeks, pp. 231–256. https://doi.org/10.5772/24283

De Wet, G.C., 1979. Simon van der Stel's journey to Namaqualand in 1685. Human & Rousseau, Cape Town.

DEA, 2018. South Africa: Final country report of the LDN Target Setting Programme. https://knowledge.unccd.int/sites/default/files/ldn_targets/South%20Africa%20LDN%20TSP%20Country%20Report.pdf.

Dean, W.R.J., Hoffman, M.T., Meadows, M.E., Milton, S.J., 1995. Desertification in the semi-arid Karoo, South Africa: review and reassessment. J. Arid Environ. 30, 247–264. https://doi.org/10.1016/S0140-1963(05)80001-1

DeAngelis, D.L., Waterhouse, J.C., 1987. Equilibrium and Nonequilibrium Concepts in Ecological Models. Ecol. Monogr. 57, 1–21.

del Barrio, G., Sanjuan, M.E., Hirche, A., Yassin, M., Ruiz, A., Ouessar, M., Valderrama, J.M., Essifi, B., Puigdefabregas, J., 2016. Land degradation states and trends in the northwestern Maghreb drylands, 1998-2008. Remote Sens. 8, 1–25. https://doi.org/10.3390/rs8070603

Denbow, J.R., Wilmsen, E.N., 1986. Advent and Course of Pastoralism in the Kalahari. Sci. New Ser. 234, 1509–1515.

DESIRE, 2008. Manual for describing land degradation indicators. http://www.desire-his.eu/index.php/en/component/docman/doc_download/18-wp21-manual-for-describing-land-degradation-indicators.

Desmet, P.G., 2007. Namaqualand-A brief overview of the physical and floristic environment. J. Arid Environ. 70, 570–587.

https://doi.org/10.1016/j.jaridenv.2006.11.019

Desmet, P.G., 1996. The vegetation and restoration potential of the arid coastal belt between Port Nolloth and Alexander Bay, Namaqualand, South Africa. University of Cape Town.

Desmet, P.G., Cowling, R.M., 1999. Biodiversity, habitat and range-size aspects of a flora from a winter-rainfall desert in north-western Namaqualand, South Africa. Plant Ecol. 142, 23–33.

Desmet, P.G., Dayaram, A., 2016. Integrated Report of proposed changes to the VEGMAP for Bushmanland, Namaqualand and Sandveld as proposed by Dr Philip Desmet at the National Vegetation Map Committee Meeting 2012.

Dewar, G., 2006. Survival and culture in the coastal desert of Namaqualand: What people ate and where they sat to eat it. The Digging Stick 23, 1–4.

Dewar, G., Stewart, B.A., 2017. Early Maritime Desert Dwellers in Namaqualand, South Africa: A Holocene Perspective on Pleistocene Peopling. J. Isl. Coast. Archaeol. 12, 44–64. https://doi.org/10.1080/15564894.2016.1216476

Diedhiou, A., Mahfouf, J.-F., 1996. Comparative influence of land and sea surfaces on the Sahelian drought: a numerical study. Ann. Geophys. 14, 115–130. https://doi.org/10.1007/s00585-996-0115-6

Diouf, A., Lambin, E.F., 2001. Monitoring land-cover changes in semi-arid regions: Remote sensing data and field observations in the Ferlo, Senegal. J. Arid Environ. 48, 129–148. https://doi.org/10.1006/jare.2000.0744

Dixon, A.P., Faber-Langendoen, D., Josse, C., Morrison, J., Loucks, C.J., 2014. Distribution mapping of world grassland types. J. Biogeogr. 41, 2003–2019. https://doi.org/10.1111/jbi.12381

Dormann, C.F., Elith, J., Bacher, S., Buchmann, C., Carl, G., Carré, G., Marquéz, J.R.G., Gruber, B., Lafourcade, B., Leitão, P.J., Münkemüller, T., Mcclean, C., Osborne, P.E., Reineking, B., Schröder, B., Skidmore, A.K., Zurell, D., Lautenbach, S., 2013. Collinearity: A review of methods to deal with it and a simulation study evaluating their performance. Ecography (Cop.). 36, 027–046.

https://doi.org/10.1111/j.1600-0587.2012.07348.x

Dougill, A.J., Fraser, E.D.G., Reed, M.S., 2010. Research, part of a Special Feature on Resilience and Vulnerability of Arid and Semi-Arid Social Ecological Systems Anticipating Vulnerability to Climate Change in Dryland Pastoral Systems: Using Dynamic Systems Models for the Kalahari.

Dougill, A.J., Thomas, D.S.G., Heathwaite, A.L., 1999. Environmental Change in the Kalahari: Integrated Land Degradation Studies for Nonequilibrium Dryland Environments. Ann. Assoc. Am. Geogr. 89, 420–442. https://doi.org/10.1111/0004-5608.00156

Downing, T.E., Lüdeke, M.K.B., 2002. International desertification: Social geographies of vulnerability and adaptation., in: Reynolds, J.F., Stafford Smith, D.M. (Eds.), Global Desertification: Do Humans Cause Deserts? Dahlem University Press, Berlin, pp. 233–252.

Driver, A., Maze, K., Lombard, A.T., Nel, J., Rouget, M., Turpie, J.K., Cowling, R.M., Desmet, P., Goodman, P., Harris, J., Jonas, Z., Reyers, B., Sink, K., Strauss, T., 2004. South African National Spatial Biodiversity Assessment: Summary Report. Pretoria.

Driver, A., Sink, K.J., Nel, J.L., Holness, S., van Niekerk, L., Daniels, F., Jonas, Z., Majiedt, P.A., Harris, L., Maze, K., 2011. National Biodiversity Assessment 2011. Cape Town.

du Toit, H.S., Gadd, S.M., Kolbe, G.A., Stead, A., van Reenen, R.J., 1923. Final Report of the Drought Investigation Commission. Cape Town.

du Toit, P.C. V, 2000. Estimating Grazing Index Values for Plants from Arid Regions 53, 529–536.

du Toit, P.C. V, Botha, W. van D., Olivier, D.J., Blom, C.D., Meyer, E.M., Becker, H.R., Barnard, G.Z.J., 1995. Estimating grazing-index values for Karoo plants 15.

Duan, B., Fang, S., Zhu, R., Wu, X., Wang, S., Gong, Y., Peng, Y., 2019. Remote estimation of rice yield with unmanned aerial vehicle (UAV) data and spectral mixture analysis. Front. Plant Sci. 10, 1–14.

https://doi.org/10.3389/fpls.2019.00204

Easdale, M.H., 2016. Zero net livelihood degradation-the quest for a multidimensional protocol to combat desertification. Soil 2, 129–134. https://doi.org/10.5194/soil-2-129-2016

Eisfelder, C., Kuenzer, C., Dech, S., 2012. Derivation of biomass information for semi-arid areas using remote-sensing data. Int. J. Remote Sens. 33, 2937–2984. https://doi.org/10.1080/01431161.2011.620034

Elmore, A., Mustard, J., 2000. Quantifying vegetation change in semiarid environments: precision and accuracy of spectral mixture analysis and the normalized difference vegetation index. Remote Sens. Environ. 73, 87–102.

ESA, 2020. Overview [WWW Document]. United Sp. Eur. URL https://www.esa.int/Applications/Observing_the_Earth/Copernicus/Overview4 (accessed 2.4.20).

Esler, K.J., Cowling, R.M., 1995. The comparison of selected life-history characteristics of Mesembryanthema species occurring on and off Mima-like mounds (heuweltjies) in semi-arid southern Africa. Vegetatio 116, 41–50.

ESRI, 2011. ArcGIS Desktop: Release 10. https://desktop.arcgis.com/en/arcmap/.

Evans, J., Geerken, R., 2004. Discrimination between climate and human-induced dryland degradation. J. Arid Environ. 57, 535–554. https://doi.org/10.1016/S0140-1963(03)00121-6

Farr, T.G., Rosen, P.A., Caro, E., Crippen, R., Duren, R., Hensley, S., Kobrick, M., Paller, M., Rodriguez, E., Roth, L., Seal, D., Shaffer, S., Shimada, J., Umland, J., Werner, M., Oskin, M., Burbank, D., Alsdorf, D.E., 2007. The shuttle radar topography mission. Rev. Geophys. 45.

Fensholt, R., Horion, S., Tagesson, T., Ehammer, A., Ivits, E., Rasmussen, K., 2015. Global-scale mapping of changes in ecosystem functioning from earth observation-based trends in total and recurrent vegetation. Glob. Ecol. Biogeogr. 24, 1003–1017. https://doi.org/10.1111/geb.12338

Fensholt, R., Langanke, T., Rasmussen, K., Reenberg, A., Prince, S.D., Tucker, C.,

Scholes, R.J., Le, Q.B., Bondeau, A., Eastman, R., Epstein, H., Gaughan, A.E., Hellden, U., Mbow, C., Olsson, L., Paruelo, J., Schweitzer, C., Seaquist, J., Wessels, K.J., 2012. Greenness in semi-arid areas across the globe 1981-2007 - an Earth Observing Satellite based analysis of trends and drivers. Remote Sens. Environ. 121, 144–158. https://doi.org/10.1016/j.rse.2012.01.017

Fensholt, R., Rasmussen, K., Kaspersen, P., Huber, S., Horion, S., Swinnen, E., 2013. Assessing land degradation/recovery in the african sahel from long-term earth observation based primary productivity and precipitation relationships. Remote Sens. 5, 664–686. https://doi.org/10.3390/rs5020664

Fisher, J., Montanarella, L., Scholes, R.J., 2018. Benefits to people from avoiding land degradation and restoring degraded land., in: Montanarella, L., Scholes, R.J., Brainach, A. (Eds.), The IPBES Assessment Report on Land Degradation and Restoration. Secretariat of the Intergovernmental Science-Policy Platform on Biodiversity and Ecosystem Services, Bonn, Germany, pp. 1–51.

Folland, C.K., Palmer, T.N., Parker, D.E., 1986. Sahel rainfall and worldwide sea temperatures, 1901-1985. Nature 320, 602–607.

Foody, G.M., 1996. Approaches for the production and evaluation of fuzzy land cover classifications from remotely sensed data Foody, G. M. Int. J. Remote Sens. 17, 1317–1340. https://doi.org/10.1080/01431169608948706

Francis, M.L., Fey, M. V., Prinsloo, H.P., Ellis, F., Mills, A.J., Medinski, T. V., 2007. Soils of Namaqualand: Compensations for aridity. J. Arid Environ. 70, 588–603. https://doi.org/10.1016/j.jaridenv.2006.12.028

Fraser, E.D.G., Dougill, A.J., Hubacek, K., Quinn, C.H., Sendzimir, J., Termansen, M., 2011. Assessing vulnerability to climate change in dryland livelihood systems: Conceptual challenges and interdisciplinary solutions. Ecol. Soc. 16, 01. https://doi.org/10.5751/ES-03402-160303

Fratkin, E., 2001. East African Pastoralism in Transition : Maasai , Boran , and Rendille Cases. Afr. Stud. Rev. 44, 1–25.

Frederiksen, P., 1993. Satellite based assessment and monitoring of land degradation in semi-arid tropical africa - aspects of the soil/vegetation complex. EARSel Adv.

Remote Sens. 2, 102–110.

Friedel, M.H., 1991. Range Condition Assessment and the Concept of Thresholds: A Viewpoint. J. Range Manag. 44, 422–426.

Funk, C., Peterson, P., Landsfeld, M., Pedreros, D., Verdin, J., Shukla, S., Husak, G., Rowland, J., Harrison, L., Hoell, A., Michaelsen, J., 2015. The climate hazards infrared precipitation with stations - A new environmental record for monitoring extremes. Sci. Data 2, 1–21. https://doi.org/10.1038/sdata.2015.66

Gao, X., Huete, A.R., Ni, W., Miura, T., 2000. Optical-biophysical relationships of vegetation spectra without background contamination. Remote Sens. Environ. 74, 609–620. https://doi.org/10.1016/S0034-4257(00)00150-4

Georganos, S., Abdi, A.M., Tenenbaum, D.E., Kalogirou, S., 2017. Examining the NDVI-rainfall relationship in the semi-arid Sahel using geographically weighted regression. J. Arid Environ. 146, 64–74. https://doi.org/10.1016/j.jaridenv.2017.06.004

Giannini, A., 2016. 40 Years of Climate Modeling: The Causes of Late-20th Century Drought in the Sahel, in: Behnke, R., Mortimore, M. (Eds.), The End of Desertification: Disputing Environmental Change in the Drylands. Springer, pp. 265–291. https://doi.org/10.1007/978-3-642-16014-1

Gibbs, H.K., Salmon, J.M., 2015. Mapping the world's degraded lands. Appl. Geogr. https://doi.org/10.1016/j.apgeog.2014.11.024

Gillson, L., Hoffman, M.T., 2007. Rangeland ecology in a changing world. Science, 315, 53–54. https://doi.org/10.1126/science.1136577

Gleason, H.A., 1917. The Structure and Development of the Plant Association. Bull. Torrey Bot. Club 44, 463–481.

González-Dugo, M.P., Mateos, L., 2008a. Spectral vegetation indices for benchmarking water productivity of irrigated cotton and sugarbeet crops. Agric. Water Manag. 95, 48–58. https://doi.org/10.1016/j.agwat.2007.09.001

González-Dugo, M.P., Mateos, L., 2008b. Spectral vegetation indices for benchmarking water productivity of irrigated cotton and sugarbeet crops. Agric.

Water Manag. 95, 48–58. https://doi.org/10.1016/j.agwat.2007.09.001

Gonzalez-Roglich, M., Zvoleff, A., Noon, M., Liniger, H., Fleiner, R., Harari, N., Garcia, C., 2019. Synergizing global tools to monitor progress towards land degradation neutrality: Trends.Earth and the World Overview of Conservation Approaches and Technologies sustainable land management database. Environ. Sci. Policy 93, 34–42. https://doi.org/10.1016/j.envsci.2018.12.019

Gonzalez, P., 2001. Desertification and a shift of forest species in the West African Sahel. Clim. Res. 17, 217–228. https://doi.org/10.3354/cr017217

Gonzalez, P., Tucker, C.J., Sy, H., 2012. Tree density and species decline in the African Sahel attributable to climate. J. Arid Environ. 78, 55–64. https://doi.org/10.1016/j.jaridenv.2011.11.001

Gorelick, N., Hancher, M., Dixon, M., Ilyushchenko, S., Thau, D., Moore, R., 2017. Google Earth Engine: Planetary-scale geospatial analysis for everyone. Remote Sens. Environ. 202, 18–27. https://doi.org/10.1016/j.rse.2017.06.031

Government of South Africa, 1951. Report of the Desert Encroachment Committee. Pretoria.

Greenville, A.C., Dickman, C.R., Wardle, G.M., 2017. 75 years of dryland science : Trends and gaps in arid ecology literature. PLoS One 12, 1–10. https://doi.org/10.4227/05/588e6a779edf5.

Grove, R.H., 1995. Green imperialism: colonial expansion, tropical island Edens and the origins of environmentalism. Cambridge University Press.

Haensler, A., Hagemann, S., Jacob, D., 2010. Climate history of Namibia and western South Africa, in: Jürgens, N., Schmiedel, U., Hoffman, M.T. (Eds.), Biodiversity in Southern Africa – Volume 2: Patterns and Processes at Regional Scale. Klaus Hess Publishers, Göttingen & Windhoek, pp. 2–5.

Hahn, B.D., Richardson, F.D., Hoffman, M.T., Roberts, R., Todd, S.W., Carrick, P.J., 2005. A simulation model of long-term climate, livestock and vegetation interactions on communal rangelands in the semi-arid Succulent Karoo, Namaqualand, South Africa. Ecol. Modell. 183, 211–230.

https://doi.org/10.1016/j.ecolmodel.2004.07.028

Hair, J.F., Ringle, C.M., Sarstedt, M., 2011. PLS-SEM: Indeed a silver bullet. J. Mark. Theory Pract. 19, 139–151. https://doi.org/10.2753/MTP1069-6679190202

Hair, J.F.J., Sarstedt, M., Hopkins, L., Kuppelwieser, V.., 2014. Partial least squares structural equation modeling (PLS-SEM) An emerging tool in business research. Eur. Bus. Rev. 26, 106–121. https://doi.org/10.1108/EBR-10-2013-0128

Hamada, Y., Stow, D.A., Roberts, D.A., Franklin, J., Kyriakidis, P.C., 2013. Assessing and monitoring semi-arid shrublands using object-based image analysis and multiple endmember spectral mixture analysis. Environ. Monit. Assess. 185, 3173–3190. https://doi.org/10.1007/s10661-012-2781-z

Hanan, N.P., Prevost, Y., Diouf, A., Diallo, O., 1991. Assessment of Desertification Around Deep Wells in the Sahel Using Satellite Imagery. J. Appl. Ecol. 28, 173–186.

Harwood, T.D., Donohue, R.J., Williams, K.J., Ferrier, S., McVicar, T.R., Newell, G., White, M., Anderson, B., 2016. Habitat Condition Assessment System: a new way to assess the condition of natural habitats for terrestrial biodiversity across whole regions using remote sensing data. Methods Ecol. Evol. 7, 1050–1059. https://doi.org/10.1111/2041-210X.12579

Hengl, T., Nussbaum, M., Wright, M.N., Heuvelink, G.B.M., Gräler, B., 2018. Random forest as a generic framework for predictive modeling of spatial and spatio-temporal variables. PeerJ 6, 1–49. https://doi.org/10.7717/peerj.5518

Henseler, J., Ringle, C.M., Sinkovics, R.R., 2009. The Use of Partial Least Squares Path Modeling in International Marketing. Adv. Int. Mark. 20, 277–320. https://doi.org/10.1108/S1474-7979(2009)0000020014

Herrmann, S.M., Hutchinson, C.F., 2005. The changing contexts of the desertification debate. J. Arid Environ. 63, 538–555. https://doi.org/10.1016/j.jaridenv.2005.03.003

Herrmann, S.M., Sop, T.K., 2016. The Map is not the Territory: How Satellite Remote Sensing and Ground Evidence Have Re-shaped the Image of Sahelian

Desertification, in: Behnke, R., Mortimore, M. (Eds.), The End of Desertification: Disputing Environmental Change in the Drylands. Springer, pp. 117–145. https://doi.org/10.1007/978-3-642-16014-1

Higginbottom, T.P., Symeonakis, E., 2014. Assessing land degradation and desertification using vegetation index data: Current frameworks and future directions. Remote Sens. 6, 9552–9575. https://doi.org/10.3390/rs6109552

Higginbottom, T.P., Symeonakis, E., Meyer, H., 2018. Mapping fractional woody cover in semi-arid savannahs using multi-seasonal composites from Landsat data. ISPRS J. Photogramm. Remote Sens. 139, 88–102.

Hill, D.J., Tarasoff, C., Whitworth, G.E., Baron, J., Bradshaw, J.L., Church, J.S., 2017. Utility of unmanned aerial vehicles for mapping invasive plant species: a case study on yellow flag iris (Iris pseudacorus L.). Int. J. Remote Sens. 38, 2083–2105. https://doi.org/10.1080/01431161.2016.1264030

Hill, J., Stellmes, M., Udelhoven, T., Röder, A., Sommer, S., 2008. Mediterranean desertification and land degradation. Mapping related land use change syndromes based on satellite observations. Glob. Planet. Change 64, 146–157. https://doi.org/10.1016/j.gloplacha.2008.10.005

Hirzel, A., Guisan, A., 2002. Which is the optimal sampling strategy for habitat suitability modelling. Ecol. Modell. 157, 331–341. https://doi.org/10.1016/S0304-3800(02)00203-X

Hoffman, M.T., 2018. Land use, land cover and vegetation change in southern Africa, in: Holmes, P.J., Boardman, J. (Eds.), Southern African Landscapes and Environmental Change. Routledge, Oxon & New York, pp. 91–111.

Hoffman, M.T., 2015. Environmental change in twentieth-century South Africa and its implications for land reform, in: Cousins, B., Walker, C. (Eds.), Land Divided, Land Restored: Land Reform in South Africa for the 21st Century. Jacana Media, Cape Town, pp. 56–67.

Hoffman, M.T., 1997. Human impacts on vegetation, in: Cowling, R.M., Richardson, F.D. (Eds.), Vegetation of Southern Africa. Cambridge University Press, Cambridge, pp. 507–534.

Hoffman, M.T., Allsopp, N., Rohde, R.F., 2007a. Special Issue Sustainable Land Use in Namaqualand. J. Arid Environ. 70, 561–846.

Hoffman, M.T., Allsopp, N., Rohde, R.F., 2007b. Sustainable land use in Namaqualand, South Africa: Key issues in an interdisciplinary debate. J. Arid Environ. 70, 561–569. https://doi.org/10.1016/j.jaridenv.2006.11.021

Hoffman, M.T., Ashwell, A., 2001. Nature Divided: Land Degradation in South Africa. Cape Town University Press, Cape Town.

Hoffman, M.T., Cowling, R.M., 1990. Vegetation change in the semi-arid, eastern Karoo over the last two hundred years: An expanding Karoo - fact or fiction? S. Afr. J. Sci. 86, 286–294.

Hoffman, M.T., Rohde, R.F., 2011. Rivers Through Time: Historical Changes in the Riparian Vegetation of the Semi-Arid, Winter Rainfall Region of South Africa in Response to Climate and Land Use. J. Hist. Biol. 44, 59–80. https://doi.org/10.1007/s10739-010-9246-4

Hoffman, M.T., Rohde, R.F., 2007. From pastoralism to tourism: The historical impact of changing land use practices in Namaqualand. J. Arid Environ. 70, 641–658. https://doi.org/10.1016/j.jaridenv.2006.05.014

Hoffman, M.T., Skowno, A.L., Bell, W., Mashele, S., 2018. Long-term changes in land use, land cover and vegetation in the Karoo drylands of South Africa: implications for degradation monitoring §. African J. Range Forage Sci. 35, 209–221. https://doi.org/10.2989/10220119.2018.1516237

Hoffman, M.T., Todd, S.W., 2000. A National Review of Land Degradation in South Africa: The Influence of Biophysical and Socio-economic Factors. J. South. Afr. Stud. 26, 743–758. https://doi.org/10.1080/713683611

Hoffman, M.T., Todd, S.W., Ntshona, Z., Turner, S., 1999. Land Degradation in South Africa.

Holden, C.E., Woodcock, C.E., 2016. An analysis of Landsat 7 and Landsat 8 underflight data and the implications for time series investigations. Remote Sens. Environ. 185, 16–36. https://doi.org/10.1016/j.rse.2016.02.052

Holling, C.S., 1973. Resilience and Stability of Ecological Systems. Annu. Rev. Ecol. Syst. 4, 1–23.

Horowitz, M., 1982. On Listening to Herders: An Essay on Pastoral Demystification. Proc. 3rd Int. Symp. Vet. Epidemiol. Econ. 416–425.

Hoscilo, A., Balzter, H., Bartholomé, E., Boschetti, M., Brivio, P.A., Brink, A., Clerici, M., Pekel, J.F., 2015. A conceptual model for assessing rainfall and vegetation trends in sub-Saharan Africa from satellite data. Int. J. Climatol. 35, 3582–3592. https://doi.org/10.1002/joc.4231

Hostert, P., Roder, A., Hill, J., 2003. Coupling spectral unmixing and trend analysis for monitoring of long-term vegetation dynamics in Mediterranean rangelands. Remote Sens. Environ. 87, 183–197.

Huang, J., Yu, H., Guan, X., Wang, G., Guo, R., 2016. Accelerated dryland expansion under climate change. Nat. Clim. Chang. 6, 166–171. https://doi.org/10.1038/nclimate2837

Huete, A.R., 1988. A soil-adjusted vegetation index (SAVI). Remote Sens. Environ. 25, 295–309. https://doi.org/10.1016/0034-4257(88)90106-X

Hulme, M., Barrow, E.M., Arnell, N.W., Harrison, P. a., Johns, T.C., Downing, T.E., 1999. Relative impacts of human-induced climate change and natural climate variability. Nature 397, 688–691. https://doi.org/10.1038/17789

Hunt, R.E., 1994. Relationship between woody biomass and PAR conversion efficiency for estimating net primary production from NDVI. Int. J. Remote Sens. https://doi.org/10.1080/01431169408954203

Huntsinger, L., 2016. The Tragedy of the Common Narrative: Re-telling Degradation in the American West, in: Behnke, R., Mortimore, M. (Eds.), The End of Desertification: Disputing Environmental Change in the Drylands. Springer, pp. 293–323. https://doi.org/10.1007/978-3-642-16014-1

Hutchinson, G.E., 1953. The Concept of Pattern in Ecology Source, in: Proceedings of the Academy of Natural Sciences of Philadelphia. Academy of Natural Sciences, pp. 1–12.

Hyam, R., 1972. The Failure of South African Expansion, 1908–1948. Africana Publishing, New York.

Ibrahim, Y.Z., Balzter, H., Kaduk, J., Tucker, C.J., 2015. Land degradation assessment using residual trend analysis of GIMMS NDVI3g, soil moisture and rainfall in Sub-Saharan West Africa from 1982 to 2012. Remote Sens. 7, 5471–5494. https://doi.org/10.3390/rs70505471

IIASA, 2009. Land Degradation Assessment in Drylands Project (LADA) Final Report: Compilation of Selected Global Indicators of Land Degradation, Land Degradation Assessment in Drylands Project (LADA) Final Report, PR. No. 39701.

IPBES, 2018. The IPBES assessment report on land degradation and restoration. Bonn, Germany.

Jafari, R., Lewis, M.M., Ostendorf, B., 2008. An image-based diversity index for assessing land degradation in an arid environment in South Australia. J. Arid Environ. 72, 1282–1293. https://doi.org/10.1016/j.jaridenv.2008.02.011

Jenkins, R.E., Bedford, W.B., 1973. The use of natural areas to establish environmental baselines. Biol. Conserv. 5, 168–174.

Jiang, H., 2016. Taking Down the “Great Green Wall”: The Science and Policy Discourse of Desertification and Its Control in China, in: Behnke, R., Mortimore, M. (Eds.), The End of Desertification: Disputing Environmental Change in the Drylands. Springer, pp. 513–536. https://doi.org/10.1007/978-3-642-16014-1

Jones, A., 2000. Effects of cattle grazing on North American arid ecosystems: A quantitative review. West. North Am. Nat. 60, 155–164.

Jönsson, P., Eklundh, L., 2004. TIMESAT - A program for analyzing time-series of satellite sensor data. Comput. Geosci. 30, 833–845. https://doi.org/10.1016/j.cageo.2004.05.006

Kairis, O., Kosmas, C., Karavitis, C., Ritsema, C., Salvati, L., Acikalin, S., Alcal??, M., Alfama, P., Atlhopheng, J., Barrera, J., Belgacem, A., Sol??-Benet, A., Brito, J., Chaker, M., Chanda, R., Coelho, C., Darkoh, M., Diamantis, I., Ermolaeva, O., Fassouli, V., Fei, W., Feng, J., Fernandez, F., Ferreira, A., Gokceoglu, C.,

Gonzalez, D., Gungor, H., Hessel, R., Juying, J., Khatteli, H., Khitrov, N., Kounalaki, A., Laouina, A., Lollino, P., Lopes, M., Magole, L., Medina, L., Mendoza, M., Morais, P., Mulale, K., Ocakoglu, F., Ouessar, M., Ovalle, C., Perez, C., Perkins, J., Pliakas, F., Polemio, M., Pozo, A., Prat, C., Qinke, Y., Ramos, A., Ramos, J., Riquelme, J., Romanenkov, V., Rui, L., Santaloia, F., Sebego, R., Sghaier, M., Silva, N., Sizemskaya, M., Soares, J., Sonmez, H., Taamallah, H., Tezcan, L., Torri, D., Ungaro, F., Valente, S., de Vente, J., Zagal, E., Zeiliguer, A., Zhonging, W., Ziogas, A., 2014. Evaluation and Selection of Indicators for Land Degradation and Desertification Monitoring: Types of Degradation, Causes, and Implications for Management. Environ. Manage. 54, 971–982. https://doi.org/10.1007/s00267-013-0110-0

Kandel, A., 1986. Fuzzy Mathematical Techniques with Applications. Addison-Wesley, Massechusettes.

Kennedy, R.E., Townsend, P.A., Gross, J.E., Cohen, W.B., Bolstad, P., Wang, Y.Q., Adams, P., 2009. Remote sensing change detection tools for natural resource managers: Understanding concepts and tradeoffs in the design of landscape monitoring projects. Remote Sens. Environ. 113, 1382–1396. https://doi.org/10.1016/j.rse.2008.07.018

Keppel-Jones, A., 1951. South Africa and the High Commission Territories. Int. J. 6, 85–93.

Kiage, L.M., 2013. Perspectives on the assumed causes of land degradation in the rangelands of Sub-Saharan Africa. Prog. Phys. Geogr. 37. https://doi.org/10.1177/0309133313492543

Knyazikhin, Y., Martonchik, J. V., Myneni, R.B., Diner, D.J., Running, S.W., 1998. Synergistic algorithm for estimating vegetation canopy leaf area index and fraction of absorbed photosynthetically active radiation from MODIS and MISR data. J. Geophys. Res. Atmos. 103, 32257–32275. https://doi.org/10.1029/98JD02462

Kohler, F., Kotiaho, J., Navarro, L., Desrousseaux, M., Wegner, G., Bhagwat, S., Reid, R., Wang, T., 2018. Concepts and perceptions of land degradation and restoration., in: Montanarella, L., Scholes, R.J., Brainach, A. (Eds.), The IPBES Assessment Report on Land Degradation and Restoration. Secretariat of the

Intergovernmental Science-Policy Platform on Biodiversity and Ecosystem Services, Bonn, Germany, pp. 53–134.

Kokaly, R.F., Clark, R.N., Swayze, G.A., Livo, E., Hoefen, T.M., Pearson, N.C., Wise, R.A., Benzel, W.M., Lowers, H.A., Driscoll, R.L., Klein, A.J., 2017. USGS Spectral Library Version 7, U.S. Geological Survey Data Series. https://doi.org/10.1111/j.1467-9310.1980.tb01113.x

Kong, T.M., Austin, D.E., Kellner, K., Orr, B.J., 2014. The interplay of knowledge, attitude and practice of livestock farmers' land management against desertification in the South African Kalahari. J. Arid Environ. 105, 12–21. https://doi.org/10.1016/j.jaridenv.2014.02.002

Kong, T.M., Marsh, S.E., van Rooyen, A.F., Kellner, K., Orr, B.J., 2015. Assessing rangeland condition in the Kalahari Duneveld through local ecological knowledge of livestock farmers and remotely sensed data. J. Arid Environ. 113, 77–86. https://doi.org/10.1016/j.jaridenv.2014.10.003

Kosmas, C., Karavitis, C., Kairis, O., Kounalaki, A., Fassouli, V., Tsesmelis, D., 2012. Using Indicators for Identifying Best Land Management Practices for Combating Desertification.

Kostka, B., 2004. A short history of nearly everything [WWW Document]. URL http://www.stripedmouse.com/site1_4_1.htm (accessed 6.15.17).

Kotzé, E., Sandhage-Hofmann, A., Meinel, J.A., du Preez, C.C., Amelung, W., 2013. Rangeland management impacts on the properties of clayey soils along grazing gradients in the semi-arid grassland biome of South Africa. J. Arid Environ. 97, 220–229. https://doi.org/10.1016/j.jaridenv.2013.07.004

Kuhn, M., 2019. caret: Classification and Regression Training.

Kust, G.S., Andreeva, O. V, Cowie, A.L., 2017. Land Degradation Neutrality: Concept development, practical applications and assessment. J. Environ. Manage. 195, 16–24. https://doi.org/10.1016/j.jenvman.2016.10.043

Lamb, P.J., 1978. Large-scale Tropical Atlantic surface circulation patterns associated with Subsaharan weather anomalies. Tellus 30, 240–251. https://doi.org/Article

Lamprey, H., 1975. Report on the Desert Encroachment Reconnaissance in Northern Sudan, Khartoum. Khartoum, Sudan.

Lander, F., Russell, T., 2018. The archaeological evidence for the appearance of pastoralism and farming in southern Africa. PLoS One 13, 1–21. https://doi.org/10.1371/journal.pone.0198941

Lausch, A., Bannehr, L., Beckmann, M., Boehm, C., Feilhauer, H., Hacker, J.M., Heurich, M., Jung, A., Klenke, R., Neumann, C., Pause, M., Rocchini, D., Schaepman, M.E., Schmidtlein, S., Schulz, K., Selsam, P., Settele, J., Skidmore, A.K., Cord, A.F., 2016. Linking Earth Observation and taxonomic, structural and functional biodiversity: Local to ecosystem perspectives. Ecol. Indic. 70, 317–339. https://doi.org/10.1016/j.ecolind.2016.06.022

Lavauden, L., 1927. Les Forêts du Sahara. Rev. des Eaux Forêts 65, 265–277.

Lawrence, R.L., Ripple, W.J., 1998. Comparisons among vegetation indices and bandwise regression in a highly disturbed, heterogeneous landscape: Mount St. Helens, Washington. Remote Sens. Environ. 64, 91–102. https://doi.org/10.1016/S0034-4257(97)00171-5

le Roux, A., Odendaal, F.J., 1992. Report on the study of natural recovery of overburden dumps on DBCM properties in Namaqualand. Report for De Beers Namaqualand Mines, Kleinzee. Kleinzee.

Lebert, T., 2004. Municipal commonage as a form of land redistribution: A case study of the new farms of Leliefontein, a communal reserve in Namaqualand, South Africa.

Lebert, T., Rohde, R.F., 2007. Land reform and the new elite: Exclusion of the poor from communal land in Namaqualand, South Africa. J. Arid Environ. 70, 818–833. https://doi.org/10.1016/j.jaridenv.2006.03.023

Lefsky, M.A., Cohen, W.B., 2003. Selection of Remotely Sensed Data, in: Wulder, M., Franklin, S.E. (Eds.), Remote Sensing of Forest Environments. Kluwer Academic, Boston, pp. 13–46. https://doi.org/10.1007/978-1-4615-0306-4_2

Liaqat, M.U., Cheema, M.J.M., Huang, W., Mahmood, T., Zaman, M., Khan, M.M.,

2017. Evaluation of MODIS and Landsat multiband vegetation indices used for wheat yield estimation in irrigated Indus Basin. Comput. Electron. Agric. 138, 39–47. https://doi.org/10.1016/j.compag.2017.04.006

Liaw, A., Wiener, M., 2002. Classification and Regression by randomForest. R News 2, 18–22.

Lindeque, L., 2009. Mapping land degradation and conservation in South Africa, LADA Project. https://doi.org/10.1007/s00384-009-0654-x

Liu, S., Liu, R., Liu, Y., 2010. Spatial and temporal variation of global LAI during 1981-2006. J. Geogr. Sci. 20, 323–332. https://doi.org/10.1007/s11442-010-0323-6

Lu, B., He, Y., 2018. Optimal spatial resolution of Unmanned Aerial Vehicle (UAV)-acquired imagery for species classification in a heterogeneous grassland ecosystem. GIScience Remote Sens. 55, 205–220. https://doi.org/10.1080/15481603.2017.1408930

Lu, B., He, Y., 2017. Species classification using Unmanned Aerial Vehicle (UAV)-acquired high spatial resolution imagery in a heterogeneous grassland. ISPRS J. Photogramm. Remote Sens. 128, 73–85. https://doi.org/10.1016/j.isprsjprs.2017.03.011

Lüdeke, M.B., Petschel-Held, G., Schellnhuber, H.-J., 2004. Syndromes of Global Change: The First Panoramic View. GAIA - Ecol. Perspect. Sci. Soc. 13, 42–49. https://doi.org/10.14512/gaia.13.1.10

Luther-Mosebach, J., Dengler, J., Schmiedel, U., Röwer, I.U., Labitzky, T., Gröngröft, A., 2012. A first formal classification of the Hardeveld vegetation in Namaqualand, South Africa. Appl. Veg. Sci. 15, 401–431. https://doi.org/10.1111/j.1654-109X.2011.01173.x

MacKellar, N.C., Hewitson, B.C., Tadross, M.A., 2007. Namaqualand's climate: Recent historical changes and future scenarios. J. Arid Environ. 70, 604–614. https://doi.org/10.1016/j.jaridenv.2006.03.024

Maggs, T., Whitelaw, G., 1991. A Review Of Recent Archaeological Research On Food-Producing Communities In Southern Africa. J. Afr. Hist. 32, 3–24.

https://doi.org/10.1017/S0021853700025317

Mahto, A., 2019. splitstackshape: Stack and Reshape Datasets After Splitting Concatenated Values.

Mambo, J., Archer, E., 2007. An Assessment of Land Degradation in the Save Catchment of Zimbabwe Published by : Wiley on behalf of The Royal Geographical Society (with the Institute of An assessment of land degradation in the Save catchment of Zimbabwe 39, 380–391.

Mandanici, E., Bitelli, G., 2016. Preliminary comparison of sentinel-2 and landsat 8 imagery for a combined use. Remote Sens. 8. https://doi.org/10.3390/rs8121014

Manfreda, S., McCabe, M.F., Miller, P.E., Lucas, R., Madrigal, V.P., Mallinis, G., Dor, E. Ben, Helman, D., Estes, L., Ciraolo, G., Müllerová, J., Tauro, F., de Lima, M.I., de Lima, J.L.M.P., Maltese, A., Frances, F., Caylor, K., Kohv, M., Perks, M., Ruiz-Pérez, G., Su, Z., Vico, G., Toth, B., 2018. On the use of unmanned aerial systems for environmental monitoring. Remote Sens. 10, 1–28. https://doi.org/10.3390/rs10040641

Marvin, D.C., Asner, G.P., 2016. Spatially explicit analysis of field inventories for national forest carbon monitoring. Carbon Balance Manag. 11. https://doi.org/10.1186/s13021-016-0050-0

Masubelele, M.L., Hoffman, M.T., Bond, W.J., 2015. Biome stability and long-term vegetation change in the semi-arid, south-eastern interior of South Africa: A synthesis of repeat photo-monitoring studies. South African J. Bot. 101, 139–147. https://doi.org/10.1016/j.sajb.2015.06.001

Maswanganye, S.E., 2018. A comparison of remotely-sensed precipitation etimates with observed data from rain guages in the Western Cape, South Africa. University of the Western Cape.

May, H., Lahiff, E., 2007. Land reform in Namaqualand, 1994-2005: A review. J. Arid Environ. 70, 782–798. https://doi.org/10.1016/j.jaridenv.2006.08.015

McAuliffe, J.R., Hoffman, M.T., McFadden, L.D., Jack, S., Bell, W., King, M.P., 2019. Whether or not heuweltjies: Context-dependent ecosystem engineering by the

southern harvester termite, Microhodotermes viator. J. Arid Environ. 163, 26–33. https://doi.org/10.1016/j.jaridenv.2018.11.012

McBratney, A.B., De Gruijter, J.J., 1992. A continuous approach to soil classification by modified fuzzy-k-means with extragrades. J. Soil Sci. 43, 159–175.

McBratney, A.B., Odeh, I.O.A., 1997. Application of fuzzy sets in soil science: Fuzzy logic, fuzzy measurements and fuzzy decisions. Geoderma 77, 85–113. https://doi.org/10.1016/S0016-7061(97)00017-7

Mcgwire, K., Minor, T., Fenstermaker, L., 1992. Hyperspectral Mixture Modeling for Quantifying Sparse Vegetation Cover in Arid Environments 4257.

McGwire, K., Minor, T., Fenstermaker, L., 2000. Hyperspectral mixture modeling for quantifying sparse vegetation cover in arid environments. Remote Sens. Environ. 72, 360–374. https://doi.org/10.1016/S0034-4257(99)00112-1

McKittrick, M., 2015. An Empire of Rivers: The Scheme to Flood the Kalahari, 1919-1945. J. South. Afr. Stud. 41, 485–504. https://doi.org/10.1080/03057070.2015.1025339

Meadows, M.E., Hoffman, M.T., 2002. The nature, extent and causes of land degradation in South Africa: legacy of the past, lessons for the future? Area 34, 428–437. https://doi.org/10.1111/1475-4762.00100

Merchant, C., 1987. The theoretical structure of eceological revolutions. Environ. Rev. 11, 265–274.

Metternicht, G., Akhtar-Schuster, M., Castillo, V., 2019. LDN Framework and Policies [Special Issue]. Environ. Sci. Policy 100.

Michez, A., Piégay, H., Jonathan, L., Claessens, H., Lejeune, P., 2016. Mapping of riparian invasive species with supervised classification of Unmanned Aerial System (UAS) imagery. Int. J. Appl. Earth Obs. Geoinf. 44, 88–94. https://doi.org/10.1016/j.jag.2015.06.014

Middleton, N., 2018. Rangeland management and climate hazards in drylands: dust storms, desertification and the overgrazing debate. Nat. Hazards 92, 57–70. https://doi.org/10.1007/s11069-016-2592-6

Midekisa, A., Holl, F., Savory, D.J., Andrade-Pacheco, R., Gething, P.W., Bennett, A., Sturrock, H.J.W., 2017. Mapping land cover change over continental Africa using Landsat and Google Earth Engine cloud computing. PLoS One 12, 1–15. https://doi.org/10.1371/journal.pone.0184926

Midgley, G.F., Musil, C.F., 1990. Substrate effects of zoogenic soil mounds on vegetation composition in the Worcester – Robertson valley, Cape Province. South African J. Bot. 56, 158–166. https://doi.org/10.1016/s0254-6299(16)31083-3

Midgley, G.F., Thuiller, W., 2007. Potential vulnerability of Namaqualand plant diversity to anthropogenic climate change. J. Arid Environ. 70, 615–628. https://doi.org/10.1016/j.jaridenv.2006.11.020

Milton, S.J., Dean, W.R.J., Du Plessis, M.A., Siegfried, W.R., 1994. A Conceptual Model of Arid Rangeland Degradation. Bioscience 44, 70–76. https://doi.org/10.2307/1312204

Milton, S.J., Hoffman, M.T., 1994. The application of state-and-transition models to rangeland research and management in Arid Succulent and Semi-Arid Grassy Karoo, South Africa. African J. Range Forage Sci. 11, 18–26. https://doi.org/10.1080/10220119.1994.9638349

Mitchell, J.J., Glenn, N.F., Anderson, M.O., Hruska, R.C., Halford, A., Baun, C., Nydegger, N., 2012. Unmanned aerial vehicle (UAV) hyperspectral remote sensing for dryland vegetation monitoring, in: Workshop on Hyperspectral Image and Signal Processing, Evolution in Remote Sensing. Shanghai, China. https://doi.org/10.1109/WHISPERS.2012.6874315

Moore, J.M., Picker, M.D., 1991. Heuweltjies (earth mounds) in the Clanwilliam district, Cape Province, South Africa: 4000-year-old termite nests. Oecologia 86, 424–432. https://doi.org/10.1007/BF00317612

Mortimore, M., 2016. Changing Paradigms for People-Centred Development in the Sahel, in: Behnke, R., Mortimore, M. (Eds.), The End of Desertification: Disputing Environmental Change in the Drylands. Springer, pp. 65–98. https://doi.org/10.1007/978-3-642-16014-1

Moss, M.R., 2000. Landscape Ecology: the Need for a Discipline?, in: Richling, A., Lechnio, J., Malinowska, E. (Eds.), Landscape Ecology: Theory and Applications for Practical Purposes. Polish Association for Landscape Ecology, Warsaw, pp. 174–187.

Mucina, L., Jürgens, N., Le Roux, A., Rutherford, M.C., Schmiedel, U., Esler, K.J., Powrie, L.W., Desmet, P.G., Milton, S.J., 2006a. Succulent Karoo Biome, in: Mucina, L., Rutherford, M.C. (Eds.), The Vegetation of South Africa, Lesotho and Swaziland. Strelizia, Pretoria, pp. 220–299.

Mucina, L., Rutherford, M.C., 2006. The vegetation of South Africa, Lesotho and Swaziland., Strelitzia 19. Strelitzia, Pretoria. https://doi.org/10.1007/s

Mucina, L., Rutherford, M.C., Powrie, L., 2006b. The logic of the map: Approaches and procedures, in: Mucina, L., Rutherford, M.C. (Eds.), The Vegetation of South Africa, Lesotho and Swaziland. Strelitzia, Pretoria, pp. 13–29.

Myers, N., Mittermeier, R.A., Mittermeier, C.G., da Fonseca, G.A.B., Kent, J., 2000. Biodiversity hotspots for conservation priorities. Nature 403, 853–858. https://doi.org/10.1038/35002501

Myint, S.W., Okin, G.S., Angeles, L., 2009. Modeling Land-Cover Types Using Multiple Endmember Spectral Mixture Analysis in a Desert City Soe W . Myint and Gregory S . Okin. https://doi.org/10.1080/01431160802549328

Myneni, R.B., Los, S.O., Tucker, C.J., 1996. Satellite-based identification of linked vegetation index and sea surface temperature anomaly areas from 1982-1990 for Africa, Australia and South America. Geophys. Res. Lett. 23, 729–732.

Nachtergaele, F.O., Petri, M., Biancalani, R., van Lynden, G., van Velthuizen, H., Bloise, M., 2011. An Information database for land degradation assessment at global level., in: Global Land Degradation Information System (GLADIS).

Nagendra, H., 2001. Using remote sensing to assess biodiversity. Int. J. Remote Sens. 22, 2377–2400. https://doi.org/10.1080/01431160117096

NASA, 2020. Landsat Science [WWW Document]. URL https://landsat.gsfc.nasa.gov/ (accessed 2.4.20).

Nash, M.S., Chaloud, D.J., 2011. Partial Least Square Analyses of Landscape and Surface Water Biota Associations in the Savannah River Basin. ISRN Ecol. 2011, 1–11.

Nenzhelele, E., Todd, S.W., Hoffman, M.T., 2018. Long-term impacts of livestock grazing and browsing in the Succulent Karoo: a 20-year study of vegetation change under different grazing regimes in Namaqualand §. African J. Range Forage Sci. 35, 277–287. https://doi.org/10.2989/10220119.2018.1519640

Nicholson, S.E., Kim, J., 1997. the Relationship of the El Ni O–Southern Oscillation To African Rainfall. Int. J. Climatol. 17, 117–135. https://doi.org/10.1002/(SICI)1097-0088(199702)17:2<117::AID-JOC84>3.0.CO;2-O

Nicholson, S.E., Tucker, C.J., Ba, M.B., 1998. Desertification, Drought, and Surface Vegetation: An Example from the West African Sahel. Bull. Am. Meteorol. Soc. 79, 815–829. https://doi.org/10.1175/1520-0477(1998)079<0815:DDASVA>2.0.CO;2

Nickel, S., Schröder, W., 2017. Fuzzy modelling and mapping soil moisture for observed periods and climate scenarios. An alternative for dynamic modelling at the national and regional scale? Ann. For. Sci. 74. https://doi.org/10.1007/s13595-017-0667-5

NRCAN, 2016. Radiometric resolution [WWW Document]. Satell. Imag. air photos. URL https://www.nrcan.gc.ca/maps-tools-publications/satellite-imagery-air-photos/remote-sensing-tutorials/satellites-sensors/radiometric-resolution/9379 (accessed 9.8.19).

O'Connor, B., Secades, C., Penner, J., Sonnenschein, R., Skidmore, A., Burgess, N.D., Hutton, J.M., 2015. Earth observation as a tool for tracking progress towards the Aichi Biodiversity Targets. Remote Sens. Ecol. Conserv. 1, 19–28. https://doi.org/10.1002/rse2.4

Oberski, D., 2016. Mixture models: Latent profile and latent class analysis. Mod. Stat. Methods HCI 275–287. https://doi.org/10.1007/978-3-319-26633-6_12

Okin, G.S., Roberts, D.A., 2002. Remote Sensing in Arid Regions: challenges and

Opportunities. Man. Remote Sens. 4, 1–30.

Okin, G.S., Roberts, D.A., Murray, B., Okin, W.J., 2001. Practical limits on hyperspectral vegetation dicrimination in arid and semiarid environments. Remote Sens. Environ. 77, 212–225.

Okin, W.J., Okin, G.S., Roberts, D.A., Murray, B., 1999. Multiple endmember spectral mixture analysis: endmember choice in an arid shrubland, in: 1999 AVIRIS Workshop. Pasadena, CA, pp. 323–332.

Okujeni, A., van der Linden, S., Tits, L., Somers, B., Hostert, P., 2013. Support vector regression and synthetically mixed training data for quantifying urban land cover. Remote Sens. Environ. 137, 184–197.

Oldeland, J., Dorigo, W., Lieckfeld, L., Lucieer, A., Jürgens, N., 2010. Combining vegetation indices, constrained ordination and fuzzy classification for mapping semi-natural vegetation units from hyperspectral imagery. Remote Sens. Environ. 114, 1155–1166. https://doi.org/10.1016/j.rse.2010.01.003

Oldeman, L.R., Hakkeling, R.T.A., Sombroek, W.G., 1991. World map of the status of human-induced soil degradation: An explanatory note. (No. 2), Global Assessment ofSoil Degradation (GLASOD).

Orr, B.J., Cowie, A.L., Castillo Sanchez, V.M., Chasek, P., Crossman, N.D., Erlewein, A., Ouwagie, G., Maron, M., Metternicht, G.I., Minelli, S., Tengberg, A.E., Walter, S., Welton, S., 2017. Scientific Conceptual Framework for Land Degradation Neutrality.

Pandey, P.C., Rani, M., Srivastava, P.K., Sharma, L.K., Nathawat, M.S., 2013. Land degradation severity assessment with sand encroachment in an ecologically fragile arid environment: a Geospatial Perspective. QScience Connect 43, 17. https://doi.org/10.5339/connect.2013.43

Parolin, P., 2001. Seed expulsion in fruits of Mesembryanthema (Aizoaceae): A mechanistic approach to study the effect of fruit morphological structures on seed dispersal. Flora 196, 313–322. https://doi.org/10.1016/S0367-2530(17)30060-9

Paruelo, J.M., Lauenroth, W.K., 1995. Regional patterns of NDVI in North American

shrublands and grasslands. Ecology 76, 1888–1898.

Penn, N.G., 1995. The Northern Cape Frontier Zone, 1700-c.1815. University of Cape Town.

Pentz, J.A., 1945. An agro-ecological survey of Natal. Dep. Agric. For. Bull. 250.

Perrings, C., Naeem, S., Ahrestani, F., Bunker, D.E., Burkill, P., Canziani, G., Elmqvist, T., Ferrati, R., Fuhrman, J., Jaksic, F., Kawabata, Z., Kinzig, A., Mace, G.M., Milano, F., Mooney, H., Prieur-Richard, A.H., Tschirhart, J., Weisser, W., 2010. Ecosystem services for 2020. Science, 330, 323–324. https://doi.org/10.1126/science.1196431

Petschel-Held, G., Block, A., Cassel-Gintz, M., Kropp, J., Lüdeke, M.K.B., Moldenhauer, O., Reusswig, F., Schellnhuber, H.J., 1999. Syndromes of Global Change: A qualitative modelling approach to assist global environmental management. Environ. Model. Assess. 4, 295–314. https://doi.org/10.1023/A:1019080704864

Pettorelli, N., Laurance, W.F., O'Brien, T.G., Wegmann, M., Nagendra, H., Turner, W., 2014. Satellite remote sensing for applied ecologists: Opportunities and challenges. J. Appl. Ecol. 51, 839–848. https://doi.org/10.1111/1365-2664.12261

Pettorelli, N., Owen, H.J.F., Duncan, C., 2016. How do we want Satellite Remote Sensing to support biodiversity conservation globally? Methods Ecol. Evol. 7, 656–665. https://doi.org/10.1111/2041-210X.12545

Pettorelli, N., Vik, J.O., Mysterud, A., Gaillard, J.M., Tucker, C.J., Stenseth, N.C., 2005. Using the satellite-derived NDVI to assess ecological responses to environmental change. Trends Ecol. Evol. 20, 503–510. https://doi.org/10.1016/j.tree.2005.05.011

Pickup, G., Bastin, G., Chewings, V.H., 1994. Remote-Sensing-Based Condition Assessment for Nonequilibrium Rangelands Under Large- Scale Commercial Grazing. Ecol. Appl. 4, 497–517.

Pickup, G., Chewings, V.H., 1994. A grazing gradient approach to land degradation assessment in arid areas from remotely-sensed data. Int. J. Remote Sens. 15,

597–617.

Pleurdeau, D., Imalwa, E., Détroit, F., Lesur, J., Veldman, A., Bahain, J.J., Marais, E., 2012. “Of sheep and men”: Earliest direct evidence of caprine domestication in southern Africa at Leopard Cave (Erongo, Namibia). PLoS One 7, 1–10. https://doi.org/10.1371/journal.pone.0040340

Pole Evans, I.B., 1936. A vegetation map of South Africa. Bot. Surv. Mem. South Africa 15.

Prince, S.D., 2019. Challenges for remote sensing of the Sustainable Development Goal SDG 15.3.1 productivity indicator. Remote Sens. Environ. 234, 111428. https://doi.org/10.1016/j.rse.2019.111428

Prince, S.D., 2016. Where Does Desertification Occur? Mapping Dryland Degradation at Regional to Global Scales, in: Behnke, R., Mortimore, M. (Eds.), The End of Desertification: Disputing Environmental Change in the Drylands. Springer, pp. 225–263. https://doi.org/10.1007/978-3-642-16014-1

Prince, S.D., Becker-Reshef, I., Rishmawi, K., 2009. Detection and mapping of long-term land degradation using local net production scaling: Application to Zimbabwe. Remote Sens. Environ. 113, 1046–1057. https://doi.org/10.1016/j.rse.2009.01.016

Prince, S.D., Podwojewski, P., 2019. Desertification: Inappropriate images lead to inappropriate actions. L. Degrad. Dev. 1–6. https://doi.org/10.1002/ldr.3436

Prince, S.D., Von Maltitz, G., Zhang, F., Byrne, K., Driscoll, C., Eshel, G., Kust, G., Martínez-Garza, C., Metzger, J.P., Midgley, G.F., Moreno-Mateos, D., Sghaier, M., Thwin, S., 2018. Status and trends of land degradation and restoration and associated changes in biodiversity and ecosystem functions, in: Montanarella, L., Scholes, R.J., Brainich, A. (Eds.), The IPBES Assessment Report on Land Degradation and Restoration. Secretariat of the Intergovernmental Science-Policy Platform on Biodiversity and Ecosystem Services, Bonn, Germany, pp. 221–338.

Qi, J., Chehbouni, A., Huete, A.R., Kerr, Y.H., Sorooshian, S., 1994. A modified soil adjusted vegetation index. Remote Sens. Environ. 48, 119–126.

https://doi.org/10.1016/0034-4257(94)90134-1

R Core Team, 2019. R: A language and environment for statistical computing.

Reed, M.S., Buenemann, M., Atlhopheng, J., Akhtar-Schuster, M., Bachmann, F., Bastin, G., Bigas, H., Chanda, R., Dougill, A.J., Essahli, W., Evely, A.C., Fleskens, L., Geeson, N., Glass, J.H., Hessel, R., Holden, J., Ioris, A.A.R., Kruger, B., Liniger, H., Mphinyane, W., Nainggolan, D., Perkins, J., Raymond, C.M., Ritsema, C.J., Schwilch, G., Sebego, R., Seely, M., Stringer, L.C., Thomas, R., Twomlow, S., Verzandvoort, S., 2011. Cross-scale monitoring and assessment of land degradation and sustainable land management: A methodological framework for knowledge management. L. Degrad. Dev. 22, 261–271. https://doi.org/10.1002/ldr.1087

Ren, H., Zhou, G., Zhang, F., 2018. Using negative soil adjustment factor in soil-adjusted vegetation index (SAVI) for aboveground living biomass estimation in arid grasslands. Remote Sens. Environ. 209, 439–445. https://doi.org/10.1016/j.rse.2018.02.068

Ren, H., Zhou, G., Zhang, X., 2011. Estimation of green aboveground biomass of desert steppe in inner mongolia based on red-edge reflectance curve area method. Biosyst. Eng. 109, 385–395. https://doi.org/10.1016/j.biosystemseng.2011.05.004

Reynolds, J.F., Grainger, A., Stafford Smith, D.M., Bastin, G., Garcia-Barrios, L., Fernández, R.J., Janssen, M.A., Jürgens, N., Scholes, R.J., Veldkamp, A., Verstraete, M.M., Von Maltitz, G., Zdruli, P., 2011. Scientific concepts for an integrated analysis of desertification. L. Degrad. Dev. 22, 166–183. https://doi.org/10.1002/ldr.1104

Reynolds, J.F., Smith, D.M.S., Lambin, E.F., Ii, B.L.T., Mortimore, M., Batterbury, S.P.J., Downing, T.E., Dowlatabadi, H., Fernández, R.J., Herrick, J.E., Huber-sannwald, E., Jiang, H., Leemans, R., Lynam, T., Maestre, F.T., Ayarza, M., Walker, B., 2007. Global Desertification : Building a Science for Dryland Development. Science, 316, 847–852.

Reynolds, J.F., Stafford-smith, D.M., Lambin, E., 2003. Do humans cause deserts?

An old problem through the lens of a new framework: the Dahlem desertification paradigm, in: Allsopp, N., Palmer, A.R., Milton, S.J., Kirkman, K.P., Kerley, G.I.H., Hurt, C.R., Brown, C.J. (Eds.), VIIth International Rangelands Congress. Document Transformation Technologies, Durban, South Africa, pp. 2042–2048.

Reynolds, J.F., Stafford Smith, D.M. (Eds.), 2002. Global Desertification: Do Humans Cause Deserts? Dahlem University Press, Berlin.

Rigdon, E.E., 2014. Rethinking Partial Least Squares Path Modeling : Breaking Chains and Forging Ahead. Long Range Plann. 47, 161–167. https://doi.org/10.1016/j.lrp.2014.02.003

Riginos, C., Hoffman, M.T., 2003. Changes in Population Biology of Two Succulent Shrubs along a Grazing Gradient. J. Appl. Ecol. 40, 615–625.

Roberts, D. a., Gardner, M., Church, R., Ustin, S., Scheer, G., Green, R.O., 1998. Mapping Chaparral in the Santa Monica Mountains Using Multiple Spectral Mixture Models. Remote Sens. Environ. 65, 267–279. https://doi.org/10.1016/S0034-4257(98)00037-6

Roberts, D.A., Dennison, P.E., Roth, K.L., Dudley, K., Hulley, G., 2015. Relationships between dominant plant species, fractional cover and land surface temperature in a Mediterranean ecosystem. Remote Sens. Environ. 167, 152–167.

Roberts, D.W., 1996. Landscape vegetation modelling with vital attributes and fuzzy systems theory. Ecol. Modell. 90, 175–184. https://doi.org/10.1016/0304-3800(95)00164-6

Rocchini, D., Ricotta, C., 2007. Are landscapes as crisp as we may think? Ecol. Modell. 204, 535–539. https://doi.org/10.1016/j.ecolmodel.2006.12.028

Rodríguez-Caballero, E., Knerr, T., Weber, B., 2015. Importance of biocrusts in dryland monitoring using spectral indices. Remote Sens. Environ. 170, 32–39. https://doi.org/10.1016/j.rse.2015.08.034

Rohde, R.F., Hoffman, M.T., 2008. One Hundred Years of Separation: The Historical Ecology of a South African ‘Coloured Reserve.’ Africa (Lond). 78, 189–222. https://doi.org/10.3366/e0001972008000132

Rondeaux, G., Steven, M., Baret, F., 1996. Optimization of Soil-Adjusted Vegetation Indices. Remote Sens. Environ. 55, 95–107. https://doi.org/10.1016/0034-4257(95)00186-7

Rosch, E., 1975. Cognitive representations of semantic categories. J. Exp. Psychol. Gen. 104, 192–233.

Rosch, E., 1973. Natural categories. Cogn. Psychol. 4, 328–350. https://doi.org/10.1016/0010-0285(73)90017-0

Rose, R.A., Byler, D., Eastman, J.R., Fleishman, E., Geller, G., Goetz, S., Guild, L., Hamilton, H., Hansen, M., Headley, R., Hewson, J., Horning, N., Kaplin, B.A., Laporte, N., Leidner, A., Leimgruber, P., Morisette, J., Musinsky, J., Pintea, L., Prados, A., Radeloff, V.C., Rowen, M., Saatchi, S., Schill, S., Tabor, K., Turner, W., Vodacek, A., Vogelmann, J., Wegmann, M., Wilkie, D., Wilson, C., 2015. Ten ways remote sensing can contribute to conservation. Conserv. Biol. 29, 350–359. https://doi.org/10.1111/cobi.12397

Rouse, R.W.H., Haas, J.A.W., Deering, D.W., 1973. Monitoring Vegetation Systems in the Great Plains with ERTS. Third Earth Resour. Technol. Satell. Symp. Vol. I Tech. Present. NASA SP-351 309–317.

Rowell, D.P., Folland, C.K., Maskell, K., Ward, M.N., 1995. Variability of summer rainfall over tropical north Africa (1906–92): Observations and modelling. Q. J. R. Meteorol. Soc. 121, 669–704. https://doi.org/10.1002/qj.49712152311

Sabins, F., 1987. Remote sensing: Principles and interpretation. W.H. Freeman and Company, New York.

Salih, A.A.M., Ganawa, E.T., Elmahl, A.A., 2017. Spectral mixture analysis (SMA) and change vector analysis (CVA) methods for monitoring and mapping land degradation/desertification in arid and semiarid areas (Sudan), using Landsat imagery. Egypt. J. Remote Sens. Sp. Sci. 20, S21–S29. https://doi.org/10.1016/j.ejrs.2016.12.008

Salvati, L., Rontos, K., Salvia, R., Zambon, I., 2019. Land Degradation: A Sociological Perspective, in: Zambon, I., Salvati, L., Ferrara, C. (Eds.), Land Degradation: The Main Challenge. Nova Science Publishers, Inc., New York, pp. 23–58.

Samanta, A., Ganguly, S., Vermote, E., Nemani, R.R., Myneni, R.B., 2012. Why is Remote Sensing of Amazon Forest Greenness so Challenging? Earth Interact. 16, 120420140647003. https://doi.org/10.1175/ei440.1

Sampson, S.G., 1986. Veld damage in the Karoo caused by its pre-Trekboer inhabitants: preliminary observations in the Seacow Valley. Nat. 30, 37–42.

Samuels, M.I., 2013. Pastoral mobility in a variable and spatially constrained South African environment. University of Cape Town.

Samuels, M.I., 2006. Patterns of resource use by livestock during and after drought in a communal rangeland in Namaqualand. University of the Western Cape.

Samuels, M.I., Allsopp, N., Hoffman, M.T., 2019. Traditional Mobile Pastoralism in a Contemporary Semiarid Rangeland in Namaqualand, South Africa. Rangel. Ecol. Manag. 72, 195–203. https://doi.org/10.1016/j.rama.2018.08.005

Samuels, M.I., Allsopp, N., Knight, R.S., 2007. Patterns of resource use by livestock during and after drought on the commons of Namaqualand, South Africa. J. Arid Environ. 70, 728–739. https://doi.org/10.1016/j.jaridenv.2006.11.006

SANBI, 2019. The Vegetation Map of South Africa, Lesotho and Swaziland (2006-2018). http://bgis.sanbi.org/Projects/Detail/186.

SANBI, 2006. Vegetation Map of South Africa, Lesotho and Swaziland. https://bgis.sanbi.org/SpatialDataset/Detail/330.

Sanchez, G., 2012. plsdepot: Partial Least Squares (PLS) Data Analysis Methods. https://cran.r-project.org/package=plsdepot.

Sankey, T.T., McVay, J., Swetnam, T.L., McClaran, M.P., Heilman, P., Nichols, M., 2018. UAV hyperspectral and lidar data and their fusion for arid and semi-arid land vegetation monitoring. Remote Sens. Ecol. Conserv. 4, 20–33. https://doi.org/10.1002/rse2.44

Santin-Janin, H., Garel, M., Chapuis, J.L., Pontier, D., 2009. Assessing the performance of NDVI as a proxy for plant biomass using non-linear models: A case study on the kerguelen archipelago. Polar Biol. 32, 861–871. https://doi.org/10.1007/s00300-009-0586-5

Sarstedt, M., Ringle, C.M., Henseler, J., Hair, J.F., 2014. On the Emancipation of PLS-SEM : A Commentary on Rigdon (2012). Long Range Plann. 47, 154–160. https://doi.org/10.1016/j.lrp.2014.02.007

Schellnhuber, H.J., Block, A., Cassel-Gintz, M., Kropp, J., Lammel, G., Lass, W., Lienenkamp, R., Loose, C., Lüdeke, M.K.B., Moldenhauer, O., Petschel-Held, G., Plochl, M., Reusswig, F., 1997. Syndromes of global change. Gaia 6, 19–34.

Schloss, A.L., Kicklighter, D.W., Kaduk, J., Wittenberg, U., 1999. Comparing global models of terrestrial net primary productivity (NPP): Comparison of NPP to climate and the Normalized Difference Vegetation Index (NDVI). Glob. Chang. Biol. 5, 25–34. https://doi.org/10.1046/j.1365-2486.1999.00004.x

Schmidt, A., 2002. Strip-mine rehabilitation in Namaqualand. University of Stellenbosch.

Schmiedel, U., Dengler, J., Etzold, S., 2012. Vegetation dynamics of endemic-rich quartz fields in the Succulent Karoo, South Africa, in response to recent climatic trends. J. Veg. Sci. 23, 292–303. https://doi.org/10.1111/j.1654-1103.2011.01346.x

Schmiedel, U., Linke, T., Christiaan, R., Falk, T., Gröngröft, A., Haarmeyer, D.H., Hanke, W., Henstock, R., Hoffman, M.T., Kunz, N., Labitzky, T., Luther-Mosebach, J., Lutsch, N., Meyer, S., Petersen, A., Röwer, I.U., van der Merwe, H., van Rooyen, M.W., Vollan, B., Weber, B., 2010. Environmental and socio-economic patterns and processes in the Succulent Karoo—frame conditions for the management of this biodiversity hotspot, in: Hoffman, M.T., Schmiedel, U., Jurgens, N. (Eds.), Biodiversity in Southern Africa – Volume 3: Implications for Landuse and Management. Klaus Hess Publishers, pp. 110–150.

Schmiedel, U., Oldeland, J., 2018. Vegetation responses to seasonal weather conditions and decreasing grazing pressure in the arid Succulent Karoo of South Africa§. African J. Range Forage Sci. 35, 303–310. https://doi.org/10.2989/10220119.2018.1531926

Scholes, R.J., 2009. Syndromes of dryland degradation in southern Africa. African J. Range Forage Sci. 26, 113–125. https://doi.org/10.2989/AJRF.2009.26.3.2.947

Scholes, R.J., Biggs, R., 2005. A Biodiversity Intactness Index. Nature 434, 45–50.

Schulze, B.R., 1965. General Survey. Climate of South Africa. Part 8. Pretoria.

Schumann, B.D., Todd, S.W., Haarmse, C., 2018. Evaluating riparian restoration in the Nama Karoo, in: Arid Zone Ecology Forumq. AZEF, Robertson, South Africa.

Schwarz, E., 1919. Kalahari of Thirstland Redemption. T. Maskew Miller.

Scoones, I., 1999. New Ecology and the Social Sciences: What Prospects for a Fruitful Engagement? Annu. Rev. 28, 479–507.

Senf, C., Lastovicka, J., Okujeni, A., Heurich, M., van der Linden, S., 2020. A generalised regression-based unmixing model for mapping forest cover fractions throughout three decades of Landsat data. Remote Sens. Environ. 240, 111691.

Serbetar, I., 2012. Partial Least Squares Regression Analysis: Example of Motor Fitness Data. Croat. J. Educ. Hrvat. časopis za Odgoj i Obraz. 14, 917–932.

Settle, J.J., Drake, N.A., 1993. Linear mixing and the estimation of ground cover proportions 1161. https://doi.org/10.1080/01431169308904402

Shackleton, S.E., Shackleton, C.M., 2015. Not just farming: Natural resources and livelihoods in land and agrarian reform., in: Cousins, B., Walker, C. (Eds.), Land Divided, Land Restored: Land Reform in South Africa for the 21st Century. Jacana Media, Cape Town, pp. 191–205.

Shaw, J., 1875. On the changes going on in the vegetation of South Africa through the introduction of the Merino sheep. Bot. J. Linn. Soc. 14, 202–208.

Sims, N., Green, C., Newnham, G., England, J., Held, A., 2017. Good Practice Guidance: SDG Indicator 15.3.1.

Sims, N.C., England, J.R., Newnham, G.J., Alexander, S., Green, C., Minelli, S., Held, A., 2019. Developing good practice guidance for estimating land degradation in the context of the United Nations Sustainable Development Goals. Environ. Sci. Policy 92, 349–355. https://doi.org/10.1016/j.envsci.2018.10.014

Skowno, A.L., Poole, C.J., Raimondo, D.C., Sink, K.J., Van Deventer, H., Van Niekerk, L., Harris, L.R., Smith- Adao, L.B., Tolley, K.A., Zengeya, T.A., Foden, W.B.,

Midgley, G.F., Driver, A., 2019. National Biodiversity Assessment 2018: The status of South Africa's ecosystems and biodiversity. Synthesis Report., South African National Biodiversity Institute, an entity of the Department of Environment, Forestry and Fisheries.

Smith, A.B., 1992. Origins and Spread of Pastoralism in Africa. Annu. Rev. Anthropol. 21, 125–141.

Smith, W.K., Dannenberg, M.P., Yan, D., Herrmann, S., Barnes, M.L., Barron-gafford, G.A., Biederman, J.A., Ferrenberg, S., Fox, A.M., Hudson, A., Knowles, J.F., Macbean, N., Moore, D.J.P., Nagler, P.L., Reed, S.C., Rutherford, W.A., Scott, R.L., Wang, X., Yang, J., 2019. Remote Sensing of Environment Remote sensing of dryland ecosystem structure and function : Progress , challenges , and opportunities. Remote Sens. Environ. 233, 111401. https://doi.org/10.1016/j.rse.2019.111401

Somers, B., Asner, G.P., 2013. Multi-temporal hyperspectral mixture analysis and feature selection for invasive species mapping in rainforests. Remote Sens. Environ. 136, 14–27.

Somers, B., Asner, G.P., Tits, L., Coppin, P., 2011. Endmember variability in Spectral Mixture Analysis: A review. Remote Sens. Environ. 115, 1603–1616. https://doi.org/10.1016/j.rse.2011.03.003

Somers, B., Verbesselt, J., Ampe, E.M., Sims, N., Verstraeten, W.W., Coppin, P., 2010. Spectral mixture analysis to monitor defoliation in mixed-aged Eucalyptus globulus Labill plantations in southern Australia using Landsat 5-TM and EO-1 Hyperion data. Int. J. Appl. Earth Obs. Geoinf. 12, 270–277. https://doi.org/10.1016/j.jag.2010.03.005

Sommer, S., Zucca, C., Grainger, A., Cherlet, M., Zougmore, R., Sokona, Y., Hill, J., Peruta, R.D., Roehrig, J., Wang, G., 2011. Application of Indicator Systems for Monitoring and Assessment of Desertification form National to Global Scales. L. Degrad. Dev. 22, 184–197. https://doi.org/10.1002/ldr.1084

Sonnenschein, R., Kuemmerle, T., Udelhoven, T., Stellmes, M., Hostert, P., 2011. Differences in Landsat-based trend analyses in drylands due to the choice of

vegetation estimate. Remote Sens. Environ. 115, 1408–1420.

Speranza, C.I., Adenle, A., Boillat, S., 2019. Land Degradation Neutrality - Potentials for its operationalisation at multi-levels in Nigeria. Environ. Sci. Policy 94, 63–71. https://doi.org/10.1016/j.envsci.2018.12.018

Stavi, I., Lal, R., 2015. Achieving Zero Net Land Degradation: Challenges and opportunities. J. Arid Environ. 112, 44–51. https://doi.org/10.1016/j.jaridenv.2014.01.016

Stebbing, E.P., 1935. The Encroaching Sahara : The Threat to the West African Colonies. The Geogra 85, 506–519.

Stellmes, M., Röder, A., Udelhoven, T., Hill, J., 2013. Mapping syndromes of land change in Spain with remote sensing time series, demographic and climatic data. Land use policy 30, 685–702. https://doi.org/10.1016/j.landusepol.2012.05.007

Sterk, G., Boardman, J., Verdoodt, A., 2016. Desertification: history, causes and options for its control. L. Degrad. Dev. 27, 1783–1787.

Sternberg, T., 2012. Piospheres and Pastoralists: Vegetation and Degradation in Steppe Grasslands. Hum. Ecol. 40, 811–820. https://doi.org/10.1007/s

Stocking, M., Murnaghan, N., 2000. Land Degradation – Guidelines for Field Assessment. Norwich.

Stoms, D.M., Hargrove, W.W., 2000. Potential NDVI as a baseline for monitoring ecosystem functioning. Int. J. Remote Sens. 21, 401–407. https://doi.org/10.1080/014311600210920

Stringer, L.C., 2006. The UN Convention to Combat Desertification. Accessed May 27, 2014. [WWW Document]. URL http://www.scidev.net/global/ desert-science/policy-brief/the-un-convention-to-combat-desertification.html. (accessed 6.2.17).

Stringer, L.C., Reed, M.S., 2007. Land Degradation Assessment in Southern Africa: Integrating Local and Scientific Knowledge Bases. L. Degrad. Dev. 18:, 99–116.

Stringer, L.C., Reed, M.S., Fleskens, L., Thomas, R.J., Le, Q.B., Lala-Pritchard, T.,

2017. A New Dryland Development Paradigm Grounded in Empirical Analysis of Dryland Systems Science. L. Degrad. Dev. 28, 1952–1961. https://doi.org/10.1002/ldr.2716

Sugden, J.M., 1989. Late Quaternary palaeoecology of the central and marginal uplands of the Karoo, South Africa. University of Cape Town.

Suggitt, A.J., Gillingham, P.K., Hill, J.K., Huntley, B., Kunin, W.E., Roy, D.B., Thomas, C.D., 2011. Habitat microclimates drive fi ne-scale variation in extreme temperatures 1–8. https://doi.org/10.1111/j.1600-0706.2010.18270.x

Swift, J., 1996. Desertification: Narratives, winners and losers., in: Leach, M., Mearns, R. (Eds.), The Lie of the Land: Challenging Received Wisdom on the African Environment. James Currey, Oxford.

Symeonakis, E., Drake, N., 2004. Monitoring desertification and land degradation over sub-Saharan Africa. Int. J. Remote Sens. 25, 573–592. https://doi.org/10.1080/0143116031000095998

Symeonakis, E., Karathanasis, N., Koukoulas, S., Panagopoulos, G., 2016. Monitoring Sensitivity to Land Degradation and Desertification with the Environmentally Sensitive Area Index: The Case of Lesvos Island. L. Degrad. Dev. 27, 1562–1573. https://doi.org/10.1002/ldr.2285

Tapia, R., 2004. Optimization of sampling schemes for vegetation mapping using fuzzy classification. Interntional Institute for Geo-Information Science and Earth Observation. Enschede, the Netherlands.

Thomas, D.S., Middleton, N.J., 1994. Desertification: Exploding the myth. John Wiley & Sons;Chichester.

Thomas, D.S., Shaw, P.A., 1991. The Kalahari Environment. Cambridge University Press, Cambridge.

Thomas, D.S.G., 1997. Science and the desertification debate. J. Arid Environ. 37, 599–608. https://doi.org/10.1006/jare.1997.0293

Thompson, M., Vlok, J., Cowling, R.M., Cundill, S.L., Mudau, N., 2005. A land transformation map of the Little Karoo. CEPF Funded Proj.

Thompson, M., Vlok, J., Rouget, M., Hoffman, M.T., Balmford, A., Cowling, R.M., 2009. Mapping grazing-induced degradation in a semi-arid environment: A rapid and cost effective approach for assessment and monitoring. Environ. Manage. 43, 585–596. https://doi.org/10.1007/s00267-008-9228-x

Thorp, K.R., French, A.N., Rango, A., 2013. Effect of image spatial and spectral characteristics on mapping semi-arid rangeland vegetation using multiple endmember spectral mixture analysis (MESMA). Remote Sens. Environ. 132, 120–130. https://doi.org/10.1016/j.rse.2013.01.008

Thrash, I., 2000. Determinants of the extent of indigenous large herbivore impact on herbaceous vegetation at watering points in the north-eastern lowveld, South Africa. J. Arid Environ. 61–72. https://doi.org/10.1006/jare.1999.0452

Todd, S.W., 2009. Field-Based Assessment of Degradation in the Namakwa District. Final Report: Mapping Degradation in the Arid Subregions of the BIOTA South Transect. SANBI, Cape Town.

Todd, S.W., Hoffman, M.T., 2009. A fence line in time demonstrates grazing-induced vegetation shifts and dynamics in the semiarid Succulent Karoo. Ecol. Appl. 19, 1897–1908.

Todd, S.W., Hoffman, M.T., 1999. A fence-line contrast reveals effects of heavy grazing on plant diversity and community composition in Namaqualand, South Africa. Plant Ecol. 142, 169–178. https://doi.org/10.1023/a:1009810008982

Tong, X., Brandt, M., Hiernaux, P., Herrmann, S.M., Tian, F., Prishchepov, A. V., Fensholt, R., 2017. Revisiting the coupling between NDVI trends and cropland changes in the Sahel drylands: A case study in western Niger. Remote Sens. Environ. 191, 286–296. https://doi.org/10.1016/j.rse.2017.01.030

Toulmin, C., Brock, K., 2016. Desertification in the Sahel: Local Practice Meets Global Narrative, in: Behnke, R., Mortimore, M. (Eds.), The End of Desertification: Disputing Environmental Change in the Drylands. Springer, pp. 37–63. https://doi.org/10.1007/978-3-642-16014-1

Transon, J., d'Andrimont, R., Maugnard, A., Defourny, P., 2018. Survey of hyperspectral Earth Observation applications from space in the Sentinel-2 context.

Remote Sens. 10, 1–32. https://doi.org/10.3390/rs10020157

Tully, K., Sullivan, C., Weil, R., Sanchez, P., 2015. The State of soil degradation in sub-Saharan Africa: Baselines, trajectories, and solutions. Sustainability 7, 6523–6552. https://doi.org/10.3390/su7066523

Turnbull, L., Wainwright, J., Brazier, R.E., 2008. A conceptual framework for understanding semi-arid land degradation: ecohydrological interactions across multiple-space and time scales. Ecohydrology 1, 23–34. https://doi.org/10.1002/eco

Turner, W., Rondinini, C., Pettorelli, N., Mora, B., Leidner, A.K., Szantoi, Z., Buchanan, G., Dech, S., Dwyer, J., Herold, M., Koh, L.P., Leimgruber, P., Taubenboeck, H., Wegmann, M., Wikelski, M., Woodcock, C., 2015. Free and open-access satellite data are key to biodiversity conservation. Biol. Conserv. 182, 173–176. https://doi.org/10.1016/j.biocon.2014.11.048

UN, 2015. Resolution adopted by the General Assembly on 25 September 2015, in: Transforming Our World: The 2030 Agenda for Sustainable Development. p. 35. https://doi.org/10.1163/157180910X12665776638740

UN, 2012. The future we want: Outcome document of the United Nations Conference on Sustainable Development, in: Rio+20 United Nations Conference on Sustainable Development. United Nations, Rio de Janeiro, pp. 1–72. https://doi.org/10.1126/science.202.4366.409

UN General Assembly, 1977. Plan of Action to Combat Desertification. United Nations Conf. Desertif. 32/172, 106–107.

UNCCD, 2017. Drylands, in: Dudley, N., Alexander, S. (Eds.), The Global Land Outlook. United Nations Convention to Combat Desertification, Bonn, pp. 246–269. https://doi.org/10.2307/j.ctv7cjw5h.7

UNCCD, 2016. Report of the Conference of the Parties on its twelfth session, held in Ankara from 12 to 23 October 2015, in: Conference of the Parties. pp. 1–80.

UNCCD, 2013. Glossary for performance and impact indicators, financial flows and best practices Summary, in: Committee for the Review of the Implementation of

the Convention. Bonn, pp. 1–24. https://doi.org/10.4324/9780203135365

UNCCD, 2009. UNCCD 1st Scientific Conference: Synthesis and recommendations., in: Conference of the Parties. UNCCD Secretariat, Bonn.

UNCCD, 2007. Report of the Conference of the Parties on its eighth session, held in Madrid from 3 to 14 September 2007 (ICCD/COP(8)/16/Add.1), Decision 3/COP.8: The Strategy. Madrid. https://doi.org/10.1177/107049659700600204

UNCCD, 1994. United Nations Convention to Combat Desertification in those countries experiencing serious drought and/or serious desertification, particularly in Africa. United Nations Convention to Combat Desertification, p. 54. https://doi.org/10.1159/000153199

UNCED, 1992. Agenda 21, in: United Nations Conference on Environment & Development. https://doi.org/10.1007/s11671-008-9208-3

UNEP, 1997. World Atlas of Desertification, Second Edition. Arnold, London.

UNEP, 1992. World Atlas of Desertification, First Edition. Arnold, London.

UNEP, 1991. Status of desertification and implementation of the United Nations Plan of Action to Combat Desertification : report of the Executive Director : United Nations Environment Programme. Nairobi.

UNEP, 1984. General assessment of progress in the implementation of the Plan of Action to Combat Desertification 1978–1984: Report of the Executive Director. Governing Council, twelfth Session, UNEP/GC.12/9. Nairobi.

United Nations, 1994. Elaboration of an International Convention to Combat Desertification in countries experiencing serious drought and/or desertification, particularly in Africa., United Nations General Assemby.

Václavík, T., Lautenbach, S., Kuemmerle, T., Seppelt, R., 2013. Mapping global land system archetypes. Glob. Environ. Chang. 23, 1637–1647. https://doi.org/10.1016/j.gloenvcha.2013.09.004

Vågen, T., Winowiecki, L.A., Abegaz, A., Hadgu, K.M., 2013a. Landsat-based approaches for mapping of land degradation prevalence and soil functional

properties in Ethiopia. Remote Sens. Environ. 134, 266–275. https://doi.org/10.1016/j.rse.2013.03.006

Vågen, T., Winowiecki, L.A., Tondoh, J.E., 2013b. The Land Degradation Surveillance (LDSF) Field Guide. v4. 1-9.

Vågen, T., Winowiecki, L.A., Tondoh, J.E., Desta, L.T., Gumbricht, T., 2016. Mapping of soil properties and land degradation risk in Africa using MODIS reflectance. Geoderma 263, 216–225. https://doi.org/http://dx.doi.org/10.1016/j.geoderma.2015.06.023

Valentyn, F., 1971. Description of the Cape of Good Hope with matters concerning it., Series II. ed. Van Riebeeck Society, Cape Town.

van Haren, N., Fleiner, R., Liniger, H., Harari, N., 2019. Contribution of community-based initiatives to the sustainable development goal of Land Degradation Neutrality. Environ. Sci. Policy 94, 211–219. https://doi.org/10.1016/j.envsci.2018.12.017

van Rheede van Oudtshoorn, K., van Rooyen, M.W., 1999. Dispersal Biology of Desert Plants, Adaptations of Desert Organisms. Springer-Verlag, Berlin. https://doi.org/10.1017/CBO9781107415324.004

van Rooyen, M.W., Le Roux, A., Geldenhuys, C., van Rooyen, N., Broodryk, N.L., van der Merwe, H., 2015. Long-term vegetation dynamics (40 yr) in the Succulent Karoo, South Africa: Effects of rainfall and grazing. Appl. Veg. Sci. 18, 311–322. https://doi.org/10.1111/avsc.12150

Verón, S.R., Paruelo, J.M., Oesterheld, M., 2006. Assessing desertification. J. Arid Environ. 66, 751–763. https://doi.org/10.1016/j.jaridenv.2006.01.021

Verstraete, M.M., Hutchinson, C.F., Grainger, A., Stafford Smith, M., Scholes, R.J., Reynolds, J.F., Barbosa, P., Léon, A., Mbow, C., 2011. Towards a global drylands observing system: Observational requirements and institutional solutions. L. Degrad. Dev. 22, 198–213. https://doi.org/10.1002/ldr.1046

Vetter, S., 2005. Rangelands at equilibrium and non-equilibrium: Recent developments in the debate. J. Arid Environ. 62, 321–341.

https://doi.org/10.1016/j.jaridenv.2004.11.015

Visser, I., Speekenbrink, M., 2010. depmixS4: An R Package for Hidden Markov Models. J. Stat. Softw. 36, 1–21. https://doi.org/10.18637/jss.v036.i07

Vogler, K.C., Ager, A.A., Day, M.A., Jennings, M., Bailey, J.D., 2015. Prioritization of forest restoration projects: Tradeoffs between wildfire protection, ecological restoration and economic objectives. Forests 6, 4403–4420. https://doi.org/10.3390/f6124375

Vogt, J. V., Safriel, U., Von Maltitz, G., Sokona, Y., Zougmore, R., Bastin, G., Hill, J., 2011. Monitoring and assessment of land degradation and desertification: Towards new conceptual and integrated approaches. L. Degrad. Dev. 22, 150–165. https://doi.org/10.1002/ldr.1075

Von Maltitz, G., Gambizo, J., Kellner, K., Rambau, T., Lindeque, L., Kgope, B., 2019. Experiences from the South African land degradation neutrality target setting process. Environ. Sci. Policy 101, 54–62. https://doi.org/10.1016/j.envsci.2019.07.003

Von Maltitz, G., Lindeque, L., Kellner, K., 2018. A changing narrative on desertification and degradation in South Africa, in: Squires, V.R., Ariapour, A. (Eds.), Desertification: Past, Current and Future Trends. Nova Science Publishers, Inc., New York, pp. 29–72.

Walker, C., Cousins, B., 2015. Land divided, land restored: Introduction, in: Cousins, B., Walker, C. (Eds.), Land Divided, Land Restored: Land Reform in South Africa for the 21st Century. Jacana Media, Cape Town, pp. 1–23.

Wang, R., Wan, B., Guo, Q., Hu, M., Zhou, S., 2017. Mapping regional urban extent using NPP-VIIRS DNB and MODIS NDVI data. Remote Sens. 9, 1–25. https://doi.org/10.3390/rs9080862

Washington-Allen, R.A., Niel, T.G. Van, Ramsey, R.D., West, N.E., 2004. Remote Sensing – Based Piosphere Analysis. GIScience Remote Sens. 41, 136–154. https://doi.org/10.2747/1548-1603.41.2.136

Waterhouse, G., 1932. Simon van der Stel's Journal of his Expedition to Namaqualand,

1685-6. Longmans, Green & Co., London.

Watkeys, M.K., 1999. Soils of the arid south western zone of southern Africa., in: Dean, W.R.J., Milton, S.J. (Eds.), The Karoo: Ecological Patterns and Processes. Cambridge University Press, Cambridge.

Webley, L., 2007. Archaeological evidence for pastoralist land-use and settlement in Namaqualand over the last 2000 years. J. Arid Environ. 70, 629–640. https://doi.org/10.1016/j.jaridenv.2006.03.009

Wessels, K.J., 2009. Letter to the editor: Comments on “Proxy global assessment of land degradation” by Bai et al. (2008). Soil Use Manag. 25, 91–92. https://doi.org/10.1111/j.1475-2743.2009.00195.x

Wessels, K.J., Bergh, F. van den, Roy, D.P., Salmon, B.P., Steenkamp, K.C., MacAlister, B., Swanepoel, D., Jewitt, D., 2016. Rapid land cover map updates using change detection and robust random forest classifiers. Remote Sens. 8, 1–24. https://doi.org/10.3390/rs8110888

Wessels, K.J., Prince, S.D., 2007. Monitoring land degradation with long-term satellite data in South Africa. Gr. Earth Obs. 1-3. http://hdl.handle.net/10204/2787.

Wessels, K.J., Prince, S.D., Carroll, M., Malherbe, J., 2007a. Relevance of Rangeland Degradation in Semiarid Northeastern South Africa to the Nonequilibrium Theory. Ecol. Appl. 17, 815–827.

Wessels, K.J., Prince, S.D., Frost, P.E., Van Zyl, D., 2004. Assessing the effects of human-induced land degradation in the former homelands of northern South Africa with a 1 km AVHRR NDVI time-series. Remote Sens. Environ. 91, 47–67. https://doi.org/10.1016/j.rse.2004.02.005

Wessels, K.J., Prince, S.D., Malherbe, J., Small, J., Frost, P.E., VanZyl, D., 2007b. Can human-induced land degradation be distinguished from the effects of rainfall variability? A case study in South Africa. J. Arid Environ. 68, 271–297. https://doi.org/10.1016/j.jaridenv.2006.05.015

Wessels, K.J., Prince, S.D., Zambatis, N., MacFadyen, S., Frost, P.E., Van Zyl, D., 2006. Relationship between herbaceous biomass and 1-km ^{2} Advanced Very

High Resolution Radiometer (AVHRR) NDVI in Kruger National Park, South Africa. Int. J. Remote Sens. 27, 951–973. https://doi.org/10.1080/01431160500169098

Wessels, K.J., Steenkamp, K., Von Maltitz, G., Archibald, S., 2011. Detecting inter-annual variability in the phenological characteristics of southern Africa's vegetation using satellite imagery. Rangelands 88–91.

Wessman, C.A., Bateson, C.A., Benning, T.L., 1997. Detecting Fire and Grazing Patterns in Tallgrass Prairie Using Spectral Mixture Analysis. Ecol. Appl. 493–511.

Westoby, M., Walker, B., Noy-meir, I., 1989. Opportunistic Management for Rangelands Not at Equilibrium. Soc. Range Manag. 42, 266–274.

Wiens, J.A., 1984. On understanding a nonequilibrium world: myth and reality in community patterns and processes., in: Strong, D.R., Simberloff, D., Abele, L., Thistle, A.B. (Eds.), Ecological Communities: Conceptual Issues and the Evidence. Princeton University Press, New Jersey, pp. 439–458.

Willemen, L., Nangendo, G., Belnap, J., Bolashvili, N., Denboba, M.A., Douterlungne, D., Langlais, A., Mishra, P.K., Molau, U., Pandit, R., Stringer, L.C., Budiharta, S., Fernández Fernández, E., Hahn, T., 2018. Decision support to address land degradation and support restoration of degraded land., in: Montanarella, L., Scholes, R.J., Brainach, A. (Eds.), The IPBES Assessment Report on Land Degradation and Restoration. Secretariat of the Intergovernmental Science-Policy Platform on Biodiversity and Ecosystem Services, Bonn, Germany, pp. 591–648.

Winslow, M.D., Vogt, J. V., Thomas, R.J., Sommer, S., Martius, C., Akhtar-Schuster, M., 2011. Special Issue on Understanding Dryland Degradation Trends. L. Degrad. Dev. 22, 145–312.

Wold, S., Ruhe, A., Wold, H., Dunn, W.J., 1984. The collinearity problem in linear regression. The partial least squares (PLS) approach to generalised inverses. SIAM J. Sci. Stat. Comput. 5, 735–743.

Wright, J.B., 1977. Hunters, herders and early farmers in southern Africa. Theor. A J. Soc. Polit. Theory 49, 19–36.

Wu, C., Murray, A.T., 2003. Estimating impervious surface distribution by spectral mixture analysis 84, 493–505.

Wu, J., Wang, D., Bauer, M.E., 2007. Assessing broadband vegetation indices and QuickBird data in estimating leaf area index of corn and potato canopies. F. Crop. Res. 102, 33–42. https://doi.org/10.1016/j.fcr.2007.01.003

Wunder, S., Bodle, R., 2019. Achieving land degradation neutrality in Germany: Implementation process and design of a land use change based indicator. Environ. Sci. Policy 92, 46–55. https://doi.org/10.1016/j.envsci.2018.09.022

WWF South Africa, 2019. Integrated annual report. Cape Town.

WWF South Africa, 2018. Conservation for the future: Innovate, collaborate to ensure protected area expansion., in: Bonthuys, J., Marais, E. (Eds.), WWF-SA's Land Programme Partners Forum. WWF-SA, Cape Town, pp. 1–16.

Xiaosong, D.X., Lai, F., 2012. Using partial least squares in operations management research : A practical guideline and summary of past research. J. Oper. Manag. 30, 467–480. https://doi.org/10.1016/j.jom.2012.06.002

Xie, Y., Sha, Z., Yu, M., 2008. Remote sensing imagery in vegetation mapping : a review 1, 9–23. https://doi.org/10.1093/jpe/rtm005

Xie, Z., Phinn, S.R., Game, E.T., Pannell, D.J., Hobbs, R.J., Briggs, P.R., McDonald-Madden, E., 2019. Using Landsat observations (1988–2017) and Google Earth Engine to detect vegetation cover changes in rangelands - A first step towards identifying degraded lands for conservation. Remote Sens. Environ. 232, 1–15. https://doi.org/10.1016/j.rse.2019.111317

Xue, J., Ge, Y., Ren, H., 2017. Spatial upscaling of green aboveground biomass derived from MODIS-based NDVI in arid and semiarid grasslands. Adv. Sp. Res. 60, 2001–2008. https://doi.org/10.1016/j.asr.2017.07.016

Xue, Y., 1997. Biosphere feedback on regional climate in tropical North Africa. Q. J. R. Meteorol. Soc. 123, 1483–1515. https://doi.org/10.1002/qj.49712354203

Yang, J., Weisberg, P.J., Bristow, N.A., 2012. Landsat remote sensing approaches for monitoring long-term tree cover dynamics in semi-arid woodlands: Comparison of

vegetation indices and spectral mixture analysis. Remote Sens. Environ. 119, 62–71. https://doi.org/10.1016/j.rse.2011.12.004

Yengoh, G.T., Dent, D., Olsson, L., Tengberg, A.E., Tucker, C.J., 2014. The use of the Normalized Difference Vegetation Index (NDVI) to assess land degradation at multiple scales: a review of the current status, future trends, and practical considerations. https://doi.org/10.1007/978-3-319-24112-8

Youngentob, K.N., Roberts, D.A., Held, A.A., Dennison, P.E., Jia, X., Lindenmayer, D.B., 2011. Mapping two Eucalyptus subgenera using multiple endmember spectral mixture analysis and continuum-removed imaging spectrometry data. Remote Sens. Environ. 115, 1115–1128. https://doi.org/10.1016/j.rse.2010.12.012

Zadeh, L., 2008. Is there a need for fuzzy logic? Inf. Sci. (Ny). 178, 2751–2779. https://doi.org/10.1016/j.ins.2008.02.012

Zadeh, L., 1965. Fuzzy sets. Inf. Control 8, 338–353. https://doi.org/10.1016/S0019-9958(65)90241-X

Zanchetta, A., Bitelli, G., 2017. A combined change detection procedure to study desertification using opensource tools. Open Geospatial Data, Softw. Stand. 2, 1–12. https://doi.org/10.1186/s40965-017-0023-6

Zeng, N., Neelin, J.D., Lau, K., Tucker, C.J., 1999. Enhancement of Interdecadal Climate Variability in the Sahel by Vegetation Interaction. Sci. New Ser. 286, 1537–1540.

Zhou, L., Tian, Y., Myneni, R.B., Ciais, P., Saatchi, S., Liu, Y.Y., Piao, S., Chen, H., Vermote, E.F., Song, C., Hwang, T., 2014. Widespread decline of Congo rainforest greenness in the past decade. Nature 508, 86–90. https://doi.org/10.1038/nature13265

Zhu, X., Liu, D., 2015. Improving forest aboveground biomass estimation using seasonal Landsat NDVI time-series. ISPRS J. Photogramm. Remote Sens. 102, 222–231. https://doi.org/10.1016/j.isprsjprs.2014.08.014

Appendix

Google Earth Engine scripts

A. Extracting topographic variables from digital elevation data:

https://code.earthengine.google.com/7c3cc8ed64ed6e5cc9e32b7aade33a4b

```
/*This script extracts values for slope angle, slope aspect, and   elevation for
 *the project area from the Shuttle Radar Topography Mission (Farr et al. 2007)
 *digital elevation data. Slope angle is reported in degrees, slope aspect
 *values are converted from degrees to between -1 and 1, and elevation are
 *reported as metres above sea level.
 */

// Import site locations and name them sites
// Draw polygon round area of interest and name it projPoly

// Load the SRTM image.
var SRTM = ee.Image('USGS/SRTMGL1_003');

// Apply an algorithm to an image deriving slope.
var slope = ee.Terrain.slope(SRTM);

// Get the slope aspect (in degrees)
var aspect = ee.Terrain.aspect(SRTM);

// Convert so that 1 = north, and -1 = south, east and west are both 0
var aspectNS = aspect.divide(180).multiply(Math.PI).cos();

// Export the elevation, aspect and slope angle values for each site as tables
var plotElevation = SRTM.reduceRegions({
collection: sites,
reducer: ee.Reducer.median(),
scale: 30,
});

Export.table(plotElevation, "PlotElevation", {fileformat:"CSV"});

var plotAspect = aspect.reduceRegions({
collection: sites,
reducer: ee.Reducer.median(),
scale: 30,
});

Export.table(plotAspect, "PlotAspect", {fileformat:"CSV"});

var plotSlope = slope.reduceRegions({
collection: sites,
reducer: ee.Reducer.median(),
scale: 30,
});

Export.table(plotSlope, "PlotSlope", {fileformat:"CSV"});

// Export images representing the three variables for the project area (to drive)
Export.image.toDrive({
  image: SRTM,
  description: 'ProjArea_elevation',
  scale: 30,
  region: projPoly
```

```
});

Export.image.toDrive({
  image: slope,
  description: 'ProjArea_slope',
  scale: 30,
  // maxPixels: 1e9,
  region: projPoly
});

Export.image.toDrive({
  image: aspectNS,
  description: 'ProjArea_aspectNS',
  scale: 30,
  region: projPoly
});

// Export images representing the three variables for the project area (to assets)
Export.image.toAsset({
  image: SRTM,
  description: 'Elevation',
  scale: 30,
  region: projPoly
});

Export.image.toAsset({
  image: aspectNS,
  description: 'SlopeAspect',
  scale: 30,
  region: projPoly
});

Export.image.toAsset({
  image: slope,
  description: 'SlopeAngle',
  scale: 30,
  region: projPoly
});
```

B. Landsat 8 vegetation indices:

https://code.earthengine.google.com/68f9c4368f22b974abd647032f487b89

```
/*This script extracts values for 5 vegetation indices (NDVI, EVI, SAVI, MSAVI,
 *OSAVI) from USGS Landsat 8 Surface Reflectance Tier 1 data
 */

// Import site locations and name them sites
// Draw polygon round area of interest and name it projPoly

// Create a variable from the different bands for landsat8
var Landsat_8_BANDS = ['B2',   'B3',    'B4',  'B5',  'B6',  'B7', 'pixel_qa'];
var STD_NAMES = ['blue', 'green', 'red', 'nir', 'swir1', 'swir2', 'pixel_qa'];

var getQABits = function(image, start, end, newName) {
    // Compute the bits we need to extract.
    var pattern = 0;
    for (var i = start; i <= end; i++) {
       pattern += Math.pow(2, i);
    }
    // Return a single band image of the extracted QA bits, giving the band
    // a new name.
    return image.select([0], [newName])
```

```
                  .bitwiseAnd(pattern)
                  .rightShift(start);
};

// A function to mask out cloud shadow pixels.
var cloud_shadows = function(image) {
  // Select the QA band.
  var QA = image.select(['pixel_qa']);
  // Get the internal_cloud_algorithm_flag bit.
  return getQABits(QA, 3,3, 'Cloud_shadows').eq(0);
  // Return an image masking out cloudy areas.
};

// A function to mask out cloudy pixels.
var clouds = function(image) {
  // Select the QA band.
  var QA = image.select(['pixel_qa']);
  // Get the internal_cloud_algorithm_flag bit.
  return getQABits(QA, 5,5, 'Cloud').eq(0);
  // Return an image masking out cloudy areas.
};

var maskClouds = function(image) {
  var cs = cloud_shadows(image);
  var c = clouds(image);
  image = image.updateMask(cs);
  return image.updateMask(c);
};

// This function adds quality bands to the images (NDVI, EVI, SAVI, MSAVI, OSAVI).
var addQualityBands = function(image) {
  return image
    .addBands(image.normalizedDifference(['nir', 'red']).rename('ndvi'))
    .addBands(image.expression(
      '2.5 * ((NIR - RED) / (NIR + 6 * RED - 7.5 * BLUE + 1))', {
        'NIR': image.select('nir'),
        'RED': image.select('red'),
        'BLUE': image.select('blue')
  }).rename('evi'))
    .addBands(image.expression(
      '((NIR - RED) / (NIR + RED +0.5))*(1.5)', {
        'NIR': image.select('nir'),
        'RED': image.select('red')
  }).rename('savi'))
  .addBands(image.expression(
      '(2 * NIR + 1 - sqrt(pow((2 * NIR + 1), 2) - 8 * (NIR - RED)) ) / 2', {
        'NIR': image.select('nir'),
        'RED': image.select('red')
  }).rename('msavi'))
  .addBands(image.expression(
      '((NIR - RED) / (NIR + RED +0.16))', {
        'NIR': image.select('nir'),
        'RED': image.select('red')
  }).rename('osavi'))
};

//Import LANDSAT SR collections and add the quality bands
var landsat8 = ee.ImageCollection('LANDSAT/LC08/C01/T1_SR')
    .filterDate('2017-01-01', '2017-11-01')
    //.filter(ee.Filter.calendarRange(9,10,'month'))//Filter to specified months
    .select(Landsat_8_BANDS, STD_NAMES)
    .filterBounds(projPoly).map(maskClouds)
    .map(addQualityBands);

// Create a variable which gets the median value from the landsat 8 collection
var median = landsat8.median();

// Create variables for median ndvi, evi, and savi over the collection
```

```
var Lndvi = median.select(["ndvi"]);
var Levi = median.select(["evi"]);
var Lsavi = median.select(["savi"]);
var Lmsavi = median.select(["msavi"]);
var Losavi = median.select(["osavi"]);

// Create index variables for each individual site
// var plotndvi = ndvi.reduceRegions({
//   collection: sites,
//   reducer: ee.Reducer.median(),
//   scale: 30,
// });
// var plotevi = evi.reduceRegions({
//   collection: sites,
//   reducer: ee.Reducer.median(),
//   scale: 30,
// });
// var plotsavi = savi.reduceRegions({
//   collection: sites,
//   reducer: ee.Reducer.median(),
//   scale: 30,
// });
// var plotmsavi = msavi.reduceRegions({
//   collection: sites,
//   reducer: ee.Reducer.median(),
//   scale: 30,
// });
// var plotosavi = osavi.reduceRegions({
//   collection: sites,
//   reducer: ee.Reducer.median(),
//   scale: 30,
// });

//Export the plot index values as tables.
// Export.table(plotndvi, "Landsat_ndvi_2017", {fileformat:"CSV"});
// Export.table(plotevi, "Landsat_evi_2017", {fileformat:"CSV"});
// Export.table(plotsavi, "Landsat_savi_2017", {fileformat:"CSV"});
// Export.table(plotmsavi, "Landsat_msavi_2017", {fileformat:"CSV"});
// Export.table(plotosavi, "Landsat_osavi_2017", {fileformat:"CSV"});

//Export index value images for the project area (to assets)
Export.image.toAsset({
  image: Lndvi,
  description: 'Lndvi',
  assetId: 'Lndvi',
  region: projPoly,
  scale: 30
});
Export.image.toAsset({
  image: Levi,
  description: 'Levi',
  assetId: 'Levi',
  region: projPoly,
  scale: 30
});
Export.image.toAsset({
  image: Lsavi,
  description: 'Lsavi',
  assetId: 'Lsavi',
  region: projPoly,
  scale: 30
});
Export.image.toAsset({
  image: Lmsavi,
  description: 'Lmsavi',
  assetId: 'Lmsavi',
  region: projPoly,
  scale: 30
```

```
});
Export.image.toAsset({
  image: Losavi,
  description: 'Losavi',
  assetId: 'Losavi',
  region: projPoly,
  scale: 30
});
```

C. Sentinel-2A vegetation indices:

https://code.earthengine.google.com/27057d51465ecf1d833e3e8887b60dec

```
/*This script extracts values for 5 vegetation indices (NDVI, EVI, SAVI, MSAVI,
 *OSAVI) from Sentinel-2 MSI: MultiSpectral Instrument, Level-2A data
 */

// Import site locations and name them sites
// Draw polygon round area of interest and name it projPoly

// Define study period
var startDate = '2017-01-01';
var endDate = '2017-11-01';

// Function to mask clouds using the Sentinel-2 QA band.
function maskS2clouds(img) {
  var qa = img.select('QA60').int16();

  // Bits 10 and 11 are clouds and cirrus, respectively.
  var cloudBitMask = Math.pow(2, 10);
  var cirrusBitMask = Math.pow(2, 11);

  // Both flags should be set to zero, indicating clear conditions.
  var mask = qa.bitwiseAnd(cloudBitMask).eq(0).and(
             qa.bitwiseAnd(cirrusBitMask).eq(0));

  // Return the masked and scaled data.
  return img.updateMask(mask);
}

var Sentinel_bands = ['QA60', 'B1','B2','B3','B4','B5','B6','B7','B8','B8A',
'B9','B10', 'B11','B12'];
var STD_NAMES = ['QA60','cb', 'blue', 'green', 'red', 're1','re2','re3','nir',
'nir2', 'waterVapor', 'cirrus','swir1', 'swir2'];

// This function adds quality bands to the images (NDVI, EVI, SAVI, MSAVI, OSAVI).
var addQualityBands = function(image) {
  return image
    .addBands(image.normalizedDifference(['nir', 'red']).rename('ndvi'))
    .addBands(image.expression(
      '2.5 * ((NIR - RED) / (NIR + 6 * RED - 7.5 * BLUE + 1))', {
        'NIR': image.select('nir'),
        'RED': image.select('red'),
        'BLUE': image.select('blue')
  }).rename('evi'))
    .addBands(image.expression(
      '((NIR - RED) / (NIR + RED +0.5))*(1.5)', {
        'NIR': image.select('nir'),
        'RED': image.select('red')
  }).rename('savi'))
  .addBands(image.expression(
      '(2 * NIR + 1 - sqrt(pow((2 * NIR + 1), 2) - 8 * (NIR - RED)) ) / 2', {
        'NIR': image.select('nir'),
        'RED': image.select('red')
```

```
  }).rename('msavi'))
  .addBands(image.expression(
      '((NIR - RED) / (NIR + RED +0.16))', {
        'NIR': image.select('nir'),
        'RED': image.select('red')
  }).rename('osavi'))
};

//Get s2 data
var s2s = ee.ImageCollection('COPERNICUS/S2')
                  .filterDate(startDate, endDate)
                  .filterBounds(projPoly)
                  .select(Sentinel_bands,STD_NAMES)
                  .map(addQualityBands);

//Apply cloud mask
var s2MaskedQA = s2s.map(maskS2clouds);
//Map.addLayer(s2MaskedQA.median(),vizParams,'QA Cloud Masked Median');

// Create a variable which gets the median value from the sentinel collection
var median = s2MaskedQA.median();

// Create variables for median ndvi, evi, and savi over the collection
var Sndvi = median.select(["ndvi"]);
var Sevi = median.select(["evi"]);
var Ssavi = median.select(["savi"]);
var Smsavi = median.select(["msavi"]);
var Sosavi = median.select(["osavi"]);

// Create variables which are the median ndvi, evi, savi, msavi, and osavi values
for each individual plot
// var plotndvi = ndvi.reduceRegions({
//   collection: plots,
//   reducer: ee.Reducer.median(),
//   scale: 10,
// });
// var plotevi = evi.reduceRegions({
//   collection: plots,
//   reducer: ee.Reducer.median(),
//   scale: 10,
// });
// var plotsavi = savi.reduceRegions({
//   collection: plots,
//   reducer: ee.Reducer.median(),
//   scale: 10,
// });
// var plotmsavi = msavi.reduceRegions({
//   collection: plots,
//   reducer: ee.Reducer.median(),
//   scale: 10,
// });
// var plotosavi = osavi.reduceRegions({
//   collection: plots,
//   reducer: ee.Reducer.median(),
//   scale: 10,
// });

// Export the plot index values as tables. There may be a way to combine the values
into a single table before exporting.
// Export.table(plotndvi, "Sentinel_ndvi_2017", {fileformat:"CSV"});
// Export.table(plotevi, "Sentinel_evi_2017", {fileformat:"CSV"});
// Export.table(plotsavi, "Sentinel_savi_2017", {fileformat:"CSV"});
// Export.table(plotmsavi, "Sentinel_msavi_2017", {fileformat:"CSV"});
// Export.table(plotosavi, "Sentinel_osavi_2017", {fileformat:"CSV"});

Export.image.toAsset({
  image: Sndvi,
  description: 'Sndvi',
```

```
  assetId: 'Sndvi',
  region: projPoly,
  scale: 30
});
Export.image.toAsset({
  image: Sevi,
  description: 'Sevi',
  assetId: 'Sevi',
  region: projPoly,
  scale: 30
});
Export.image.toAsset({
  image: Ssavi,
  description: 'Ssavi',
  assetId: 'Ssavi',
  region: projPoly,
  scale: 30
});
Export.image.toAsset({
  image: Smsavi,
  description: 'Smsavi',
  assetId: 'Smsavi',
  region: projPoly,
  scale: 30
});
Export.image.toAsset({
  image: Sosavi,
  description: 'Sosavi',
  assetId: 'Sosavi',
  region: projPoly,
  scale: 30
});
```

D. Landsat 8 spectral unmixing cover estimates:

https://code.earthengine.google.com/9922f5ad9f4e56cd2432fa21963fe7e5

```
/*This script derives proportional estimates of cover for bare ground,
 *perennial plant cover, and bare rock from USGS Landsat 8 Collection 1 Tier 1
 *TOA Reflectance data using a spectral unmixing algorithm
 */

// Import site locations and name them sites
// Draw polygon round area of interest and name it projPoly

var bands = ['B2', 'B3', 'B4', 'B5', 'B6', 'B7'];

// This function masks clouds for Landsat 8
var maskClouds = function(image) {
  var quality = image.select('BQA');
  var cloud01 = quality.eq(61440);
  var cloud02 = quality.eq(53248);
  var cloud03 = quality.eq(28672);
  var mask = cloud01.or(cloud02).or(cloud03).not();
  return image.updateMask(mask);
};

//import collection
var collection = ee.ImageCollection(l8)
    .filterDate('2013-04-11', '2017-10-30')
    .filterBounds(projarea)
    .map(maskClouds)
    .select(bands);
```

```
//create image
var image = ee.Image(collection.sort('CLOUD_COVER').first());
// print(image);

// Create a median composite.
var medianComp = collection.median();

//create endmember values
var bareMean = medianComp.reduceRegion({
  reducer: ee.Reducer.mean(),
  geometry: bare,
  scale: 30,
  tileScale: 16,
}).values();
var vegMean = medianComp.reduceRegion({
  reducer: ee.Reducer.mean(),
  geometry: veg,
  scale: 30,
  tileScale: 16,
}).values();
var rockMean = medianComp.reduceRegion({
  reducer: ee.Reducer.mean(),
  geometry: rock,
  scale: 30,
  tileScale: 16,
}).values();

//unmix image
var autoUnmix = image.unmix([bareMean,vegMean,rockMean] ,true,true);
print(autoUnmix);

//unmix through time
var colUnmix = collection.map(function (i) {
  return i.unmix([bareMean,vegMean,rockMean], true, true)}
  );

var colUnmix = collection.combine(colUnmix); //Need to combine to origional
collection to retain metadata for plotting

// print(colUnmix, ' unmixed collection');

Map.addLayer(colUnmix);
```

E. Sentinel-2A spectral unmixing cover estimates:

https://code.earthengine.google.com/a4d1a8d618e8c8df1a2932e587282cfb

```
/*This script derives proportional estimates of cover for bare ground,
 *perennial plant cover, and bare rock from Sentinel-2 MSI: MultiSpectral
 *Instrument, Level-2A data using a spectral unmixing algorithm
 */

// Import site locations and name them sites
// Draw polygon round area of interest and name it projPoly

// Define study period
var startDate = '2017-01-01';
var endDate = '2017-10-31';

// Function to mask clouds using the Sentinel-2 QA band.
function maskS2clouds(img) {
  var qa = img.select('QA60').int16();
// Bits 10 and 11 are clouds and cirrus, respectively.
  var cloudBitMask = Math.pow(2, 10);
```

```
  var cirrusBitMask = Math.pow(2, 11);
// Both flags should be set to zero, indicating clear conditions.
  var mask = qa.bitwiseAnd(cloudBitMask).eq(0).and(
             qa.bitwiseAnd(cirrusBitMask).eq(0));
// Return the masked and scaled data.
  return img.updateMask(mask);
}

var Sentinel_bands = ['QA60', 'B1','B2','B3','B4','B5','B6','B7','B8','B8A',
'B9','B10', 'B11','B12'];
var STD_NAMES = ['QA60','cb', 'blue', 'green', 'red', 're1','re2','re3','nir',
'nir2', 'waterVapor', 'cirrus','swir1', 'swir2'];

//Get s2 data
var s2s = ee.ImageCollection('COPERNICUS/S2')
                  .filterDate(startDate, endDate)
                  .filterBounds(projPoly)
                  .select(Sentinel_bands,STD_NAMES);
// print(s2s, 'sentinel collection');

//Get the raw median
var vizParams = {bands: ['red', 'green', 'blue'], min: 0, max: 3000};
// Map.addLayer(s2s.median(),vizParams,'Raw Median');

//Apply cloud mask
var s2MaskedQA = s2s.map(maskS2clouds);

// Create median composite
var medianS2 = s2MaskedQA.median();

// Get the mean, max and min spectrum in each of the endmember polygons.
var bareMean = medianS2.reduceRegion(ee.Reducer.mean(), bare, 10).values();
var rockMean = medianS2.reduceRegion(ee.Reducer.mean(), rock, 10).values();
var vegMean = medianS2.reduceRegion(ee.Reducer.mean(), veg, 10).values();

// Automatic unmixing method......
var Sunmix = medianS2.unmix([bareMean, vegMean, rockMean],true,true);
// Map.addLayer(Sunmix);
// print(Sunmix, 'unmixed image');

var SBare = Sunmix.select('band_0');
var SVeg = Sunmix.select('band_1');
var SRock = Sunmix.select('band_2');

// Export unmixed images to asset
Export.image.toAsset({
  image: SRock,
  description: 'SRock',
  scale: 30,
  region: projPoly,
  maxPixels: 1e12
});

Export.image.toAsset({
  image: SVeg,
  description: 'SVeg',
  scale: 30,
  region: projPoly,
  maxPixels: 1e12
});

Export.image.toAsset({
  image: SBare,
  description: 'SBare',
  scale: 30,
  region: projPoly,
  maxPixels: 1e12
});
```

```
// Export unmixed images to drive
// Export.image.toDrive({
//   image: SBare,
//   description: 'SentinelBare',
//   scale: 10,
//   maxPixels: 1e12,
//   region: projPoly
// });

// Export unmix value for each plot
// var plotMESMA = autoUnmix.reduceRegions({
//   collection: plots,
//   reducer: ee.Reducer.median(),
//   scale: 10,
//   tileScale: 16,
// });

// //print(plotMESMA);
// Export.table(plotMESMA, "Sentinel_unmix_3groups", {fileformat:"CSV"});
```

F. Landsat 8 spectral unmixing bare ground estimate change over time:

https://code.earthengine.google.com/cbb1e082e2f23804e165d46f3edfe1d7

```
/*This script determines the trendline slope and percentile range of bare ground
 *spectral unmixing proportional cover estimates from USGS Landsat 8 Collection
 *1 Tier 1 TOA Reflectance data
 */

// Import site locations and name them sites
// Draw polygon round area of interest and name it projPoly

// print(projarea);

var timeField = 'system:time_start';
// Use the reflective bands.
var l5bands = ['B1', 'B2', 'B3', 'B4', 'B5', 'B7'];
var bands = ['B2', 'B3', 'B4', 'B5', 'B6', 'B7'];

// This function masks clouds for Landsat 8
var maskClouds = function(image) {
  var quality = image.select('BQA');
  var cloud01 = quality.eq(61440);
  var cloud02 = quality.eq(53248);
  var cloud03 = quality.eq(28672);
  var mask = cloud01.or(cloud02).or(cloud03).not();
  return image.updateMask(mask);
};

// Use this to mask clouds in Landsat 5 and 7 imagery
var cloud_thresh = 10; // set cloud threshold
// create cloud score function for LS 7 imagery taking advantage of the built in
algorithm cloudscore
var cloudfn = function(image){
  var CloudScore = ee.Algorithms.Landsat.simpleCloudScore(image); //use add the
cloud likelihood band to the image
  var quality = CloudScore.select('cloud'); //isolate the cloud likelihood band
  var cloud01 = quality.gt(cloud_thresh); //get pixels above the threshold
  var cloudmask = image.mask().and(cloud01.not()); //create a mask from high
likelihood pixels
  return image.updateMask(cloudmask); //mask those pixels from the image
};
```

```
//load collection for unmixing
var forSMA = ee.ImageCollection('LANDSAT/LC08/C01/T1_TOA')
    .filterDate('2017-01-01', '2017-10-31')
    .filterBounds(projarea)
    .map(maskClouds)
    .select(bands);
    // .map(addVariables);

// Load Landsat Image Collections.
var l8collection = l8
    .filterBounds(projarea)
    .filterDate('2013-04-11','2019-07-31')
    .map(maskClouds)
    .select(bands);
    // .map(addVariables);
var l7collection = l7
    .filterBounds(projarea)
    .filterDate('1999-01-01','2013-04-11')
    .map(maskClouds)
    .select(l5bands);
    // .map(addVariables);
var l5collection = l5
    .filterBounds(projarea)
    .filterDate('1984-01-01','1999-01-01')
    .map(maskClouds)
    .select(l5bands);
    // .map(addVariables);

var l7Renamed = l7collection.select(
    ['B1', 'B2', 'B3', 'B4', 'B5', 'B7'], // old names
    ['B2', 'B3', 'B4', 'B5', 'B6', 'B7']  // new names
);
var l5Renamed = l5collection.select(
    ['B1', 'B2', 'B3', 'B4', 'B5', 'B7'], // old names
    ['B2', 'B3', 'B4', 'B5', 'B6', 'B7']  // new names
);

// print(l8collection);
// print(l7Renamed);
// print(l5Renamed);

var collection = ee.ImageCollection(l5Renamed.merge(l7Renamed).merge(l8collection))
                  .sort('system:time_start')
                  .select(['B2', 'B3', 'B4', 'B5', 'B6', 'B7']);
// print(collection);

// var image = ee.Image(collection.sort('CLOUD_COVER').first());

// Create a median composite.
var medianComp = forSMA.median();

// Get the mean spectrum in each of the endmember polygons.
var bareMean = medianComp.reduceRegion({
  reducer: ee.Reducer.mean(),
  geometry: bare,
  scale: 30,
  tileScale: 16,
}).values();
var vegMean = medianComp.reduceRegion({
  reducer: ee.Reducer.mean(),
  geometry: veg,
  scale: 30,
  tileScale: 16,
}).values();
var rockMean = medianComp.reduceRegion({
  reducer: ee.Reducer.mean(),
  geometry: rock,
  scale: 30,
```

```
  tileScale: 16,
}).values();

//////////////Unmixing through
time/////////////////////////////////////////////////////////////////////////////
//Map unmixing over each image in a collection
var colUnmix = collection.map(function (i) {
  return i.unmix([bareMean,vegMean,rockMean], true, true)
});

var colUnmix = collection.combine(colUnmix); //Need to combine to origional
collection to retain metadata for plotting

////////// Linear regression
//////////////////////////////////////////////////////////////////
var addVariables = function(image) {
  var date = ee.Date(image.get(timeField)) // Compute time in fractional years
since the epoch.
  var years = date.difference(ee.Date('1970-01-01'), 'year')
  return image
.addBands(ee.Image(years).rename('t').float()) // Add a time band.
    .addBands(ee.Image.constant(1)); // Add a constant band.
};

var linearCollection = colUnmix.map(addVariables);
// print(linearCollection);

// Reduce the collection with the linear fit reducer. Independent variable are
followed by dependent variables.
var linearBare = linearCollection.select(['t', 'band_0'])
  .reduce(ee.Reducer.linearFit());
var bareTrend = linearBare.select('scale').rename('bareTrend');

var plotBareTrend = linearBare.reduceRegions({
 collection: plots,
 reducer: ee.Reducer.median(),
 scale: 30,
});
// Export.table(plotBareTrend, "BareProportionTrend", {fileformat:"CSV"});

// // Amplitude

var reduced = colUnmix.reduce(ee.Reducer.percentile([5,25,50,75,95]));
// print(reduced, ' percentile reduction');

// get bare amplitude
var bareRange =
reduced.select('band_0_p95').subtract(reduced.select('band_0_p5')).rename('bareAmpl
itude');
// print(bareRange, 'bare amplitude image');
// Map.addLayer(bareVariability, {min:0.01, max:0.99});

// then just extract values for your sampling locations from the amplitude image...
var plotBareVariability = bareRange.reduceRegions({
  collection: plots,
  reducer: ee.Reducer.median(),
  scale: 30,
  tileScale: 16
});
// Export.table(plotBareVariability, "Variability_bare_proportion",
{fileformat:"CSV"});

Export.image.toDrive({
  image: bareTrend,
  description: 'BareTrend',
  scale: 30,
  region: projPoly,
  maxPixels: 1e9
```

```
});

Export.image.toDrive({
  image: bareRange,
  description: 'BareRange',
  scale: 30,
  region: projPoly,
  maxPixels: 1e9
});
```

G. Partial least square regression project area projection:

https://code.earthengine.google.com/14ab1a323bd6456a198caae12a05eeb5

```
/*This script projects the regression coefficients from a partial least squares
 *regression model to develop images for estimated bare ground and estimated
 *perennial plant cover for the project area
 */

// Import site locations and name them sites
// Draw polygon round area of interest and name it projPoly

// stack variables into image
var stack =
Levi.addBands(Lmsavi).addBands(Lndvi).addBands(Losavi).addBands(Lsavi).addBands(LBa
re).addBands(LVeg).addBands(LRock).addBands(Sndvi).addBands(Sevi).addBands(Ssavi).a
ddBands(Smsavi).addBands(Sosavi).addBands(SBare).addBands(SVeg).addBands(SRock);
// print(stack);

//////// create map for perennial cover

var per =
stack.expression("intercept+(a*x1)+(b*x2)+(c*x3)+(d*x4)+(e*x5)+(f*x6)+(g*x7)+(h*x8)
+(i*x9)+(j*x10)+(k*x11)+(l*x12)+(m*x13)", {
  'intercept':ee.Image(7.2286829),
  'a':ee.Image(-8.8843203),
  'b':ee.Image(-16.4787721),
  'c':ee.Image(-24.1500871),
  'd':ee.Image(-24.1484140),
  'e':ee.Image(-16.0965944),
  'f':ee.Image(-13.0038829),
  'g':ee.Image(-0.1200955),
  'h':ee.Image(64.7860885),
  'i':ee.Image(108.0897218),
  'j':ee.Image(108.1542219),
  'k':ee.Image(72.4610391),
  'l':ee.Image(-22.3040971),
  'm':ee.Image(21.8265843),
  'x1':stack.select('evi'),
  'x2':stack.select('msavi'),
  'x3':stack.select('ndvi'),
  'x4':stack.select('osavi'),
  'x5':stack.select('savi'),
  'x6':stack.select('band_0'),
  'x7':stack.select('band_1'),
  'x8':stack.select('msavi_1'),
  'x9':stack.select('ndvi_1'),
  'x10':stack.select('osavi_1'),
  'x11':stack.select('savi_1'),
  'x12':stack.select('band_0_1'),
  'x13':stack.select('band_1_1')
});

// print(per);
```

```
var bar =
stack.expression("intercept+(a*x1)+(b*x2)+(c*x3)+(d*x4)+(e*x5)+(f*x6)+(g*x7)+(h*x8)
+(i*x9)+(j*x10)+(k*x11)+(l*x12)+(m*x13)", {
  'intercept':ee.Image(31.601574),
  'a':ee.Image(18.577378),
  'b':ee.Image(38.743007),
  'c':ee.Image(54.970941),
  'd':ee.Image(54.974129),
  'e':ee.Image(36.653965),
  'f':ee.Image(25.426900),
  'g':ee.Image(-5.092543),
  'h':ee.Image(-45.193400),
  'i':ee.Image(-79.886711),
  'j':ee.Image(-79.962583),
  'k':ee.Image(-53.797337),
  'l':ee.Image(39.463357),
  'm':ee.Image(-38.682795),
  'x1':stack.select('evi'),
  'x2':stack.select('msavi'),
  'x3':stack.select('ndvi'),
  'x4':stack.select('osavi'),
  'x5':stack.select('savi'),
  'x6':stack.select('band_0'),
  'x7':stack.select('band_1'),
  'x8':stack.select('msavi_1'),
  'x9':stack.select('ndvi_1'),
  'x10':stack.select('osavi_1'),
  'x11':stack.select('savi_1'),
  'x12':stack.select('band_0_1'),
  'x13':stack.select('band_1_1')
});

// print(bar);

// Export.image.toAsset({
//   image: per,
//   description: 'pls2_per_pred',
//   assetId: 'pls2_per_pred',
//   region: projPoly,
//   scale: 30
// });

// Export.image.toAsset({
//   image: bar,
//   description: 'pls2_bare_pred',
//   assetId: 'pls2_bare_pred',
//   region: projPoly,
//   scale: 30
// });

// Export.image.toDrive({
//   image: per,
//   description: 'pls5_sumPer',
//   scale: 30,
//   region: projPoly
// });

// Export.image.toDrive({
//   image: bar,
//   description: 'pls5_sumAnBg',
//   scale: 30,
//   region: projPoly
// });

// Export predicted bare ground and perennial plant cover for test plots

var testplotsVeg = per.reduceRegions({
```

```
      collection: testPlots,
      reducer: ee.Reducer.median(),
      scale: 30,
      tileScale: 16
});
var testplotsBar = pba.reduceRegions({
      collection: testPlots,
      reducer: ee.Reducer.median(),
      scale: 30,
      tileScale: 16
});
var testplotsArch = Arch.reduceRegions({
      collection: testPlots,
      reducer: ee.Reducer.median(),
      scale: 30,
      tileScale: 16
});

Export.table(testplotsVeg, "pls7_sumPer_predicted_testPlots", {fileformat: "CSV"});
Export.table(testplotsBar, "pls7_sumAnBg_predicted_testPlots", {fileformat:
"CSV"});
Export.table(testplotsArch, "archetype_testPlots", {fileformat: "CSV"});
```

H. Trendline slope value of CHIRPS precipitation data:

https://code.earthengine.google.com/28d853745e19f24ac7c05962c02a47f9

```
/*This script extracts values for the trendline slope of CHIRPS Pentad: Climate
 *Hazards Group InfraRed Precipitation with Station Data (version 2.0 final)
 *derived precipitation data
 */

// Import site locations and name them sites
// Draw polygon round area of interest and name it projPoly

//dates
var start_date = '1984-01-01';
var end_date = '2018-06-30';

//Filter chirps data
var chirps = ee.ImageCollection('UCSB-CHG/CHIRPS/PENTAD')
  .filterDate(start_date,end_date)
  .filterBounds(projPoly)
  .select('precipitation');

var precip = chirps.filterDate('1984-01-01','2018-06-30').mean();

////////////////////////////////////////////////////////////////////////
// Export trend image
var createTimeBand = function(img) {
    var year = ee.Date(img.get('system:time_start')).get('year').subtract(1984)
    return              ee.Image(year).byte().addBands(img).set('system:time_start',
img.get('system:time_start'))};

var ChirpsTrend = chirps.map(createTimeBand);
//print(ChirpsTrend)

var     trendImg     =     ChirpsTrend.reduce({reducer:     ee.Reducer.linearFit(),
parallelScale:4 });
print(trendImg, 'Trend image');

var RainfallTrend = trendImg.select('scale');

print(RainfallTrend, 'Rainfall trend');
```

```
// Export.image.toDrive({
//   image: RainfallTrend,
//   description: 'RainfallTrend',
//   scale: 30,
//   region: projPoly
// });

Export.image.toAsset({
  image: RainfallTrend,
  description:'RainfallTrend3',
  scale: 30,
  region: projPoly
});
```